2000

Beach development behind detached breakwater.

Axe, Philip George

BEACH DEVELOPMENT BEHIND DETACHED BREAKWATERS

by

PHILIP GEORGE AXE

September 2000

BEACH DEVELOPMENT BEHIND DETACHED BREAKWATERS

by

PHILIP GEORGE AXE

A thesis submitted to the University of Plymouth
in partial fulfilment for the degree of

DOCTOR OF PHILOSOPHY

School of Civil and Structural Engineering
Faculty of Technology

September 2000

Abstract

Beach development behind detached breakwaters

Philip George Axe

Concurrent wave and morphology data were collected around a coastal protection scheme on the U.K. south coast. The scheme consists of eight detached breakwaters protecting a renourished sand and shingle beach, and is situated in a strongly macro-tidal environment. The development of the beach morphology is described. The beach trapped sand and shingle moving eastwards into it, and lost material from the eastern end. While the beach was designed to maintain a shingle beach, it was found that the scheme was most effective at trapping sand, which led to tombolo formation behind the updrift breakwaters.

Current engineering design methods for describing beach development were applied to the scheme. Empirical techniques were found to be poor predictors of the salient length, although the simplest methods were reasonable guides to the scheme response over a variety of tidal levels. The US Army Corps of Engineers one-line model GENESIS (Hanson, 1989) was applied to the scheme. Using observed values of beach, structure and wave conditions, it was necessary to exaggerate transport due to longshore gradients in wave height relative to transport due to oblique wave approach to correctly describe salient formation. While it was possible to reduce model calibration errors, model validation was not successful. This was due to the inability of the model to allow tombolo formation, and also due to the lack of a 'constant' beach profile, due to the different behaviour of the sand and shingle.

Empirical orthogonal function analysis was carried out on the beach survey data. From the limited records available, it was clear that the scheme reduced profile variance behind it, compared to the updrift and downdrift shorelines. The scheme also led to more complex 3D seasonal movements of beach material, in contrast to the predominantly 2D response updrift.

Table of Contents

List of Figures

Chapter 5

Chapter 6

Acknowledgements

I would like to acknowledge the support of Prof. Geoff Bullock, Dr. Andrew Chadwick and Professor David Huntley, in particular for their patience while I wrote up away from Plymouth.

I would also like to acknowledge the encouragement and support I received from my current supervisor at POL, Dr. Philip Woodworth. I must thank my colleague, Dr. Suzana Ilic, for her help and support during the endless hours processing and checking data, and her technical advice, coffee and recipes throughout the project.

I would like to acknowledge the help of Paul Bird and the technicians and divers of the School of Civil and Structural Engineering, and also of the University diving and sailing centre, Coxside. Particularly, I would like to thank Tony, Ian and Steve for their help in fabricating and deploying the equipment and ground tackle. I would like to also thank Dr. David Pope, Richard Brown and Bob Gayler of Brighton University Department of Civil and Environmental Engineering for their work with the IWCM. David Green, Roger Spencer, Ian Trayner, Chris White and Brian Chapman, of Arun District Council, for their help with provision of boats (at strange hours of the morning) and time to download data, and also for their help with the provision of aerial survey data.

Thanks to Dr. Adam and Mrs. Angela Crawford, for their support and advice, on both technical and administrative matters,

More social thanks go to Drs. Yolanda Foote, Mark Davidson, Paul Russell and Dave Simmonds for their advice, help and beer.

Thanks to my wife, Kristina, for her patience in having only known (and married) me as someone who will be ready 'soon'.

Author's Declaration

At no time during the registration for the degree of Doctor of Philosophy has the author been registered for any other University award.

This study was financed with the aid of funding from the Engineering and Physical Sciences Research Council, The Standing Conference on Problems Associated with the Coastline, and Arun District Council. Support to attend Coastal Dynamics '97 and European Geophysical Society General Assembly (1999) was provided by the Natural Environment Research Council's Centre for Coastal and Marine Sciences.

A programme of advanced study was undertaken, which included attendance at the courses and conferences listed on the following page, in addition to departmental seminars at the School of Civil and Structural Engineering and Institute of Marine Studies, University of Plymouth.

Dr. Hans Hanson, of the University of Lund, Sweden, was visited in June 1996.

Signed.....

Date.....

Courses attended:

HSE iv University of Plymouth, Scientific diving (1993-1994)

Coastal Engineering and Shoreline Management, one week EPSRC short course held at the School of Civil and Structural Engineering, University of Plymouth, 1995

Coastal Geology, taught by Prof. Paul Komar, short course held at ICCE'96

MAST Advanced Study course on Hydro- and Morphodynamic Processes in Coastal Seas, Held at Renesse, Netherlands, Summer 1998.

Conferences attended

25th International Conference on Coastal Engineering (ICCE), Orlando, Florida. September 1996

Coastal Dynamics '97, Plymouth, U.K., June 1997

General Assembly of the European Geophysical Society, Den Haag, Netherlands, April 1999

Publications

Axe, P.G., S. Ilic and A.J. Chadwick, 1996, 'Evaluation of beach modelling techniques behind detached breakwaters', *Proceedings of the 25th International Conference on Coastal Engineering*, ed. B. Edge, ASCE, New York, pp. 2036-2047

Axe, P.G., and A.J. Chadwick, 1997, 'Beach variability behind detached breakwaters', *Proceedings of Coastal Dynamics '97*, ASCE, New York, pp. 744-753

Bird, P.A.D., Davidson, M.A., Ilic, S., Bullock G.N., Chadwick, A.J., Axe P.G., and Huntley D.A., 1995, 'Wave reflection, transformation and attenuation characteristics of rock island breakwaters', *Proceedings ICE conference on Coastal Structures and Breakwaters '95*, Thomas Telford Publications, London.

Ilic S., Axe P.G., Chadwick A.J., Davidson M.A., Bird P.A.D., Bullock G.N., and Pope D.J., 1995, 'The role of offshore breakwaters in coastal defence', *Proceedings of 1st Croatian Conference on Water*, Dubrovnik, Croatia

Notation

B	Breakwater length
C_{ij}, Q_{ij}	co- and quadrature spectra
Cg	wave group velocity
D_B	Berm height
D_C	Closure depth
D_{Lto}	Maximum depth of longshore transport
D_G	depth at groyne tip
D_S	depth at structure
E	wave energy density
G	Gap width
Ge	Distance between shoreline ellipse centre, and breakwater tip (McCormick, 1993)
G(f,θ)	directional spreading function
H	wave height
I	immersed weight transport rate
K_R	Refraction coefficient
K_S	Shoaling coefficient
K_D	Diffraction coefficient
P	recorded pressure
$P_E(\theta)$	proportion of energy at a breakwater tip
Q	sediment transport rate
R	radius length (between a breakwater tip and shoreline)
S	distance from breakwater to shoreline
S_{max}	wave energy concentration parameter
S(f)	wave frequency spectrum
S(f,θ)	directional wave frequency spectrum
S_{ij}	momentum flux tensor
T_p	peak wave period
X	distance of salient apex from breakwater

λ(x,t); λ(y,t);
e(x,t);e(y,t) eigenvalues and their respective eigenfunctions

a	wave amplitude
d_{50}	median grain size
g	gravitational acceleration
h	water depth (or beach height)
k	wave number
l	wavelength
p	sediment porosity
q	source or sink of sand
u_*	friction velocity
z	sensor height
tan β	beach slope
α,θ	wave angles
γ	wave breaking criterion
ζ	water level
η	surface elevation
ϕ	angle the radius makes with a tangent to the shoreline
φ	velocity potential
ρ	density
τ_0	bed shear stress
ξ_b	Irribarren number

Subscripts

o	offshore
b	breaking
s	significant
L	limiting
m0	zeroth moment

1 Introduction

This thesis describes a study of the development of a renourished beach protected by detached breakwaters on the U.K. south coast. The study involved an extensive field measurement programme, analysis of this data and evaluation of modelling techniques.

To provide a context for the work presented in this thesis, this chapter summarises coastal engineering problems in the United Kingdom due to predicted sea level change, and the problem of ageing coastal structures. The response to these pressures is described. An overview of coastal protection schemes along the U.K. south coast is presented, and experience in the use of detached breakwaters and shingle beach modelling is shown to highlight the need for increased field data resources, and modelling experience.

The experimental site at Elmer is described in terms of its position in the littoral cell structure of the UK south coast; its geology; and its recent development and engineering history. The experiment is described, and the author's role in this collaborative project is presented.

1.1 Coastal protection and the UK

In the UK as a whole, it is estimated that around 3 million people live on or below the +5 m (above mean sea level) contour, with the fastest growing populations in Cambridgeshire, Dorset and the Isle of Wight. **Figure 1-1** shows those areas that are most prone to flooding or suffering coastal erosion. The south east of England is also the region most at risk from the post-glacial readjustment of Great Britain due to the removal of ice loading since the last ice age. Land settlement, due to groundwater (and locally, hydrocarbon) abstraction, the increase in storm surge activity and expected acceleration in sea level rise, due to predicted global warming, exacerbate these problems.

The Ministry of Agriculture, Fisheries and Food (MAFF) are responsible for grant aid for coastal protection works in the United Kingdom. This government department recommends that allowance be made for a relative sea level rise of between 4 mm/year in the north-west and north-east of Britain, and 6 mm/year in the

south and south east (Pethick and Burd, 1993). This compares with global estimates of about 1.5 mm/year from global tide gauge records reported by Aubrey and Emery (1993).

Surveys by the U.K. National Rivers Authority (now part of the Environment Agency) in 1992, and by MAFF (1994), state that of the 3763 km of English coastline, 1000 km is protected against tidal flooding (sea defence), and 860 km is protected against coastal erosion (coast protection). It is estimated that of these works, 13% have a design life of 5 years or less.

On the UK south coast, these pressures have led to the commissioning of shoreline management plans. Where there is the need, and favourable benefit cost ratios and environmental considerations allow, engineering protection schemes have been constructed. Recent examples of these are presented in **Table 1-1**. From this table, it can be noted that of the eleven schemes involving beach renourishment, four schemes include detached breakwaters, two involve diffracting T-shaped groynes, and eight schemes involve shingle as the beach nourishment material. All of the schemes are in macro-tidal environments.

1.2 Current design experience

The use of detached breakwaters for beach stabilisation and coastal protection in the U.K. is relatively recent, with the first documented case being at Leasowe Bay on the Wirral (Barber and Davies, 1985). This is shown in **Figure 1-2**). Outside of the U.K., their use has been in predominantly micro-tidal regimes, such as the U.S. Great Lakes, or the Mediterranean. For example, more than 500 detached breakwaters exist along 300 km of the central Adriatic Italian shoreline (Liberatore, 1992). In Japan, detached breakwaters protect 572 km of coastline, and techniques for predicting three dimensional beach topography change have been developed for sandy beaches. This pool of experience in Japan is however largely inaccessible to western engineers, as only between 5 and 15% of Japanese coastal engineering literature has been written in English (Horikawa K. 1996).

Scheme location	Construction date	Description
Pevensey Levels	1996	Shingle beach renourishment , in conjunction with T-shaped groynes
Seaford	1987	First major shingle beach recharge in the U.K., Terminal groyne and periodic recycling of material
Brighton	1996	Storm water reservoir behind shingle beach
Elmer	1993	Shingle beach nourishment stabilised by eight detached breakwaters and a terminal groyne
Felpham	1996/7	Proposed shingle beach renourishment stabilised by T-shaped groynes
Hayling Island	1996	Shingle beach renourishment and recycling
Monks Bay, Isle of Wight	1995	Single offshore breakwater
Hurst Spit, Christchurch Bay	1989	Shingle beach nourishment
Bournemouth	1988-90	Beach recharge using sand dredged from Poole Harbour
Sandbanks, Poole	1996	
Lyme Regis	1997 (proposed)	Three detached offshore breakwaters, storm water storage in new seawalls, and beach nourishment
Sidmouth	1995	Two detached breakwaters, two groynes, armouring of seawall and shingle beach nourishment
Towan Beach, Restormel	1994	Beach groundwater control system

Table 1-1 Recent coastal protection measures along the U.K. south coast

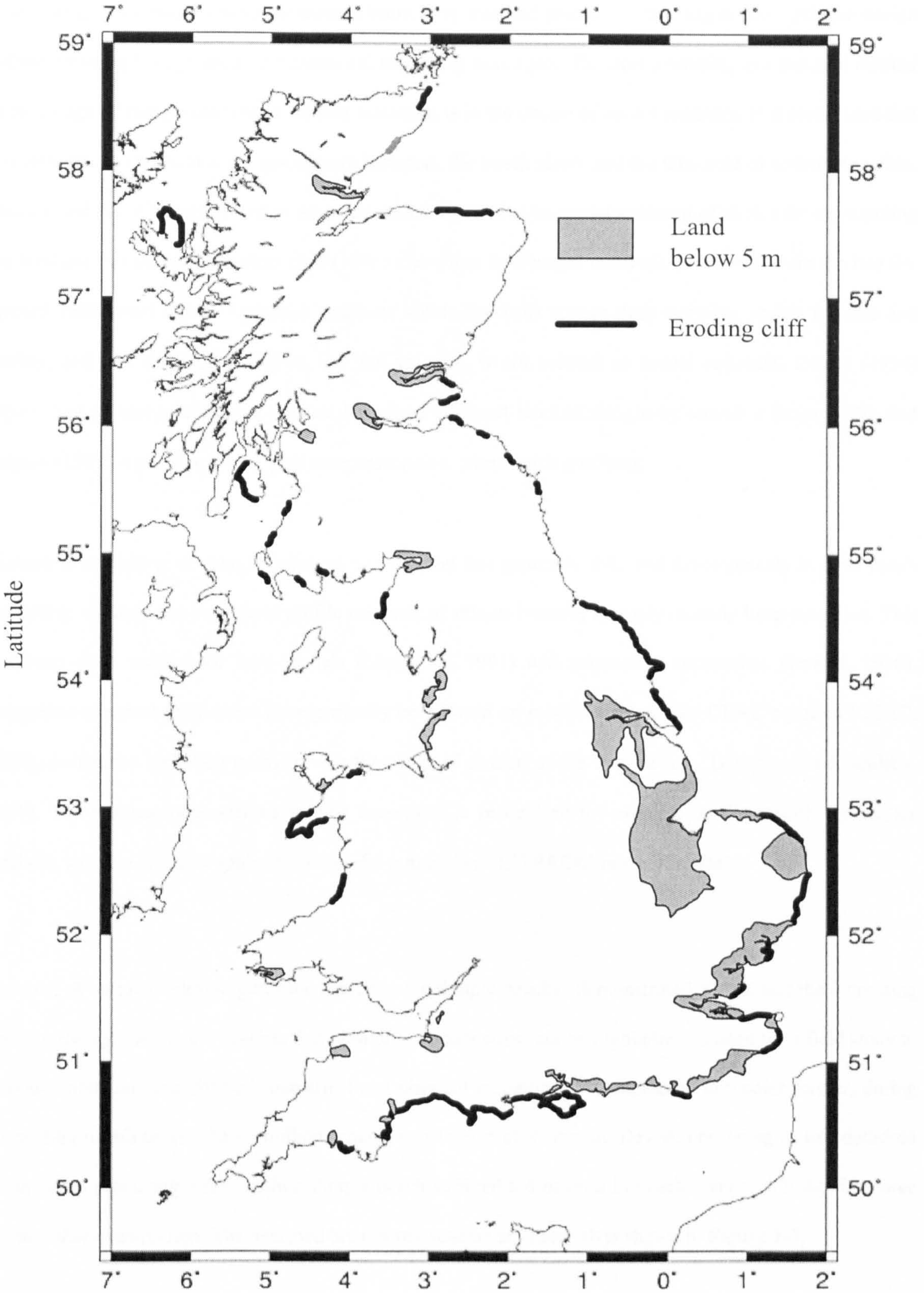

Figure 1-1 Eroding cliff lines and areas below +5 m above Ordnance Datum in England, Wales and Scotland (after Rendel, Palmer and Tritton Ltd, 1996)

In the design of a major coastal defence scheme, it is standard practice to investigate and optimise design options by using both physical and numerical modelling techniques. Physical modelling is a standard method in the design of shingle beaches. A current limitation is in the choice of model sediment. It is recognised that it is important to reproduce the on-offshore transport, the beach slope, and the threshold of sediment motion. This has led HR Wallingford Ltd to adopt crushed anthracite as its model sediment of choice for representing the behaviour of shingle. Loveless *et al* (1996) claim that lightweight materials are ejected from the bed (by upward percolation due to hydraulic gradients within the bed) sooner than materials scaled for size and density, and thus anthracite, with its low fall velocity, is not suitable as model sediment. Coates (1994) reports that anthracite also over-predicts longshore transport rates of shingle by around a factor of 40, and Janssen (1993) warns that it may give unrepresentative, steep beach gradients.

Numerical modelling of shingle transport and beaches has generally followed developments in sand beach modelling, although the very rapid profile response of shingle beaches has only recently been modelled. This has been done using both bore models (Chadwick, 1991) and parametric approaches (Powell, 1990). Longshore transport predictions have generally been based on modifications to the CERC equation (CERC, 1984), sometimes including terms for the threshold of motion of the shingle (e.g. Damgaard and Soulsby, 1996). The problem of modelling shingle movement is recognised for example by the Danish Hydraulics Institute, who use an upper grain size limit of 5 mm in their 'LITPACK' range of models.

The lack of validated design guidance available for shingle beaches demonstrated above, and the increasing need to manage the shingle beaches that exist or are under construction highlights the need for a field study to provide validation data for both numerical and physical modelling. To emphasize this point further, during the writing of this thesis, the £6 million scheme constructed at Sidmouth, Devon, consisting of two detached breakwaters protecting a renourished shingle beach suffered a 4 m drop in beach level within the first three months after construction. The detached breakwater scheme at Sidmouth is shown in **Figure 1-3**.

It is the aim of this study to collect field data to evaluate currently available models of beach development, and to produce guidance for practising engineers on model application. The next part of this chapter is a description of the fieldwork site, its location, geology, and its recent development as a headland area.

Figure 1-2 Looking west over detached breakwaters at Leasowe Bay, Wirral. (Photograph by author)

Figure 1-3 Sidmouth breakwaters and renourished beach looking south west, September 1995, on completion (Photograph by author)

1.3 Site description

1.3.1 Location

Elmer lies on the U.K. south coast, 24 km west of Brighton. It lies 15 km from the western boundary of the Selsey Bill - Thames estuary coastal cell. This primary cell is divided into numerous sub cells. Elmer lies in the centre of the Selsey Bill - Brighton Marina sub cell (Bray *et al*, 1995). Within this sub cell, 'partial hard' cell boundaries exist at Pagham Harbour (~10 km west of the study site) and at the mouth of the Arun (~5 km to the east). Given the predominant west to east drift direction along this coastline, the Pagham boundary is expected to have a controlling influence on the natural supply of beach material to this site. This is illustrated in **Figure 1-4**.

The study site is the most seaward protrusion along an otherwise straight stretch of coastline, and has thus behaved as a headland area. This can be seen in **Figure 1-5**. This feature has arisen as a result of the development of Elmer as a residential zone since around 1912, and its subsequent protection with groynes and seawalls. In 1963, the coastal protection authorities responsible for this frontage erected mass concrete coast defence walls (crest levels of 5.5 m Above Ordnance Datum in the east, 4.8m AOD in the west) and re-built the groyne field. Further work was required during the 1970s, and between 1976 and 1990 over 99,000m^3 of shingle was added to the beach by Arun District Council and Southern Water. These works did not stop the lowering of beach levels, and by 1990, beach levels had fallen sufficiently to expose the toe steps of the 1963 sea wall. Further loss of beach material would cause the undercutting and failure of the wall Authority (Robert West and Partners, 1991).

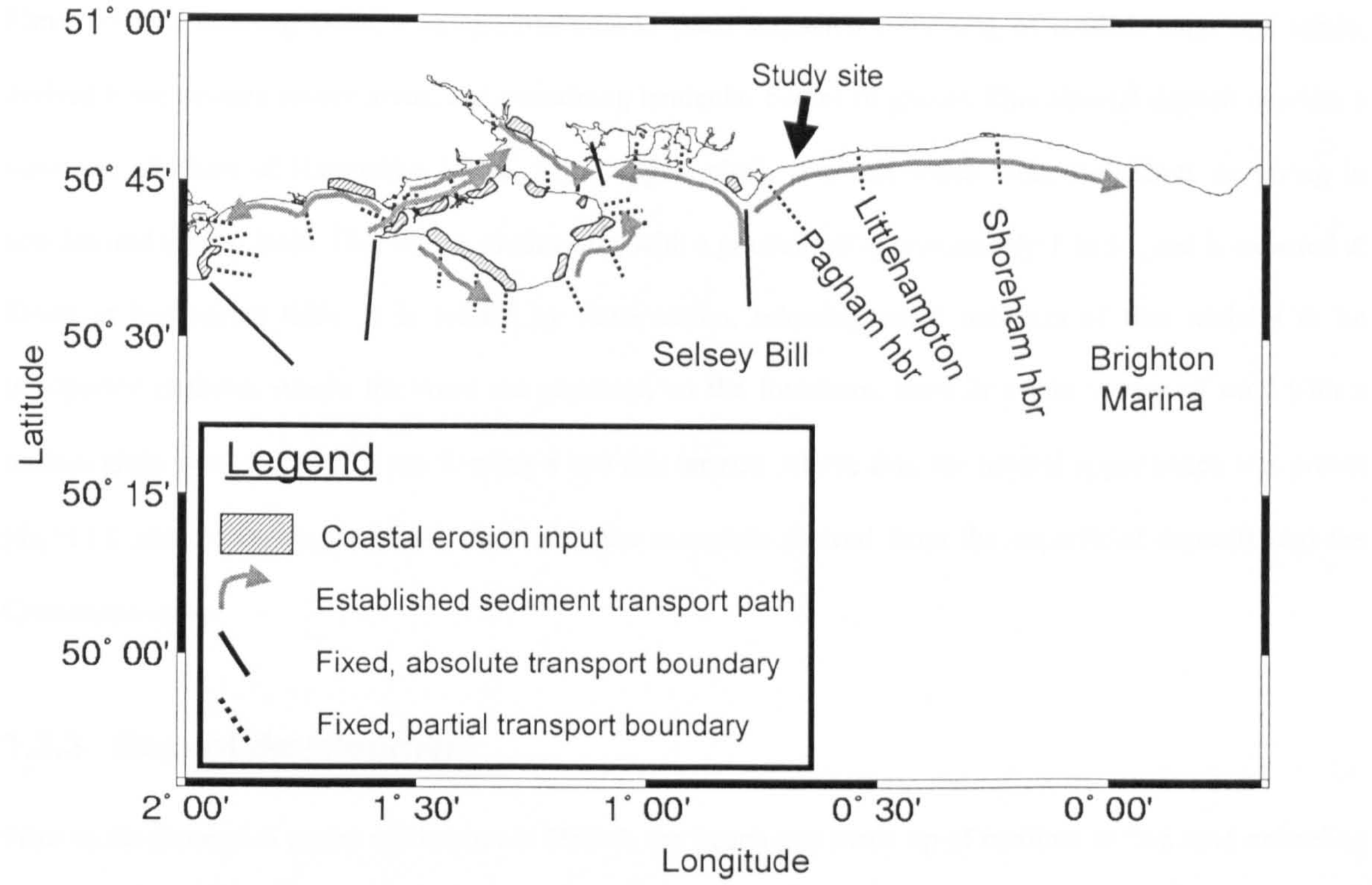

Figure 1-4 Location of Elmer in terms of the regional littoral cell structure. Information on sources of sediment and transport boundaries taken from Bray *et al*, 1995

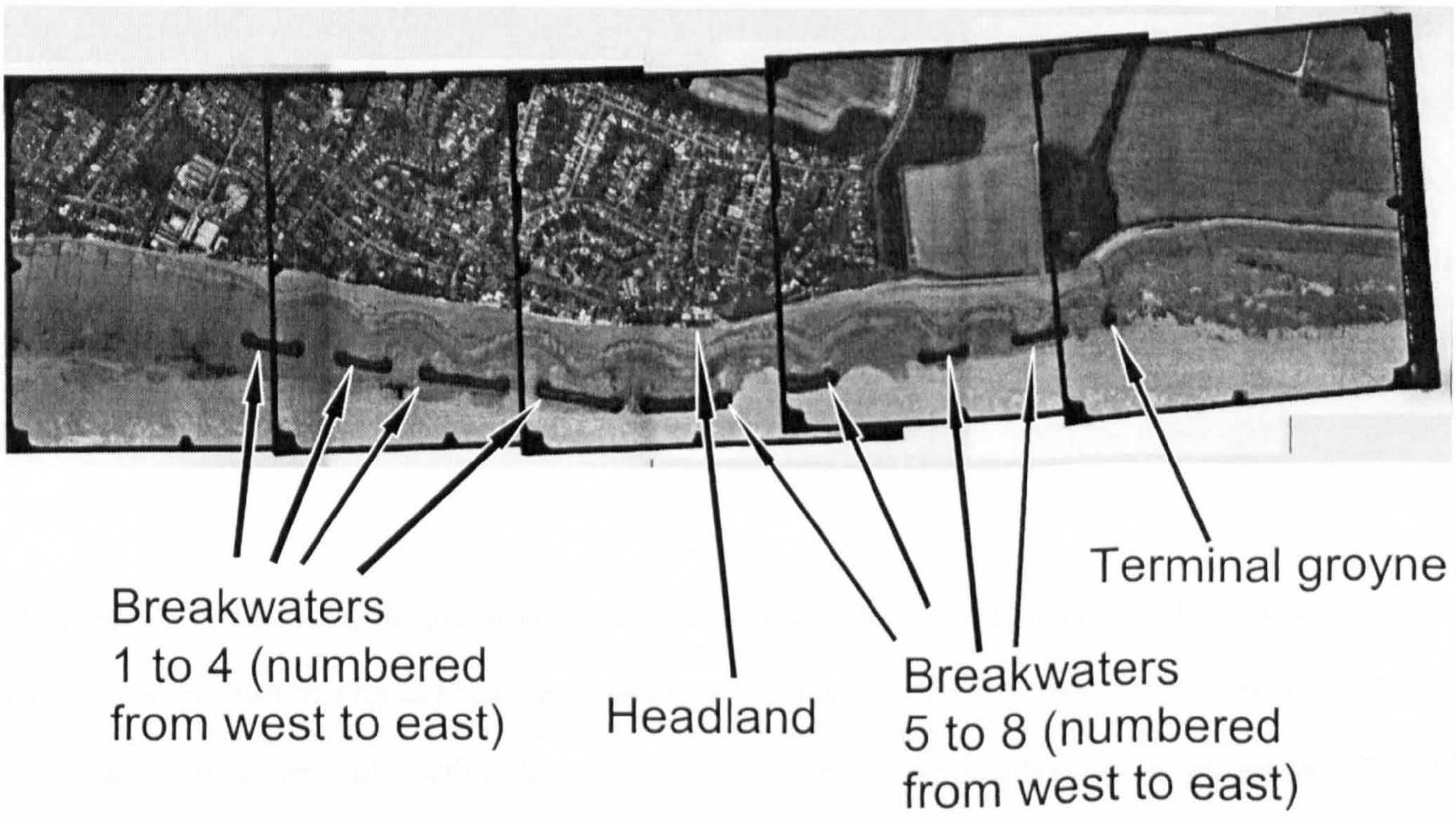

Figure 1-5 Elmer frontage, showing headland, breakwater and groyne positions (from aerial photograph)

1.3.2 Geology

Elmer lies on Reading Beds, a terrigenous coastal plain sequence consisting of reddish clays and sands, derived from western source areas, and containing lenticular bodies of gravel. This alluvial deposit overlies a wave cut platform of Hampshire Chalk. This 'upper' chalk is a soft white rock, with flints occurring in nodules and tabular beds. This slopes southwards, with a gradient of approximately 1 in 50, and is exposed at Elmer at low spring tides. It is eroded by wave action, releasing small numbers of flint nodules to be transported onshore. Above the wave cut platform, on the foreshore, there is a thin veneer of sand with a median grain size (d_{50}) of 115 μm forming a low tide terrace. Above this, the natural upper beach was gravel (d_{50}=11.0 mm), composed of hard chert and flint materials derived from the superficial deposits and the Cretaceous strata.

1.3.3 Recent development

Prior to the protection works carried out in 1992-3, the beach was made up of medium to fine sand extending from the sea wall to the chalk platform. In addition to these deposits, there was fine, medium and coarse shingle, small amounts of sand and shingle admixtures, some soft to firm alluvial deposits, and the Upper Chalk.

Updrift coastal works and groyne systems prevented longshore transport of material into the study area. This was demonstrated by a beach recharge that took place at Middleton-on-Sea. The material was observed to move less than 250 m over several years. Onshore transport of shingle was identified by consultants' report (Robert West and Partners, 1991) as being a potentially significant sediment source.

In the east of the scheme, shingle levels were highest, although still sufficiently low to expose old timber faggot work and the toe piles and bracing of the Poole Place groyne. These levels were very sensitive to local conditions, and a week of south-easterly winds and waves in April 1991 led to an accumulation of approximately 1 m of shingle against the Poole Place groyne. Elsewhere along the frontage, shingle coverage was patchy, with the shingle deposits being no more than 0.5 m thick at the top of the beach in places (Robert West and Partners, 1991).

In the winter of 1989, severe storms led to flooding of the residential hinterland. As an emergency measure, the coast protection authorities constructed two rock-island breakwaters to reduce the severity of wave conditions at the most vulnerable part of the frontage. A rock revetment was also constructed at this time. Longer-term works were planned, consisting of a 139,000 m^3 beach fill along the Arun District Council (ADC) frontage, using coarse material from offshore sources. This beach material was to act as the coastal defence structure, and be stabilised by eight shore-parallel offshore breakwaters and a terminal rock groyne in place of the older groyne at Poole Place.

Following the recommendations of consultants, and physical model tests at HR Wallingford (HR Wallingford Ltd., 1992a, HR Wallingford Ltd., 1992b), Arun District Council (ADC) and the National Rivers Authority (NRA) commissioned the construction of an offshore breakwaters scheme, in conjunction with a beach replenishment. The timber groyne at Poole Place was to be replaced with a rock structure. The beach nourishment was to allow the formation of salients behind the breakwaters without depleting the existing beach. The formation of these features would provide sufficient shingle in front of the concrete sea walls to prevent overtopping. Salients are believed to behave as permeable groynes, only trapping a proportion of material transported alongshore. It was also envisaged that any material transported into the scheme from offshore would be retained. Overtopping predictions made from the physical model tests indicated that in front of the ADC frontage, a shingle beach crest 4.5 m Above Ordnance Datum (AOD) with a berm width of 10 m would reduce overtopping to within acceptable levels for a 100 year return storm.

Originally two breakwaters were constructed of 7 tonne blocks of carboniferous limestone as an emergency measure. These were situated immediately seaward of the headland, approximately where breakwaters 3 and 4 now stand. Between 1992 and 1993, the number of structures was increased to eight. Breakwater lengths vary between 70 and 140 m and crests are 4.5 m above ordnance datum, although in order to reduce the down drift impact of the scheme, the crest level of the eastern end breakwater is 1.5 m lower than the others. The slope of the seaward face of the initial, emergency breakwaters was 1 in 1.5, although this has since been reduced to 1 in 2 by the addition of 8 tonne Norwegian syenite armour stone. Each breakwater end is finished with a round head, with slope of 1 in 2.5. Schematic diagrams of a typical breakwater are shown in Figure

1-6. A fuller description of the site, and details of the construction, may be found in Holland and Coughlan (1994).

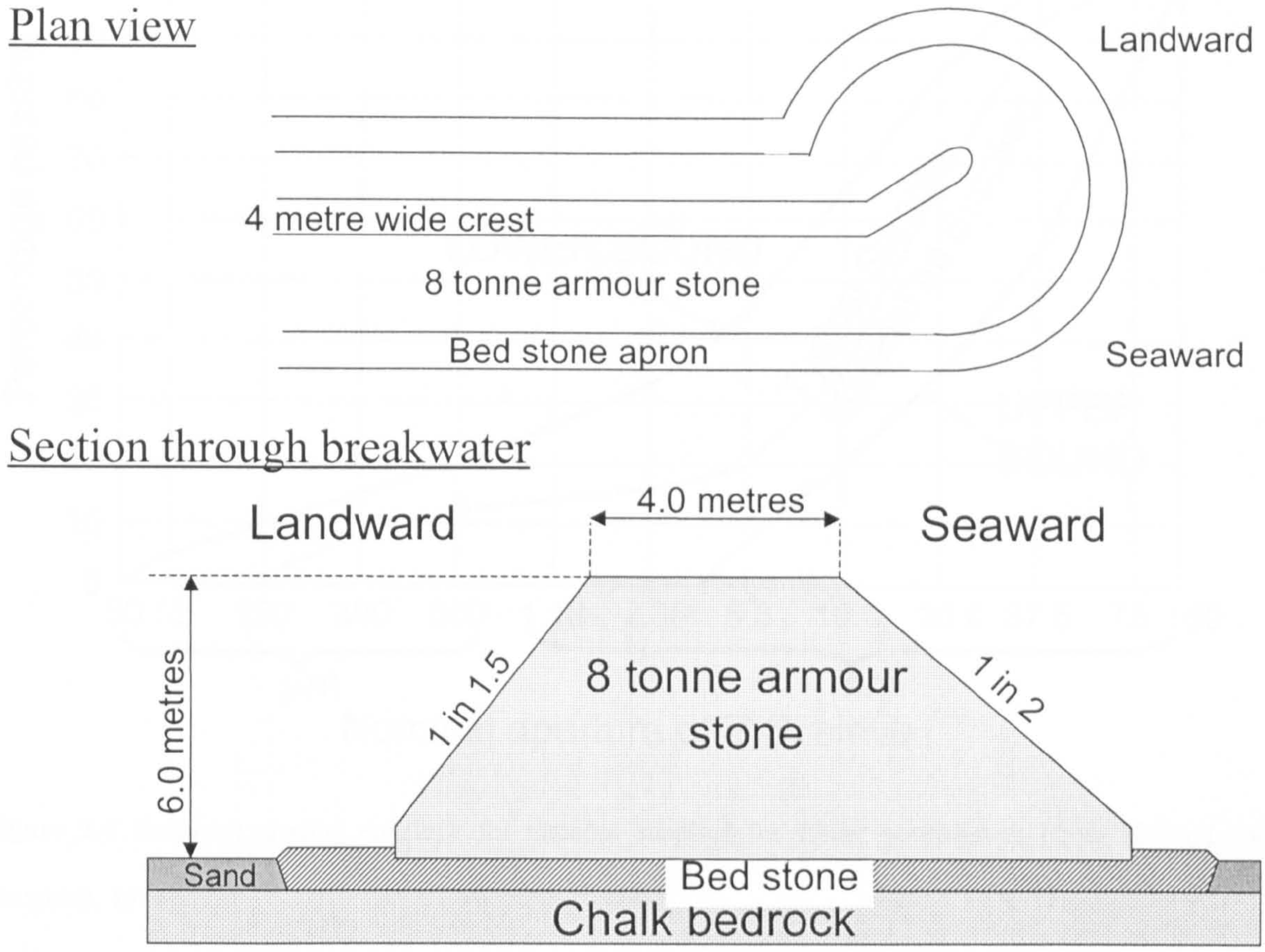

Figure 1-6 Schematic diagram showing plan and sectional views through a typical Elmer breakwater (after Holland and Coughlan, 1994)

Beach nourishment material was acquired from offshore dredging areas on the Owers Bank (approximately 10km south east of Selsey Bill), using bottom suction dredgers. This type of dredger was used to allow the finest material to be lost during the dredging, which allowed the material to fit the required grading curve. The design grading curve is presented as Figure 1-7. The material was transferred from the dredgers to split bottom barges 1-2 miles offshore. The barges then deposited the material at the site over high water. At the following low water, the material was initially pushed and later carried into position. The design requirement was for 139,000 m^3 of beach fill on the Arun Frontage, and 100,000m^3 along the NRA frontage (Holland and Coughlan,. 1994)

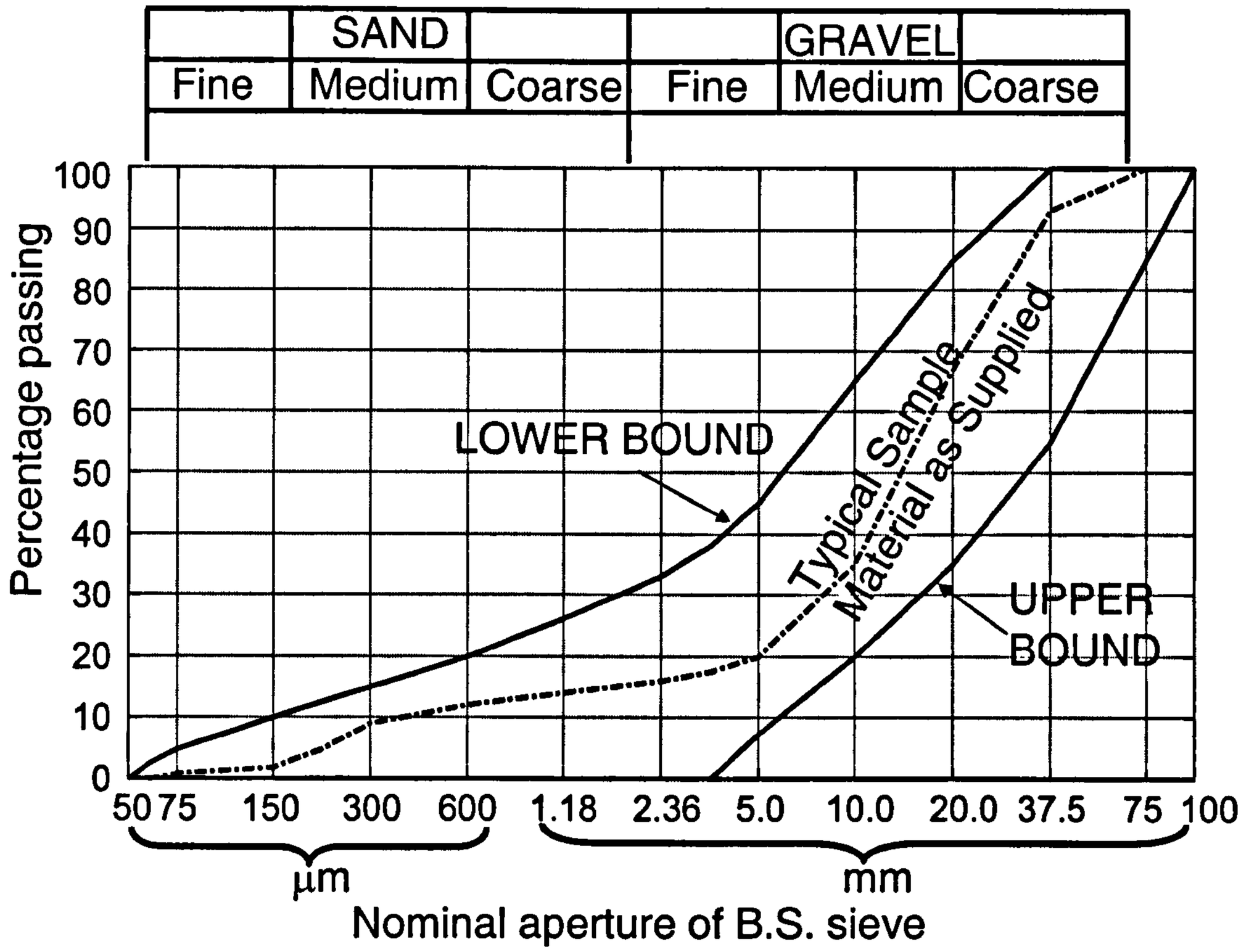

Figure 1-7 Sediment grading envelope for material supplied for Elmer nourishment (from Holland and Coughlan, 1994)

1.4 Beach development behind detached breakwaters

The work presented here was funded by the Engineering and Physical Sciences Research Council (EPSRC), by the Standing Conference on Problems Associated with the Coastline (SCOPAC), and by Arun District Council. The project was a collaborative venture between the civil engineering departments at the universities of Brighton and Plymouth. It involved experimental design to satisfy requirements for wave and morphological modelling, as well as data collection, processing and analysis.

The experiment consisted of a 14-month fieldwork period, in which directional wave recorders were deployed 700 m offshore of, and also shoreward of the detached breakwaters described in 1.3.3. Concurrent beach monitoring, involving aerial surveys for large-scale morphology change, and particle size analyses were also undertaken. A short period of current metering and float tracking was also included.

The author was responsible for the offshore wave recording, the organisation of the beach surveys and the current metering. He was also involved with the operation of an additional wave recorder deployed immediately seaward of the breakwaters, used to investigate their reflection performance. In preparing for these activities, he was also responsible for the operation of the pressure transducer array deployed at Felpham during the inter-comparison between wave recorders used in this study.

Offshore pressure data were processed to provide surface elevation data. This and the system calibration was performed by the author under the supervision of Dr. P.A.D. Bird. Directional analysis of both offshore and inshore wave data was performed by Ilic (1999).

Further analysis of wave and morphology data were carried out by the author. Evaluation of beach modelling techniques, and the use of empirical orthogonal functions to describe beach changes were also the author's work.

The next chapter discusses the existing literature on the prediction of beach development behind detached breakwaters.

2 Literature Review

This chapter describes previous use of detached breakwaters in a variety of environments. Theoretical requirements for understanding processes behind detached breakwaters are presented, in terms of wave theory and morphodynamics. Finally, modelling approaches intended to describe beach development at a variety of time scales are presented and discussed. Requirements for developing the existing knowledge are developed from this description.

2.1 Previous studies of breakwater schemes

Offshore breakwaters have been used for over a century to give shelter for harbours. For example the Plymouth (UK) breakwater, a rubble mound structure, was constructed in the middle of the 19th century. The application of detached breakwaters to the problem of beach protection is more recent. The earliest example is that constructed at Venice Beach, California, a single unit built close to the shoreline in 1905, to protect an alongshore amusement pier. Further single units were constructed at Santa Barbara, California (1929), to protect a harbour by sheltering the entrance, and by trapping longshore sediment to prevent siltation. The largest single such breakwater in the US is at Santa Monica, California. Constructed in 1934, it is 610 m long

Multiple units have been constructed to protect recreational beaches. The largest array of these is at Presque Isle, on Lake Erie, where 55 structures were placed along with a sand beach fill to protect an 11 km long sand spit. Chasten *et al* (1993) described US experience of detached breakwater design as limited, with only 21 projects, consisting of 225 breakwater units, existing in the United States and the Hawaiian Islands. Outside of the US, breakwaters have been employed and monitored in Israel (Nir, 1982), Italy (Liberatore, 1992), Spain and Denmark. Perhaps the greatest pool of experience lies in Japan, where at least 4000 breakwater segments have been constructed (Rosatti and Truitt, 1990).

U.K. sites are limited to Leasowe Bay, initially a single breakwater and the first such structure in the U.K. This was constructed in 1976 (Barber and Davies, 1985), and was studied by Copeland (1985), leading to the development of a mild slope equation-based wave propagation model, MSWAVE, to model the effect of the

structure on waves and wave induced currents. This site has since been developed further, and a photograph of the site in 1997 is presented in the previous chapter.

Other schemes have been built, or are under construction, at Happisburgh and Winterton (Pethick and Burd, 1993), at Monks Bay, on the Isle of Wight, and most recently, at Sidmouth in Devon. A scheme of eight breakwaters, fronting a replenished shingle beach at Elmer, West Sussex, is the subject of the study presented in this thesis.

Toyoshima (1976,1982) illustrates some of the problems associated with the use of these structures. Near Kaike in Japan, a beach had been accreting steadily until engineering works in a nearby river reduced the sand supply, causing the beach to erode. Initially groynes were used, followed by concrete wall, but both failed to protect the frontage or the beach. In 1966, a detached breakwater was proposed, and eventually constructed of tetrapods on a rubble core. This was successful in producing accretion behind it, but erosion was enhanced adjacent to it. This was countered by the construction of another three structures adjacent to the original. Eventually, by 1982, 11 such structures were required, protecting the entire frontage.

Part of the problem was the lack of beach fill placed with the breakwaters, which simply captured material from the adjacent beaches. Also, a potential problem with these structures can be the undesired formation of tombolos, which interrupt longshore sediment transport, as the breakwater, when joined to the shore behaves as a T-shaped groyne.

The Sidmouth scheme also experienced problems, described by Ingles (1996). The two breakwaters protected the renourished beach from wave attack from the south and west. A series of strong easterly winds however removed material from in front of the sea wall shown in the previous chapter, and moved it behind the breakwater. Beach levels dropped by 3 metres in front of the sea wall.

Macro-tidal environments and coarse beach material are common in the U.K., though rarely treated in models. Thus, there is a need to obtain design guidance for engineers to aid in the future design of schemes, and to establish the limits of applicabiliy of detached breakwater technology. The monitoring of detached breakwater schemes, the collation of data describing scheme performance, and the testing of engineering tools all help deliver this guidance.

2.2 Waves on beaches and around structures

2.2.1 Wave diffraction around structures

The diffraction of light waves around an object was discovered by the Italian Francesco Grimaldi (1618-1663), and was known to Newton. Despite not fitting Newton's 'corpuscular' theory of light, Newton did not see diffraction as a justification for a wave theory of light. Huygens, who believed in a wave theory, did not believe in diffraction. Fresnel was first to correctly apply Huygens principle of secondary wavelets to explain diffraction (Halliday and Resnick, 1978). Thomas Young described the phenomenon in terms of light waves, and was the first to realise that it was an edge effect.

For reflection to occur, the transverse dimensions of the reflector must be substantially larger than the wavelength of the incident beam. If this condition is not met, then the radiation will be scattered in all directions from it. This is diffraction. Two kinds of diffraction theory are employed in traditional optics - Fresnel diffraction and Fraunhofer diffraction. Fresnel diffraction is the more general solution, and occurs when the slit (or light source) and screen (on which the resulting pattern is displayed) are a finite distance from the diffracting aperture. Fraunhofer diffraction is a mathematically simpler special case of Fresnel diffraction. For this case, the screen is an infinite distance from the diffracting aperture, and thus wave fronts of diffracted waves are assumed to be parallel to the screen when they reach it, so there is no difference in phase over the area of the screen.

Traditional geometrical optics describes light in terms of rays. These rays are assumed to travel in straight lines (except when travelling through media of varying optical density), and energy is assumed to be conserved along a ray. This restriction precludes traditional geometrical optics from describing diffraction and scattering phenomena, and prevents the accurate description of energy levels along a ray in the region of a caustic, where rays cross. The advent of Maxwell's equations in the late 19th century, describing the wave motion of light in terms of an electromagnetic potential allowed Sommerfeld (1896) to develop a theory describing electromagnetic wave diffraction. It is this theory that has proved the basis of attempts to describe water wave diffraction, first by Lamb (1932), and then by Penney and Price (1952). The work by Penney and Price forms the basis of the current British Standard (British Standards Institute, 1984) technique for the calculation of wave energy diffracted around a breakwater arm in water of constant depth. The method described in the British Standard is only applicable for monochromatic waves.

In addition to the Penney and Price (1952) solution, Morse and Rubinstein (1938) gave an exact solution for the diffraction of sound and electromagnetic waves by a slit in an infinite plane. Carr and Stelzriede (1952) applied this solution to water waves. Diagrams based on this method are given in the Shore Protection Manual (Coastal Engineering Research Center, 1984) for waves diffracted by a breakwater slit.

In addition to these methods, Lamb (1932) published a solution for diffraction through a gap where the gap width (G) was much smaller than the wavelength (l) of the water waves. Lacombe (1952) derived an approximate solution based on Huygens' construction. Memos (1980) and Smallman and Porter (1985) have developed exact solutions for the diffraction of waves between two breakwater arms forming an angle. The table below gives the region of validity for each theory.

Lamb (1932)	Carr and Stelzriede (1952)	Penney and Price (1952)	Lacombe (1952)	Memos (1980)	Smallman and Porter (1985)
G/l<0.5	0.5<G/l<3	G/l>1	G/l>1	G/l>1	G/l>0.5

Table 2-1 Range of validity for diffraction theories, where G is the gap width, and l is the wavelength

Goda (1985) warns of the dangers of applying these diffraction diagrams in engineering situations, and proposes an extension to the Sommerfeld solution for the calculation of diffraction coefficients for random waves. Diffraction coefficients are non-dimensional parameters relating the wave height at a point in the diffracted region - or '*shadow zone*' - to the incident wave height. For a certain situation, values of Goda's diffraction coefficients are higher than those based on a monochromatic wave condition. The Goda method considers the directional spreading in the incident wave field, which allows greater energy penetration into the shadow zone. Monochromatic descriptions of wave diffraction give lower estimates of wave heights in the sheltered zone than are observed in the field.

Pos and Kilner (1987) used laboratory tests to study wave diffraction through a breakwater slit. They used monochromatic waves guided by splitter plates, and measured the wave heights before the diffracted waves had the chance to reflect from the walls of the tank by photogrammetry. By comparing the physical model results with numerical (mild-slope) model predictions, they were able to study the ability of the model to predict wave energy in the shadow zone.

They found that the numerical model underestimated the amount of energy in the shadow zones for large gap widths, and observed 'secondary waves' at the breakwater tips. They postulated that these were the mechanism by which wave energy is transferred away from the main axis of the slit. Diffraction is an edge effect, so it would be expected that waves travelling through the centre of the slit would be largely unaffected by the slit sides, and diffraction would only occur at the breakwater tips. This hypothesis is reinforced by the observation that as the gap width was decreased, these secondary waves coalesced to cover the entire gap width, giving circular wave fronts through the slit. Thus for narrow gap widths the slit behaves as a point source.

Further tests were done by Briggs *et al* (1995). They diffracted wave spectra around a single breakwater arm. They observed that, as predicted by Goda (1985), wave energy in the shadow zone is underestimated by monochromatic diffraction models. Additionally, they found that the directional spread of the incident waves was the most important parameter in deciding the energy in the breakwater lee.

2.2.2 Wave breaking and wave induced currents

Linear wave theory gives a relation between wave celerity and water depth. As a wave group propagates into shallower water, its velocity changes. To maintain a constant energy flux, as the group velocity is reduced, so the wave amplitude must increase. This leads to an increase in wave height with shoaling. If the wave front is approaching the beach obliquely, then Snell's law (which states that the ratio of the wave phase speed to the sine of the angle between the wave number vector and the shore normal is a constant) indicates that the wave must turn such that the wave fronts become more parallel to the shoreline. This is refraction. Both these processes lead to a change in wave height, which may be described simply in terms of refraction and shoaling coefficients. When the wave height grows to a certain proportion of the water depth, then wave breaking occurs, the water motion becomes more turbulent and mass transport is associated with the waves. The limiting ratio of wave height to water depth has been investigated by many researchers, and is usually taken to be some function of the offshore wave steepness, and the beach slope. Generally, it is accepted to lie somewhere in the range of 0.55 to 1.4 (Nelson, 1997). Once waves break, the energy associated with them is available to do work, as well as to dissipate through turbulence and viscosity.

It has long been known that oblique waves incident on a straight beach induce a longshore current. Putnam et al (1949) suggested that the magnitude of this current is related to the energy, or the momentum, of the

incident waves. The energy approach is a difficult one to model, due to the various dissipative mechanisms that exist. The momentum approach was described by Longuet-Higgins and Stewart (1962,1964). This approach is described below.

The concept of *'radiation stresses'* introduced by Longuet-Higgins and Stewart (1962) is analogous to the concept of thermal wind, or radiation pressure, that is known in electromagnetic radiation. Lamb (1932) described the momentum associated with surface waves. The magnitude is proportional to the square of the wave height, and the direction is the same as the direction of wave motion. If a wave is reflected, then the direction of the momentum vector is changed, and so a force must be exerted on the reflector. The term *radiation stress* was adopted, rather than *radiation pressure*, as the stress term does not imply that the forces are distributed evenly throughout the domain of interest.

The detailed derivation of the radiation stress terms are given in Longuet-Higgins and Stewart (1962), while a more descriptive derivation is presented in Longuet-Higgins and Stewart (1964). The reader is referred to these papers for details of the derivation. This section of the review describes the implications of radiation stress theory for the case of waves on a beach with detached breakwaters.

The momentum flux tensor S_{ij} parallel and perpendicular to the direction of wave propagation is given by

$$S_{ij} = \begin{bmatrix} E\left(\frac{1}{2} + \frac{2kh}{\sinh 2kh}\right) & 0 \\ 0 & E\frac{kh}{\sinh kh} \end{bmatrix}$$

Equation 2-1

, where E is the wave energy density, given by

$$E = \frac{1}{2}\rho g a^2$$

Equation 2-2

and k is the wavenumber vector, h the water depth, ρ the water density, g acceleration due to gravity and a the wave amplitude.

Consider waves approaching normal to a beach. The radiation stress gives a horizontal transfer of horizontal momentum. Assuming that the wave input is constant, then the rate of momentum transfer is also constant. E

in Equation 2-2 is a function of the wave amplitude which, after breaking decreases as h, the water depth decreases. This leads to a variation in the radiation stress. Looking at the flux of horizontal momentum entering shallow water, the mean water level $\overline{\zeta}$ can be shown to vary with the change in radiation stress:

$$\frac{d\overline{\zeta}}{dx} = -\frac{1}{\rho g h}\frac{dS_{11}}{dx}$$

Equation 2-3

This equation shows the variation of the depth-integrated mean pressure gradient with the gradient of the radiation stress. This equation can be integrated to show the set down in mean sea level that increases towards the breakpoint, and the set up of the mean water surface towards the shoreline shoreward of the breakpoint. This shoreward setup is important, as it can cause a rise in the sea level up to 40% of the rms incident wave height.

Where the waves approach obliquely to the beach, there is a component of the momentum flux in an alongshore direction as well as in the cross shore. It can be shown that the momentum flux into the surf zone is proportional to the energy flux. The local stress in the surf zone is proportional to the wave energy dissipation rate. The combination of the tangential bottom stress (due to the wave orbital motion and a small mean flow) gives a mean stress in the alongshore direction. Longuet-Higgins (1970a, 1970b) demonstrated that the resulting current velocity was proportional to the longshore component of the wave orbital velocity, and that this velocity was a maximum at the break point. By including the effects of horizontal mixing, the maximum in the velocity distribution was shifted shorewards, and the zone of flow broadened in the cross-shore direction.

Behind a detached breakwater, there is an alongshore difference in wave height, due to diffraction. This leads to a difference between the wave set up behind the breakwater (in the shadow zone) and the set up away from the breakwater. This difference in water level results in a longshore current into the shadow zone. Oblique wave fronts of the diffracted waves also contribute to this current. Where a breakwater is shore parallel, with similar diffraction occurring at its other tip, or an obstruction along its length, then this flow into the shadow region must be balanced by a return flow. This return flow is observed in physical and numerical models to join up with the incoming flow, such that a gyre forms behind each half of the breakwater. The width of the return flow is observed in the field and laboratory tests to be narrow and energetic. At present, this is difficult to reproduce in numerical models, which tend to represent the return flow as a broader feature.

The description given above presents a simple picture of wave induced currents as steady phenomena, driven by a constant energy flux. Given that the forcing of these currents is by random waves, the currents themselves are not steady. Along a straight beach with a 'steady' longshore current, meanders form which propagate downstream. These features are observed as a fluctuation of the current observed on the beach - possibly periodic - and so this may be considered as wave like behaviour. These features have been termed shear waves. Also, these descriptions only give depth integrated descriptions of the flow, and take no account of the effects of undertow or the internal beach hydraulics.

Behind detached breakwaters (or diffracting groynes) the return flow does not always form a simple gyre. Intermittent bursts of current have been observed in tank tests, transporting water and also sediment offshore of the breakwater. Recent laboratory tests by Ilic (pers. comm.) found only a single gyre on the shoreward side of a detached breakwater in physical model tests. Recent work by Peregrine and Bokhove (1998) on wave propagation across a broken bar suggest that vorticity effects may lead to the generation of mean flows within the surf zone.

2.2.3 Wave modelling

The previous section described wave transformation from deep water to the shoreline, and introduced the processes that need to be understood for the confident description of hydrodynamics around detached breakwaters. This section describes techniques for modelling wave conditions in the near shore zone, given a certain offshore wave condition, however that condition has been obtained. The simple technique of ray tracing is presented, as is wave transformation modelling based on the mild-slope equation. The section then briefly reviews techniques for modelling waves in the surf zone, and methods for calculating the hydrodynamics necessary for input into morphological models.

Ray tracing

This is perhaps the simplest method for describing wave transformations. It makes use of the analogy between water wave propagation and geometrical optics. It uses wave-averaged energy conservation derived from the basic equations integrated over depth and averaged over a wave period. Snell's law can be used to describe wave refraction, while changes in wave height due to refraction are interpreted in terms of the spacing of wave *rays* (orthogonals to the wave front). The constant energy flux assumed to exist between two adjacent rays means that as ray spacing increases, the wave height decreases, and vice versa. Height changes

due to shoaling are calculated in terms of a shoaling coefficient (the square root of the ratio of the offshore to inshore group velocity), while those due to refraction are calculated using a refraction coefficient. Additional parameters may be added to represent bottom friction, and also to approximate wave diffraction around structures (e.g. Kraus, 1984).

The simplicity of the technique has led to its use for many years. Johnson *et al* (1948) published guidance as to how to manually construct refraction diagrams. Numerical methods are also used. The ray tracing programs INRAY and OUTRAY are commercially available from HR Wallingford Ltd, and a ray tracing approach is used as the internal wave model in the morphology model GENESIS (Hanson, 1989).

A limitation to this simple view of wave modelling is that it allows the formations of caustics. When wave rays are focussed, for example by means of a circular shoal, the rays converge towards a point, leading to estimates of very high - potentially infinite - wave heights. These results are physically incorrect, as energy would be transferred away from the caustic point, for example by wave breaking and by diffraction. In numerical models that rely on this approach, infinite wave heights may not be achieved at a caustic due to *numerical diffraction*, in reality a diffusion of energy due to the resolution and characteristics of the numerical scheme.

This approach to wave modelling is linear, so spectral wave representations may be made by modelling a range of wave frequencies and directions, and summing the result. Goda (1985) presents guidance as to how to calculate effective refraction coefficients for a spectral representation.

Mild - slope equation

Berkhoff (1972) developed a combined refraction/diffraction equation for wave propagation, based on the assumption of irrotational flow in the equations of wave motion. This assumption allows the use of a velocity potential that satisfies Laplace's equation:

$$\nabla^2 \varphi = 0$$

Equation 2-4

where ∇ is the gradient operator, and φ is the velocity potential. Assuming a rigid and impermeable bottom and linear free surface boundary conditions allows a vertically integrated model describing wave propagation to be derived. Wave energy flux is not conserved along rays, allowing the model to be used in areas with significant diffraction. This model is only approximately valid if the bottom is not horizontal. It does

however give a good approximation for bottom slopes of up to 1 in 3 - hence its name- the 'mild-slope' equation. It has the following form:

$$\frac{\partial}{\partial x}\left(G\frac{\partial \Phi}{\partial x}\right)+\frac{\partial}{\partial y}\left(G\frac{\partial \Phi}{\partial y}\right)+k^2 G\Phi=0$$

Equation 2-5

where k is given from the dispersion relation, and G is given as follows:

$$G=g\frac{\frac{1}{4}\sinh(2kh)+\frac{1}{2}kh}{k(\cosh(kh))^2}$$

Equation 2-6

A parabolic approximation to the equation, proposed by Radder (1979) does not allow waves to propagate in the negative x direction (therefore no reflection can take place). Also, wave diffraction is limited to the effects along a wave front (or a line of equal phase), while that due to a curvature in wave amplitude (in the direction of propagation) is neglected.

Elliptic solutions of Equation 2-5 (such as Copeland, 1985; Madsen and Larsen, 1987; Li and Anastasiou, 1992) allow the incorporation of reflection effects. Also, being a linear model, superposition of results from different frequencies and directions can be used to estimate spectral wave transformations.

Surf zone models

Hamm, *et al* (1993), in their review of wave transformations, recommended that wave modules in morphodynamic models should be kept as simple as possible, due to the need to update the wave model due to changes in bathymetry, sea level and wave climate. They do however recommend that modellers consider the directionality and randomness of the wave field, the refraction of waves by currents (especially in areas of horizontal shear) due to structures, river mouths and tidal inlets. Additionally, they claim that energy dissipation, non-linearities due to uneven topography, and low frequency (infra-gravity) waves need to be modelled accurately. The models described in the previous section do not meet all of these requirements, and much work has been undertaken in the modelling of waves in the surf zone - which is the area where the sediment transport that we are interested in takes place, and also the place where non-linearities , energy dissipation, low frequency motions and shear currents become important.

This section briefly describes bore models and Boussinesq models which, although initially used to describe wave propagation up to breaking, can provide a description of wave motions in surf zone, including interactions with currents. Cnoidal wave theory may be used to describe the propagation of waves after breaking. For a description of this approach to wave modelling, the reader is referred to Svendsen and Brink-Kjær (1973).

Bore models

Bore models describe the motion of waves after breaking as they propagate across the surf zone. The wave is assumed to propagate as a translatory wave (bore or hydraulic jump). Models are based on the depth-averaged, inviscid, shallow water wave equations, and the bore is modelled as a discontinuity in the water elevation. Along the bore, mass and momentum are conserved. These conditions assume there is a surf zone for the bores to propagate across, and that the beaches are of 'small' slope - although bore models have been used to describe wave run up on rough slopes (Kobayashi *et al*, 1989) and on shingle beaches (Chadwick, 1991). The models are limited to use in the inner surf zone, after wave breaking is complete, as the non-linear shallow water equations predict the steepening of the front face of a wave, but cannot realistically predict the location of wave breaking. The lack of frequency dispersion in the non-linear shallow water equations also restricts bore model use to very shallow water.

Boussinesq models

Boussinesq equations are an attractive alternative to the non-linear shallow water equations, as they incorporate frequency dispersion, and can be applied to a much wider wave spectrum, and to larger coastal areas (Madsen *et al*, 1997). While wave breaking is not automatic in Boussinesq models, it can be introduced through the use of limiting steepness criteria and dissipation mechanisms.

The time domain approach of Schäffer *et al* (1993), extended in Madsen *et al* (1997), allowed the study of wave transformation through the surf zone to the run up limit. In addition, wave breaking, decay, surf beat and wave induced currents generated in the model were evaluated.

The principle restriction of Boussinesq equations is their water depth limitation. Madsen *et al* (1991) state that the worst forms of the equations break down for a depth to deepwater wavelength ratio of larger than 0.12. The derivation presented by Madsen *et al* (1991) introduces a modification to the wave celerity term,

which improves the model performance in deeper water. The authors claimed that the modification extended the applicability of their model to a depth-to-deep water wavelength ratio of 0.6, although Madsen and Sørensen (1992) showed that the model limit over uneven topography was a ratio of 0.5.

2.3 Sediment transport and beach morphology

2.3.1 Morphology changes

In deterministic morphology modelling, it is assumed that beach changes occur due to sediment transport forced by the interaction of various hydrodynamic phenomena. Classically, sediment transport is considered to move as *bed load* and, if fluid turbulence is sufficient, as *suspended load*. Bed load transport occurs where material is relatively coarse, and shear stresses are relatively small. Grains are assumed to move in a thin layer close to the bed, by rolling, gliding or jumping (saltating). Where material is coarse and shear stresses are large, then this transport takes place in several layers above the bed, and there is *sheet flow*. Where lift forces due to turbulent eddies are greater than the settling velocity of particles, sediment may be held in suspension and transported without being in contact with the bed. This is *suspended load* transport. Figure 2-1 shows the boundaries between different modes of transport for a range of grain sizes, under a range of friction (shear) velocities. The shear velocity is related to the bed shear stress by Equation 2-7, where τ_0 is the bed shear stress, and ρ is the fluid density.

$$u_* = \sqrt{\frac{\tau_0}{\rho}}$$

Equation 2-7

To model this behaviour, it is necessary to describe the transport either in terms of the bed load and suspended load components ('*total-load*' models), or to simply assume a relationship that relates the total volume of material transported to some fluid behaviour, without detailing the mechanisms that move the material ('*bulk energy*' models).

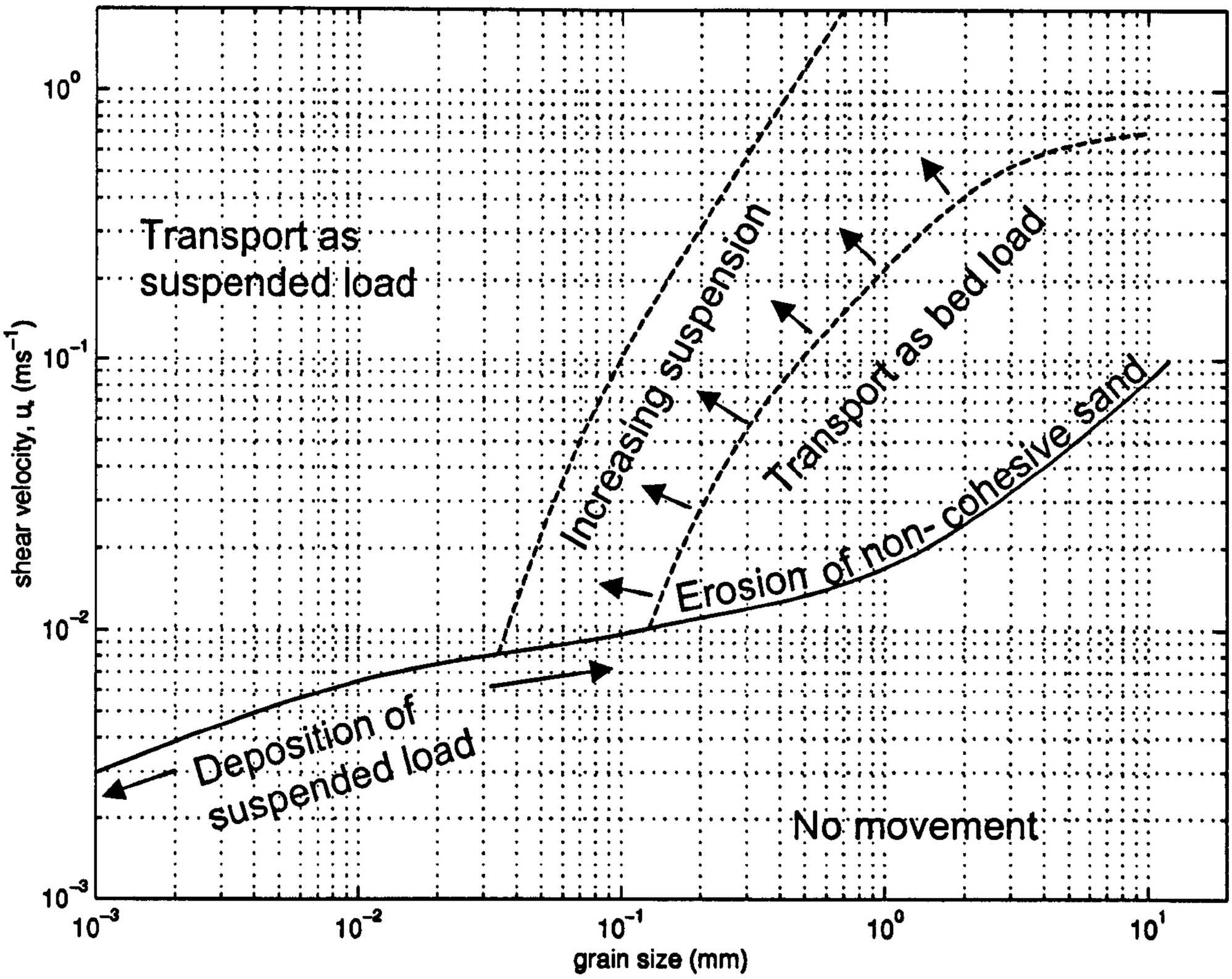

Figure 2-1 Threshold curve for sediment movement, with transition between bed load and suspended load indicated. (after Open University, 1989)

2.3.2 Bulk Sediment Transport Equations

Early attempts to estimate longshore sediment transport rates were based on the assumption that it is proportional to wave energy flux. Munch-Petersen (1938) proposed

$$Q_S = K_1 E_o \cos\alpha_o$$

Equation 2-8

Q_S is the *volumetric* sediment transport rate. E_o and α_o are the deep water wave energy density and direction respectively. K_1 is some constant. This approach developed steadily. Of particular note in the equation of Komar and Inman (1970), which is expressed in the form

$$I_1 = KP_1$$

Equation 2-9

I_l is the 'immersed weight' transport rate, and is related to Q_s by the following:

$$I_1 = (\rho_s - \rho)g(1-p)Q_S$$

Equation 2-10

'ρ_s' and 'ρ' are the sediment and fluid densities respectively. This is related to weight by 'g', the acceleration due to gravity. The effect of interstices between the sediment grains is represented by a porosity term 'p'. This conventionally is given a value of 0.4. P in Equation 2-9 is the 'wave power' in the alongshore direction. Equation 2-9 was adopted by the US Army Corps of Engineers, and is generally referred to as the CERC equation.

In addition to the '*bulk estimators*' based on the approach described above, there are also a range of '*total load*' models for estimating sediment transport. These describe the total transport in terms of the sum of different modes of transport - generally separate bed load and suspended load components. Kamphuis *et al* (1986) describe these as 'shear stress modification' methods. These models are frequently developments of methods for estimating transport rates in fluvial environments.

The Bijker (1971) method is a good example of the total load approach. This uses a current velocity distribution, which is then coupled to a unidirectional bed load transport model (based on Frijlink, 1952) and also to a suspended load model (based on Einstein, 1950). The shear stresses resulting from the estimated velocity distribution is modified to account for wave action, and also the presence of bedforms, before being used in the transport calculations. Similar approaches have been proposed by, among others: Swart (1976), using a modified Engelund and Hansen (1967) approach; by Walton and Chiu (1979) using a modification to Bagnold's (1966) expression; and Swart and Fleming (1980), using a modified Ackers and White formula. Bailard (1981) also proposes a total load transport model based on the energetics approach (Inman and Bagnold, 1963; Bagnold, 1966).

These approached require some assumption of the bed roughness, to generate reasonable levels of turbulence to maintain the suspended load. This in turn requires knowledge of the bed, and the presence or absence of ripples. There are usually further assumptions regarding the nature of the fluid flow. Kamphuis *et al* (1986) suggest that the more complex formulations are of use when looking in detail at transport mechanisms - either under controlled conditions, such as in a laboratory, or for short periods, when bed and flow conditions are assumed to be unchanging. Over longer spatial or temporal scales, averaging of model input conditions

becomes necessary, and removes the advantage that these methods hold over the simpler '*bulk energy*' approaches.

The simplicity of the 'bulk energy' approaches encouraged further development, and the introduction of terms to extend the limits of applicability. Osaza and Brampton (1980) introduced a second term to represent the influence of wave height gradients – improving the estimates of transport behind diffracting structures. Hanson and Kraus (1989) adopted this method in the one-line model GENESIS. Their equation is as follows:

$$Q = \left(H^2 Cg\right)_b \left(a_1 \sin 2\alpha - a_2 \cos\alpha \frac{\partial H}{\partial x}\right)_b$$

Equation 2-11

where the two coefficients a_1 and a_2 are defined thus:

$$a_1 = \frac{K_1}{16\left(\frac{\rho_s}{\rho} - 1\right)(1-p)1.416^{\frac{5}{2}}}$$

Equation 2-12

$$a_2 = \frac{K_2}{8\left(\frac{\rho_s}{\rho} - 1\right)(1-p)(\tan\beta)1.416^{\frac{5}{2}}}$$

Equation 2-13

K_1 and K_2 are calibration values. ρ_s and ρ are densities of sediment and water, p is sediment porosity, $\tan\beta$ is the average bottom slope from the shoreline to the depth of longshore transport. The factor of 1.416 converts from significant to root-mean-square wave height.

Kamphuis (1991) developed a formula based on a series of controlled laboratory tests. The formula predictions were then compared with field data. This formula was found to under predict slightly for gravel sized particles:

$$Q_I = 1.3\times10^{-3}\rho\left(H_s^2 T_p^{1.5}(\sin 2\alpha)^{0.6}\right)_b d_{50}^{-0.25}(\tan\beta)^{0.75}$$

Equation 2-14

Q_I is the immersed mass transport rate, in kg/s, and the subscript b refers to the condition at the breakpoint.

Kamphuis (1994) modified this formula to include a term that allows for variation in longshore wave heights. In this revised version, the 'sin' based angle term is replaced with:

$$\left[\sin 2\alpha_b - \frac{K_1 \cos\alpha_b}{\tan\beta}\frac{\partial H_{sb}}{\partial x}\right]$$

Equation 2-15

where K_1 is a weighting coefficient with a value of between 1 and 2.

In addition to this formula, Chadwick (1989) proposed a modification to the CERC formula for use with coarse sediment based on the developments of Brampton and Motyka (1985), van Hijum and Pilarczyk (1982) and a field study on the south coast of the UK. This is of the form:

$$Q = \frac{K}{\left(\frac{\rho}{\rho_s}-1\right)\left(\frac{1}{1-p}\right)}\frac{\left(H_{rms}^2 Cg\sin 2\alpha\right)_b}{16} - P_o$$

Equation 2-16

P_O has a value of 12.2, p is the voids ratio (set to 0.47) and K has a value of 0.0384.

There have been various exercises evaluating sediment transport predictors. Van de Graaff and van Overeem (1979) reviewed the various available formulae. Due to a lack of reliable high quality laboratory or field data on longshore sediment transport, they were forced to compare the predictions of the various models with those of the CERC formula (which had previously been extensively validated). They found that Bijker's formula (1971) provided a better fit to the validation data than the Ackers and White (1973), the modified Ackers and White (van de Graaff and van Overeem, 1979), or Engelund and Hansen's (1967) formulae. Fleming *et al* (1986) evaluated 10 bulk transport predictors with field data collected in the C2S2 study. The Davies and Kamphuis (1985) model performed better than the CERC or the Acker's and White (1973) formulae. Osaza and Brampton (1980) have made use of a modified form of Komar and Inman's (1970) 'Scripps' equation.

Schoonees and Theron (1994) compared the accuracy of bulk transport formulae against an extensive database of field sediment transport rates from literature sources. This showed that the Kamphuis (1991), van Hijum and Pilarczyk (1982) and Chadwick (1991) formulae gave the best fit to field data over a wide variety of grain sizes.

2.3.3 Macro-tidal beaches

The eastern English Channel is a macro-tidal environment. In macro-tidal environments, the beach morphodynamic states are expected to change with the tidal water level (Wright *et al*, 1982). This would be

expected as the break point will move offshore with lowering water levels (for a constant wave height), and with a $y^{2/3}$ type beach profile, the surf zone will widen as the break point moves further offshore than the run-up limit. This section describes the differences in behaviour expected of a macro-tidal beach compared to those in micro- and meso-tidal areas.

The dynamics of natural macro-tidal beaches have been studied by, for example, Wright *et al* (1982), Jago and Hardisty (1984) and Davidson *et al* (1993). Wright *et al* (1982) commented on the lack of rhythmic and aperiodic longshore features in the beach topography of Cable Beach, Australia, which experiences a 9 m spring tidal range. The only features observed on an otherwise featureless site were beach cusps, which appeared intermittently at the limit of the high water swash zone. They postulated that this absence of features may be due to the need for a 'spin up' time to allow long period (surf beat) induced phenomena to influence the topography. Jago and Hardisty (1984), studying a beach in south west Wales, also observed a lack of rhythmic topography. They observed that the narrow surf zone at high water associated with plunging breakers produced asymmetric flows in the swash zone, leading to steeper beach gradients than observed at low water, where the beach was more dissipative and swash zone flows were more symmetrical. Davidson et al, working on Spurn Head, a spit on the North Sea coast of the U.K., observed a marked asymmetry in transport processes between the flood and ebb tides, with highest levels of suspension and transport associated with offshore transport on the falling tide.

In an attempt to understand the reason for the simple topography observed on macro-tidal beaches, Fisher and O'Hare (1996) used a simple, energetics based empirical model that investigated the influence of the flow asymmetry structure observed by Davidson *et al* (op. cit.) on the cross shore bed topography. The varying tidal level acted to prevent the formation of a well defined bar. This model was sensitive to tidal range, with greater ranges leading to a smoother beach profile.

2.4 Modelling beach changes around structures

The previous section described the processes that lead to changes in beach topography, on natural beaches and in the vicinity of structures. It also described the expected influence of a macro-tidal environment on beach profile development. This next section describes modelling techniques used to attempt to describe these processes at various time and length scales.

Models provide an understanding of the physical processes governing a particular environmental problem and form an approximation of reality that allows their use by engineers with less experience of a problem than the model designer (Thompson, 1992). This section presents and discusses the components of shoreline development models, with particular reference to the problem of predicting shoreline changes in the vicinity of offshore breakwaters.

2.4.1 Geometrical plan shape models

Hsu and Silvester's (1990) approach describes the equilibrium shoreline behind a single detached breakwater under direct (normal) wave attack. The equilibrium plan form is that shape of beach that is in equilibrium with incident wave conditions such that no net littoral transport takes place. The model is empirical, based on both laboratory and field data, and predicts a parabolic shoreline. The shape of this shoreline is based on the ratio of the distance from the original shoreline to the centreline of the breakwater, to the breakwater length. No details of the wave field, beach properties or wave transmission effects are taken into account.

The origin of this work is in the study of natural bays bounded by rocky headlands. It was observed (Yasso, 1965) that many bays bounded by rocky headlands have a half-heart shape. Silvester (1970) showed that a logarithmic spiral of the form $R_2/R_1=e^{\theta \cot \phi}$ (where R_1 and R_2 are two radii of the spiral, separated by an angle of θ radians; cot is the cotangent; ϕ is the angle the radius makes with a tangent to the curve) fits the equilibrium plan form of many beaches.

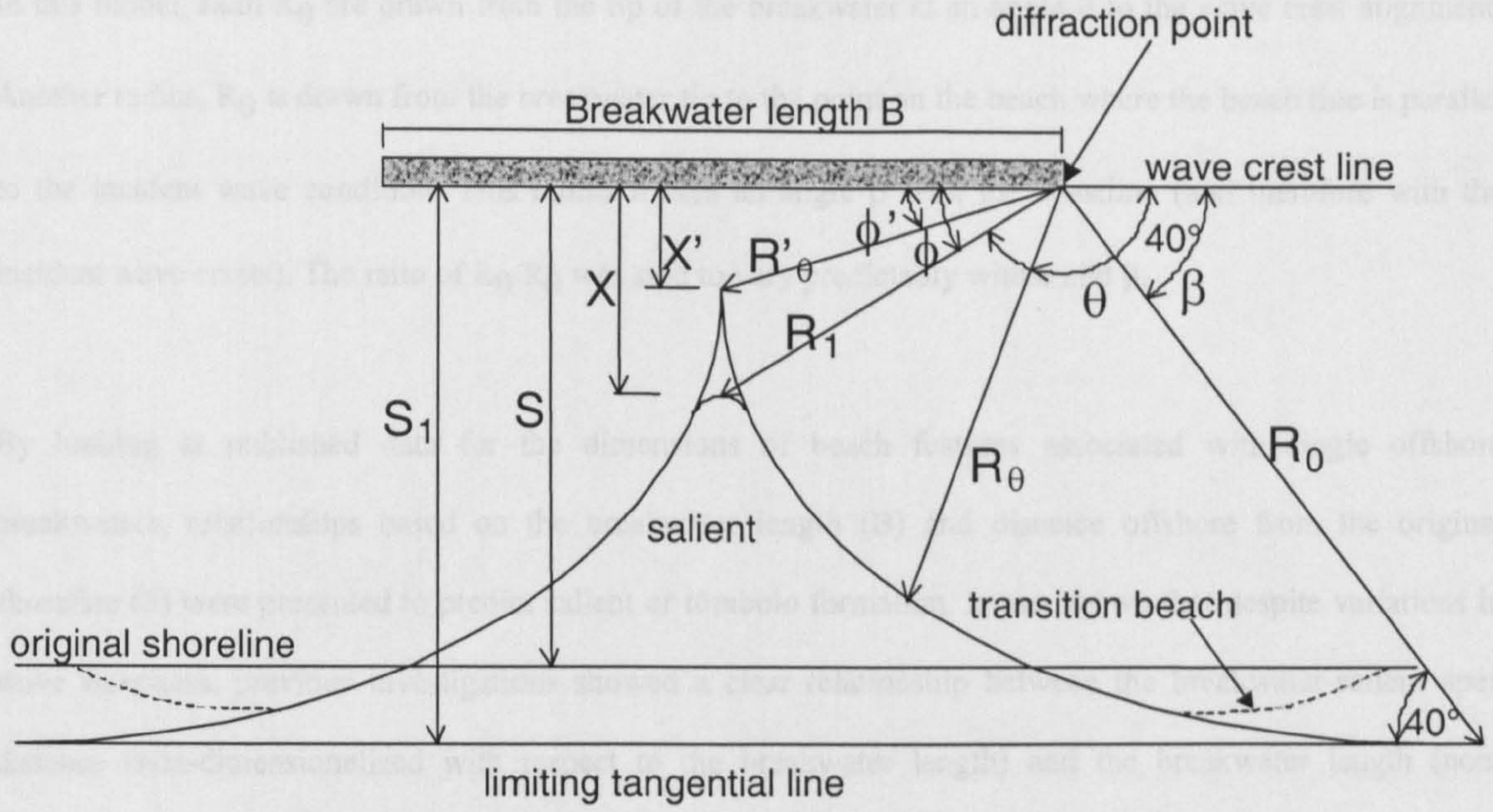

Figure 2-2 Definition sketch of breakwater and salient parameters, after Hsu and Silvester, 1990

Sketch notation is as follows:

ϕ Angle between breakwater line and salient apex, measured from the diffraction point

ϕ' Angle between breakwater line, and theoretical intersection point of the bay curves, measured from the diffraction point

β Angle between wave front and R_0

θ Angle between radii from diffraction point to shoreline, and the incident (undiffracted) wave front

B Breakwater length

R_0 Radius length from tip of breakwater at $\beta=40°$ to incident wave crest or bay limit

R_θ Radius length from tip of breakwater to shoreline, at an angle θ to the incident wave crests

R_1 Radius length from the breakwater tip to salient apex (on the breakwater centreline)

R_θ' Radius length from the breakwater tip, to the intersection point of the theoretical shoreline curves

S Distance from breakwater to original shoreline

S_1 Distance between the breakwater and the limiting tangential line of the final shoreline

X Distance of salient apex from breakwater

X' Distance between breakwater and intersection point of the theoretical shoreline curves

Work by Hsu *et al* (1987) showed limitations in the spiral shape model for sections of the beach downcoast from the headland. Instead, a parabolic form was derived for a bay in static equilibrium. This model is applicable to bays occurring adjacent to offshore breakwaters, although only for waves of normal incidence.

In this model, radii R_θ are drawn from the tip of the breakwater at an angle θ to the wave crest alignment. Another radius, R_0 is drawn from the breakwater tip to the point on the beach where the beach line is parallel to the incident wave condition. This radius makes an angle β with the coastline (and therefore with the incident wave crests). The ratio of R_θ/R_0 was said to vary predictably with θ and β.

By looking at published data for the dimensions of beach features associated with single offshore breakwaters, relationships based on the breakwater length (B) and distance offshore from the original shoreline (S) were presented to predict salient or tombolo formation. It was shown that despite variations in wave steepness, previous investigations showed a clear relationship between the breakwater-salient apex distance (non-dimensionalized with respect to the breakwater length) and the breakwater length (non-dimensionalized with respect to the initial breakwater-shoreline distance). It was suggested that wave steepness would only affect the rate at which the salients formed, as previous tests showed similar planforms developing, despite different wave steepness for each test. From the data presented, tombolos were predicted to form when the ratio of S/B was between 1.33-5.21.

Laboratory tests in a spiral wave basin by Suh and Dalrymple (1987), on both single and multiple offshore breakwaters, were used to examine the importance of the breakwater length, spacing and offshore distance. In addition to these tests, they presented an extensive review of previous experiments in both laboratory and field. In the tank tests, it was found that when breakwaters are separated by a gap more than twice the wavelength of the incident waves, the shoreline behind the structures behaves as if the breakwaters are single units - the coastline taking on a log-spiral type form. As the gap was reduced, an elliptic shoreline developed in the embayments, with the ellipses centred on the midpoints of the gaps. Differences between laboratory experiments and field examples were also observed, with salient growth being greater in the field.

Further work was presented by McCormick (1993), who used the same field data set to determine a parametric relationship to describe the shoreline position in terms of bed slope, and wave conditions. An elliptic (rather than parabolic) shoreline plan was chosen, based on photographs presented in Dally and Pope (1986). The ellipses were defined as having centres along the longshore axis at an offshore distance in line with line of the breakwaters. The model was derived for normally incident waves, and then extended to allow for non-normal wave attack. In order to apply the model to multiple breakwaters, the value of the 'semi-gap width' is required (this is equal to half the distance between two adjacent breakwater tips). If this value is

greater than the distance from the breakwater gap to the theoretical centre of the ellipse, then the breakwaters can be considered to be independent, and can be treated as single units. After using physical model data to develop the model, it was applied to an array of 11 offshore breakwaters situated at Bay Ridge, Maryland, USA.

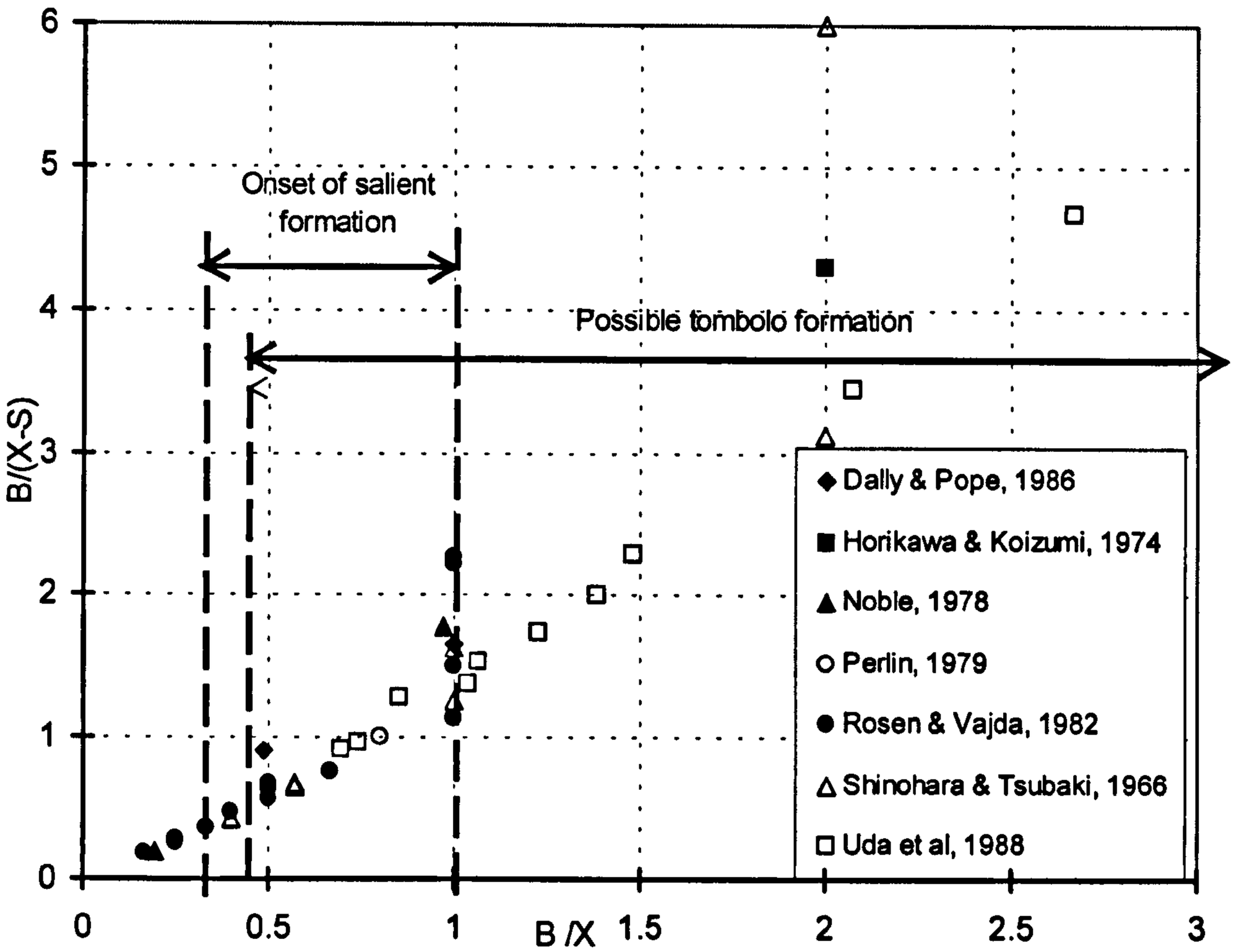

Figure 2-3 Tests showing salient lengths and offshore distances for single detached breakwaters, after Hsu and Silvester (1990)

2.4.2 One-line models

The one-line, or 1D, form of coastline model calculates shoreline change as a function of the alongshore direction. In order to do this, it must be assumed that the beach profile remains constant and unchanged - it simply moves on or offshore as the coast erodes or accretes. Obviously this type of model cannot predict changes based on cross-shore sediment transport, although it is useful in predicting the long-term evolution of a beach.

Principle Parameters

In its simplest form, the one-line model solves the 1D conservation of mass equation and the 1D equation of motion. This was first done by Pelnard-Considère (1956), who combined the equations to form a diffusion type equation, where the parameter A represents wave and sediment characteristics, y is the cross shore beach position, x is the longshore ordinate, and t represents time.

$$\frac{\partial y}{\partial t} + A\frac{\partial^2 y}{\partial x^2} = 0$$

Equation 2-17

This formula was coded by Perlin and Dean (1978), who compared Pelnard-Considère's analytical solution of the equation for sediment bypassing a groyne with two different numerical solutions- one implicit and one explicit. They also compared the results to those obtained with a two-line model. Hanson (1989) gives the following expression for the continuity of sand:

$$\frac{\partial y}{\partial t} + \frac{\left(\frac{\partial Q}{\partial x} + q\right)}{(D_B + D_C)} = 0$$

Equation 2-18

where Q is the longshore sand transport rate (in m^3/s); q is a term to describe any line sources or sinks of sand in the alongshore direction; D_B is the average berm height above mean sea level and D_C is the depth of closure. The sum (D_B+D_C) is termed the active beach height, and represents the vertical distance over which the longshore transport occurs (in the timescale of the simulation).

This type of model has been applied to describe shoreline position in hypothetical and prototype cases. Leblond (1972) produced a model to predict the plan shape of headland bays. This model predicted a logarithmic spiral shape beach plan, fitting the observations of Silvester and Ho (1972). Matsuoka and Ozawa (1983) applied a simple one-line model to laboratory tests, as well as to the problem of predicting actual beach response to the detached breakwaters. They applied their model to the first detached breakwater built at Kaike (an area with simple bottom topography) and to an array of three structures built at Nishiki (an area with complex offshore bathymetry). The one-line technique was used to model shingle beaches by Brampton and Motyka (1985). One-line models are available in most coastal engineering model suites (for example, GENESIS, within the US Army Corps of Engineers Shoreline Modeling System, within LitPack, from the Danish Hydraulics Institute, and UNIBEST, from Delft Hydraulics). GENESIS, LitPack and

Unibest solve the one-line equation for shoreline change in different ways. Unibest (UNIform BEach Sediment Transport) initially calculates the along shore and cross shore distribution of longshore sediment transport due to waves and tidal currents, in the Unibest LT module. It does this using a linear wave refraction model. Non-linear processes (wave breaking and bottom friction) are taken into account, and wave decay in the surf zone is modelled assuming random waves over an arbitrary beach profile. Wave diffraction effects are not taken into account. Water level changes, including wave induced set up and set down are included, and sediment stirring, through wave breaking, and sediment-flow interactions are also represented. These calculations are done for each grid point along, and across, the modelled shoreline, while the sediment transport capacity is calculated using a choice of five different transport formulae. By changing the wave and current conditions, and the shoreline orientation, a set of 'coastal constants' is obtained, which define the longshore transport rates for each coastal orientation. This 'coastal constant' is then input into the coastline change module, Unibest-CL.

Unibest-CL calculates the shoreline development, based on the computed coastal constants, taking into account the change of transport rate according to:

- changes in coastal orientation
- blocking of the littoral drift, (for example by a groyne or headland)
- fixing the coastline position with a seawall
- sediment sources and sinks
- variation in wave energy along the coast

Litpack ('LITtoral Processes And Coastline Kinetics') is a similarly modular system. Initially, the cross shore distribution of wave height, setup and longshore transport is calculated for an arbitrary beach profile by the Litdrift routine. Net and gross sediment transport is calculated taking into account changes in water level and beach profile changes. The module output is the cross shore distribution of water level, longshore current, wave height, wave angle, water flux, bed load, suspended load, total load, and cumulative total load. Annual drift estimates are made on the basis of a weighted sum of input conditions in the database, or from the time series of offshore input conditions.

LitLine is the one-line shoreline change module. This takes the longshore transport estimates from LitDrift, and simulates the coastal response to gradients in longshore sediment transport capacity, whether they be due to natural features, or coastal structures. Wave diffraction around structures is taken into account. The model output is shoreline position, sediment transport rates, water depth in front of revetments, and accumulated volumes of sediment deposited and bypassed. Litpack assumes a long, uniform coastline, and also assumes that sediment transport rates are stationary during the entire simulation period.

Possibly the most extensively applied one-line model currently in use is GENESIS (Hanson, 1989; Hanson and Kraus, 1989; Hanson and Kraus 1990). This model was first developed to describe shoreline changes at Oarai beach, Japan, where conditions were dominated by a long angled groyne, and a large breakwater (Kraus and Harikai, 1983). It has since been applied to the problem of shoreline development behind breakwater schemes in the US (Hanson and Kraus, 1991), and wave transmission through single and multiple detached breakwaters (Hanson and Kraus, 1990; Hanson, Kraus and Nakashima, 1989). The model uses the modification of the CERC equation described in Equation 2-11, so longshore current distributions in the cross shore, wave current interactions, partition between suspended and bed load and water level changes are not represented. This simplified approach allows the changing shoreline orientation to be fed back into the sediment transport calculations.

In GENESIS, to solve Equation 2-18 the alongshore sediment transport rate, Q is found using equation Equation 2-11. To solve this, the breaking wave conditions (height and group velocity) are required. To calculate wave breaking, an internal ray-tracing model is used. The method used in GENESIS to do this is described in detail below.

Calculation of Wave Breaking Conditions

Wave group velocity at breaking is calculated from the wave period and water depth at the breakpoint. The time series of wave conditions used by the model are held in an input file. In the model steering ('START') file, the user specifies the depth of water in which these wave conditions were observed (or modelled). The waves are transformed from this offshore input position to the breakpoint by the internal wave model. This model calculates wave conditions at breaking due to shoaling and refraction, assuming plane, parallel offshore depth contours. A modification to the calculated wave condition is then made in the presence of diffracting structures.

Shoreline wave conditions due to shoaling and refraction are calculated using refraction and shoaling coefficients, such that

$$H_{out} = K_R K_S H_{in}$$

Equation 2-19

where K_R is a refraction coefficient calculated using

$$K_R = \left[\frac{\cos\theta_{in}}{\cos\theta_{out}}\right]^{1/2}$$

Equation 2-20

and K_S is a shoaling coefficient defined as

$$K_S = \left[\frac{Cg_{in}}{Cg_{out}}\right]^{1/2}$$

Equation 2-21

where Cg is the wave group velocity (in metres per second) defined by linear theory, and the subscripts *in* and *out* describe the initial or final wave conditions.

To solve these equations, the wavelengths at the initial and final depths are needed. The GENESIS internal wave transformation model uses an approximation to linear wave theory by Hunt (1979) to solve for the wavelength. Knowledge of these wavelengths allows the wave angle to be calculated using Snell's law.

$$\frac{\sin\theta_b}{L_b} = \frac{\sin\theta_I}{L_I}$$

Equation 2-22

The breaking criterion is found from

$$\gamma = \frac{H_b}{D_b} = b - a\frac{H_0}{L_0}$$

Equation 2-23

where H_0/L_0 is the deepwater wave steepness and a and b are found from Equation 2-24 and Equation 2-25 (from Smith and Kraus, reported in Hanson and Kraus, 1989).

$$a = 5.00[1 - \exp(-43\tan\beta)]$$

Equation 2-24

$$b = \frac{1.12}{[1 + \exp(-60\tan\beta)]}$$

Equation 2-25

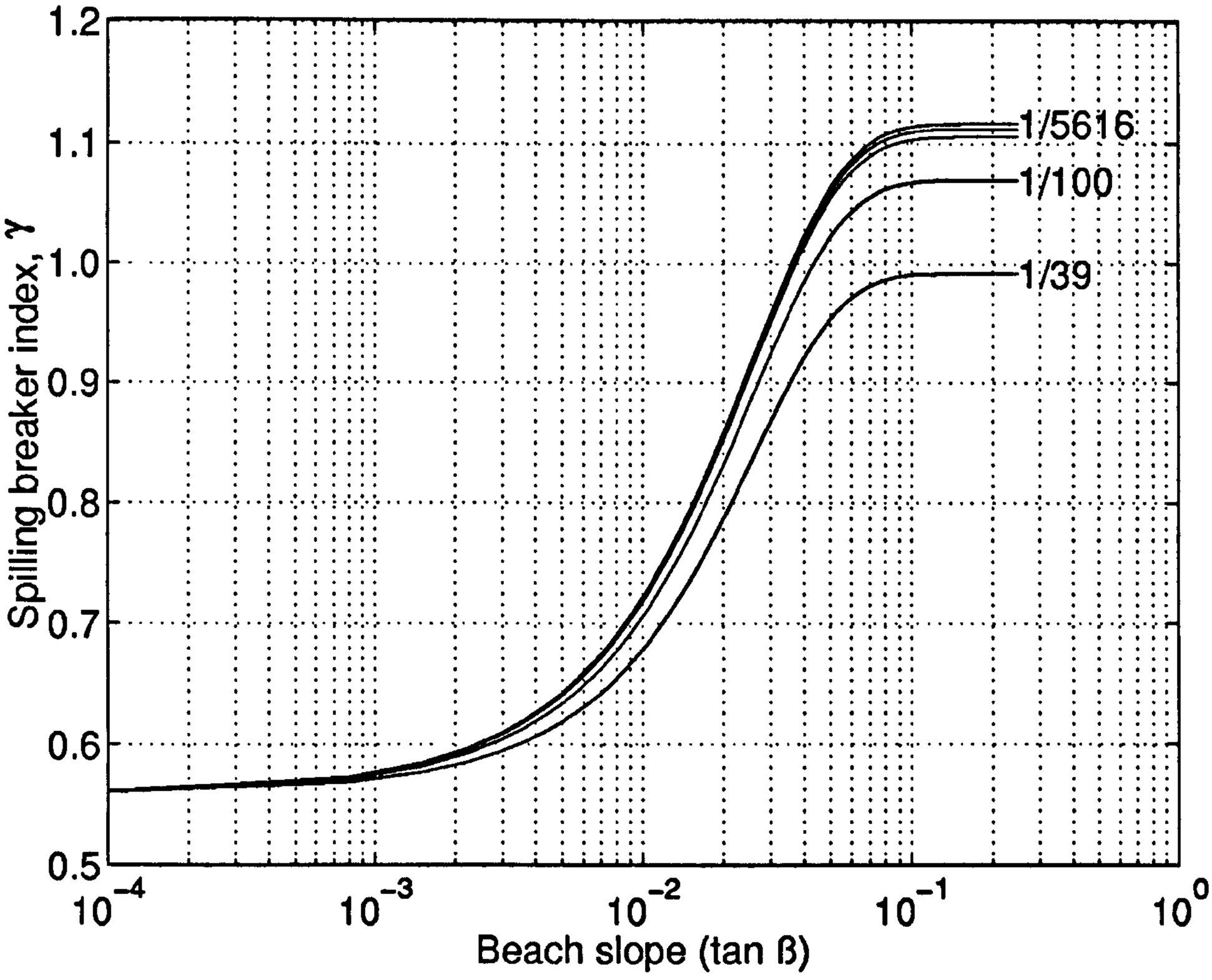

Figure 2-4 Spilling breaker index γ versus mean beach slope tanβ, based on Equation 2-23.

Deep-water wave steepnesses used of 1/39, 1/100, 1/350, 1/624, 1/1404 and 1/5616 are equivalent to a wave height of 1 metre, and wave periods of 5, 8, 15, 20, 30 and 60 seconds respectively.

Figure 2-4 shows the variation of γ with beach slope (based on Equation 2-23) for a selection of deepwater wave steepness values. To arrive at the breaking wave height due to refraction and shoaling alone, Equation 2-19 through to Equation 2-23 are solved by iteration. The mean beach slope, tan β, is found from the beach grain size according to Moore's (1982) development of Dean's (1977) equation, and also the maximum depth of longshore transport such that:

$$\tan\beta = \left[\frac{A^3}{D_{LTo}}\right]^{1/2}$$

Equation 2-26

Grain size enters this equation through the parameter A, given by Moore in terms of the median beach grain size d_{50} as follows:

$A = 0.41(d_{50})^{0.94}$ if $d_{50} < 0.4$ mm,

$A = 0.23(d_{50})^{0.32}$ if $0.4 < d_{50} < 10.0$ mm,

$A = 0.23(d_{50})^{0.28}$ if $10.0 < d_{50} < 40.0$ mm,

$A = 0.46(d_{50})^{0.11}$ if $d_{50} \geq 40.0$ mm,

The maximum depth of longshore transport is given in Hanson and Kraus (1989) as

$$D_{LTo} = (2.3 - 10.9H_o)\frac{H_o}{L_o}$$

Equation 2-27

Equation 2-27 as reported by Hanson and Kraus (1989), appears to be incorrect. Values of H_O greater than 2.3/10.9 metres results in a negative value of the D_{LTo}, which returns a complex value for the beach slope. Hallermeier (1983) uses

$$D_{LTo} = 2.3H_s - 10.9\frac{H_s^2}{L_s} \approx 2H_s$$

Equation 2-28

Influence of Diffraction

When the tips of offshore breakwaters and long groynes are offshore of the surf zone, GENESIS treats them as diffracting structures. Wave breaking conditions at the shoreline behind these structures are governed by wave refraction and shoaling, as in the rest of the model domain, and also by wave diffraction. Figure 2-5 is a schematic showing wave diffraction around one end of a detached breakwater. Waves approach the beach at the bottom of the picture. To calculate the wave height at P_2, in the shadow zone behind the breakwater, the breaking wave height of the ray at P_3 is multiplied by a diffraction coefficient. This coefficient is dependent on the diffraction angle (θ_D in Figure 2-5) and the water depth at P_1. The depth at P_1 could be calculated from the beach slope and distance from the shoreline, but in GENESIS is set by the user in the START file. The diffraction angle is the angle between the line from P_1 to P_2 and the path that the wave would have taken in the absence of the diffracting structure (P_1 to P_3). Thus, the wave height at P_2 is given by

$$H_b = K_D(\theta_D, d_{P1})H_b'$$

Equation 2-29

To determine the function K_D the method of Goda, Takayama and Suzuki (1978) is used, employing the energy concentration parameter $S(max)_o$ defined by Mitsuyasu (1975). The subscript *o* refers to deep water. Kraus (1984) presents a figure to allow *S(max)* to be found from the deep-water wave steepness. This figure is reproduced as Figure 2-6.

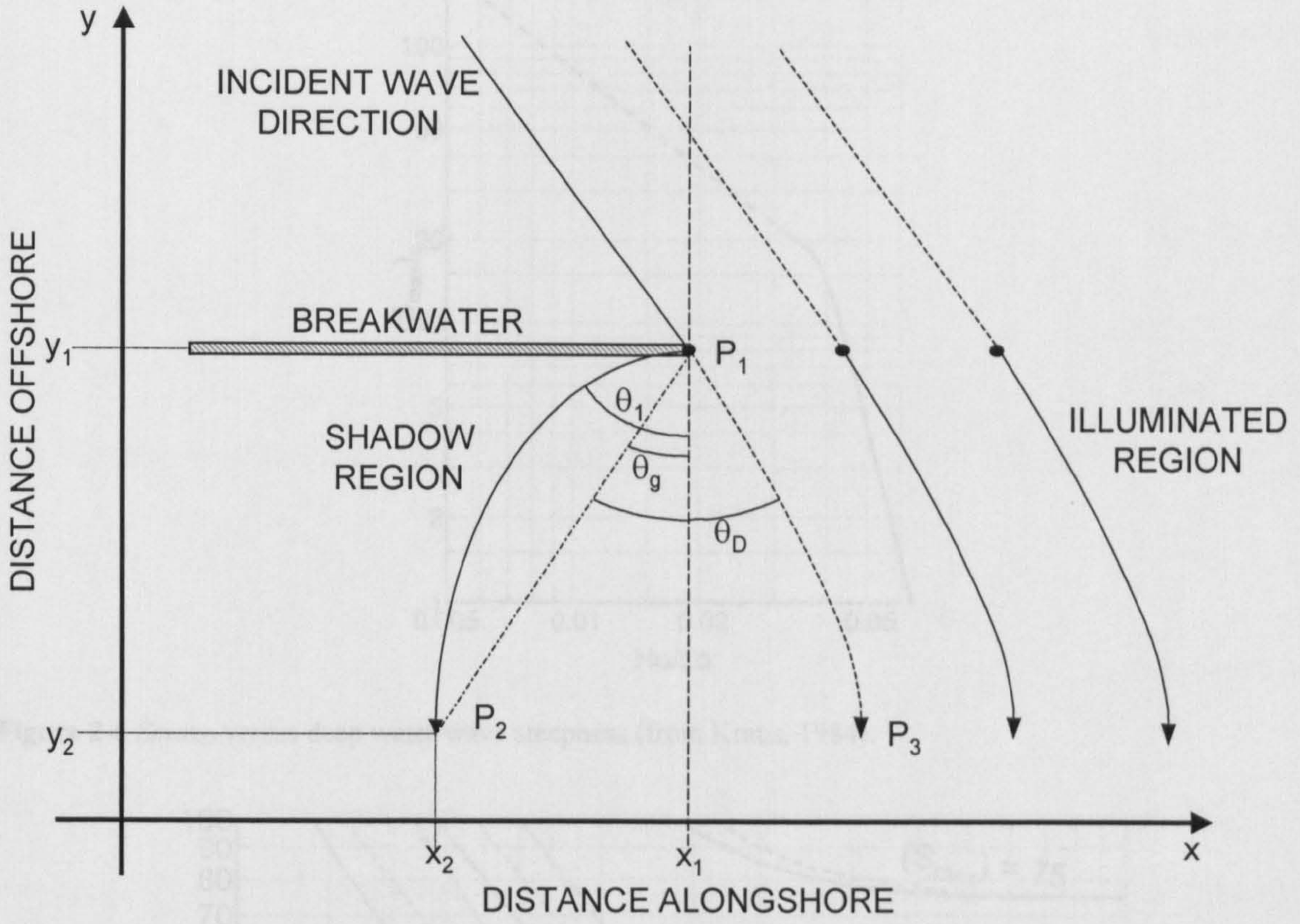

Figure 2-5 Definition of parameters in Kraus' (1984) wave diffraction approximation, adopted in GENESIS (after Hanson and Kraus, 1989)

Goda *et al* (1978) present a set of curves to determine *S(max)* at the diffraction point, in terms of $(Smax)_o$, the ratio of local water depth d_{PI} to the deep water wavelength L_o , and a wave angle which denotes the angle between the incident waves and the interface between deep and shallow water. The size of this angle is expected to be very small, making the method to be applicable to general bathymetry. These curves are presented in Figure 2-7.

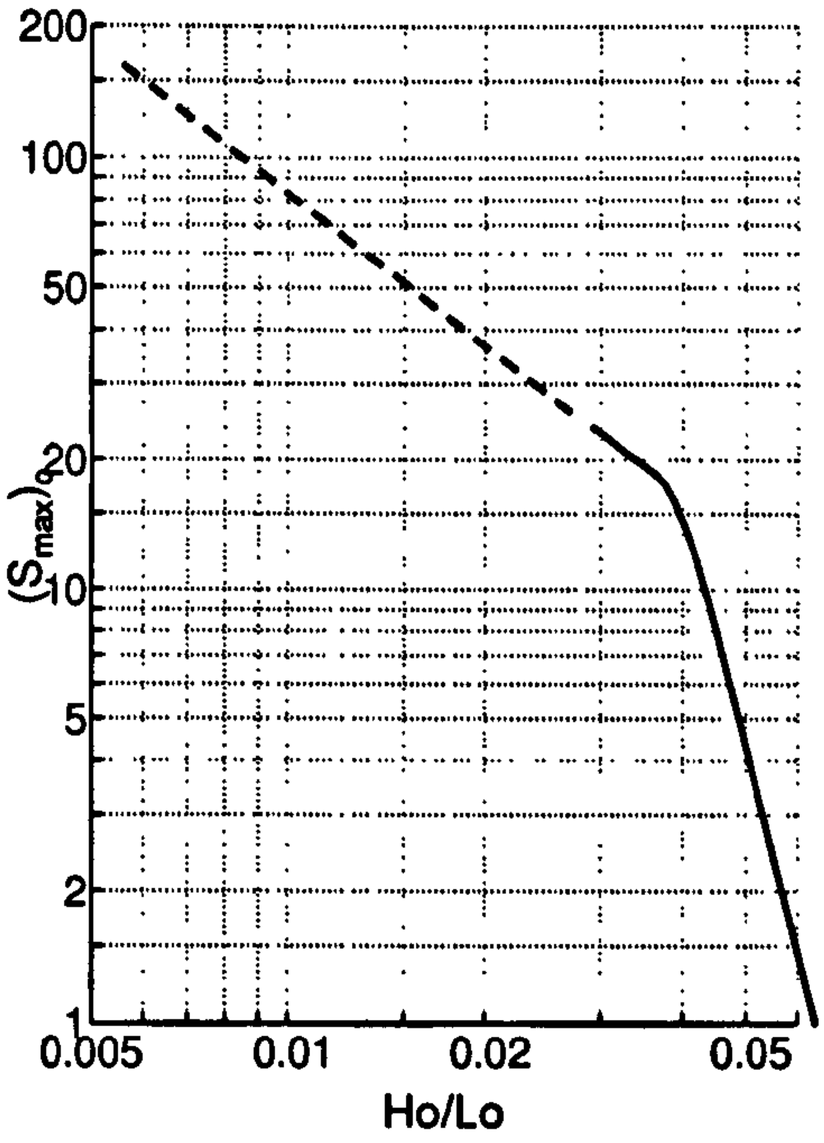

Figure 2-6 $Smax_O$ versus deep water wave steepness (from Kraus, 1984).

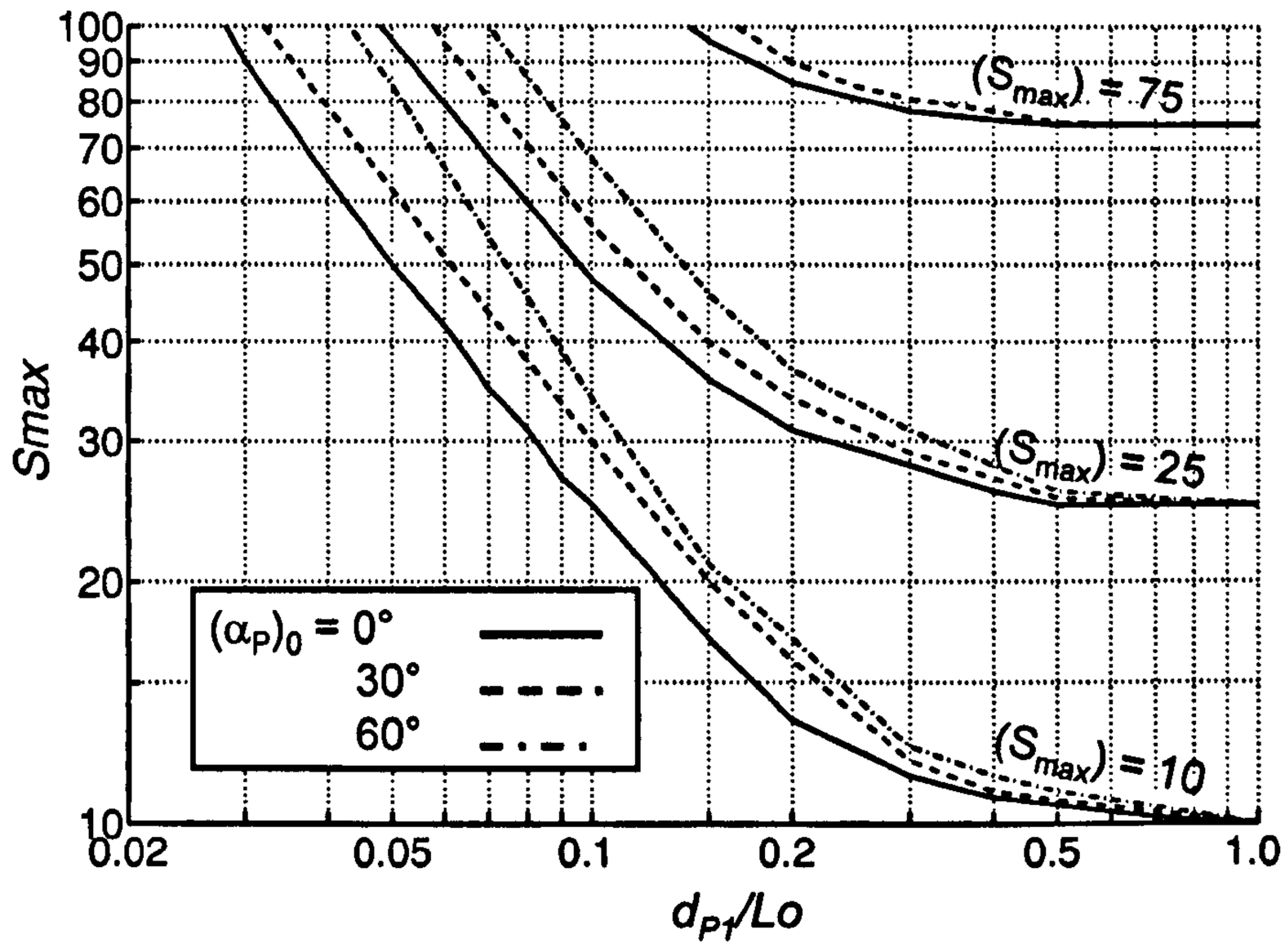

Figure 2-7 Change of maximum directional concentration parameter *Smax* due to wave refraction in shallow water (from Goda *et al*, 1978)

Having found *Smax* at the breakwater tip using Figure 2-7, the energy along a line at an angle θ_D from the line of the incident wave, is calculated as a percentage of the energy at the breakwater tip ($P_E(\theta_D)$). This can be found either by using Figure 4 in Goda *et al* (1978) or by using the following equations, which are an approximation to the curves presented by Goda *et al* (Kraus, 1984).

$$W = 5.31 + 0.270S_{max} - 0.000103S_{max}^2$$

Equation 2-30

$$A = \frac{S_{max}}{W}\theta_D$$

Equation 2-31

$$P_E(\theta_D) = 50(\tanh(A) + 1)$$

Equation 2-32

The diffraction coefficient $K_D(\theta_D)$ is then given by

$$K_D(\theta_D) = \sqrt{\frac{P_E(\theta_D)}{100}}$$

Equation 2-33

Combined refraction/diffraction

The use of θ_D in Equation 2-29 indicates that waves are assumed to follow a straight path after diffraction, and not experience any further refraction. This assumption speeds up the calculation of diffracted wave heights, but at the expense of the accuracy of the solution. Kraus (1984) states that this method would be expected to over-predict the breaking wave height, while under-predicting the breaking wave angle by a factor of up to 150%. Looking at Equation 2-29, this will have the effect of reducing the predicted transport rate, as both the $\sin\alpha_b$ and $\frac{\partial H}{\partial x}$ terms will be reduced.

Contour modification

As the shoreline position changes through a model run, the distance and angles between grid cells and sources of diffraction change. In addition, the shape of the offshore contours will change to reflect the local changes in the shoreline orientation. To account for this effect, the orientation of the shoreline is assumed to extend to the depth of the diffraction source (or reference depth). Wave refraction and diffraction is carried out in a reference frame relative to the orientation of the local shoreline. After refraction, diffraction and shoaling calculations are completed, the breaking wave angle is rotated back to the fixed co-ordinate system for use in the longshore transport calculations (Equation 2-11). Use of the contour modification routine is reported to significantly improve the accuracy of the internal wave model, giving a more realistic breaking wave angle (Kraus, 1983; Kraus and Harikai, 1983).

Modelling Beach Changes Around Coastal Structures

In front of seawalls

The common approach to the solution of this problem is to follow the method of Osaza and Brampton (1980). The beach is described by a single contour line (at mean sea level) at some position y in the cross shore direction. If the beach is backed by a seawall at a position y_{SW}, then for a non-eroding beach y will be greater than or equal to $y_{SW}+D_B/\tan\beta$, where D_B is the berm height and $\tan\beta$ is the beach slope. This is shown in Figure 2-8.

Generally, the beach has a defined berm height and when the beach contour position is at or greater than, position y_1 in Figure 2-8, then the wall does not influence sediment transport. If the beach erodes such that the berm height is less than D_B, then the berm height becomes a function of x (alongshore position) and T (time). The calculated transport rate is also affected.

Osaza and Brampton (1980) allowed the beach level to fall until there was no beach left above the mean sea level (point y_4 in Figure 2-8). At this point, longshore transport is reduced to zero. At an intermediate point (positions y_2 or y_3) the transport through that beach section is reduced from the 'standard' (no seawall) transport rate by a factor proportional to the ratio of the height of the new berm to D_B. An alternative method was also proposed, whereby the modification to the original transport rate is a factor based on the ratio of areas EFGH to ABCD (referring to Figure 2-8).

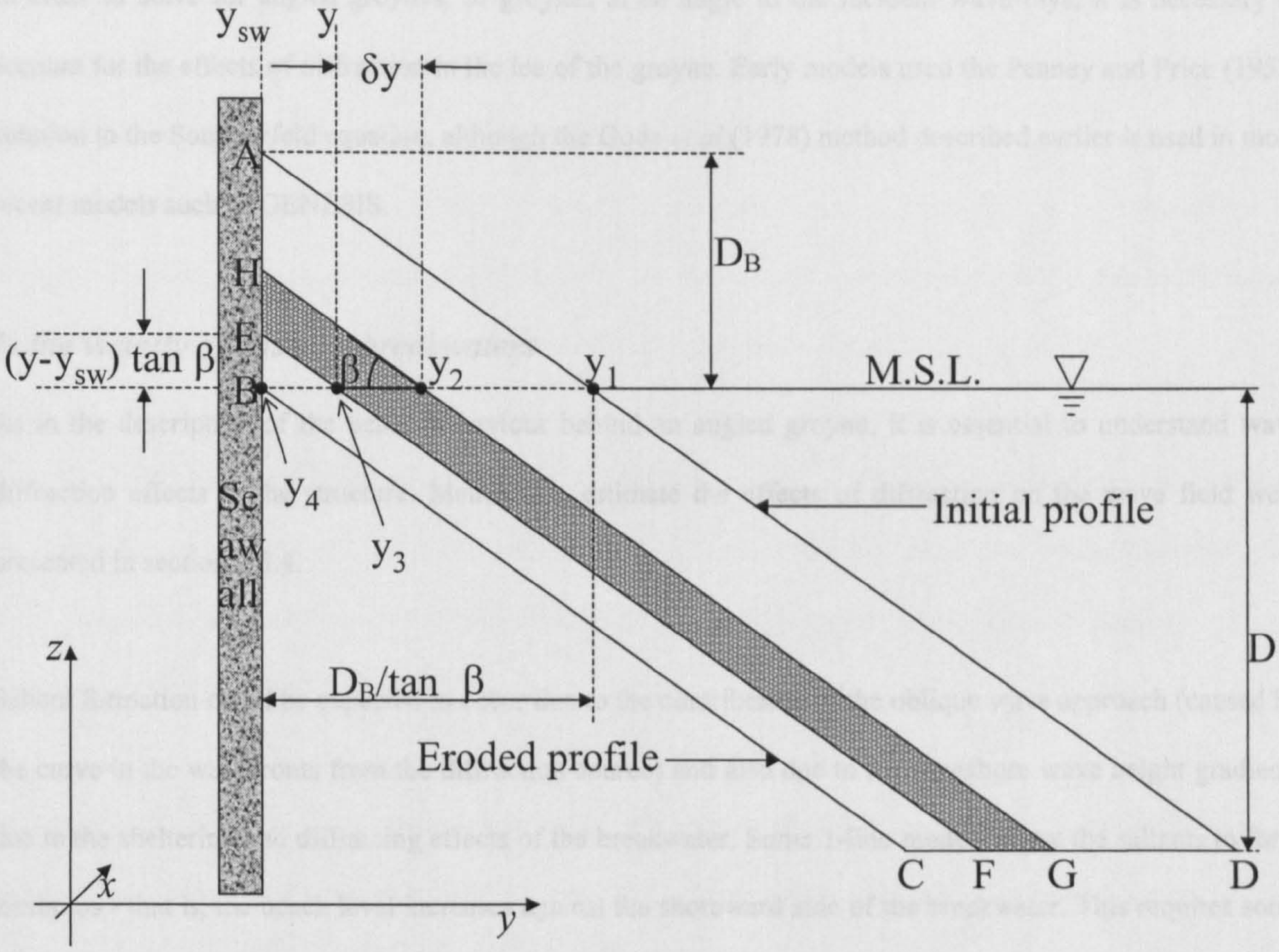

Figure 2-8 Terms used in one-line modelling of beach response in front of a seawall, after Osaza and Brampton (1980).

Adjacent to groynes

A thorough description of material bypassing groynes requires a description of cross-shore as well as longshore transport. GENESIS (Hanson, 1989) uses a simple assumption to allow the one-line model to calculate this.

Bypassing only takes place when the depth at the groyne tip D_G is less than the local depth of longshore transport. The actual volume of material bypassed is calculated by means of a bypassing factor. This is simply 1- (the depth of groyne tip : the maximum depth of longshore transport). The actual volume bypassing the structure is then the updrift transport rate × this bypassing factor. Bakker *et al* (1968) solved the problem by introducing a second contour line at the depth of closure. This allowed the profile to change in the vicinity of groynes. When the profile reaches a particular steepness, sand is assumed to be transferred to the offshore contour. Perlin and Dean (1978) solved the problem by allowing for permeable groynes. Each structure traps only a proportion of the sediment that arrives at it, allowing the rest to pass through.

In order to solve for angled groynes, or groynes at an angle to the incident wave rays, it is necessary to account for the effects of diffraction in the lee of the groyne. Early models used the Penney and Price (1952) solution to the Sommerfeld equation, although the Goda *et al* (1978) method described earlier is used in more recent models such as GENESIS.

In the vicinity of offshore breakwaters

As in the description of the beach behaviour behind an angled groyne, it is essential to understand wave diffraction effects at the structure. Methods to estimate the effects of diffraction on the wave field were presented in section 2.3.4.

Salient formation could be expected to occur due to the contribution of the oblique wave approach (caused by the curve in the wavefronts from the diffraction source) and also due to the longshore wave height gradients due to the sheltering and diffracting effects of the breakwater. Some 1-line models allow the salients to form tombolos - that is, the beach level increases against the shoreward side of the breakwater. This requires some parameterisation, similar to the groyne condition, to allow material to be bypassed around the seaward side of the tombolo. Some models (such as GENESIS) avoid this problem by terminating the model simulation if tombolos form.

2.4.3 *N* - line models

Bakker (1968) introduced the two line model as an extension to the one-line approach, allowing material to be transported around the seaward limit of coastal structures such as groynes. Perlin and Dean (1985) presented a fully implicit *N*-line finite difference model. This model used a wave power based bulk sediment transport relation. This transport was distributed across the surf zone (between the *N* contours) by a normalised, empirical relationship. Cross shore transport was calculated by comparing the modelled beach slope with a 'standard' slope (that followed a $y^{2/3}$ type profile). If the profile was steeper than that predicted by the $y^{2/3}$ relation, then transport was assumed to be offshore, while onshore transport was permitted if the profile was flatter than that described by $y^{2/3}$. The rate of cross shore transport was governed by an *activity factor* that was constant within the surf zone, but decayed exponentially seaward of it.

The model was applied to a simulated groyne field, on steep and flat beaches, and also to the problem of modelling the dispersal of a slug of nourishment material placed at the toe of the beach. A validation exercise

was carried out using data from a single detached breakwater, adjacent to a channelled inlet. The authors felt that the validation exercise was qualitatively reasonable, but the model over-predicted erosion. It was felt that this problem was due to the inability to model barred profiles, or to include currents and variations in water level. Additionally, the problems of using an empirical cross shore transport distribution, a simple longshore transport formula, and the simplifications of the wave model were cited. It is probable that better results could have been obtained if the model was 'tune-able' to the local conditions.

Brampton and Motyka (1985) considered the possibility of applying a multi-line model to describe transport on a shingle beach. They felt that a one-line model was more suited to the problem of shingle beach plan shape development, due to the current state of knowledge of the behaviour of sand/shingle beaches, and also the cheaper operational costs.

In addition to modelling multiple contour lines, Fleming (1993b) describes a multiple profile model presented by Dales and Al-Mahouk (1991), where successive profiles were modelled using a Bailard (1981) transport model and Nairn's (1988) cross shore transport model.

2.4.4 3D morphology modelling

In his review of numerical morphology modelling, de Vriend (1992) divides 3D morphology models into classes based on three different concepts. These concepts are as follows:

- ISE: Initial Sedimentation/Erosion models calculate the hydrodynamics and resulting sediment dynamics based on the initial bed topography. The resulting topography is not fed back into the hydrodynamics - only the resulting erosion/deposition at each grid point is calculated.
- MTM: Medium Term Morphodynamic models feed the topographic changes back into the hydrodynamic model. The time scale of the morphodynamic changes are considered to be similar to the time scale of the hydrodynamics (considered to be of the order of a tidal cycle).
- LTM: Long term morphodynamic models use a parameterised description of the physical processes to develop a long term description of the bed changes.

ISE models have been implemented by, for example, de Vriend and Ribberink (1988) and Dingemans *et al* (1987). Due to the lack of feedback from the bed to the flow, their application is generally limited to short time periods, such as parts of storms. These models can be used to give an understanding of the physical processes at work over these short time periods.

MTM models do allow bathymetric changes to be fed back into the hydrodynamic modules, and so can be applied over longer time scales. Models are divided into two classes. 2DH models describe the 3D development of the bed morphology, but do so based on estimates of the depth integrated flow structure, with some parameterisation used to calculate the bed shear stress. The Watanabe *et al* (1986) model uses a mild-slope equation based model to calculate radiation stresses, which are then used to produce a depth mean flow. The sediment movement due to these currents was simply added to the movement due to the waves alone. This simplification was acceptable to the authors due to the lack of understanding of sediment dynamics in combined wave current flows. Use of a Boussinesq model, such as that described in Sørensen *et al* (1998) removes the need to separate wave and current flows.

De Vriend (1986) warns of instabilities that occur, and may grow exponentially, in *'rigid lid'* models (i.e. models where the movement of the free surface is not modelled) without wave-driven currents. The waves are sufficient to introduce perturbations in the flow, and the differential equations allow these perturbations to grow. Where the numerical scheme does not permit these perturbations, it is due to numerical smoothing. An effective way to reduce this instability is the use of slope-limiting effects, such as those described by Horikawa (1988).

The other form of MTM model is the quasi-3D (sometimes called 2½D) models. These models consist of a 2DH model, linked at each grid point to a 1D vertical velocity profile model. The vertical profile model describes the variation from the mean, assumed, velocity profile that is used in the 2DH model. This secondary velocity field has a depth-averaged flow of zero. Sediment transport is described by an equilibrium concentration profile in the 2DH model, while the secondary velocity profile allows deviations from this due to suspension or deposition of material. An example of the quasi-3D approach is the QQ3-DM (Briand and Kamphuis, 1990) which uses radiation stresses to drive a depth integrated flow model, with a three layer theoretical undertow model to add vertical structure.

Kamphuis (1992) comments on the limitations of this approach to modelling. There are problems describing the hydrodynamics (effects of wave asymmetry, non-linear interactions, infra-gravity motions) and the effects of bedforms. There is a high computational cost of simulating a range of wave conditions (particularly if describing the wave field in a directional, spectral way), and the frequently poor quality of input wave data (usually from hindcasts, with poor directional resolution) cannot usually justify this approach. It is suggested

that the increased effort required to operate these models is not reflected in the quality of the data obtained. In addition, the high computational cost limits the ability of engineers to play with the model, to try a variety of different input conditions for sensitivity analyses.

The final class of models described by de Vriend (1992) are the LTM models. These involve the parameterisation of wave and sediment behaviour - and assume that shoreline changes occur over longer time scales than changes in the hydrodynamics. This may be a reasonable assumption for large areas over long time scales, but is obviously not true for catastrophic changes in beach morphology due to severe storms. These models are frequently empirical, and take the form of descriptions of the evolution of particular features. These are frequently done by assuming that a beach will take certain shape that follows a particular geometrical form (for example, the Cowell and Roy (1988) model of profile evolution). Additional empirical modelling may rely on assumptions of the fractal behaviour of large coastal areas (for example, Beltram and Southgate, 1995). These longer-term methods rely on an understanding of the behaviour of the coast as a system, rather than the deterministic interaction between well-defined (and understood) forcing and response functions.

2.4.5 Empirical orthogonal functions

In addition to the geometrical and deterministic approaches to beach modelling, a third wholly empirical approach exists based on long term beach survey records. Hsu *et al* (1994) developed an empirical model to predict beach changes due to both cross shore and longshore sediment transport where the beach is defined in terms of two eigenfunctions $e_k(x,t)$ and $e_k(y,t)$, which represent the cross shore and long shore respectively. The beach level h is described by:

$$h(x,y,t) = \sum_k e_k(x,t) e_k(y,t)$$

Equation 2-34

In turn, each eigenfunction can be split into a spatial and a temporal term as follows:

$$e_k(x,t) = \sum_m e_k^m(x) c_{kx}^m(t), e_k(y,t) = \sum_n e_k^n(y) c_{ky}(t)$$

Equation 2-35

where k represents variational terms, and c describes temporal terms. In earlier models (e.g. Hsu *et al*, 1986) these terms were simply substituted into the equation for h. This was computationally demanding however,

and so the expression was simplified, to include only one temporal term. The model was validated using field observations of 12 profiles taken every two months between October 1983 and June 1986 (resulting in 17 profiles for each section). These profiles were of a sandy beach protected by six offshore breakwaters.

The authors found that the model was successful in predicting mean trends for the beach development, but was limited in its ability to model the effect of storms or short term events on the beach. This is to be expected however, given that the model worked on a Markov process and linear regression to predict beach changes.

For the study of shingle beaches, where extreme, short lived events can have catastrophic effects on a beach (for example, the damage to shingle spits, reported in Nicholls and Wright, 1991), this model would not be suitable for application. Another drawback of this model is its need for large volumes of site-specific input data. Being based solely on field data, this model must assume that conditions do not change over the period of interest - i.e. there is no change in the sediment transport into the modelled area, and the wave climatology remains constant.

2.4.6 Physical models of detached breakwaters

Laboratory tests have been used in the study of offshore breakwaters to attempt to mimic the processes that had been observed in the field, while allowing researchers to control the conditions in the test. The first known tests, undertaken by Sauvage and Vincent (1954), demonstrated the formation of two symmetrical circulatory cells in the shadow zone behind the structure.

Rosen and Vajda (1982) used a small scale moveable bed model, with a high, impervious shore parallel detached breakwater in front of a 7 m long beach, 9 m from the wave paddle. In these tests, the effects of three wave steepnesses were tested. For each test, the beach was brought into equilibrium without the breakwater in place, and the first breakwater was placed. Initially, a 0.5 m breakwater was inserted. The beach was brought into a new equilibrium, and measured. The breakwater was replaced by a 1.0 m model, the new equilibrium beach developed and measured, and finally a 2.0 m structure was positioned and the test was repeated. At the end of these tests, the beach was brought back into equilibrium, and the tests were repeated for the breakwater positioned offshore. Monitoring of the beach position was by means of visual observation, photography, and by marking the position with small sticks. A point gauge was also employed

to measure control profiles. Current circulation patterns were visualised using flourescent dye tracing.

Results of the dye tracing showed the formation of two circulatory cells in the lee of the breakwater. In addition to these, fluctuating rip currents occasionally broke away from the circulation cell, producing a return flow to the seaward side of the breakwater. Sand was transported from both sides of the breakwater into the sheltered zone behind the structure, accumulating around the axis of symmetry. Initially, the salient developing behind the breakwater had a saddle shape, as two salients formed. Sand-bars were observed in the inshore area near the breakwater tips. On these bars, sand moved with the waves and with the currents. The shoreward faces of these features were almost vertical. These bars migrated shoreward, and joined the rest of the salient. This movement of material from offshore to the salient does not follow the more conventionally described longshore movement of material.

Development of the salient appeared to be controlled by the breakwater distance from the original shoreline. It was proposed that the spit geometry was governed by the ratio of breakwater length to the offshore distance of the structure. It was observed that variations in wave steepness affected the observed beach profile, but did not affect the actual plan shape of the equilibrium beach.

As the beach approached equilibrium for each breakwater configuration, the rate of change of the shoreline position decreased. This suggests that longshore transport of sand is reduced. Two reasons for this were proposed. The first, as suggested by Silvester and Ho (1972) in the study of equilibrium headland beaches, was that as the shoreline comes into equilibrium, longshore currents become so weak as to stop transport. The reason for this, proposed by Silvester (1970), was that at equilibrium, wave crests were parallel to the beach contours. Thus there would be no oblique wave approach, and thus no longshore transport. The second idea was that longshore transport did not stop, but continuity is maintained by a constant recirculation of material.

This second theory was discounted as both tests (Gourlay, 1976) and continuity considerations, indicated that current flows at the breakwater tips were weaker than those observed at the shoreline, and this would lead to the deposition of sediment there. Gourlay's (1976) constructed a fixed bed model, with a single breakwater arm extending out to the centre of the tank. Behind this, shaped into the bed, was typical equilibrium salient bathymetry, such that the wave fronts diffracted around the breakwater arm would always be parallel to the bottom contours. He observed that as waves diffracted into the sheltered region behind the breakwater, there

exists a longshore gradient in wave height along the breaker line, with the highest waves being outside of the shadow zone, the lowest waves within it. This longshore gradient of breaker height translates itself into a longshore gradient in wave set up. It is this wave set up that drives the current circulation behind the breakwater.

Suh and Dalrymple (1987) used a spiral wave basin to generate waves with a constant, small oblique approach (around 2^{o} at breaking). Following Rosen and Vajda (1982), they allowed their beach to come into equilibrium with the wave conditions before inserting any structure. After running several tests on single offshore breakwaters, where different breakwater lengths and offshore distances were tested, they studied a few multiple breakwater configurations, varying only the gap width and the offshore distance.

The sand trapping ability of the structures was quantified by means of a sand trapping efficiency term, the dimensionless deposited volume, which is the ratio of the volume of material deposited behind a breakwater (both above and below the waterline) to the actual volume protected by the breakwater.

2.5 Conclusions

This review has presented the methods available to describe wave induced forcing on beaches protected with detached breakwaters. The physical processes, the numerical techniques available to model them, and limitations to those numerical methods have been discussed. Likewise, methods for describing sediment transport driven by the wave field have also been discussed. These methods also range from simple predictors relating the predicted volumetric sediment transport rate to the incident wave energy flux, to complex descriptions involving estimates of shear stresses, bed roughness and sediment motion thresholds.

The design engineer requires information as to which tools are suitable for use to assist scheme design. Knowledge of the limitations of those tools is equally important. The problem of predicting beach morphology changes has been shown to be complex. Different processes are important over different length and time scales. If engineers are to predict beach response to structures, then there is a need to decide which time and space scales are of interest. Previous research suggests that it is not justifiable, practical or necessary to describe all the physics of sediment transport to make reasonable predictions of beach response. The question of what level of parameterisation is acceptable depends on the time and space scales of interest, and the quality of the available data.

The scales of interest dictate the methodology required to investigate their contribution to the morphological change. To study the short-term beach response, high temporal resolution sampling is required. This would typically mean co-located pressure transducers and current meters. The current meters would need a response time that allowed turbulence, as well as waves and mean currents to be resolved. This would suggest the need for either electromagnetic or acoustic devices. Some way of measuring sediment transport directly would also be desirable, such as acoustic or optical backscatter devices. Coherent Doppler or Cross Correlation Velocimetry would provide both current and concentration information at very high sampling rates. To represent the bed roughness accurately, some measure of the presence and size of bedforms would be necessary. Ripple profilers or sector-scanning sonar would be suitable for this task. To obtain coverage of the entire scheme at Elmer, equipment would need to be deployed along many cross-shore profiles. To measure the entire beach morphology at similar time scales would be extremely laborious, even for a short time.

The above approach would be ideal for a short-term study, for example of the beach response to a storm. To investigate the long term beach development at that temporal resolution would require the equipment to be

deployed for a long period. This would create calibration problems, as the long term stability of the equipment described above is not well known. The volume of data produced would be huge, and to make sense of it would require temporal averaging, which would filter out the detail that would have been collected at such great expense. This is before the practical and cost implications of assembling such a vast array of equipment, and the personnel to operate it, has been taken into account.

If the interest was in the longer term beach development, then it makes sense to have a reduced sampling rate. Individual suspension events are less important on this time scale, so high frequency measurements of sediment concentration profiles are of less interest. The minimum data set that models require is a description of the beach morphology (including how it changes over time), and the incident wave field. Given the importance of the directional spreading in controlling wave energy penetration into the lee of structures, and the simple need for knowledge of the direction of wave approach for 'longshore power' type transport models, it is clear that directional wave recording is necessary. It is necessary to have the wave conditions at the beach to record the strength of the wave forcing. Most models however bring waves in from an offshore point, so it makes sense to locate the wave recorder at this point, rather than have to backtrack the 'final' wave condition from the beach to offshore, only to bring it back in numerically. If more than one wave recording system were available, then one system could be placed at the offshore point, and one at the shoreline. This would also permit the validation of numerical methods of wave transformation.

The frequency of bathymetric and beach morphology surveys is of concern. If the offshore bathymetry changes rapidly, it will affect the wave field at the beach. While this will be picked up using the two wave recording systems proposed previously, the wave recorders only give point measurements, so the spatial distribution of the wave field cannot be confidently determined. In this case, frequent bathymetric surveys are required. Alternatively, if the offshore bathymetry is unchanging, then the number of surveys required can perhaps by reduced to one or maybe two. Beach morphology is expected to change as the scheme develops towards an 'equilibrium' with the wave field (if such a configuration exists), seasonally, and also due to storms. Storm response is not the time scale of interest in a medium or long term study although it might have catastrophic effects on the beach shape, which feed into the long term beach development. Given the interest in seasonal changes, then at least four evenly spaced surveys per year are desirable. The surveys should last for at least as long as the other monitoring activities (although for long term understanding of coastal change, as long a record as possible is desirable). The spatial coverage of the surveys should be such that they cover the entire beach, from the shoreward limit of the berm down to the offshore limit or 'closure

depth'. In the alongshore direction, they should extend far enough up and down-drift of the scheme to ensure that activities immediately adjacent to the scheme do not influence the beach levels. The survey line spacing should also be close enough to allow all the beach features of interest to be resolved. The accuracy of the surveys must be sufficient to allow confident estimates of volume changes to be made. Beach surveys are expensive, so while the above specification describes what is desirable, compromise might be necessary on the survey coverage.

Ancillary data that would be useful to collect would be sea level, for some understanding of surge levels, meteorological data (wind speed, direction and barometric pressure) and beach composition. The surge and meteorological data would allow comparison with long term records, to give an idea of the typicality of the observed data.

The choice of model for evaluation depends on the timescale of interest. To maximise the use of the exercise, It would be helpful to select a 'generic' model - one that is typical of the broad range of models in use in research and industry, and includes processes and parameters that are included in many of the 'rival' models. Finally, any model selected should be suitable for application to a renourished sand and shingle beach protected by detached breakwaters, in a macro-tidal environment.

The difficulty of collecting a full validation data set for short-term process-based modelling has been described. The study site is also particularly demanding, having a wide range of grain sizes and porous breakwaters (allowing wave transmission and the interaction between transmitted and diffracted wave fields). While collecting a hydrodynamic data set to better understand the wave-structure and wave-wave interaction would be of great value, any model would have to describe these processes if it was to have a chance of predicting the forcing on the sediment. There is also a question of the survivability of the equipment needed to measure sediment concentrations on a mixed sand and shingle beach.

The data set required for the validation of medium and long-term models is simpler than that required for short term modelling, although the recording commitment is needed over a longer period. A variety of medium and long-term model approaches have been presented. What type of model, and which actual model should be selected for validation? Data driven models, such as the eigenfunction approach of Hsu et al (1994), require a history of beach survey data before they are capable of being used in a predictive sense. Where a coastal engineering scheme has been implemented any trend in the previous shoreline behaviour

may have been altered, so a suitable data history does not exist. N-line models would be a reasonable choice for validation. They allow the three dimensional beach shape to be modelled, and have been applied to detached breakwater sites before (Perlin and Dean, 1985). They are not widely used in engineering consultancy however. Brampton and Motyka (1985) also suggest that a one-line approach is more suitable for a shingle beach. Three widely used one-line models (Unibest, LitLine and GENESIS) have been described earlier. Of these, Unibest does not model wave diffraction, which makes it unsuitable for use with this kind of scheme. LitLine and GENESIS do allow diffraction effects. The input module for LitLine is LitDrift, which calculates longshore transport across a profile to get gradients in the longshore transport field. These gradients are then applied to the shoreline shape. The assumption is that the beach is developing steadily due to the transport gradients, but that the changed beach morphology does not feed back into the transport calculation. This simplification is almost certainly going to be invalidated in the rapid shoreline development that could be expected around detached breakwaters. On the positive side however, the transport calculations in LitDrift do take into account tidal currents and variable tidal levels. GENESIS has a simpler transport formulation than the other two models, but has been applied extensively in the United States, and a large body of literature exists describing its application - in particular to detached breakwater sites. The model does allow feedback of the beach plan into the transport calculations. There is limited experience in applying this model to macro-tidal field sites - although one study describes its use to predict the development of a gravel spit in Alaska (Chu *et al*, 1987). The model also has the benefit of being freely available. The major limitation of the model is its inability to model full tombolo formation, although this was not expected to cause a problem at the project outset, as the Elmer scheme was designed to produce salients, rather than tombolos.

The GENESIS model has been widely reported in the literature, and has been applied to many sites. Despite this, no evaluation of this model has been carried out using good, long term directional wave information, and concurrent beach surveys. Based on this, and the above considerations, GENESIS was selected for evaluation. The next chapter describes the fieldwork carried out to collect the data required for model evaluation.

3. Field Experiment

3.1 Introduction

This chapter describes the fieldwork exercise. The data requirements for the project are discussed, and the experiment design is presented. The second part of the chapter describes the wave recorders used and the measurements taken. Limitations of these systems are discussed. Instrument calibration procedures are presented and discussed. A summary of the available wave data is presented. The final section of the chapter describes additional measurements, taken as part of this project. A full summary of the available data is presented.

3.1.1 Sampling requirements

The previous chapter described the data requirements for evaluating medium and long-term morphological models, and justified the nomination of the US Army Corps of Engineers' model, GENESIS, for application to the Elmer site. The data requirements for evaluating the model were also discussed. To recap, these are as follows:

- Beach morphology data, at the start of the modelled period, and at regular intervals throughout the modelling period, for at least one year.
- Description of beach composition, to set the beach slope in the model (in conjunction with beach profile data)
- Directional wave recording at the offshore 'wave input point', and at the shoreline, for the whole study period.
- Offshore bathymetric data, to allow for waves to be brought inshore from the offshore prediction point.

The value of the data could also be of use to short term studies if a short, intensive monitoring period could be included at some point in the longer-term observations.

In addition to the author's requirement for data for the study of beach morphology, the fieldwork exercise was required to provide data for the evaluation of numerical models of wave shoaling, refraction, diffraction and reflection (Ilic, 1999). In order to meet these objectives, the following requirements were defined:

- Wave data recorded simultaneously, at both the shoreline and the offshore limit of the modelling domain.
- Recording equipment to be sufficiently rugged to survive storm events, and to log data automatically.
- Wave data files to be processed using the same software routines for each wave recording system
- Beach surveys to be undertaken concurrently with wave data collection.
- Data to be collected for at least one year, to avoid seasonal bias in the data collected.

Due to the need to evaluate 'one-line' modelling approaches, which are generally considered suitable for the description of medium and long term beach changes, beach survey data was not required at a high temporal resolution. In addition to these requirements, the author was fortunate that a simultaneous fieldwork exercise was underway, carried out by Davidson *et al* (1996) measuring the reflection performance of one breakwater at the site, providing additional wave data in the spring of 1994.

3.1.2 Equipment location

At the seaward limit of the numerical modelling grid used by Ilic (*op. cit.*), one University of Plymouth directional wave recorder (described in section 3.2.1) was deployed. At prototype scale, this was 650 metres offshore, towards the western end of the scheme. This provided the incident boundary conditions to be tested in the model. At the shoreward limit of the model grid, the University of Brighton wave staffs (see section 3.2.2) were deployed to provide directional wave conditions after waves were diffracted through the gap between breakwaters three and four. For a period from February to April 1994, an additional University of Plymouth wave recorder was deployed immediately seaward of breakwater four. Current metering was undertaken in the lee of the breakwater three, for one week in May 1994. Figure 3-1 shows the equipment layout.

The entire beach was surveyed, by aerial photogrammetry, over low water, from west of the scheme, to five kilometres east, at four monthly intervals from the start of the monitoring programme.

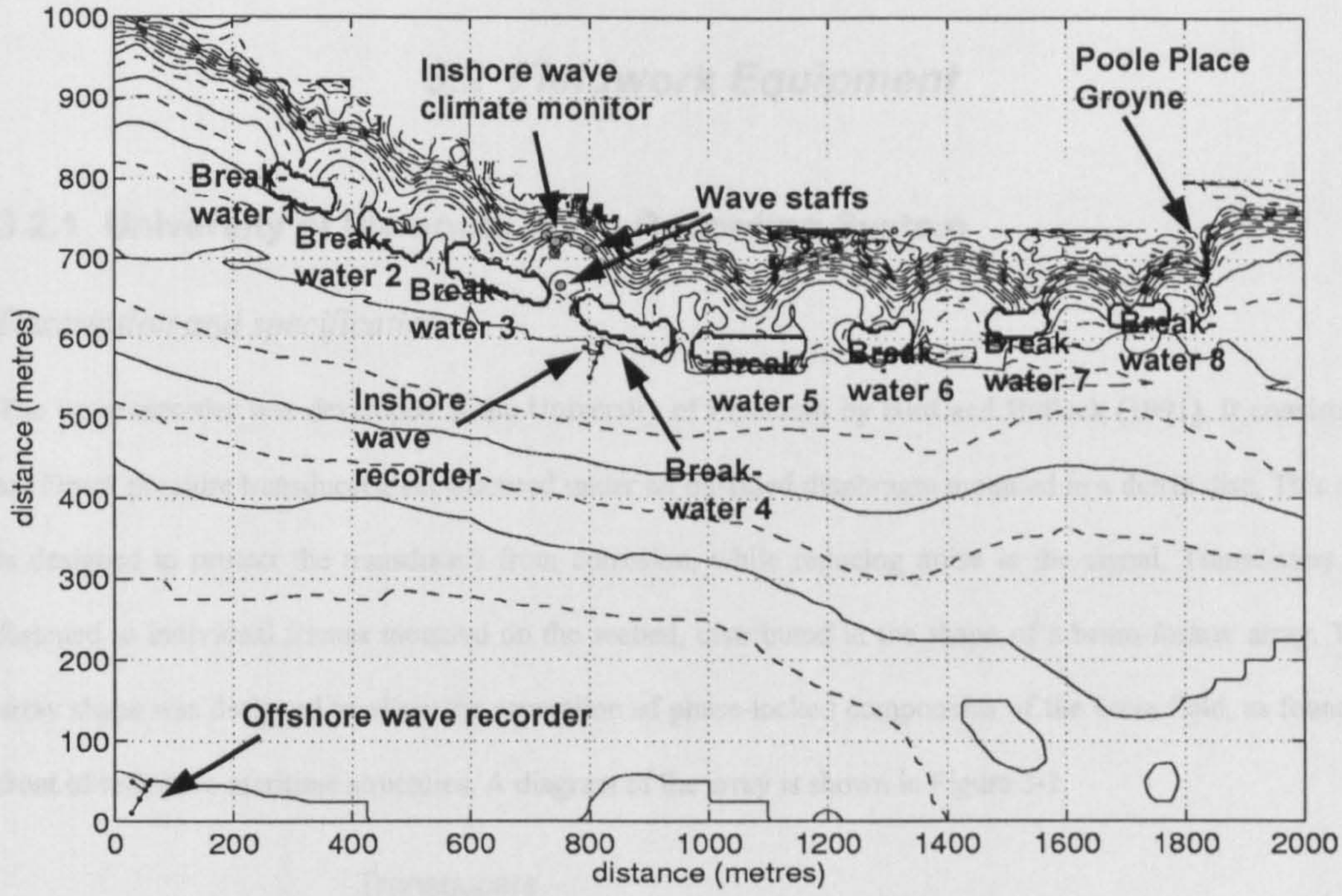

Figure 3-1 Elmer offshore bathymetry and locations of wave recording equipment

Contour lines are between -5 and +5 m OD - solid lines are at -5, -4, -3 m etc, dashed are at -4.5, -3.5 m etc. Plot also shows numbering system for breakwaters.

3.2 Fieldwork Equipment

3.2.1 University of Plymouth Wave Recording System

Description and specification

The wave recorder was developed at the University of Plymouth by Bird and Bullock (1991). It consists of six Druck pressure transducers, each housed under an oil-filled diaphragm mounted in a delrin disc. This disc is designed to protect the transducers from corrosion, while reducing noise in the signal. Transducers are fastened to individual frames mounted on the seabed, distributed in the shape of a beam-former array. This array shape was designed to allow the separation of phase-locked components of the wave field, as found in front of reflective maritime structures. A diagram of the array is shown in Figure 3-2.

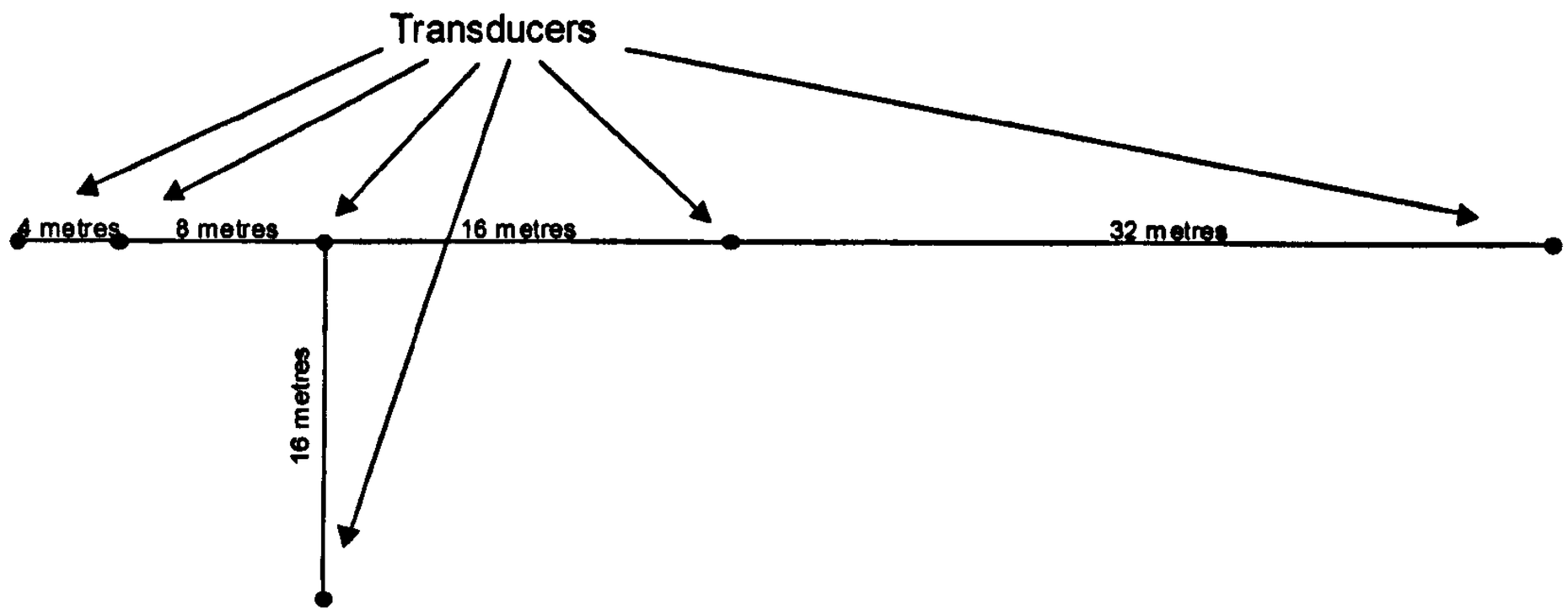

Figure 3-2 Schematic diagram of University of Plymouth wave recorder,

Relative transducer positions and nominal separations for the Elmer offshore deployment are shown.

Each transducer is connected by armoured cable to a central data logger. This contains eight 'rampacks' of CMOS semiconductor memory, sufficient to store up to 31 days of wave data. The unit also contains signal conditioning and internal calibration circuitry. Half the volume of the unit is a battery store providing power to the transducers. A data cable from the unit to the surface allows communication via an interface unit to a standard PC. For further information, the reader is recommended to study Bird (1993).

Previous uses

Prior to this study, the wave recording system (WRS) had been deployed seaward of three different structures, as part of research within the University. These were:

- Plymouth Breakwater, a rubble mound structure in 13 metres of water, and subject to severe wave attack.
- Fort Bovisand, a vertical seawall built on an inter-tidal rock ledge, 720 metres east-north-east of the eastern tip of Plymouth Breakwater. Wave recorder in ~ 7 metres of water
- Elmer 'emergency' reef-type breakwaters, constructed in autumn 1992. Wave recorder in the inter-tidal zone.

In addition to these deployments, a system supplied to Arun District Council was deployed on the sandy foreshore of a macro-tidal sand and shingle beach at Felpham, West Sussex (Axe and Bird, 1994). During this time, the wave recording system demonstrated good reliability and survivability.

Wave Recorder Deployment

Two systems were deployed at Elmer, one in the inter-tidal zone, and one 650 metres offshore of the beach, in 5.3 metres (mean water depth). Two different deployment methods were required.

For the inshore system, deployed immediately seaward of breakwater 4, Arun District Council's ground tackle was used. This consists of six steel 'chimneys', which protect and house the transducers. The data logger is mounted on a sled, and protected by a half-cylindrical steel housing. Data cables are led into this housing through narrow apertures at each end. Each part of the array is pegged into the bedrock with 0.8 metres long steel spikes. Pre-cut lengths of chain connect each section of the array, fixing the transducer spacing. This equipment was deployed at Elmer during this study, although for the EPSRC study into the Reflection Performance of Offshore Structures.

For the offshore deployment, the equipment was assembled and connected on the beach over low water as before. This time however, the transducers were mounted on brackets embedded in ¼ tonne concrete-filled tyres, and the data logger sled was without the semi-cylindrical cover. The sled was now almost 2 tonnes in weight, and had been painted in rust-inhibiting paint. Sacrificial zinc anodes were attached to all the ground tackle components. A ½ tonne concrete-filled tractor tyre was used, to act as a mooring sinker. As with the other deployment, all components were connected with pre-cut lengths of chain.

Figure 3-3 Wave recorder transducer with floats attached ready for deployment.

Photograph by R.Brown, University of Brighton

To move this equipment the ½ kilometre to the deployment site, floats were attached to each component of the array, and also to the chains. These floats consisted of polythene flasks filled with an expanding foam resin, so that if forced underwater, they would resist crushing and maintain their buoyancy. The chains were supported by many similar 5 litre floats. Transducer 6, the offset sensor, was fastened to the main axis of the array. Marker buoys were attached to each end of the array. A transducer ready for deployment is shown in Figure 3-3.

As the tide rose, the array was towed into position. An inflatable was used to keep the other end of the array straight during the tow. As the array reached the deployment site, the inshore end of the array was anchored, while the towing vessel maintained slight tension on the other end, keeping the array straight. Divers swam along the array, cutting one float from each transducer, so that the array became just negatively buoyant, and

sank. Underwater, the transducers were still buoyant enough to be moved by divers, and were manoeuvred into their correct locations. When the array was correctly positioned, the remaining floats were cut free. On the surface, all floats were recovered by the inflatable. The ½ tonne mooring sinker was deployed 10 metres east of the data logger sled. The marker buoys from the end of the array were removed, and a mooring line, consisting of 19 mm polypropylene rope, eye spliced at its lower end to a length of panzer chain, and to an orange buoy at the surface, was attached to the sinker. This mooring arrangement had the advantage of allowing a vessel to moor up to the buoy, without putting any loads onto the array. The data cable from the wave recorder was led along the seabed to the mooring block. A line from the buoy to the cable then allowed it to be raised for data to be downloaded, and then lowered to the seabed afterwards. This rather complex arrangement caused problems, and was replaced with a simpler system in February 1994, where the data cable was brought up the mooring line, and coiled below the buoy. The system was set to record data overnight. The following day, data were downloaded, the wave recorder started again, and a ring of yellow marker buoys were deployed to warn shipping away from the area.

In order to carry out directional analysis on the wave data, it was necessary to know the spacing and location of the transducers underwater. This was done using a tape survey, backed up by an EDM survey. Both surveys were carried out by divers (the author, and Mr. Steve Edmonds). The tape survey was carried out on the 4 August 94, in conjunction with an inspection of the array and a battery change for the data logger. As only a 30 metre survey tape was available, an estimate was obtained for the distance between transducers 4 and 5. The value of this distance was confirmed by the EDM survey. After this survey, it was decided that a better method would have been to drop a sinker 15 to 20 metres from the line between transducers 4 and 5, and measure the distance from this point to transducers 4,5 and 6, giving some triangulation on the location of sensor 5. This modified technique has since been used successfully in wave recorder deployments in Alderney.

Over low water, the EDM survey was completed. At this time, the water depth over the transducers was around 3 metres. A four metre long survey staff had been assembled, with a cluster of six reflectors on top. A diver located the bottom of the pole at the foot of the sensor 'chimney', while a surface swimmer kept the pole as close to vertical as possible. A survey team from Arun District Council on the beach took distance and bearing measurements on the cluster, and tied the survey in to local benchmarks. The onshore and offshore

teams communicated using two way radio. The shore team tied the survey into Ordnance Grid, and surveyed in the positions of the other instruments on the beach.

Limitations

In addition to the difficulty of surveying the offshore array, there were further problems with the wave recording system. Logging every 3.1 hours for 11 minutes at 2 Hz, the data store on the wave recorder becomes full after 31 days, and recordings cease if the system is not restarted. As the system had to be downloaded manually, through a data cable to a laptop PC, the recording routine was vulnerable to storms preventing the operator from reaching the unit. This contributed to the gap in data between 25 November 1993 to 2 February 1994. In order to minimise the risk of data loss this way, the downloading schedule was organised so that the equipment was visited every 3 weeks in summer, and every 2 weeks in winter. This safety margin was expensive to maintain, but allowed data to be recorded for the full winter period 1994 to 1995 that was missed the previous year. In addition to this problem, the record length that the instrument stores (11 minutes, at 2 Hz), is less than the more common 17 minute record. This has led to some reduction in confidence in the spectral analysis.

During deployment of the array, the connector between transducer 5 and its cable was strained. Cracks allowed water to enter, which led to corrosion of the transducer and cable. This led to a steady deterioration in the signal from this sensor, which eventually failed. Despite the sensor being replaced, no reliable data was obtained from this position.

The array stretched across 60 metres of seabed, with cables and chains joining the array components, which in turn stood 0.8 metres proud of the seabed. Despite being ringed by marker buoys, the array was still vulnerable to material such as drifting lobster pots, fishing nets and the like. During the winter of 1993-'94, the array became entangled in discarded fishing gear. The mooring buoy was lost, and the data cable had sunk, becoming wrapped around transducer 3. Divers were used to clear the site on 2 February 1994, and a new data cable, mooring line and buoy were fitted. This simpler system lasted until the end of July 1994, when barnacle fouling on the surface float cut through the mooring line. A new buoy and line were fitted, and sufficed to the end of the experiment.

The expected battery life for the wave recorder, at the stated sampling frequency and rate, is 4 months. At the end of this period, the data logger had to be recovered, and the batteries changed. When the equipment was replaced on the seabed, divers reconnected the unit to the transducers and data cable. Despite the cable ends being tagged with numbers describing which transducers they were connected to, and each diver being equipped with a laminated diagram, it was found that divers frequently connected the wrong transducers and sockets. The problem was overcome in this case by doing a wave by wave study of the relative phases of waves at each transducer. This work was carried out by Ilic. The problem is difficult to avoid with the current design of the wave recorder.

Calibration and quality control of the pressure transducers

Prior to deployment, wave recorder components are calibrated separately before the system is assembled. After assembly, a further calibration exercise takes place before deployment.

Record Timings

Timing of the offshore recorder is controlled by a real time clock in the data logger. This clock was calibrated at each download against either a recently corrected wristwatch or a GPS clock when available. Coefficients obtained from this were put into the processing software ('DECODE'), so that the processed data contained the corrected recording time. All recording was controlled in local time. The processing routines are discussed in Chapter 4.

Pressure Calibration

This wave recorder uses two internal high precision voltage sources. These provide a highly stable output that is logged alongside the output from the pressure transducers. This provides a continuous electronic calibration of the system (Bird, 1993). This information is then used in the data processing. Prior to deployment, external high precision voltage sources were connected across the data logger, and its response characteristics noted.

The pressure response of individual transducers was recorded when they were subject to varied loads from a Budenburg gauge. These two sets of data provide the initial electronic gains and offsets used in the data processing routine. The system is then assembled, and atmospheric pressure is recorded at each transducer. These values are then compared to pressure logged by an accurate aneroid barometer housed in the School of

Mechanical Engineering at the University of Plymouth. This method gives no information on the frequency response characteristics of the transducers. No calibration of the system temperature dependence over its expected operating temperature range (4° to 21°C) was carried out. This pre- deployment calibration was the same for both the inshore and offshore pressure transducer arrays.

In-situ Calibration

During such a long deployment, it was desirable to examine the stability of the system response over time. It was not feasible to recover the entire system for calibration on land, so a method was devised to calculate the calibration coefficients relative to one sensor. This could not provide absolute calibration values for the array, but it would give some idea of variability between individual transducers, and in the external circuitry of the data logger.

Transducer 1 was chosen as the benchmark for this exercise. Raw data files were converted from the hexadecimal wave recorder dump codes, to millibar pressures (using the routine 'Decode'). The pre deployment electronic calibration values were applied during this conversion. The mean pressures recorded at transducer 1 were plotted against the means recorded by the other transducers. The gradients of these lines gave the relative gains. Breaking up the record over the deployment period showed variation in gains over time. These relative gain values were put into 'DECODE', and the raw data were processed once again, to give a new set of pressure records. This removed the influence of the gains on the records. The mean pressures were re-plotted.

Transducer Offsets

After calculating the relative gains of the transducers, it was necessary to calculate the size of the offset of each signal. The differences in mean pressures recorded by each transducer were plotted over time. After correcting for the transducer gains, differences would be due to differences in depth between each sensor, and also differences in offset. Plotting sensor offset over time showed no observable variation over the entire recording period. Offset corrections were then put into the fourth stage of the 'DECODE' calibration routine, and data were reprocessed. After this final stage, the output from 'DECODE' was checked, and found to be good.

Calibration of the Inshore Pressure Transducer Array

This calibration was simpler than that carried out offshore, as the wave recorder was exposed at each low tide, allowing readings of atmospheric pressure to be taken. These were compared with the accurate aneroid barometer operated in Littlehampton by Arun District Council. This allowed the gains and offsets of the transducers to be calculated relative to this barometer.

3.2.2 Inshore Wave Climate Monitor

Description and technical specification

The Inshore Wave Climate Monitor (IWCM), developed by Chadwick *et al* (1995), consists of six resistance staffs. Four staffs are arranged in a triangular array of side 6 metres. One probe is located at each tip, with one in the centre. This provides directional wave information (after suitable processing). The two remaining poles are deployable up to 50 metres from the four pole array, and provide point measurements of surface elevation.

Each staff consists of a 6 metre plastic tube, supported by a similar length scaffolding tube. Around the plastic tube is wound 80 metres of Nichrome wire. At the top of each staff is mounted a sensor excitation and signal conditioning unit. This provides a smoothed and filtered +/- 5 Volts to each staff, with the filter unit passing all signals with a frequency less than 0.75 Hz. When operating, the Nichrome wire is exposed to the sea, which shorts out the submerged length of the wire, changing the resistance of the circuit, and hence causing a change in the voltage drop across the circuit. The voltage drop is proportional to the length of wire immersed, and so fluctuates as waves propagate past the sensor. The fluctuating signal from each sensor is taken by armoured data cable to a computer data logger up to 150 metres away. At the top of the beach, a PC fitted with an Amplicon PC 74 A/D card reads and digitises the analogue signal from each sensor. The raw data is stored on the PC hard disk, for processing either on site or back in the lab.

Previous uses

Prior to this experiment, the IWCM had been deployed at four different sites:

- Shoreham Beach. A single electronic staff was deployed in conjunction with an array for visually estimating wave direction. The system was deployed at the foot of the shingle beach, on the low tide terrace, between 2 September 1986 and 28 November 1986, when the single pole was lost in a storm.

- Wootton Creek, Isle of Wight. A single electronic staff, in a re-designed mounting frame was successfully deployed adjacent to the ferry terminal.
- Seaford Beach, Sussex. The full triangular array was deployed on the beach by Borges (1993)
- Elmer. The full array was deployed from 1 June 1992 to 2 September 1992, shoreward of the two emergency breakwaters constructed. The system recorded waves with H_{max} up to 2.46 metres. This deployment is described in Chadwick *et al* (1995).
- Felpham. One staff from the IWCM was deployed in a comparison exercise with the WRS.

Deployment and operation of the IWCM

Construction of the IWCM takes approximately two hours, and can be generally carried out over a low tide window. For this deployment however, the instrument was assembled at the top of the beach, then carried into place. The data cable was entrenched into the beach by JCB.

When operational, data logging is controlled by a BASIC program. This routine logs data every 3.1 hours, for 17 minutes at 4 Hz, but only when the water depth at the triangular array is at least 0.5 metres deep. Collected time series are displayed on screen, and automatic data processing on site is possible. Raw and processed data files are stored for downloading. The logging system is downloaded and restarted manually.

Servicing of the IWCM is simplified by its modular construction. The system can be inspected over a low tide window. Any components needing replacement can be changed at this time. Staffs showing signs of corrosion are swapped with ones from stock. Damaged components are then refurbished in the laboratory.

Limitations

Being a surface-piercing device, the monitor is particularly vulnerable to being hit by floating debris. The data cables connecting the single poles to the triangular array, and the triangular array to the logging PC, are vulnerable to damage, despite being armoured and buried into the beach. Cables became exposed as the beach crest cut back. In autumn, seaweed casts on the beach increased the loads on the cable. This finally caused the failure of the cable to the triangular array in October 1994, resulting in only non-directional information being available between October 1994 and January 1995.

In a strongly macro-tidal environment, such as Elmer, the 6 metre high poles are vulnerable to overtopping by storm waves on high spring tide. This leads to an obvious 'clipping' of the signal (analogous to saturation distortion). This clipping causes problems in the frequency analysis of the record. The effect can be minimised by fitting a crest to the record using the method described in Goda (1985).

Calibration

Calibration of the Inshore Wave Climate Monitor was carried out at Brighton University by a team led by Dr. David Pope. The calibration took two forms- static and dynamic calibration. Static calibration is carried out to relate the voltage drop across each staff to the height of water up the staff. This was done by immersing the staff a known distance into a tube of seawater.

Dynamic calibration is necessary to investigate the effect of the time lag caused by water droplets running down the staff on the output voltage. This effect was simulated by comparing this voltage change with a known drop in water level in the calibration tube. Details of this method are presented in Borges (1993). Because the nichrome wire fits in a slot in the insulating pole, the surface of each staff is smooth, and the lag time for each sensor was so small as to be negligible.

Using two independent recording systems, it was necessary to confirm that both systems were in reasonable agreement. To determine this, one sensor from the IWCM was deployed adjacent to a WRS transducer (Figure 3-4) during the deployment at Felpham, in Spring 1993. Data from the WRS was transformed from sub-surface pressure to surface elevation. These data were then compared with the surface elevation data recorded by the IWCM staff. This work was carried out and reported by Ilic (1994). The two systems were found to be in good agreement, although the WRS did slightly underestimate crest heights and trough depths when compared to the IWCM. This is typical of pressure transducer output, and may also be partly attributable to the lower sampling rate of the WRS (2 Hz compared to 4 Hz for the IWCM). The equipment deployment during the inter-comparison is shown in Figure 3-4.

Figure 3-4 Visual wave staff, resistance staff and pressure transducer during the equipment inter-comparison. The visual wave staff is the graduated staff, the resistance staff is the blue Nichrome pole, and the pressure transducer is the submerged white disc. Photograph by the author.

3.3 Additional Measurements

3.3.1 Barometric pressure

A continuous record of atmospheric pressure throughout the study period was collected by Arun District Council, from their barograph based in Littlehampton. These records were digitised by the author, and used in the calibration of the inshore wave recording system, and in all the sub-surface pressure to surface elevation calculations.

3.3.2 Beach surveys

The extent of the Elmer site precluded the use of traditional levelling techniques, using an EDM and staff. To provide a survey of the 2 km of constructed frontage, with profile lines at 30 metre intervals, the chain person would be required to walk at least 10 kilometres within a low tide window. Instead of using a large number of surveyors, it was decided to join the local authority in commissioning photogrammetric surveys of the beach. This provided both the author and Arun District Council with survey data, and split the (high) cost of the surveys. After a tendering process, the contract for five aerial surveys was awarded to Planning and Mapping Ltd, of Billingshurst, West Sussex.

Aerial surveys provided stereoscopic colour prints, at a contact scale of 1:3000 of the coastline up to 2 kilometres east of the scheme, and 1 kilometre west. Photogrammetric survey data was provided along profile lines set in discussion with Arun District Council. This gave 65 cross shore profile lines, and 4 longshore lines. Within the scheme, profile line spacing was 30 metres, with the exception of the instrumented bay, where a line spacing of 10 metres was provided. Beyond the limits of the scheme, line spacing was 50 metres. Surveys were carried out on the following dates:

2 February 1994

29 May 1994

16 September 1994

29 January 1995

16 May 1995.

Ground control for the aerial surveys was carried out by the contractor and Arun District Council. In addition to providing beach elevation information, the files supplied by the contractor included general information on

beach composition. This consisted of flags on the data, indicating a change of material. Beach material was categorised as either 'concrete' (seawall), rock (revetment or breakwaters), shingle, sand or mud. The contractors completion survey was made available by Arun District Council. All surveys were levelled to Ordnance datum.

Although photogrammetry solved the problem of surveying the large stretch of coast, the cost of each survey meant that only a few infrequent surveys were possible. Surveys were also weather and tide dependent. This last factor led to variation in the length of the some profile lines, such that the survey did not reach the depth of closure on one occasion (September 1994). The most significant drawback of these surveys concerns the level of accuracy achievable. Conventional EDM surveys can provide beach elevation information to 0.1 cm. The vertical accuracy of aerial surveys is no better than +/- 5 cm.

In addition to the photogrammetric survey data, Arun District Council supplied the results of scheme completion survey. This survey was intended to demonstrate that the scheme had been constructed according to the scheme design, and may not actually represent a true description of the state of the beach at the nominal scheme completion date (September 1993).

3.3.3 Particle size analyses

Samples of beach material were taken for analysis on two occasions. The first samples, taken in April 1994, were taken from Bay 3. Samples were taken where they appeared representative of that part of the beach, rather than at regularly spaced intervals. Five samples were taken towards the centre of the bay on the low tide terrace. Three samples were taken shoreward of breakwater 3. Four more samples were taken between the crest of the shingle and the shingle berm.

The second set of samples was taken in June 1995. Ten samples were taken between the centre of Bay 3, and the crest of the tombolo behind breakwater 3. The samples were regularly spaced along a single contour below the toe of the shingle. Samples were analysed in accordance with the dry sieving method described in British Standard 812. These data were presented in Axe (1994).

3.3.4 Photographic Record

From the start of the fieldwork programme, a photographic record of the beach was kept. At each subsequent visit to the site to download data, the beach was photographed along its length. By the end of the fieldwork, a catalogue of four hundred photographs (taken by the author and Richard Brown, technician at University of Brighton) had been assembled. These showed (generally qualitative) changes in beach levels (relative to the breakwaters), beach width (relative to the concrete revetment or seawall), and the height of escarpments in the beach material, for example.

3.3.5 Hydrographic survey data

Below the limit of the aerial surveys, bathymetric data was collected by Arun District Council. A conventional echo sounder survey was carried out from the council's 14 ft Dory. Position fixing was by DECCA (accuracy +/- 25 metres), and by horizontal sextant angles (accuracy of +/- 1 metre achievable). Survey data were reduced to Ordnance Datum. These data were digitised by the author at the NERC Image Analysis Unit , at the University of Plymouth. Data were gridded, to produce a regular bathymetric grid for numerical modelling.

3.3.6 Currents

Although tidal current information was available, no information on wave induced currents (especially shoreward of the breakwaters) was available. This information would have been desirable from both a fundamental viewpoint (to study the development of contra-rotating current cells behind breakwaters over high water) and as a verification on output from numerical models of wave propagation and sediment transport.

Six two axis Valeport electromagnetic current meters, supplied by the Institute of Marine Studies, University of Plymouth, were deployed at Elmer between 18th and 24th April 1994. These current meters were divided into two sets of three. Of these three, one head was annular, and two were spherical (although this is not believed to affect their performance). Each head was connected to a signal-conditioning unit, and then to a junction pod which was connected to the other sensors in the group, and also to the data cable. This cable was linked at its other end to data logging and power supply units at the top of the beach.

Three current meters were deployed adjacent to the IWCM, while the other three were deployed off the crest of salient 3. Data were logged at a frequency of 4 Hz for 17 minutes every 30 minutes when the lower set of equipment was immersed. After 21st April 1994, the units were logged hourly. Over each low water, each individual current meter was removed from its mount, and immersed in a bucket of seawater, to provide estimates of the current meter offsets during the deployment. Post deployment calibration took place in the towing tank at RNEC Manadon

.

3.4 Summary

The deployment and operation of all the equipment used in the Elmer fieldwork has been described. Table 3-1 summarises all data collected. The next chapter describes the processing of the data, and how it relates to other studies done in this area. The analysis of the beach data is described, and the observed beach development is reported.

Parameter measured	Method	Start date	End date	Data availability
Wave height (offshore)	Sub-surface pressure transducers	23 September 1993	14 January 1995	2437 x 11 minute samples
Wave height (inshore)	Bottom mounted pressure transducers	11 February 1994	May 1994	273 x 11 minute samples
Wave height (at the beach)	Direct measurement by resistance staffs	5 October 1993	13 December 1994	1551 records
Wave induced currents	Electromagnetic current meters, float tracking	18 April 1994	24 April 1994	63 x 17 minute samples from 6 sensors
Beach profiles	Aerial survey	September 1993	May 1995	6 surveys
Beach samples	Direct sampling	April 1994	June 1995	22 samples

Table 3-1 Summary of measured data

4. Field Data Processing and Analysis

4.1 Introduction

The first half of this chapter describes the techniques used for processing the field data. The conversion of the offshore wave recorder pressure records to surface elevation files, and the spectral and directional analysis techniques used to process this and the IWCM data are documented. Limitations of the data collection, and the data processing methods are discussed. The processing methods applied to the aerial survey data are presented, and the validation of these methods (where necessary) are described.

The second half of the chapter describes the analysis of the processed wave data, in order to compare this set of observations with 'typical' values presented by earlier researchers in this area. The beach development is described based on results of the analysis of aerial survey data.

4.2 Data Processing

4.2.1 Wave data

Pressure Records

Data are downloaded from the offshore pressure transducer array (WRS) as ASCII files. Each file consists of eight columns of data. Six columns contain the digitised signal from the six pressure transducers, while the other two columns contain calibration information from the recorder's two internal voltage sources. Each file contains up to 32 'pages' of data. Each page is 512 lines long and contains 11 minutes of data, recorded at the start of the 3.1 hour period. The first line of each is a header, containing information on the memory RAM-pack it was logged to, and also what page of the RAM-pack it is stored in. This information is kept with the data throughout processing. The other lines of data contain the pressure transducer output. The first stage of processing is to split the downloaded file into the individual pages of data. This is done using the routine 'PAGINATE' (Bird, 1993). An example of a raw 'dump' file is shown in Figure 4.1a, and the paginated data is shown in Figure 4.1b.

After pagination, data are run through the routine 'DECODE' (Bird, 1993). This takes the paginated file for input, along with a calibration file. This '.CAL' file controls DECODE, containing information on the input files to be read, the number of files to process (up to 32), the recording operation start time, and the array layout. In addition to these parameters, it also contains the calibration information described in the previous chapter. DECODE reads in the data files, and uses the reference voltage information to convert the hexadecimal output from PAGINATE into decimal, millibar pressures. The output files from DECODE contain a header of calibration information, followed by six columns of pressure data. An example of 'DECODE' output using data collected in July 1994 is shown in figure 4.1c. This data could be analysed directly to produce pressure spectra, however to allow common spectral and directional analysis routines to be used for both the Inshore Wave Climate Monitor (IWCM) and the WRS, the pressure records are converted to surface elevation. This is done using the routine 'PSURF', developed by Davidson (1993).

PSURF uses linear wave theory to convert the recorded pressure values to surface elevation over each transducer. Surface elevation η is given by

$$\eta = \frac{P}{\rho g}\left(\frac{\cosh kh}{\cosh k(z+h)}\right)$$

Equation 4-1

P is the measured pressure, ρ is water density, g is gravitational acceleration, k is wave number and z is sensor height above the bed. To solve Equation 4-1, PSURF converts pressure to an equivalent head of seawater, and de-means the data. Data are then windowed, and transformed to the frequency domain using an F.F.T. The spectral weighting function is then applied, and the smoothed frequency spectrum for each transducer is calculated. Data are then reverse transformed back to the time domain.

The $\frac{\cosh kh}{\rho g \cosh k(z+h)}$ weighting function increases rapidly with frequency (as high frequency pressure oscillations are filtered out with depth) so amplifies high frequency noise in the wave recorder signal. For this reason, instead of transforming the data up to the Nyquist frequency, a cut-off frequency of 0.33 Hz is used. Input to PSURF includes the 'decoded' pressure record, an atmospheric pressure file (containing one value of atmospheric pressure for each record, to improve the estimate of mean water depth), and information on the height of each transducer above the seabed (obtained from dive survey information).

PSURF produces four output files. The first, an information file, contains summary data for each file. This includes atmospheric pressure, mean water depth, total and gravity band (0.05 to 0.33 Hz) variance for each transducer, and also an estimate of the spectral peak frequency and significant wave height. The second file contains smoothed spectral information for each sensor. The surface elevation file consists of a header followed by (6 columns of) 1319 rows of output data. An example of this is shown in Figure 4-1d, for the same input data shown in Figures 4-1a to c. The final output file is a 'tab-delimited' text file of summary statistics for input into a spreadsheet or database.

Surface elevation records from the IWCM

The IWCM measures voltage fluctuations at each sensor. These are directly proportional to the fluctuations in surface elevation. Files downloaded at Elmer were calibrated according to the pre-deployment calibration data. The data arrived in a suitable format for further processing with no further manipulation.

Spectral and directional analysis

1. Frequency domain analysis

Data are de-trended using the second order polynomial routine in MatLab™, to remove any tidal bias in the water depth signal. This has the effect of filtering the data, so that any fluctuations in sea level due to tidal effects, or long period surf beat is removed. Data are then windowed using a Welch window. This windowing reduces spectral leakage (and thus the presence of spurious frequency components) when the data are Fourier transformed. It also reduces the variance in the input time series. To preserve the total variance when transferring data to the frequency domain, frequency domain variance is normalised to the time domain variance.

The time series were ensemble averaged with a 50% overlap, and data frequency smoothed over two frequency bins. Ensemble averaging involves the division of a record into separate segments, and the application of the F.F.T. to each segment rather than to the record as a whole. Frequency smoothing involves the summing of adjacent frequency bins. This increases the confidence of the spectral estimate, at the cost of frequency resolution. The application of both these methods gave spectral estimates with 16 and 28 degrees of freedom for the WRS and the IWCM respectively.

Figure 4.1a. Example extract from WRS dump file

```
                0705 73F9 0F01 0A03 74FC
1101 0802 72FC 1101 0703 6FFA 1201 0704
71FA 1202 0705 71FA 1101 0904 72FB 0F02
0701 72FB 0F01 0903 6FFA 0FFF 0000 0000
00CF 0735 0307 0303 0372 02FB 030F 0301
2C24 0A0D 1501 5900 0000 0000 0000 0000
Rampack number : 05   Page number : 01
2E11 0510 1501 5900 0000 0000 0000 0000
00CF 0735 03AE 03A6 041D 039C 03B7 03A4
ACA6 1C9D B8A3 ACA6 1B9D B7A3 ADA8 1B9E
B6A4 AEA7 199D B5A5 AFA9 1A9C B4A6 B0A8
199B B4A6 AFA7 1A9B B4A6 ADA6 199D B5A4
ACA6 189E B6A3 ACA5 189D B5A1 AEA7 189C
B5A4 ADA8 179B B5A6 AFA8 199B B5A5 ADA7
179C B5A6 ADA6 189D B5A4 ADA7 189D B6A2
ADA8 189E B5A3 AEA7 179D B5A4 AFA9 179C...
```

Figure 4.1b. Typical output from 'PAGINATE'

```
Rampack number : 05   Page number : 01
2E11 0510 1501 5900 0000 0000 0000 0000
00CF 0735 03AE 03A6 041D 039C 03B7 03A4
 AC A6 1C 9D B8 A3
 AC A6 1B 9D B7 A3
 AD A8 1B 9E B6 A4
 AE A7 19 9D B5 A5
 AF A9 1A 9C B4 A6
 B0 A8 19 9B B4 A6
 AF A7 1A 9B B4 A6
 AD A6 19 9D B5 A4
 AC A6 18 9E B6 A3
```

Figure 4.1c. Typical output from 'DECODE' routine,

```
% 01) FILE PATH/NAME          :dbo6r5.A01                                  %
% 02) CALIBRATION FILE        :dbo6r0_4.cal                                %
% 03) 1ST FILE DECODED @      :11 Feb 95 1704:19                           %
% 04) FILE CREATED BY         :DECODEf1                                    %
% 05) VERSION                 :1 - 11.5 94                                 %
% 06) FIRST FILE DECODED      :dbo6r5.p00                                  %
% 07)                                                                      %
% 08) WAVE RECORDER           :WR2 System 3                                %
% 09) MOD STANDARD            :Deployment B                                %
% 10) RTC ERR. (RTC/CORRECT)  :                                  1.0000%
% 11) REF. I/P FOR ADC     (V):                                  4.9935%
% 12) PROG. O/S VOLTAGE    (V):                                  1.7467%
% 13) PROG. GAIN              :                                  1.0000%
% 14) GAIN OF I/P AMP         : 4.0000 4.0000 4.0000 4.0000 4.0000 4.0000%
% 15) I/P RESISTOR      (OHMS): .0750 .0750 .0750 .0750 .0750 .0750%
% 16) TR. O/P @ ZERO P. (V, mA): 3.9929 3.9981 3.9952 3.9959 4.0040 3.9950%
% 17) TR. SENS.  (mA, mV /BAR): .0040 .0040 .0040 .0040 .0040 .0040%
% 18) OVERAL O/S ERRORS (mBAR): -2 60 -6 90 -29 70 .70 -15.40 -.50%
% 19) OVERALL GAIN ERRORS (/1): .0069 .0017 .0226 -.0081 .0023 -.0029%
% 21) LOCATION                :Elmer offshore                              %
% 22) TR. LAYOUT              :Dep B                                       %
% 23) OP. START TIME    (GMT):28 Jun 94 1240:00                            %
% 24)                                                                      %
% 25) TIME 1st READING, (GMT):19 Jul 94 0445:17                            %
% 26) DATA ELEMENT VALUES     :Abs. Pressure (mBAR)                        %
% 27) DATA ARRAY COLUMNS      :                                        6%
% 28) DATA ARRAY ROWS         :                                     1356%
% 29) READING INTERVAL    (s):                                     .5000%
% 30)                                                                      %
% 31) FINAL CALIBRATION FILE (incs Budenburg, rtc, gain and offset vals    %
% 32) generated 6/2/95                                                     %
% 33)                                                                      %
 1407 1409 1522 1406 1433 1408
 1405 1409 1521 1407 1434 1407
 1405 1409 1520 1407 1433 1407
 1406 1411 1520 1408 1432 1408
 1407 1410 1518 1407 1431 1409
 1408 1412 1519 1406 1430 1410
 1409 1411 1518 1405 1430 1410
 1408 1410 1519 1405 1430 1410
 1406 1409 1518 1407 1431 1408
 1405 1409 1517 1408 1432 1407
 1405 1408 1517 1407 1431 1405...
```

Figure 4.1d. Surface elevation file from 'PSURF'

```
% 01) FILE PATH/NAME          :c:\wr1\data\dbo6r5.C01                      %
% 02) CALIBRATION FILE        :dbo6r0_4.cal                                %
% 03) 1ST FILE DECODED @      :11 Feb 95 1704:19                           %
% 04) FILE CREATED BY         :DECODEf1    , psurf_f2                      %
% 05) VERSION                 :1 - 11.5.94 , 2 - 29.6.94                   %
% 06) FIRST FILE DECODED      :dbo6r5.p00                                  %
% 07)                                                                      %
% 08) WAVE RECORDER           :WR2 System 3                                %
% 09) MOD STANDARD            :Deployment B                                %
% 10) RTC ERR. (RTC/CORRECT)  :                                  1.0000%
% 11) REF. I/P FOR ADC     (V):                                  4.9935%
% 12) PROG. O/S VOLTAGE    (V):                                  1.7467%
% 13) PROG. GAIN              :                                  1.0000%
% 14) GAIN OF I/P AMP         : 4.0000 4.0000 4.0000 4.0000 4.0000 4.0000%
% 15) I/P RESISTOR      (OHMS): .0750 .0750 .0750 .0750 .0750 .0750%
% 16) TR. O/P @ ZERO P. (V, mA): 3.9929 3.9981 3.9952 3.9959 4.0040 3.9950%
% 17) TR SENS.   (mA, mV /BAR): .0040 .0040 .0040 .0040 .0040 .0040%
% 18) OVERAL O/S ERRORS (mBAR): -2.60 -6.90 -29.70 .70 -15.40 -.50%
% 19) OVERALL GAIN ERRORS (/1): .0069 .0017 .0226 -.0081 .0023 -.0029%
% 20)                                                                      %
% 21) LOCATION                :Elmer offshore                              %
% 22) TR. LAYOUT              :Dep B                                       %
% 23) OP. START TIME    (GMT):28 Jun 94 1240:00                            %
% 24)                                                                      %
% 25) TIME 1st READING, (GMT):19 Jul 94 0445:17                            %
% 26) DATA ELEMENT VALUES     :Surface elevation (m)                       %
% 27) DATA ARRAY COLUMNS      :                                        6%
% 28) DATA ARRAY ROWS         :                                     1356%
% 29) READING INTERVAL    (s):                                     .5000%
% 30)                                                                      %
% 31) FINAL CALIBRATION FILE (incs Budenburg, rtc, gain and offset vals    %
% 32) generated 6/2/95                                                     %
% 33)                                                                      %
   4.834   4.879   5.981   4.859   5.113   4.802
   4.845   4.868   5.929   4.858   5.067   4.877
   4.867   4.922   5.889   4.857   5.056   4.919
   4.876   4.950   5.911   4.844   5.095   4.902
   4.874   4.881   5.968   4.807   5.139   4.870
   4.864   4.829   5.993   4.785   5.136   4.839
   4.834   4.874   5.946   4.819   5.084   4.829
   4.810   4.897   5.863   4.873   5.043   4.863
   4.828   4.838   5.845   4.884   5.060   4.889
   4.847   4.816   5.928   4.864   5.107   4.854
   4.819   4.889   6.008   4.853   5.133   4.824...
```

Figure 4-1. The four stages of processing data from the University of Plymouth WRS.

Figure 4.1a shows a portion of a typical raw data file (in this case DEPB.6R5) as downloaded from the wave recorder. 4.1b shows a section of the paginated file DBO6R5.P01, taken from the raw dump file. 1c shows the header and start of the file after processing through DECODEF1, giving the pressure file DBO6R5.A01. Finally, the header and start of the surface elevation file generated by PSURF_F1 is shown in 4.1d.

Directional analysis

Barber (1963) presented the first method for the recovery of directional wave parameters from an array of gauges. His method was based on the Direct Fourier Transform, and had the virtue of being simple to apply. It did however provide a relatively poor estimate of the directional spectrum- especially when the number of wave gauges was limited. In this study, the Maximum Likelihood Method (M.L.M.) of Capon *et al* (1967) was applied. This method has been used in sea wave analysis for over a decade, due to its excellent resolving capabilities.

The aim of the M.L.M. is to minimise the variance of the difference between the spectral estimate, and the *true* spectrum, while allowing unidirectional waves (assuming no noise contamination) to be passed without bias (Pawka, 1983; Chadwick *et al*, 1995). The distribution of wave energy with frequency and direction is described by $S(f,\theta)$, the directional energy spectrum. This is related to the frequency spectrum $S(f)$ as follows:

$$S(f,\theta) = S(f).G(f,\theta)$$

Equation 4-2

$G(f, \theta)$ is the directional spreading function. To derive the directional spreading function, it is first necessary to carry out the spectral analysis for each sensor (as described above). This gives the Fourier coefficients. Taking independent pairs of sensors, the co-spectrum (C_{ij}) and quadrature spectra (Q_{ij}) must be computed. The auto-spectrum for each sensor is calculated, and the average auto spectrum, $\hat{S}(f)$ can then be calculated. The conjugate cross spectrum matrix ϕ can be calculated from the co- and quad- spectra for each frequency bin, using Equation 4-3. To apply the M.L.M., it is then necessary to invert these matrices.

$$\phi_{ij} = C_{ij} + iQ_{ij}$$

Equation 4-3

The directional spreading function $G(f, \theta)$ can then be determined using

$$G(f,\theta) = \frac{\alpha}{S(f)}\{\sum_{i=1}^{N}\sum_{j=1}^{N}\phi_{ij}^{-1}(f)\exp[-i(kx_{ij}\cos\theta + ky_{ij}\sin\theta)]\}^{-1}$$

Equation 4-4

where α is a coefficient of proportionality used to normalise the spectrum such that, as the integral of $G(f, \theta)$ by $d(\theta)$ between $+/-\pi$ is 1, so α is described by Equation 4-5.

$$\alpha = \int_{f}^{f+\Delta f} G(f,\theta)df$$

Equation 4-5

Limitations

Despite the high directional resolution of the analysis routines used on the data, two factors affect the accuracy of the estimates of directional spectra. The first of these concerns the array design used offshore, while the second concerns the choice of analysis routine used.

The design of an optimum array shape for directional wave analysis involves a number of compromises. The directional resolution possible with an array increases as the maximum distance between gauges is increased, but the minimum separation between sensors should be less than half the smallest length of the measured waves. Goda (1985) gives further guidelines on array design, warning against causing sensor redundancy by repeating vector distances between pairs of sensors in an array. The vector distances between sensor pairs should also be distributed uniformly. This will provide homogeneity in the spectral estimate with respect to direction.

The WRS, being designed for use close to structure, was designed using a beam former array shape, similar to Barber's (1963) line arrays. These array shapes give excellent directional resolution just off the normal to the axis of the array. Because of their non-uniform distribution of vector distances between sensor pairs however, the quality of the directional spectra estimates made when wave direction is outside this optimal region is poorer than would have been obtained with a more evenly distributed array, such as a pentagonal star array. Bird (1993) accepted that :

> *'even with a fairly extensive array of six transducers, the beam pattern does not give good resolution'*

It has long been known that neither the M.L.M. or the Maximum Entropy Methods perform well when used to analyse waves near reflective structures (e.g. Isobe & Kondo, 1984). Phase locking of the incident and reflected components of the sea lead to the formation of quasi standing waves, with pronounced nodal structure (see, for e.g. Davidson *et al*, 1994). Numerical tests carried out by Chadwick *et al* (1995) demonstrated the ability of the M.L.M. to recognise phase locked reflected seas, but also the inability of the M.L.M. to represent the actual wave energy distribution.

Isobe and Kondo (1984) describe a modification to the M.L.M., which improves the estimate of the energy distribution in phase locked seas. To do this however, it requires information on the position of the 'reflection line'. This line is the plane at which the waves would theoretically have been reflected for the phases of the incident and reflected waves to be as found over the measurement location. The position of this line can be found by two-dimensional techniques, such as those described in Davidson *et al* (1994).

The final technique that could have been employed is that based on Bayesian statistics. The Bayesian Directional Method (BDM) has been employed by researchers at Aalborg University (J. Helm-Petersen, pers comm.) A comparison of the M.L.M., Modified M.L.M. and the BDM has been carried out on the Elmer data by Ilic (1999). It was found that while the BDM was generally better able to allocate energy into distinct direction and frequency bins, it was array shape rather than analysis method that controlled the quality of directional spectral estimates.

Database of wave conditions

The final stage of the wave data processing was the formation of a database of the observed wave conditions. The database is in four parts. One file contains all the information collected by the IWCM inshore of the breakwaters, while the other three contain data from the offshore deployments.

The databases contain the following information:

- Recording date, time and filename
- Mean water depth at each sensor
- Signal variance at each sensor

After this information, the database presents information grouped by sensor. This information is as follows:

- Spectral moments m_0 to m_4
- Hm_0 estimated from the sample variance
- Peak frequency
- Average period
- Spectral peakness and width parameters
- Principal wave direction
- Incident and reflected spectral moments
- Incident and reflected spectral significant wave heights

4.2.2 Beach survey data

As described in the previous chapter, beach survey data were collected by aerial stereo photogrammetry. Data were supplied as ASCII text files. These consisted of a three line header (containing the survey title, dates of survey and processing) and the data in six columns. The first two columns were labels for each survey line and point. The next three columns contained the 'x', 'y' and 'z' beach co-ordinates (in a local metric grid, but with elevations relative to Ordnance Datum). The final column was a two letter flag representing beach type.

Data supplied by the contractor was plotted relative to a local co-ordinate system. The vertical datum of the surveys was the local Ordnance Datum. To map the local grid to the UK National Grid, data would be rotated by 0.346° anti-clockwise around the point 1425.063, 868.922 in the local co-ordinate system. This point then corresponded to Ordnance Survey point 497358.95, 99829.45. For the planned modelling work, and to aid gridding of the data for analysis of the survey data, the data was rotated from the original local co-ordinate system by 19.352° clockwise about point 1890, 765.

Gridding procedures

Analysis of beach volume changes, based on the aerial survey data was carried out in the following ways:

- Data were gridded to a regular 10 × 10 metre grid. Level changes between different grids were calculated.
- Gridded data produced above were contoured, and changes in contoured areas were studied
- Volumes under each profile line were calculated using Simpson's rule.

The Simpson's rule calculation was carried out as a check on the first method, while the contour based method was chosen to complement the beach modelling methods presented in the following chapter.

A variety of commercial gridding routines were evaluated, before one was selected. The first routine tested was that supplied with Graftool™ (Adept Scientific Micro Systems Ltd., 1990). This routine creates a regularly spaced grid (of up to 64 × 64 cells), and then calculates bed elevation for each cell. A weighting factor is first calculated for each point in the input data x,y,z triplets. This weighting factor is equal to the reciprocal of the distance from each input point to the desired cell, raised to some user-defined power. For positive powers, the closer a point is to the grid cell, the greater the value of its weighting function. Each weighting function is then multiplied by the bed elevation at its particular input data point, and these

weighted elevations are then summed. This total is then normalised by dividing by the sum of the weighting factors, to give the bed elevation at that grid cell. If the x and y co-ordinates of an input triplet equal the x and y co-ordinates of a gridded cell, then this procedure is bypassed, and the grid cell is allocated the same elevation value as the input point.

Data gridded in this way were studied. The routine did not realistically representing the structures on the beach, where rapid changes in bed elevation took place over short distances. Using default values for the weighting function, the profile lines crossing the breakwaters produced a series of pinnacles. Reducing the value of the weighting function reduced this, but also had the effect of flattening the beach. Points further away from each grid node were given greater significance in determining each final value of the node, so that the elevation at the node become a simple unweighted average of the elevation of a large set of survey points.

This second gridding routine was a modification of that supplied with the data analysis package MATLAB™ (Version 4.0, The MathWorks Inc., 1993). This routine also makes use of an inverse distance function. It calculates a distance matrix based on the distance of each x,y co-ordinate from the other x,y input co-ordinates. The weighting function is then calculated from the ratio of this distance matrix (transformed using Green's function) to the elevation of the input data point. The process is then reversed to give the calculated elevation at the x,y nodes on the output grid. There is a coding error in the supplied gridding routine, which results in the creation of a singular matrix. The author modified the routine slightly to avoid this problem.

The results from Matlab did appear to be more 'realistic' than those provided by Graftool. Memory limitations however meant that the entire survey area could not be gridded at once, and so overlapping segments had to be used. Comparing the overlapping sections highlighted the problem that the inverse distance method had setting values towards the grid limits - possibly due to a lack of input points beyond the limits of the grid to calculate a reasonable weighting function. It was hoped that averaging the overlapping sections, and gridding only small sections surrounded by many input points, would reduce the size of errors introduced this way.

The author also compared the results of Matlab and Surfer (Golden Software Inc., 1984) when gridding beach data from Sidmouth for a Masters degree project (Ingles, 1996). The result showed both systems to be in good agreement, and boosted confidence in the Matlab routine further. Limited computer memory

however prevented entire surveys to be gridded at once, and so the surveys were gridded in overlapping sections - with the average result at the overlap being used. Using Surfer™ permitted the entire survey area to be gridded at once, which removed errors associated with the overlaps in the Matlab.

Surfer offered eight different gridding techniques. These are as follows:

- Inverse Distance,
- Kriging,
- Minimum Curvature,
- Polynomial Regression,
- Linear Triangulation,
- Nearest Neighbor,
- Shepard's Method,
- Radial Basis Functions

These were all tested using the input data, and residuals were calculated to allow comparison with the Matlab method, and to give some idea of the magnitude of error introduced by the gridding operation. Residuals were calculated as the difference in elevation between an input data point and its nearest grid node. The root-mean-square value was taken as a measure of the gridding skill for the survey area as a whole.

Of the available methods, the nearest neighbour and linear triangulation methods from Surfer gave the smallest rms residuals (0.16 and 0.17 metres respectively). As the nearest neighbour method works on the basis of assigning each grid node the same elevation as the nearest input data point, the low residual value was unsurprising. The topography produced by the nearest neighbour method consisted of many steps, and so looked unreasonable. The linear triangulation method resulted in a smooth, realistic topography.

4.3 Data Analysis

4.3.1 Wave data

Statistical analysis of database

After processing the wave data, standard engineering analyses were carried out. These allowed the data to be compared with predictions and measurements made by other research groups, and also highlighted any peculiarities in the data. The 'standard' analyses were as follows:

- Plotting of time series of significant wave height, peak period, peak direction, water depth
- Plotting of monthly averages of wave conditions
- Production of scatter plot, wave height and direction distributions
- Extreme value statistics

Figure 4-2 and Figure 4-3 show time series of wave conditions from the offshore and inshore wave recorders respectively. These plots allowed spurious data points that may have missed earlier quality control, to be identified and flagged, so that they could be omitted from further analyses.

The production of monthly mean values gave an idea of the seasonality in the observed signals. The monthly mean water depth, significant wave height, peak wave period and direction are shown in Figure 4-4. An apparently seasonal signal can be seen clearly in the mean sea level record. The magnitude of this signal is approximately 0.3 m from trough to crest, and similar to observed monthly mean sea level values stored by the Permanent Service for Mean Sea Level for Dover and Portsmouth for the same period. Variation in the observed wave height and period are also reasonable, with higher, longer period records characterising the winter months - the result of Atlantic storm-induced swell waves, and shorter, lower waves occurring in the summer. Seasonality in the monthly average wave direction is less convincing. The values vary from 163° to 182° relative to Ordnance Survey Grid North. There may be slight evidence to suggest that wave directions in winter are from a more southerly to south of south-westerly direction, in contrast to a slightly more south of south-easterly direction in the summer. The month by month variability however is greater than any overall trend.

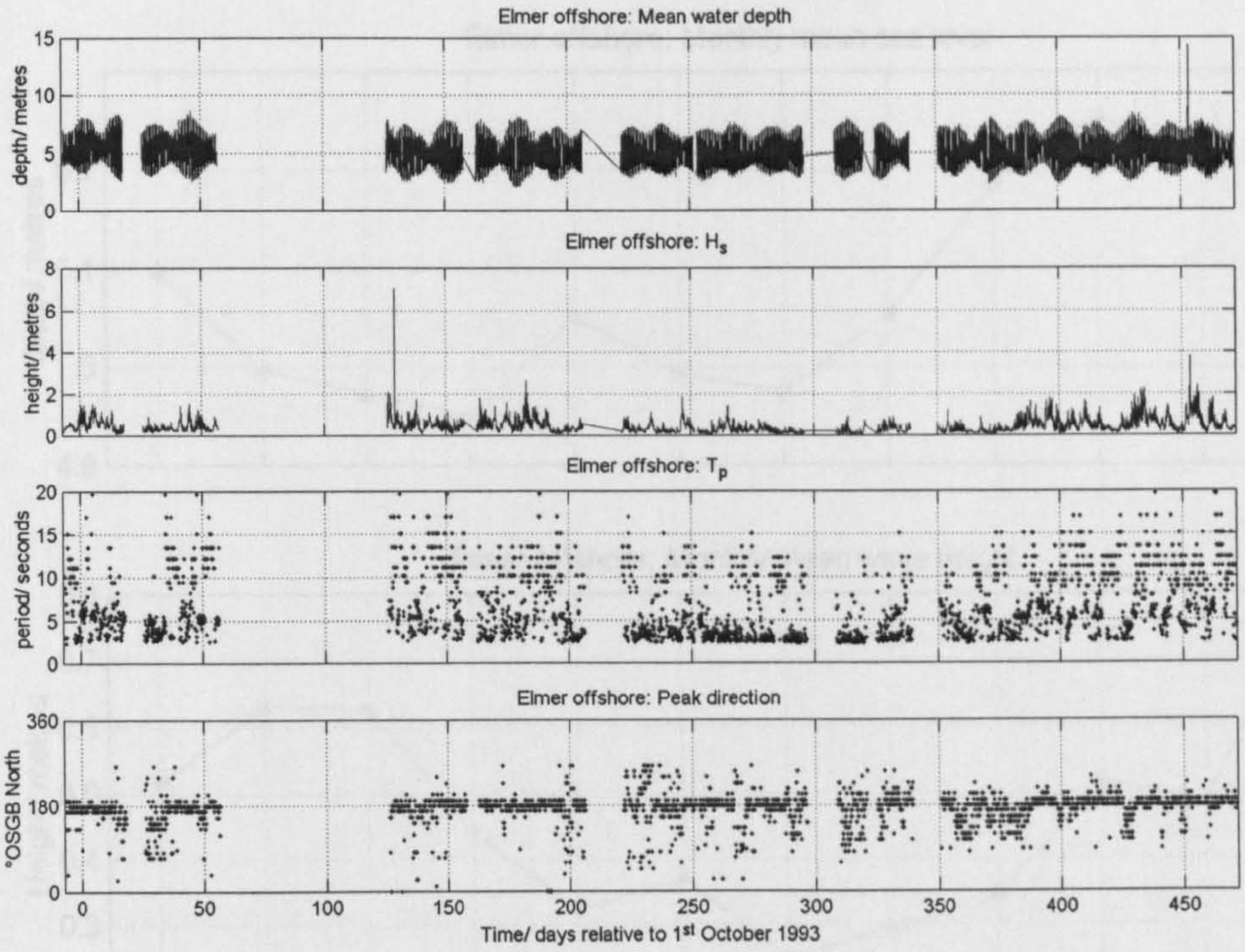

Figure 4-2 Summary plot showing time series of mean water depth, significant wave height, peak period and peak direction at the Elmer offshore array location

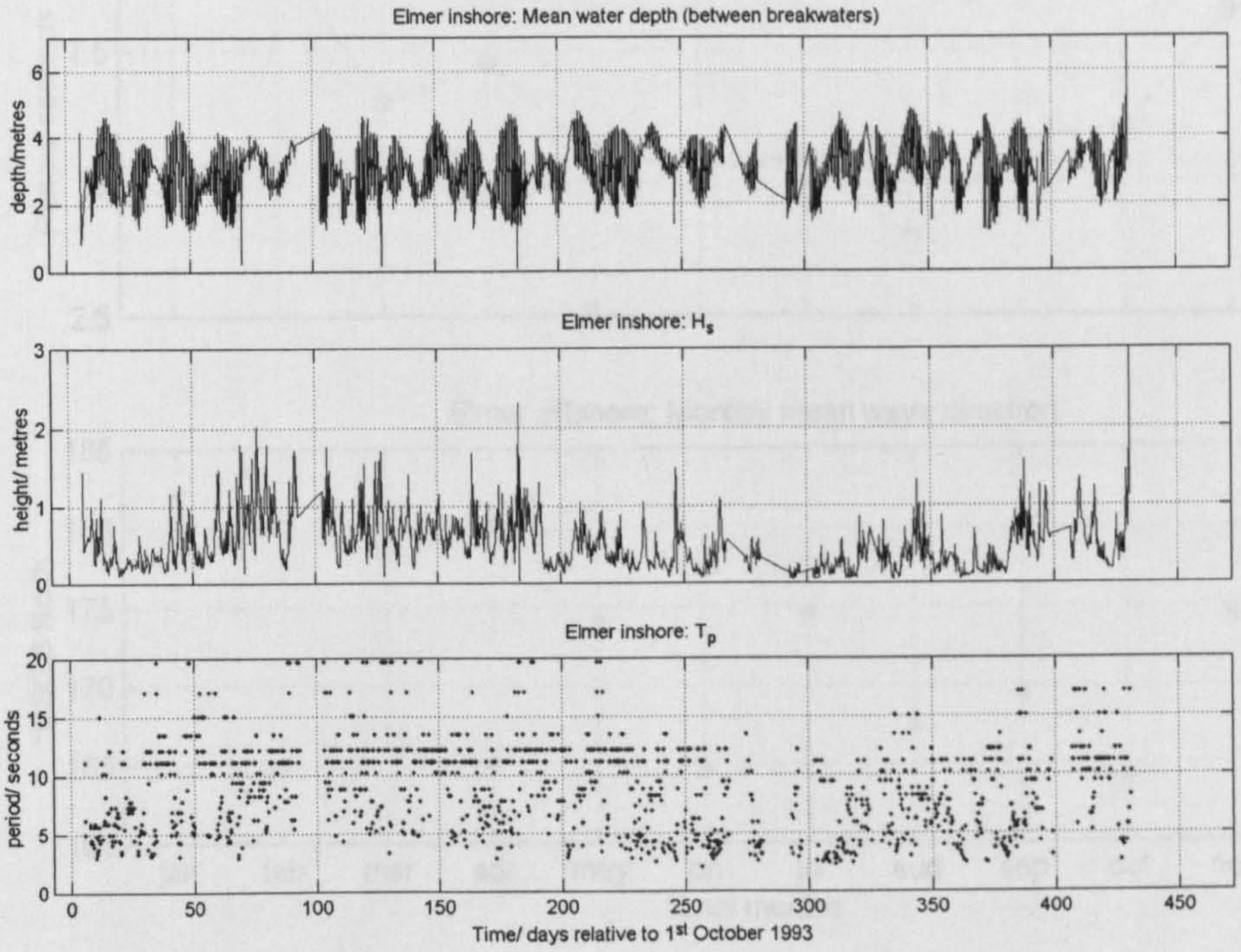

Figure 4-3 As **Figure 4-2**, but without directional information. Data from Probe 6 of the inshore wave recorder (IWCM) positioned in between breakwaters 3 and 4

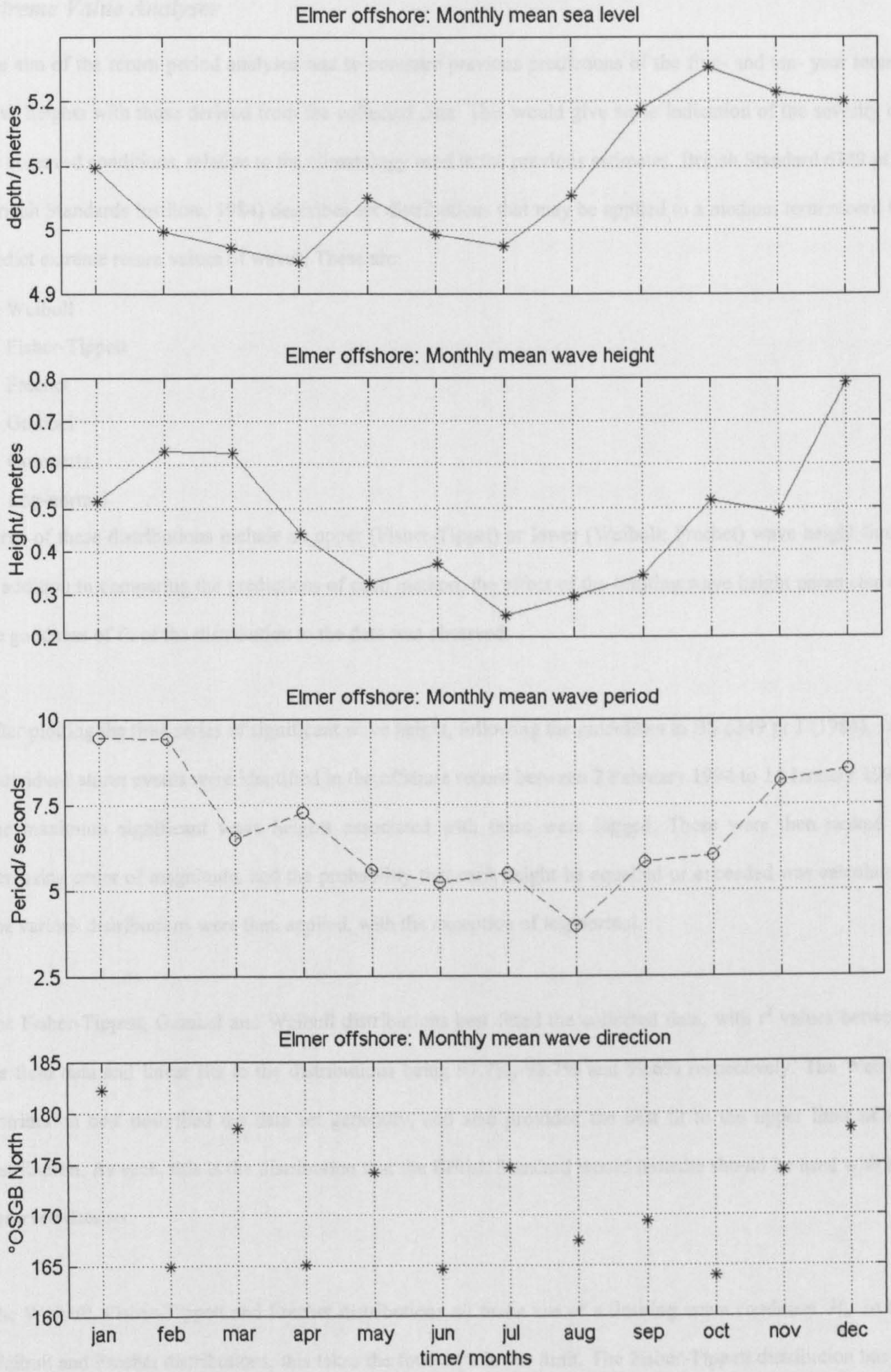

Figure 4-4 Monthly averages of water depth, significant wave height, peak period and direction observed at the Elmer offshore site.

Extreme Value Analyses

The aim of the return period analyses was to compare previous predictions of the five- and ten- year return wave heights with those derived from the collected data. This would give some indication of the severity of the observed conditions, relative to the climatology used in the previous estimates. British Standard 6349 pt.1 (British Standards Institute, 1984) describes six distributions that may be applied to a medium term record to predict extreme return values of waves. These are:

- Weibull
- Fisher-Tippett
- Frechet
- Gumbel
- Gompertz
- Log-normal

Three of these distributions include an upper (Fisher-Tippet) or lower (Weibull; Frechet) wave height limit. In addition to comparing the predictions of each method, the effect of the limiting wave height parameter on the goodness of fit of the distribution to the data was observed.

After plotting the time series of significant wave height, following the guidelines in BS 6349 pt 1 (1984), 103 'individual' storm events were identified in the offshore record between 2 February 1994 to 14 January 1995. The maximum significant wave heights associated with these were logged. These were then ranked in increasing order of magnitude, and the probability that each height be equalled or exceeded was calculated. The various distributions were then applied, with the exception of log-normal.

The Fisher-Tippett, Gumbel and Weibull distributions best fitted the collected data, with r^2 values between the field data and linear fits to the distributions being 97.7%, 98.7% and 99.6% respectively. The Weibull distribution best described the data set generally, and also provided the best fit to the upper limit of the distribution. As such, this is the distribution that the British Standard would indicate should be used with the observed data set.

The Weibull, Fisher-Tippett and Frechet distributions all make use of a limiting wave condition, H_L. In the Weibull and Frechet distributions, this takes the form of a lower limit. The Fisher-Tippett distribution has an upper limit, which may make this method suitable for use where waves are depth limited - for example in shallow water.

Both the Weibull and Fisher-Tippett distributions were found to be sensitive to changes in this limiting wave height value. The Weibull distribution was found to be much more sensitive than the Fisher-Tippett distribution, and H_L, had more effect on the wave height predictions made using these distributions.

For this data set, changes in the lower limiting value H_L for the Weibull distribution from 0.17 m to 0.2 m caused a reduced the r^2 value of the distribution from 99.6% to 98.2%. The predicted 5 year return period wave height changed from 3.0 m to 3.2 m. Increasing H_L to 0.30 m led to no significant change in the r^2 value, but did cause the predicted 5 year significant wave height to increase to 3.8m. The predicted 100 year wave height was increased from 3.9m to 5.5m.

The Fisher-Tippett distribution was much less sensitive to the upper limiting value of H_L. A one metre difference either side of the optimum value led to a 0.1% difference in r^2. A spread of values of H_L from 5 to 8m (around an optimum of 6.1m) led to predictions of the 100 year return wave being between 3.3 and 3.7m.

The guidance in the British Standard is that when using the Fisher-Tippett, Weibull or Frechet distributions, a variety of values of H_L should be tried, and the one that gives the best fit to the distribution should be used. The sensitivity of the Weibull-based estimates to the value of H_L indicates that great care should be taken when using this method for obtaining extreme wave height values. Even small differences between the selected and optimum values of H_L can cause large differences in the estimated value of the extreme wave heights. The method used here, of looking at the effect of varying H_L on the fit of the data to a perfect distribution, would appear to be a reasonable way of obtaining a reliable value for HL.

Comparison of measured data with 'typical' values

Two methods were used to assess the 'typicality' of the wave data. The first method was the comparison of the wave data with predicted wave conditions. The second method involved the comparison of wind observations from a nearby site, made during the study period, with monthly averages from the literature.

Database contents were compared with the results of a wave study carried out for Arun District Council (HR Wallingford, 1994). This study used the data generated by the UK Meteorological Office's 'Fine Mesh Wave Model'. Data covered the period October '86 to March '93, and were in the form of H_s, T_{mean} and θ, for wind and swell waves separately, and in combination. Frequency spectra, and mean wave directions for each

frequency bin, had been generated for each record. Based on this data, HR Wallingford created full directional spectra for each record at the Met. Office's offshore prediction point. Each frequency and direction component was transformed inshore using ray tracing techniques, to produce predicted wave conditions for a point on the 5 metre (below Chart Datum) contour, off Middleton-on-Sea. Data generated by this method was validated against data produced in a previous study.

This previous study provided extreme value statistics based on fourteen years of wind data (1974-1988) collected at Portland, calibrated against wave rider buoy measurements, taken in 10 m of water off Littlehampton, collected between April 1985 and March 1986 (HR Wallingford, 1988). This data had been used in the design of the Elmer scheme, both in the consultancy work carried out by Robert West and Partners (1991), and in the physical model studies (HR Wallingford, 1992a & b). The data in the 1994 report are presented in the form an annual scatter diagram, and seasonal and monthly tables of significant wave height and mean wave direction. The percentage time for which wave height thresholds were exceeded were also calculated, and a Weibull distribution fitted to the data to predict values likely to be exceeded 10%, 20% and 50% of the time.

For the second part of the comparison exercise, wind data collected at Portland, and at St. Catherine's Point Lighthouse (Isle of Wight), were compared with estimates of mean conditions. Wind data for January 1994-1995 was downloaded from the U.S. NOAA World Wide Web pages, (http://www.ncdc.noaa.gov). Monthly, seasonal and annual wind conditions were taken from Department of Energy guidance notes (Department of Energy, 1989), and from HR Wallingford (1991).

Result of Comparison

Scatter diagrams for the measured and predicted wave climate are shown in Figure 4-5 and Figure 4-6 respectively. The most obvious difference between the two figures is in the maximum wave heights. The predicted wave heights range from 0 to 4.8 m. The observations range from 0 to 2.6 m. Possible reasons for this difference are:

- waves at the observation point are depth limited
- the prediction point is further offshore, and more exposed than the recording point
- the recording period is calmer than the 10 year average used to generate the predicted data
- poor model predictions

No depth-limited waves were observed during the recording period (that is, a plot of H_{max} against depth for the offshore wave recorder showed no limiting function), although the highest predicted waves would be expected to become depth-limited offshore of the observing point under all but the highest tides. The prediction point is not more exposed than the wave recorder, being only 2 km from it in an area of simple bathymetry. The final possibility, that the HR model predictions do not describe what is observed at Elmer, are supported by the distribution of data in the scatter diagram. The HR predictions of mean conditions overestimate the number of events where the peak period of the wave field is less than about 7 seconds, and the wave height is low (less than ~1 metre). At these times, it would appear that the wave field is dominated by long period swell (of period 10 to 20 seconds). These waves would be from Atlantic storms, and have propagated up the Channel as swell. It was found that there was a strong seasonal dependence on the occurrence of the swell dominated wave spectra. The generally low wave heights associated with this swell explains why at higher wave heights, the HR predictions and the observations are in better agreement throughout the range of periods. It would appear that the long period signal is swamped by more local high energy events. In terms of predicting the frequency of occurrence of maximum wave heights, the HR predictions appear good.

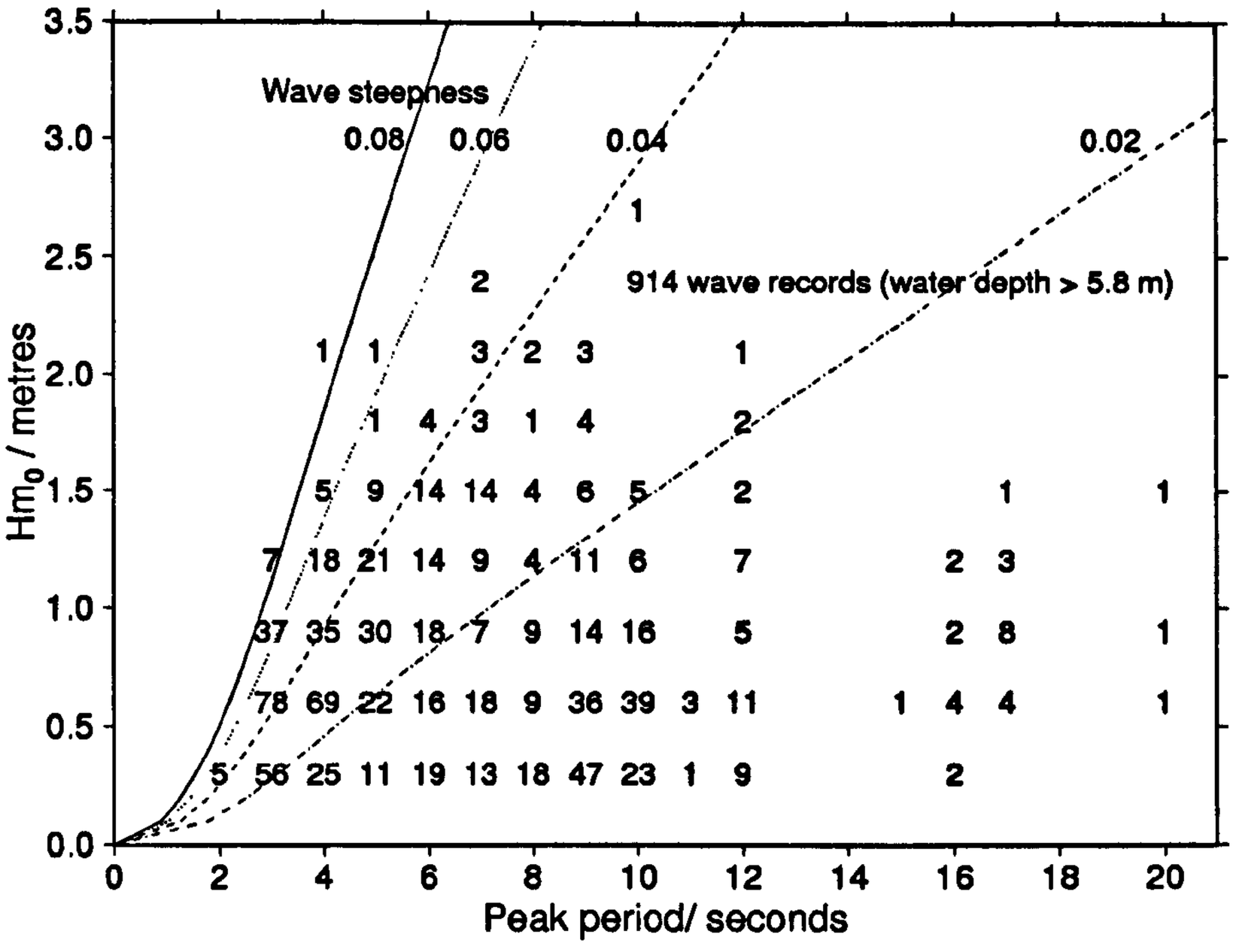

Figure 4-5 Scatter plot based on measured wave conditions at Elmer offshore position. Data based on 914 wave records (where water depth > 5.8 m). Lines for wave steepnesses of 0.02, 0.04, 0.06 and 0.08 are also shown.

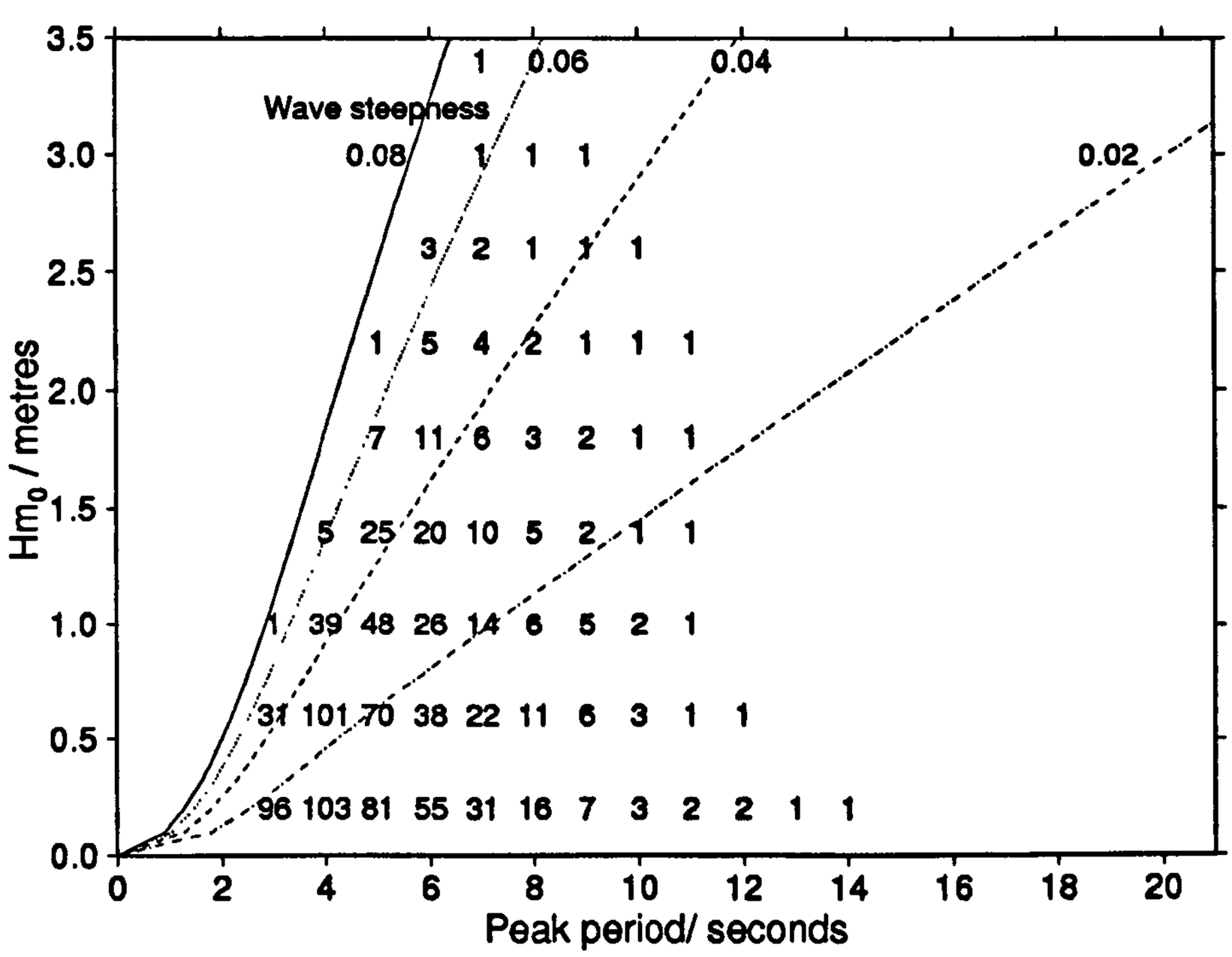

Figure 4-6 Scatter plot for offshore of Middleton-on-Sea, at the -5 metre (CD) contour, based on 'MetRay' predictions January 1987 - December 1992. From HR Wallingford Ltd. (1994).

Overall therefore, from the comparison of scatter plots, it would appear that for higher wave heights, the HR predictions are in reasonable agreement with the observations, but that the observed distribution does not extend to such high wave heights as the HR predictions. It is most likely that the lower observed wave heights were due to unusually calm weather during the observation period. It is possible that the lower observed wave heights were due to the depth limiting of some waves offshore of the wave recorder, although this was not detected in the offshore wave record (in, for example, plots of maximum wave height against water depth).

The comparison of measured and predicted wind speeds gave a similar result. Monthly wind speeds predicted for the coast from Anvil Point (Dorset) to Shoreham (~20 km east of Elmer). These data were obtained from OTH 89 299 'Metocean parameters- parameters other than waves' (Dept. of Energy, 1989). They were compared with measured wind speeds from St. Catherine's Point, in the centre of the prediction area, which were available for the period January 1994 to January 1995. The results of the comparison are shown in Table 4-1.

Month	Jan	Feb	Mar	Apr	May	Jun	Jul	Aug	Sep	Oct	Nov	Dec
Maximum predicted sustained gust (m/s)	22.4	21.8	21.1	20.4	19.1	17.7	17.1	18.4	20.4	22.4	22.4	22.4
Maximum observed sustained gust (m/s)	21	17.5	18	22	15	19	11	14	25	18	16	24
As % of prediction	94%	80%	85%	108%	79%	107%	64%	76%	122%	80%	71%	107%

Table 4-1 Comparison of predicted and measured monthly extremes of wind speed

This shows for the greater part of the year, observed maximum sustained gusts were less than those values predicted on the basis of long term records. This analysis only gives an approximate guide to how conditions during the observation period compare with longer-term conditions. The methods used here were chosen because of the problem of obtaining long term meteorological and oceanographic time series. The comparison might be made more rigorous by comparing, for example, surge activity from tide gauge records.

4.3.2 Beach data

The Elmer shoreline was constructed to match the final shoreline found in physical model tests. These tests had started with a straight beach, and were run for a 'morphological year' (i.e. exposed to model waves such that the resulting sediment transport was equivalent to that expected in a one-year period). In this way, the constructed shoreline was considered to be closer to its 'equilibrium' configuration than a straight beach. It was hoped that it would experience less reworking (and fewer losses of material) than a simple straight, plane beach.

The physical model tests were carried out by HR Wallingford Ltd (1992a & b) with an undistorted geometrical scaling of 1:80. This represented an area of 2.65 km alongshore by 0.65 km offshore. Froudian scaling was used for the waves. Wave spatial dimensions were scaled by 1:80, wave periods by $1:80^{½}$. The offshore topography was constructed in concrete, while the beach material was represented by anthracite with a specific gravity of 1.38, and particle sizes between 1.09 and 1.81 mm. The low specific gravity of anthracite was expected to represent the beach slope, and cross shore transport well, but was expected to over estimate longshore transport rate. Previous experience indicated that modelled rates were likely to be about 11 times what would be expected in the field. The rock in the breakwaters was scaled according to the Hudson formula.

The wave conditions used in the modelling are described in Table 4-2.

Return Period (years)	Still water level (m over Ordnance Datum)	Offshore wave conditions		
		Hs (metres)	T_{mean}(seconds)	Direction
5 : 1	2.80	5.64	7.93	240°, 180°
1 : 2	3.50	5.84	8.07	240°, 180°, 140°
1 : 200 (A)	3.27	8.26	9.60	240°, 180°, 140°
1 : 200 (B)	3.67	7.90	9.39	240°, 180°, 140°

Table 4-2 Wave and water level conditions used in physical model tests

The aim of the tests was to refine the number, layout and crest elevation of offshore breakwaters to be used, to reduce the overtopping along the frontage. In addition, the behaviour of the beach and structures was examined to best estimate of the volume and grading of renourishment material, and to contribute to the formulation of a beach management policy.

The Elmer beach topography, based on the post-construction survey is shown in Figure 4-7. This shows the completed shoreline behind the western two breakwaters to be straight, with parallel contours above the 0 metre OD level. The -1 metre OD contour ran seaward of the breakwaters, and shows slight indentations in the breakwater gaps. Behind breakwaters 3 and 4, tombolos existed at the 0 metre and -1 metre levels respectively, while the upper beach showed slight seaward deviations from the previously straight trend. The beach was flattened over the tombolos (beach slope between the 0 metre and -1 metre OD contours ~ 1v:40h compared with a slope of ~1v:10h for the upper, and updrift, beach). The presence of these tombolos is confirmed by a photograph of the scheme construction published in 'New Civil Engineer' (1993). Downdrift of the headland, the beach slope was unchanging (in space) between the -1 metre and +5 metre contours, although small salients were built into the shoreline behind the eastern four breakwaters.

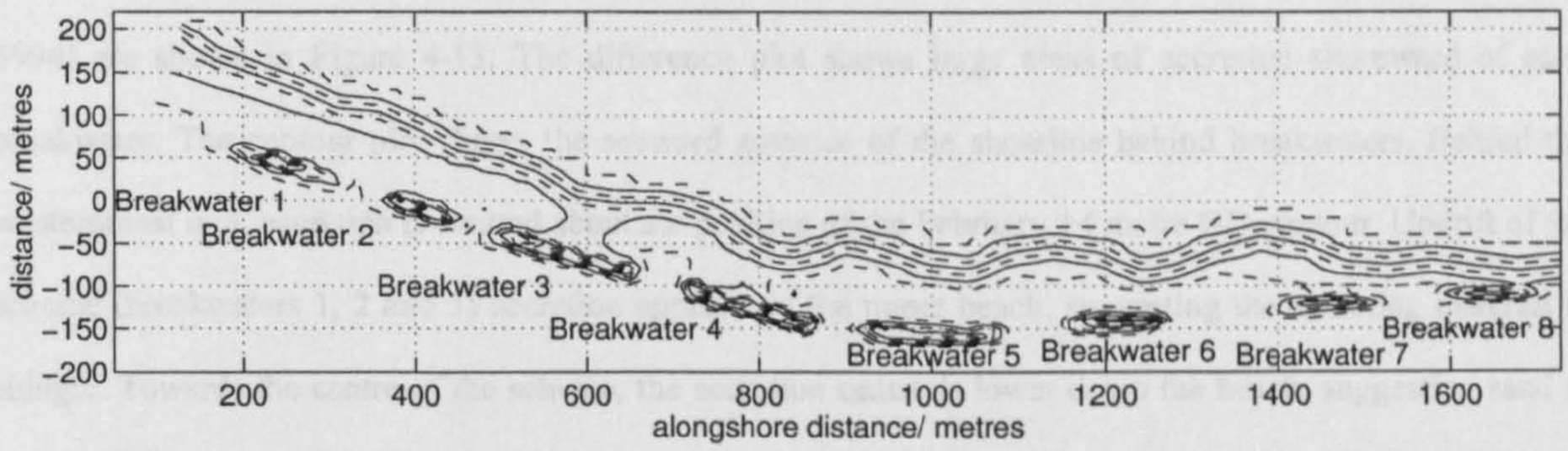

Figure 4-7 Elmer shoreline as constructed.

Levels shown as contours between -1 and +5 metres AOD. Dashed lines represent odd values, solid lines even.

The development of the beach topography was examined in terms of level changes and contour movements of the gridded surveys. Estimates of the beach volume changes were made, based on the sum of the level changes (each grid square represented 100 m^2 of beach). Estimates were also made on the basis of contour movements, to show at which levels accretion/erosion occurred. These contours were generated from the gridded data. On some of the contours produced, the contour positions were not strictly monotonic, (that is for each alongshore position, there exists only one contour position). Where the beach line did go back on itself, then the file was edited by eye. Any errors that this would introduce are expected to be small and localised.

Volume changes were also calculated by looking at area changes under each profile. Profile areas were calculated using Simpson's rule.

4.3.3 Beach Changes

The following section describes the changes in beach morphology between successive surveys. These changes might be accounted for by seasonal profile changes, so a description of annual morphology changes (February 1994 to January 1995, and May 1994 to May 1995) is included.

September 1993 to February 1994

The shoreline behind breakwaters 1 and 2, in September 1993, is shown in Figure 4-8. Level differences and contour movements between the completion survey (September 1993) and the first aerial survey (February 1994) are shown in Figure 4-13. The difference plot shows large areas of accretion shoreward of each breakwater. The contour plot shows the seaward advance of the shoreline behind breakwaters. Behind the westernmost unit, accretion is centred about the position of the February +4 metre OD contour. Updrift of the scheme (breakwaters 1, 2 and 3) accretion appears on the upper beach, suggesting the accreting material is shingle. Towards the centre of the scheme, the accretion centre is lower down the beach, suggesting sand is accreting. In the centre of the scheme, the centre of accreting areas Most accretion occurred behind breakwater 1 (~ +2 m); breakwater 7 and breakwater 8 (both > 2 m change in beach level). The accretion behind breakwater 1 is shown in Figure 4-9.

In addition to the salient growth that these level changes indicate, several areas of beach seaward of the Ordnance Datum contour show accretion of up to 0.4 m. This is apparent to the west, and seaward of, breakwater 1, and in the bay shoreward of breakwaters 4 and 5. Contour movements show this accretion as an offshore movement behind each breakwater. Behind breakwaters 1-3, the +1 metre contour advances by 37, 30 and 24 m respectively. Other contours do not move equally, indicating a flattening of the beach profile behind the breakwaters. Beach levels dropped primarily on the upper beach, shoreward of the + 1 metre OD contour. These losses were generally located just west of the bay mid-line. Beach levels dropped by around 2 m in the bay shoreward of breakwaters 5 and 6. The contour plot shows the retreat of the shoreline in the embayments. Changes in beach slope in the bays are minimal. This erosion is also apparent from

photographs of the beach at this point, which show the revetment at the back of the bay between breakwaters 4 and 5 becoming exposed, and of cliffs of height 1 metre forming in the compacted replenishment material. This is illustrated in Figure 4-10, Figure 4-11 and Figure 4-12. Gridded level changes indicate that net accretion within the scheme was +6 200 m^3 of material in this first winter period. This compares with annual longshore drift estimates of between 5000 and 20000 m^3 per year (Robert West and Partners, 1991).

Figure 4-8 Shoreline behind breakwaters 1 and 2, September 1993 (photograph by the author)

Figure 4-9 Shingle accretion behind breakwater 1 (photograph by the author)

Figure 4-10 Beach in front of bay 5 revetment, High water, September 1993. Photograph by the author

Figure 4-11 Bay 5 revetment (low tide) February 1994. Photograph by the author

Figure 4-12 Cliffing in renourished material, bay 5. April 1994. Photograph by author

Figure 4-14 shows the differences in position of the 0 to +4 metre contours between September 1993 and February 1994. This plot shows most accretion occurred at the 0 metre level, particularly behind the western two breakwaters, where the contour moved seawards by 50m. There is a similar pattern of accretion and erosion at the +1 metre level, with salient growth greatest behind the same western breakwaters (between 200 and 500 m alongshore).

Behind the eastern two breakwaters, accretion is greater at +1 metre AOD than at 0 metres, which indicates a steepening of the beach as tombolos form. Above the +1 metre contour, movement is similar to that observed below. Salient lengths are reduced, although the amount of erosion in the bays is similar between levels 0 to 3 metres. Overall, this indicates a flattening of the beach profile over the (particularly updrift) salients. Net volume changes associated with these contour movements (between 120 and 1730 m alongshore) are shown in Table 4-3.

Level	Mean contour movement	Volume change associated with this movement
0 metre contour	+6.70 m	+10 850 m^3
1 metre contour	+1.90 m	+3090 m^3
2 metre contour	-1.98 m	-3190 m^3
3 metre contour	-2.95 m	-4760 m^3
4 metre contour	-3.53 m	-5700 m^3
Total volume change		+ 290 m^3

Table 4-3 September 1993 to February 1994 volume changes - estimated on the basis of contour movements

Analysis of beach volume change based on Simpson's rule showed a net accretion of 17 600 m^3. The longshore distribution of this accretion is shown in Figure 4-15.

Over this period, the three analysis methods gave the following values for the volume change within the scheme:

Gridded survey data: + 6 200 m^3

Simpson's rule calculations: + 17 600 m^3

Contour movements (upper beach): + 290 m^3

There is a considerable discrepancy between these estimates. Each method has limitations that could contribute to the difference. The gridding method uses a weighted averaging technique to estimate the elevation of each grid node. The limits of the gridded area are not set by the survey data, but are specified by

the user in the first instance. The grids are then cropped to remove points that lie outside the surveyed areas. This cropping introduces some subjectivity. In addition, the position of survey points over each breakwater was not the same from survey to survey (although the position of each survey line was). When gridding the data, the heights of each breakwater varied from survey to survey – due to different points being used to define their shape. The breakwaters could either be left in the grid, which would have introduced large and spurious volume changes to the calculations, or edited out. This editing also introduced an element of subjectivity.

The low level of accretion in the contour-movement method is most likely because the method was not extended below the Ordnance datum contour. This was because the shoreline position was not monotonic below 0 m AOD – particularly around the breakwaters where most accretion was occurring – and the results of the contour movements were to be compared with output from a numerical model, which required the modelled contour to be monotonic. As a result, this method ignored the large volumes of sand that accreted offshore of the 0 metre contour, and were observed by the other techniques. The method is still useful however, as it suggests that if the beach was reshaping – and re-working, then the volume changes introduced by this can be accounted for by the contour movements above Ordnance Datum level. Any accretion observed below this level can be attributed by material being trapped (temporarily or permanently) by the scheme.

The Simpson's Rule method is the simplest used, as it only takes the input survey data into account. The method still suffers the same problem as the gridding technique – in that the use of different survey points on one transect over a breakwater between different surveys can cause large differences in the estimated volume of the breakwater. This introduces false volume changes that can be of a similar magnitude to the beach volume changes themselves. To avoid this, the breakwaters were edited out of the profiles before calculating the profile volumes. This also introduces some small element of subjectivity into the solution of the problem.

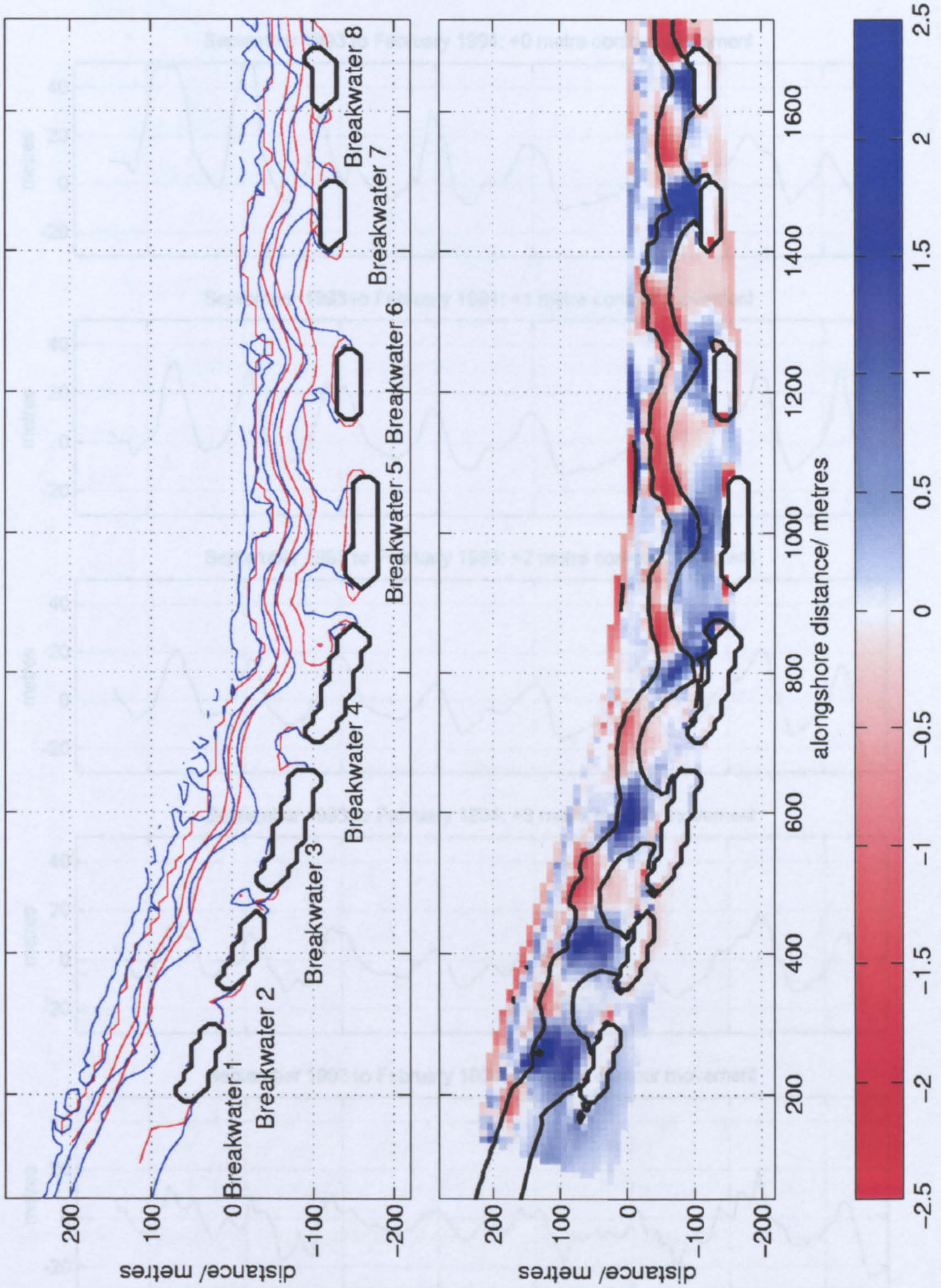

Figure 4-13 Elmer beach changes, September 1993 to February 1994.

Top figure shows -1, +1, +3 and +5 metre (AOD) contour positions for September 1993 (red) and February 1994 (blue). Lower figure shows level changes from the September position, where colour maps to level change (in m) as shown on the colour bar.

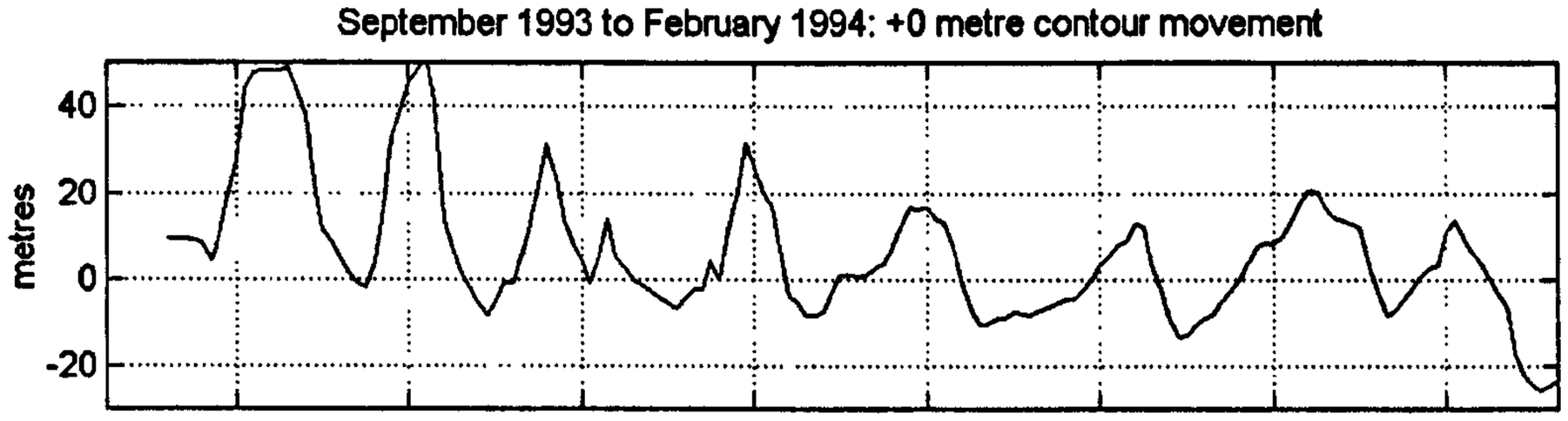

Figure 4-14 Contour movements at different levels along the Elmer frontage between September 1993 and February 1994.

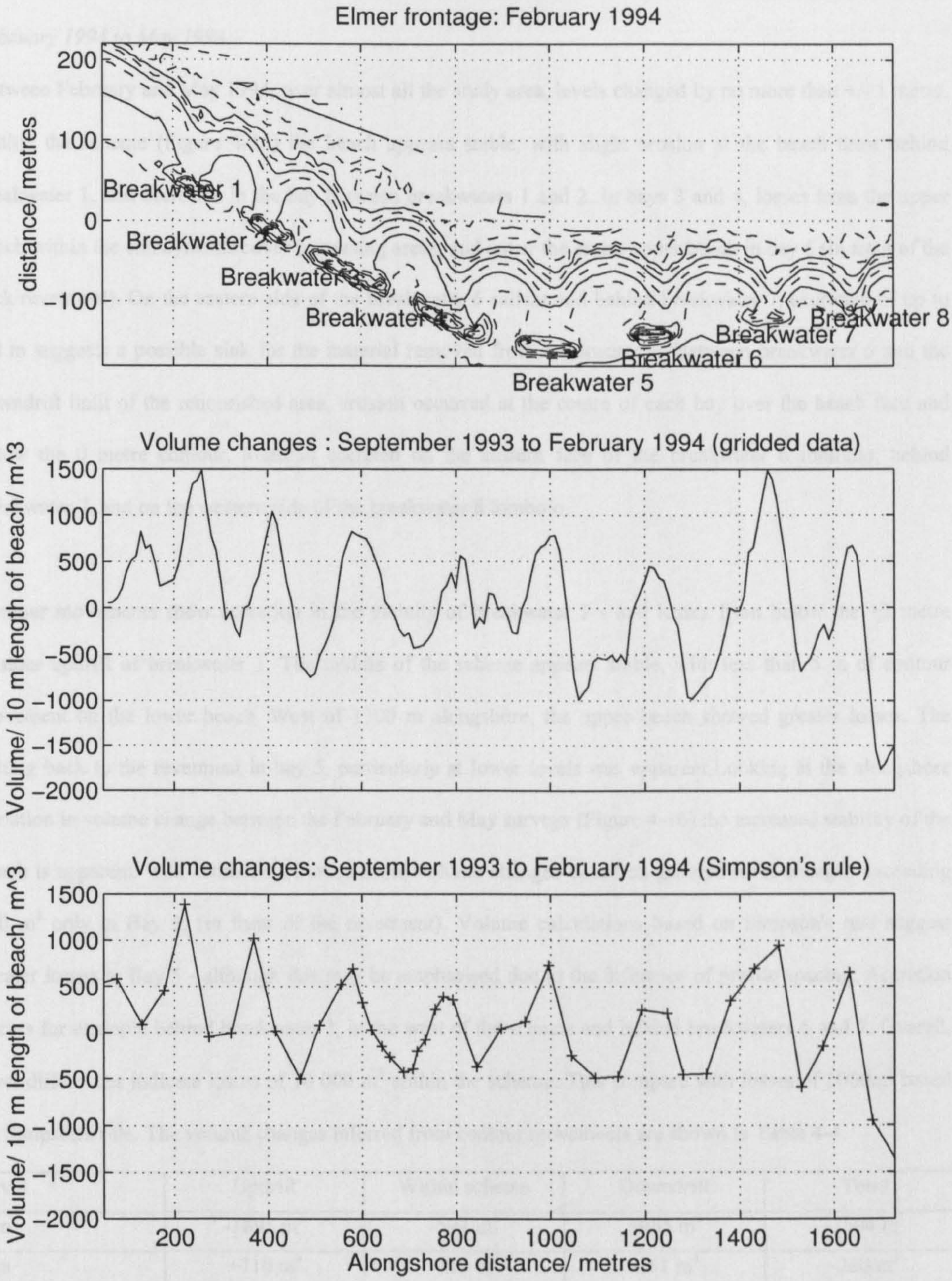

Figure 4-15 Volume changes (September 1993 – February 1994) based on summing the gridded level changes at each alongshore cell, and directly from the profile information using Simpson's rule.

Gridded data have a 10 metre resolution (hence show the net volume change over those 10 metres alongshore). The volumes calculated with Simpson's Rule were based on the actual survey line spacing (10 or 30 metres) and have been normalized to allow direct comparison with the gridded data.

February 1994 to May 1994

Between February and May 1994, over almost all the study area, levels changed by no more than +/- 1 metre. Within the scheme (Figure 4-16) the beach appears stable, with slight erosion at the beach crest behind breakwater 1, and accretion in the bay between breakwaters 1 and 2. In bays 3 and 4, losses from the upper beach within the embayments cover increasing areas, and cover the entire upper beach in bay 5 (in front of the rock revetment). On the eastern side of the breakwater 6 salient and behind breakwater 7, accretion of up to 0.8 m suggests a possible sink for the material removed from breakwater 5. Between breakwater 6 and the downdrift limit of the renourished area, erosion occurred at the centre of each bay over the beach face and below the 0 metre contour. Material accreted on the eastern face of the breakwater 6 tombolo, behind breakwater 7, and on the western side of the breakwater 8 tombolo.

Contour movements show accretion in the vicinity of breakwater 2 - and losses from below the +2 metre contour updrift of breakwater 1. The middle of the scheme appears stable, with less than 5 m of contour movement on the lower beach. West of 1300 m alongshore, the upper beach showed greater losses. The cutting back to the revetment in bay 5, particularly at lower levels was apparent.Looking at the alongshore variation in volume change between the February and May surveys (Figure 4-16) the increased stability of the beach is apparent, with estimates of cross shore volume changes based on gridded level changes exceeding 500 m^3 only in Bay 5, (in front of the revetment). Volume calculations based on Simpson's rule suggest greater losses in Bay 5 - although this may be emphasised due to the influence of profile spacing. Accretion occurs for example behind breakwater 3, in the west of the scheme and behind breakwaters 6 and 7. Overall, level differences indicate losses of 10 000 m^3 within the scheme. This compare with losses of 3000m^3 based on Simpson's rule. The volume changes inferred from contour movements are shown in Table 4-4.

Level	Updrift	Within scheme	Downdrift	Total
0 m	-1895 m^3	-594 m^3	+985 m^3	-1504 m^3
1 m	+710 m^3	-319 m^3	-651 m^3	-260 m^3
2 m	-18 m^3	-27 m^3	-284 m^3	-329 m^3
3 m	-210 m^3	-454 m^3	-361 m^3	-1025 m^3
4 m	-249 m^3	-1467 m^3	-193 m^3	-1909 m^3
Total	-1662 m^3	-2861 m^3	-504 m^3	-5027 m^3

Table 4-4 Volume changes between February and May 1994, inferred from contour movements

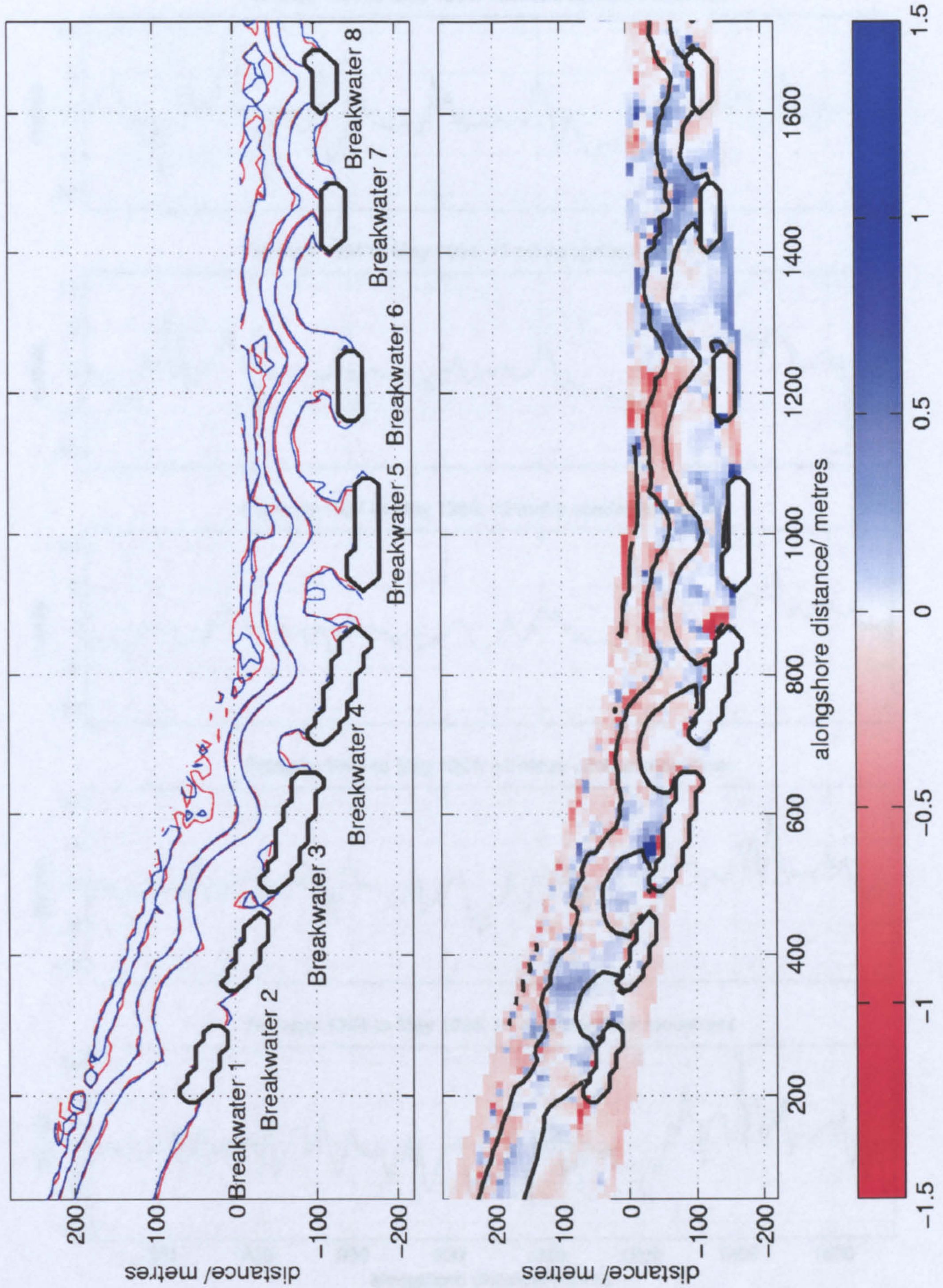

Figure 4-16 Elmer contour positions (red: February 1994, blue: May 1994) and level changes between February and May 1994.

Colour represents level change in metres corresponding to the value on the colour bar.

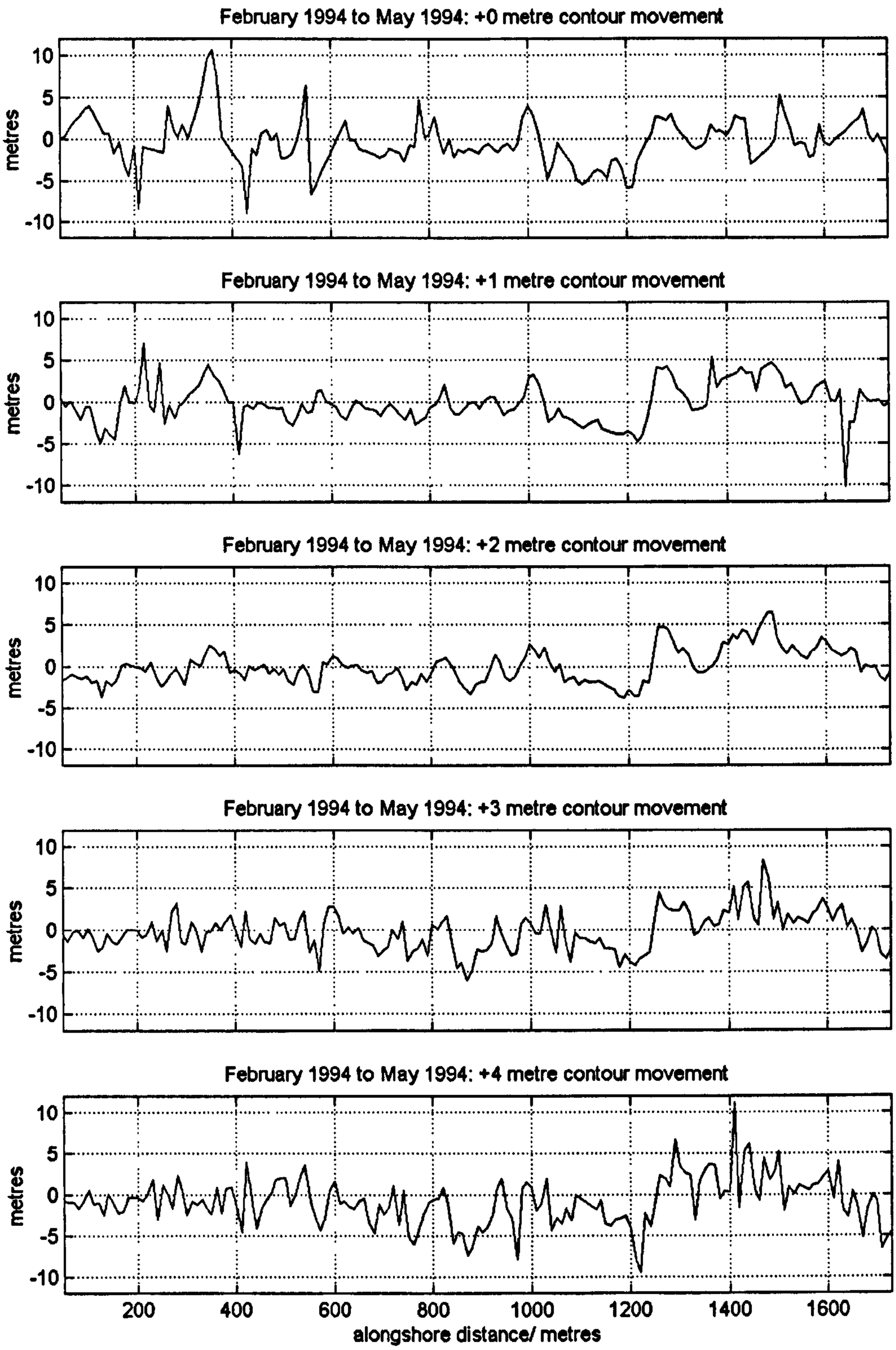

Figure 4-17 Contour movements at 0 - +4 m above Ordnance Datum, for Elmer frontage between February and May 1994

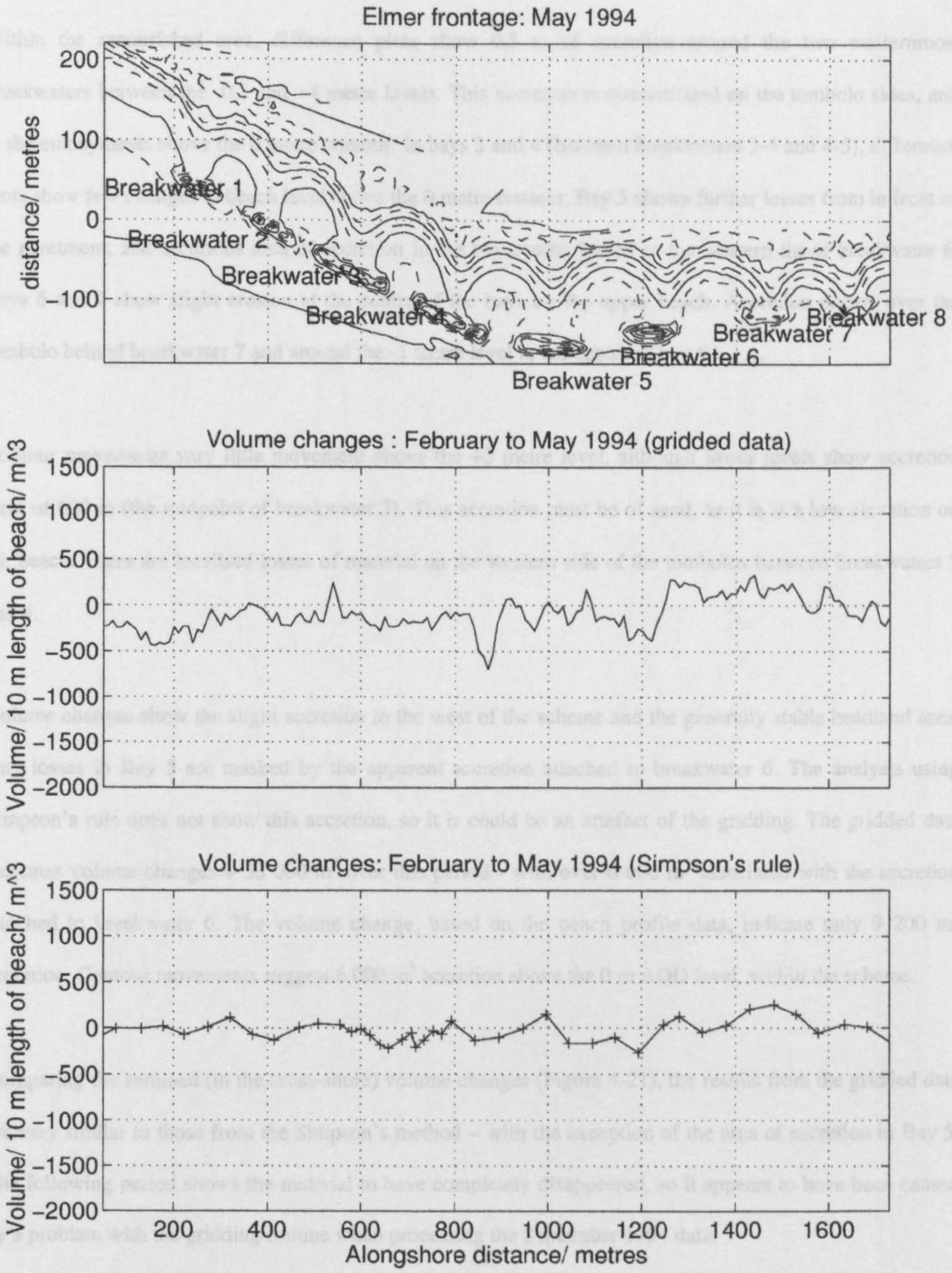

Figure 4-18 Elmer volume changes based on summing the gridded level changes at each alongshore cell (middle slide), and directly from the profile information using Simpson's rule (bottom slide). Elmer data, February to May 1994

May 1994 to September 1994

Within the renourished area, difference plots show 0.5 m of accretion around the two westernmost breakwaters between the -0.5 and +4 metre levels. This accretion is concentrated on the tombolo sides, and in the embayments above the 0 metre contour. In bays 3 and 4 (between breakwaters 3-4 and 4-5), difference plots show few changes in beach level above the 0 metre contour. Bay 5 shows further losses from in front of the revetment, and a curious area of accretion in the bay centre, linked to the western tip of breakwater 6. Bays 6 and 7 show slight erosion at the centre of the bays on the upper beach. Accretion occurs over the tombolo behind breakwater 7 and around the -1 metre level in the centre of bay 6.

Contour movements vary little movement above the +3 metre level, although lower levels show accretion west of 600 m (the midpoint of breakwater 3). This accretion must be of sand, as it is at a low elevation on the beach. There are localised losses of material on the western side of the tombolos between breakwaters 2 and 4.

Volume changes show the slight accretion in the west of the scheme and the generally stable headland area. Any losses in Bay 5 are masked by the apparent accretion attached to breakwater 6. The analysis using Simpson's rule does not show this accretion, so it is could be an artefact of the gridding. The gridded data indicates volume changes + 33 000 m^3 over this period - with over 6 000 m^3 associated with the accretion attached to breakwater 6. The volume change, based on the beach profile data, indicate only 9 200 m^3 accretion. Contour movements suggest 6 000 m^3 accretion above the 0 m AOD level, within the scheme.

Comparing the summed (in the cross-shore) volume changes (Figure 4-21), the results from the gridded data are very similar to those from the Simpson's method – with the exception of the area of accretion in Bay 5. The following period shows the material to have completely disappeared, so it appears to have been caused by a problem with the gridding routine when processing the September 1994 data.

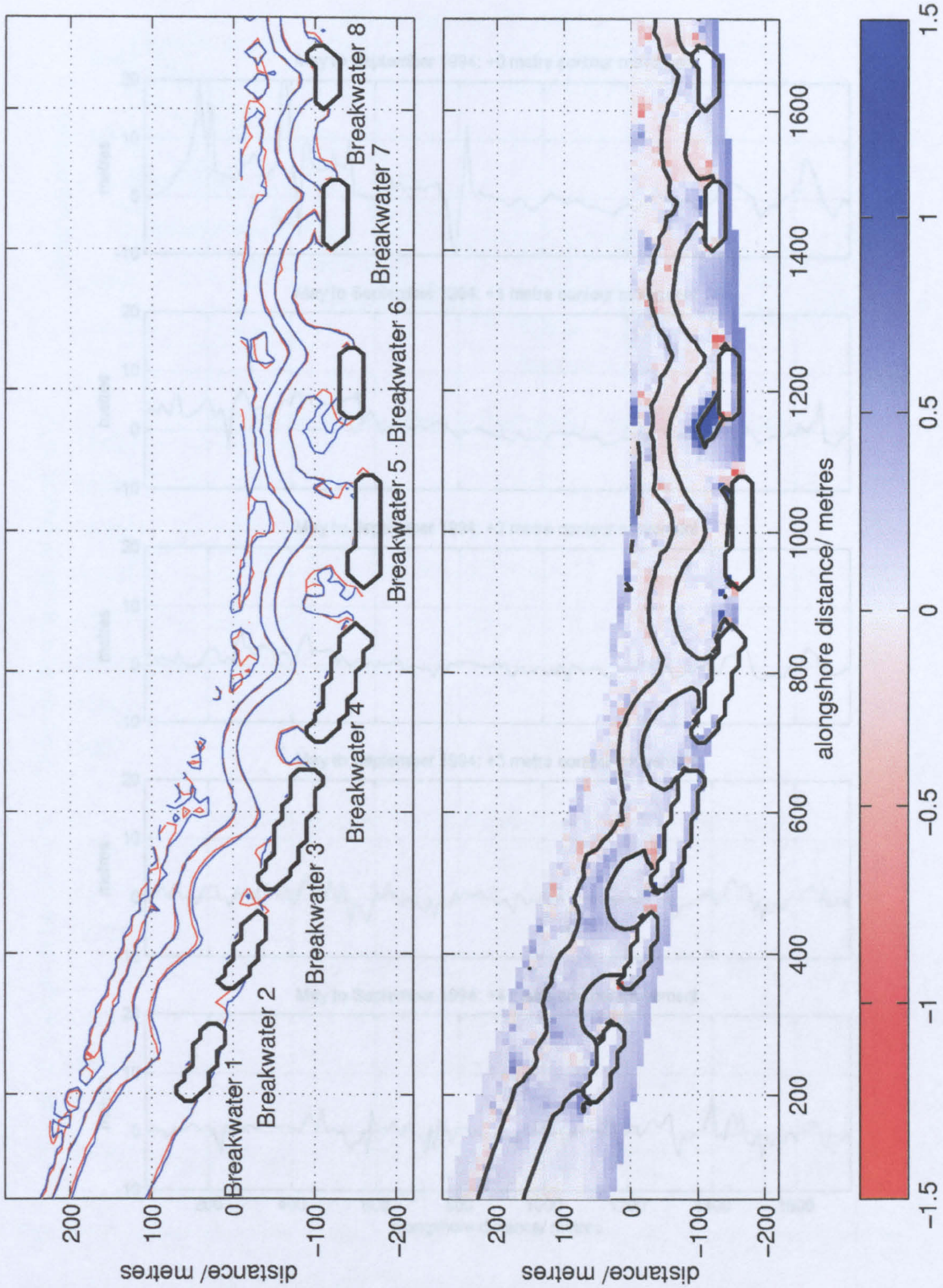

Figure 4-19 Elmer contour positions (red: May 1994; blue: September 1994) and level changes (in metres)

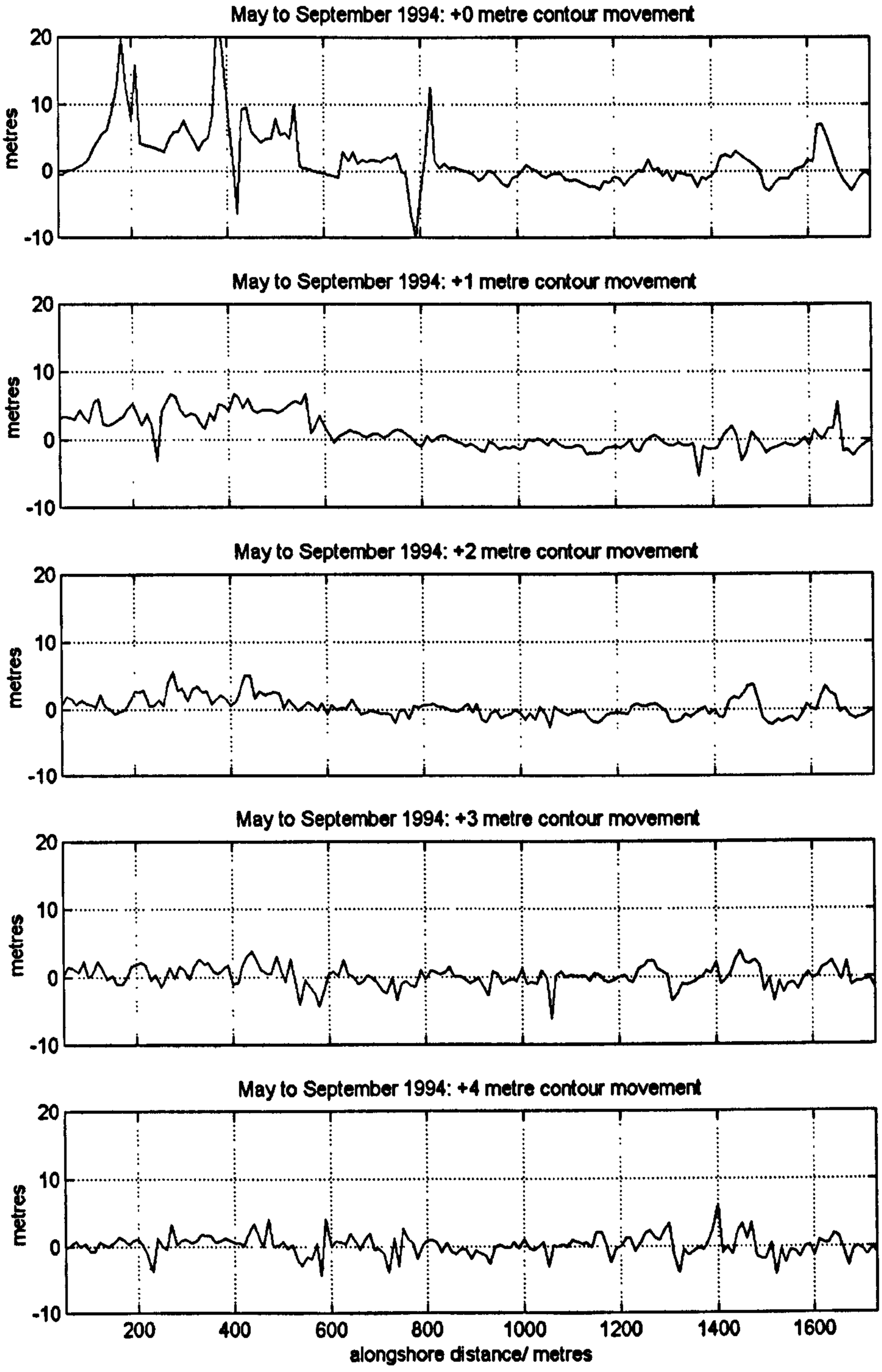

Figure 4-20 Contour movements at 0 - +4 m above Ordnance Datum. May 1994 to September 1994

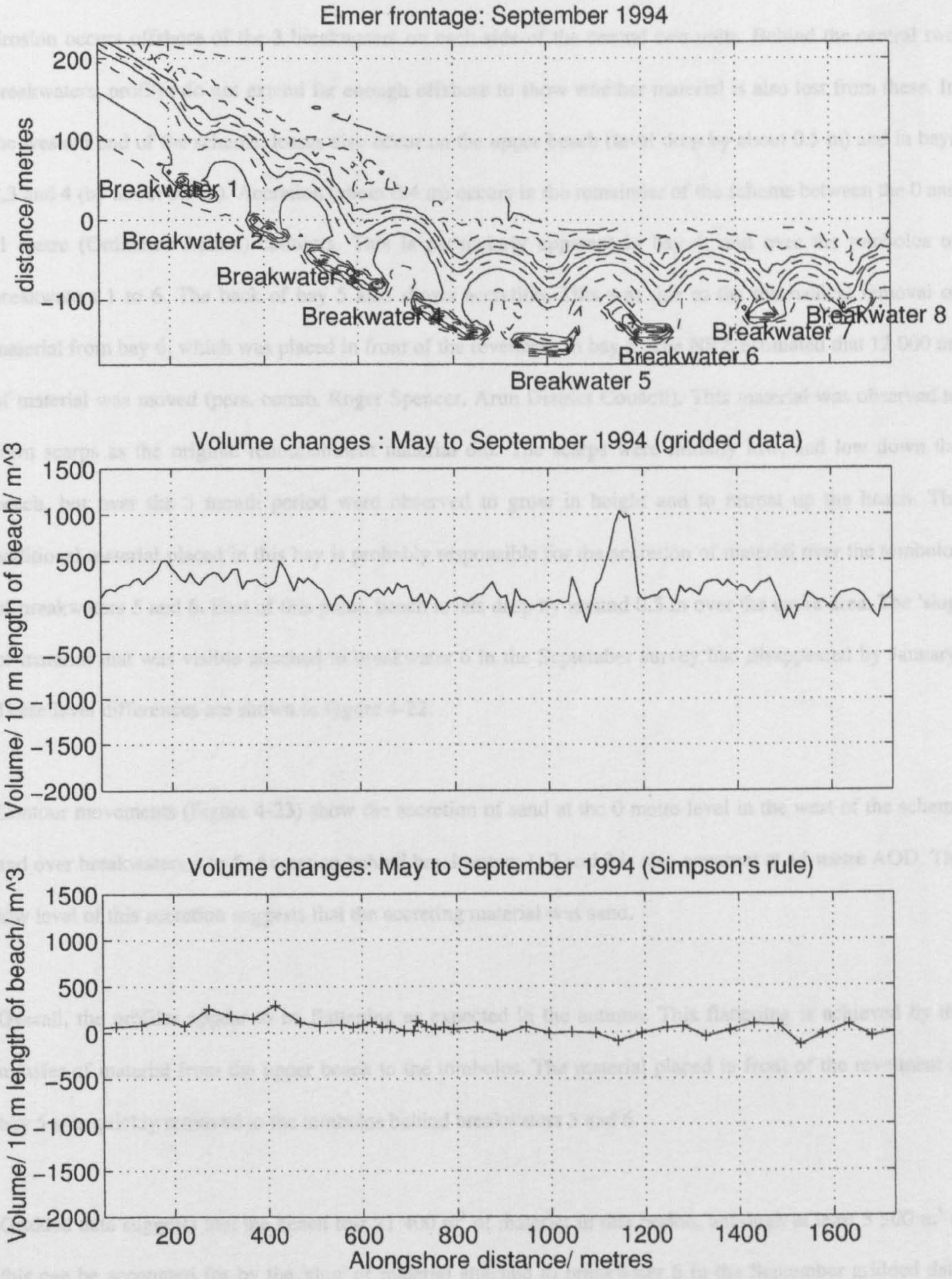

Figure 4-21 Alongshore volume changes between May and September 1994, based on summing gridded data for alongshore points (middle) and by Simpson's rule for each profile line (bottom)

September 1994 to January 1995

Erosion occurs offshore of the 3 breakwaters on each side of the central two units. Behind the central two breakwaters, profiles do not extend far enough offshore to show whether material is also lost from these. In the western end of the scheme, losses also occur on the upper beach (level drop by about 0.5 m) and in bays 2,3 and 4 (by about 0.2 m). Accretion (about 0.4 m) occurs in the remainder of the scheme between the 0 and -1 metre (Ordnance Datum) contours. This is particularly apparent in bay 1, and over the tombolos of breakwaters 1 to 6. The back of bay 5 also shows accretion. This was due to the mechanical removal of material from bay 6, which was placed in front of the revetment in bay 5. The NRA estimated that 12 000 m^3 of material was moved (pers. comm. Roger Spencer, Arun District Council). This material was observed to form scarps as the original renourishment material did. The scarps were initially low, and low down the beach, but over the 3 month period were observed to grow in height and to retreat up the beach. The additional material placed in this bay is probably responsible for the accretion of material over the tombolos of breakwaters 5 and 6. East of this point, beach levels drop by around 0.5 m over the entire area. The 'slug' of material that was visible attached to breakwater 6 in the September survey had disappeared by January. These level differences are shown in Figure 4-22.

Contour movements (Figure 4-23) show the accretion of sand at the 0 metre level in the west of the scheme and over breakwaters 1 to 5. Accretion behind breakwaters 1, 2 and 3 is also apparent at +1 metre AOD. The low level of this accretion suggests that the accreting material was sand.

Overall, the profiles appear to be flattening as expected in the autumn. This flattening is achieved by the transfer of material from the upper beach to the tombolos. The material placed in front of the revetment in bay 5 was quickly removed to the tombolos behind breakwaters 5 and 6.

Gridded data suggests that the beach lost 21 400 m^3 of material in this period, although at least 5 500 m^3 of this can be accounted for by the 'slug' of material attached to breakwater 6 in the September gridded data.

The analysis of beach profile changes showed the beach lost 7 400 m^3. Contour movements indicated losses of 3000 m^3 between 0 and +4 AOD, although the 0 metre contour showed accretion of 4 200 m^3 - demonstrating a further flattening of the beach profile.

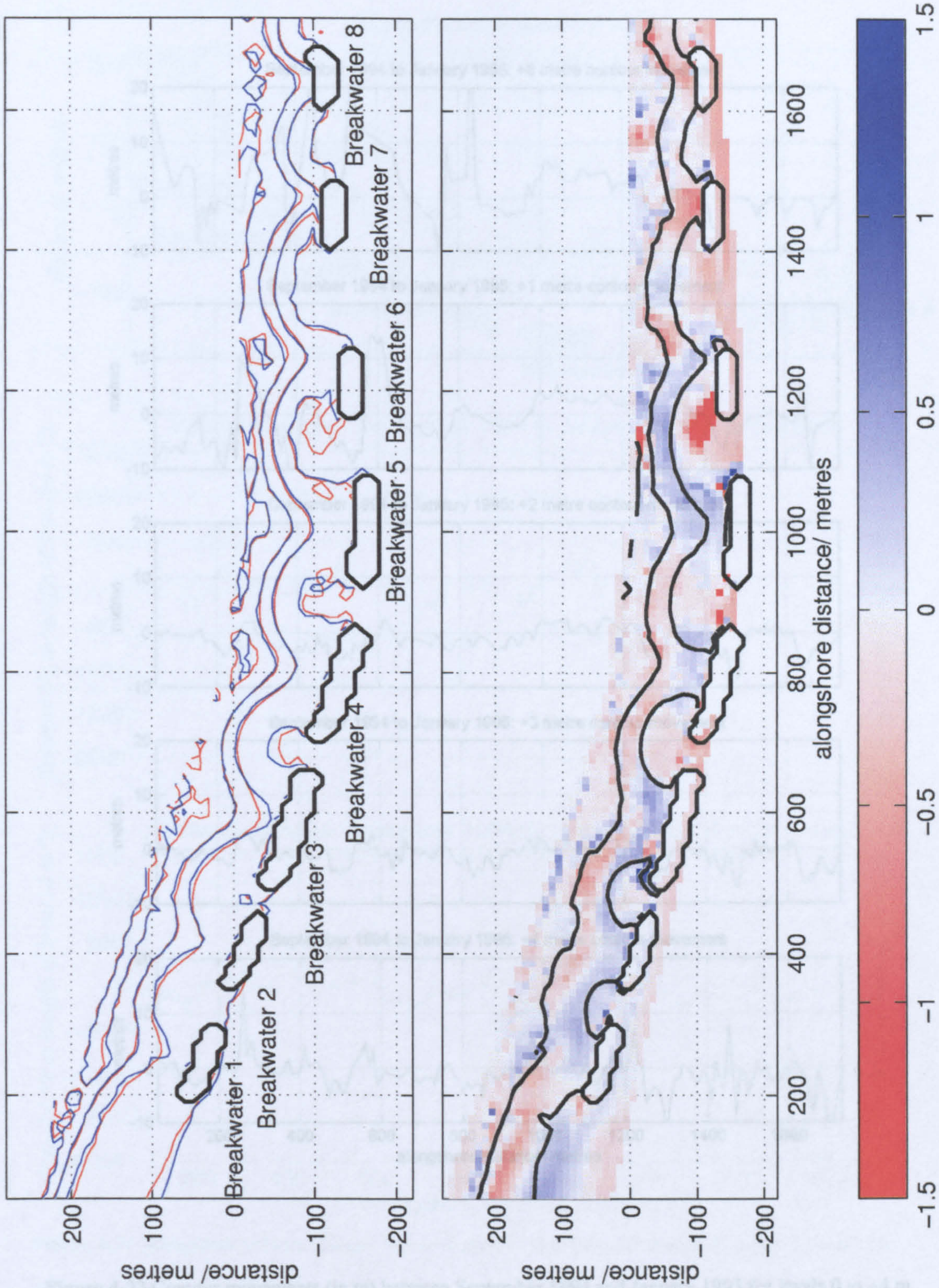

Figure 4-22 Contour positions in September 1994 (red) and January 1995 (blue) and level changes (in metres) between September 1994 and January 1995.

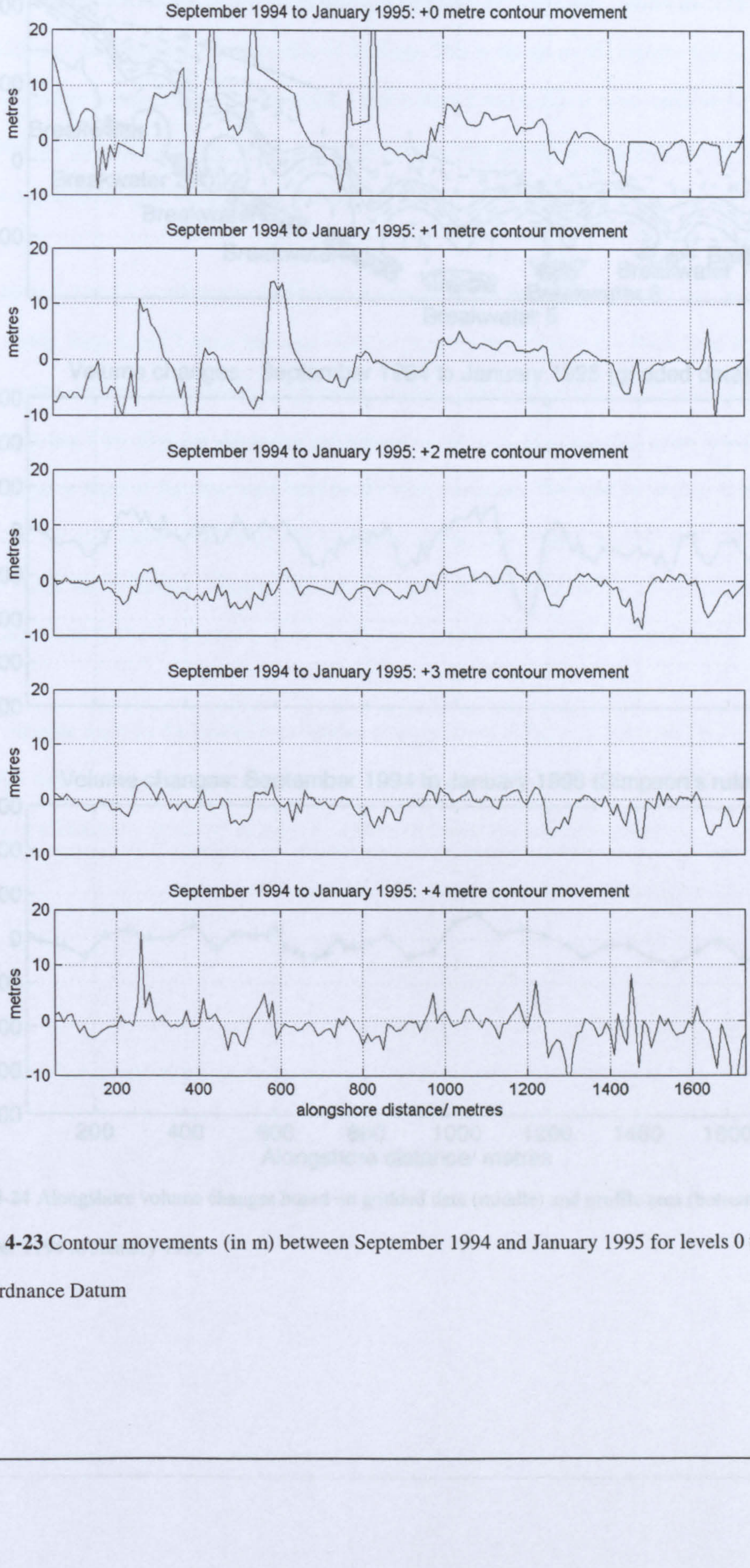

Figure 4-23 Contour movements (in m) between September 1994 and January 1995 for levels 0 to +4 m over Ordnance Datum

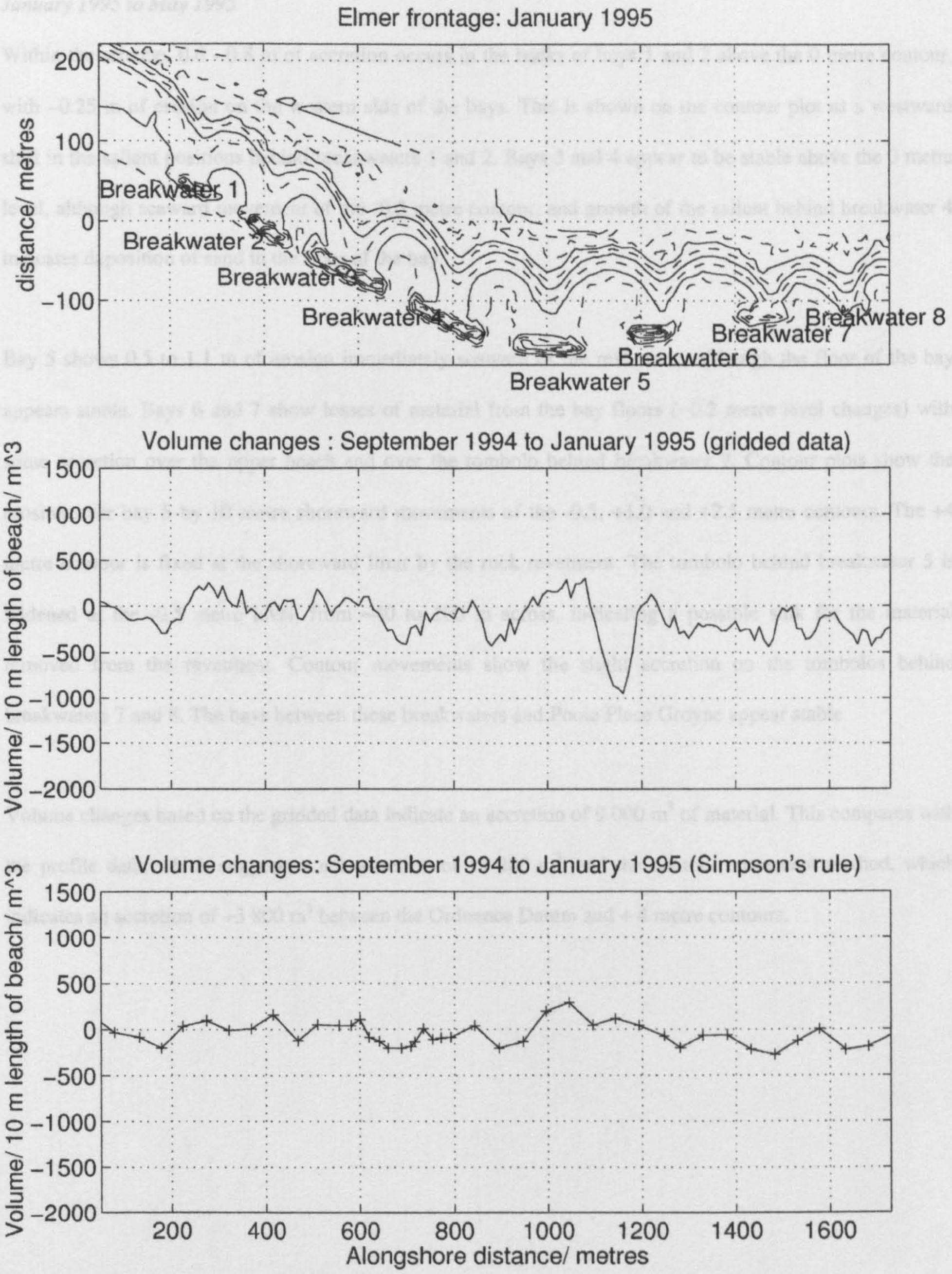

Figure 4-24 Alongshore volume changes based on gridded data (middle) and profile area (bottom), for September 1994 to January 1995

January 1995 to May 1995

Within the scheme, 0.6 - 0.8 m of accretion occurs in the backs of bays 1 and 2 above the 0 metre contour, with ~0.25 m of erosion on the western side of the bays. This is shown on the contour plot as a westward shift in the salient positions behind breakwaters 1 and 2. Bays 3 and 4 appear to be stable above the 0 metre level, although seaward movement of the -0.5 metre contour, and growth of the salient behind breakwater 4 indicates deposition of sand in the floor of the bay.

Bay 5 shows 0.5 to 1.1 m of erosion immediately seaward of the revetment, although the floor of the bay appears stable. Bays 6 and 7 show losses of material from the bay floors (~0.2 metre level changes) with some accretion over the upper beach and over the tombolo behind breakwater 7. Contour plots show the erosion over bay 5 by 10 metre shoreward movements of the -0.5, +1.0 and +2.5 metre contours. The +4 metre contour is fixed at the shoreward limit by the rock revetment. The tombolo behind breakwater 5 is widened at the -0.5 metre level, from ~40 to 100 m across, indicating a possible sink for the material removed from the revetment. Contour movements show the slight accretion on the tombolos behind breakwaters 7 and 8. The bays between these breakwaters and Poole Place Groyne appear stable.

Volume changes based on the gridded data indicate an accretion of 9 000 m^3 of material. This compares with the profile data, which suggests a net accretion of 12 200 m^3, and the contour movement method, which indicates an accretion of +3 800 m^3 between the Ordnance Datum and + 4 metre contours.

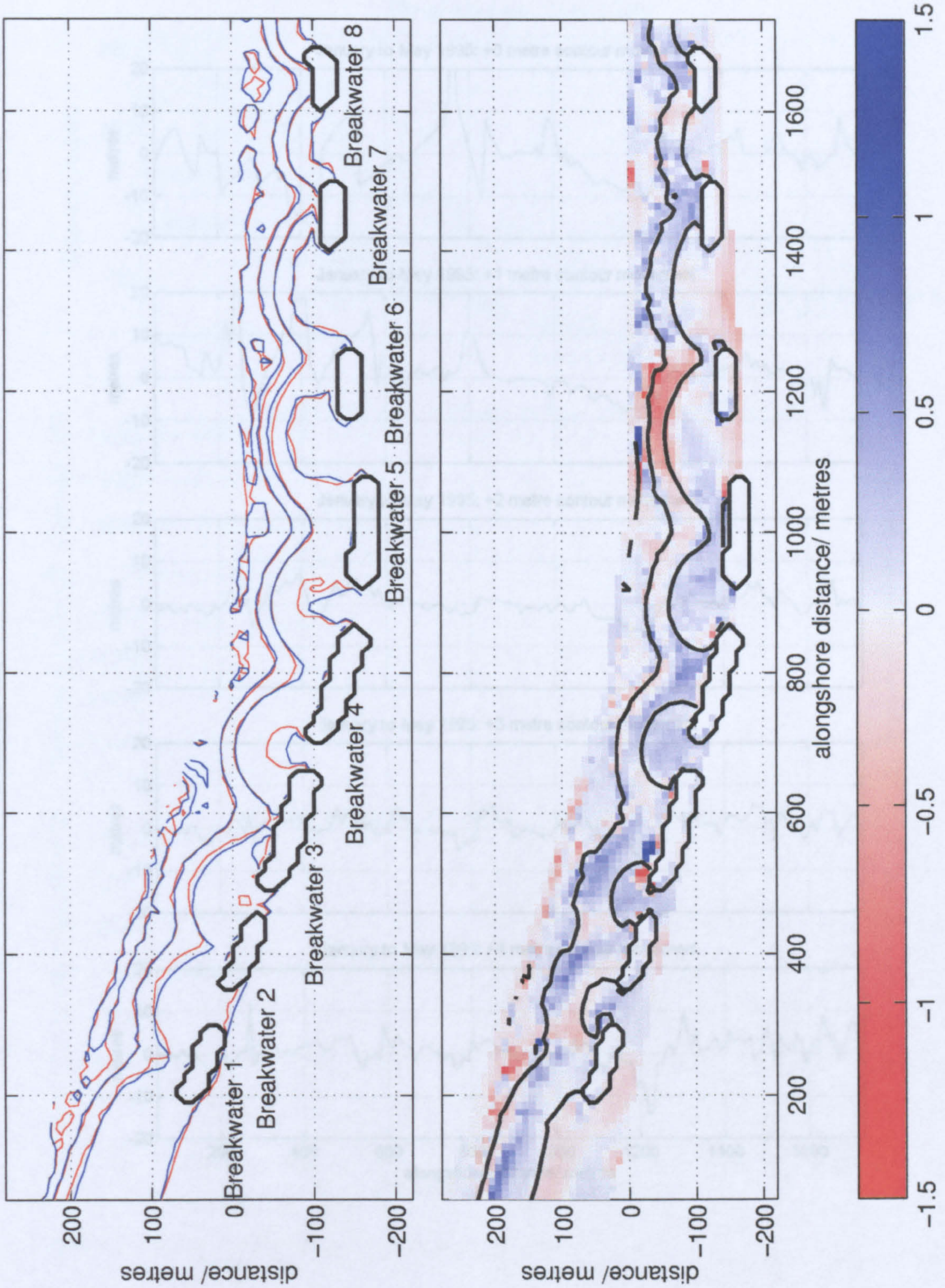

Figure 4-25 Contour positions (red: January 1995; blue: May 1995) and level difference plot

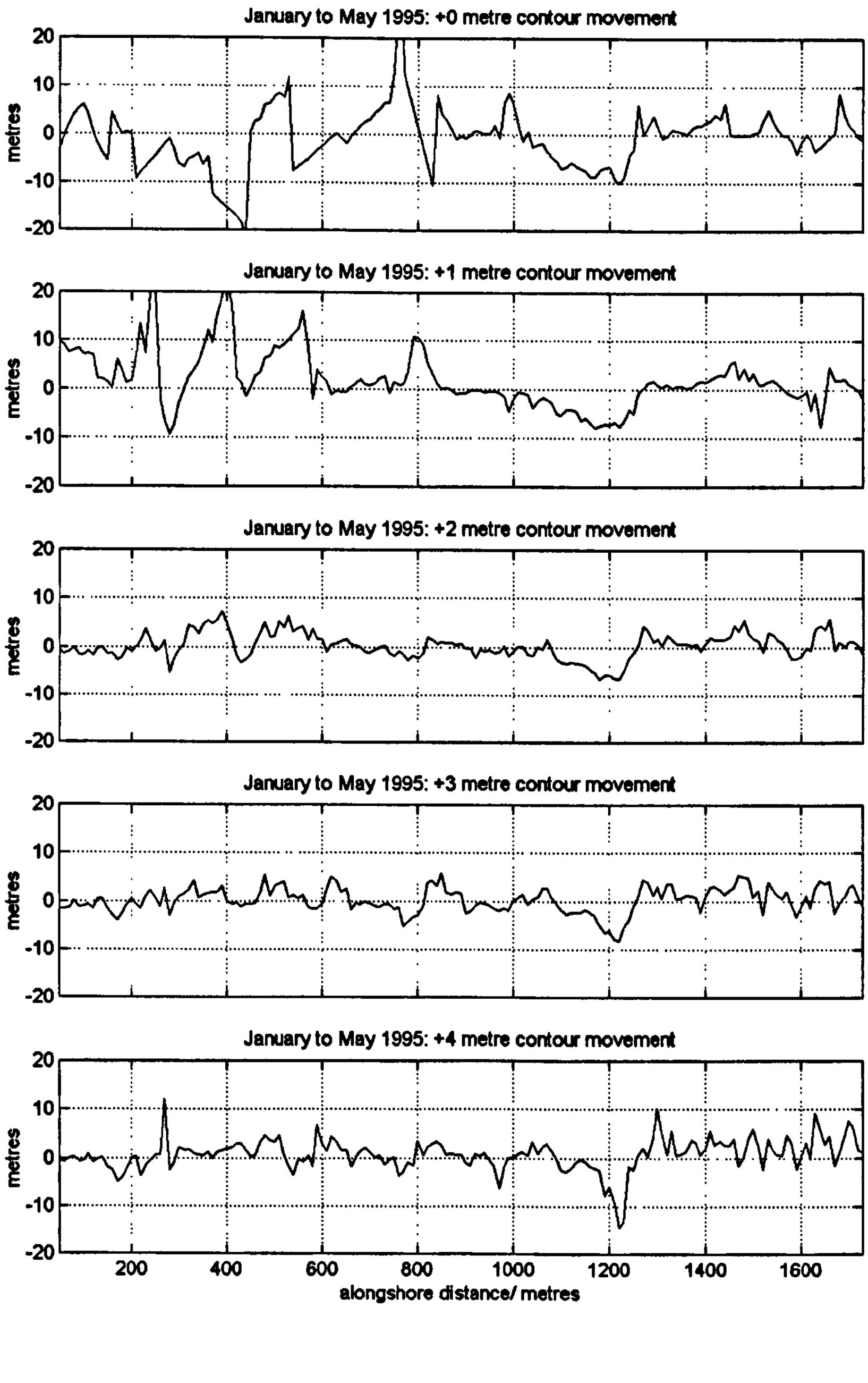

Figure 4-26 Contour movements between 0 and +4 m, from January 1995 to May 1995.

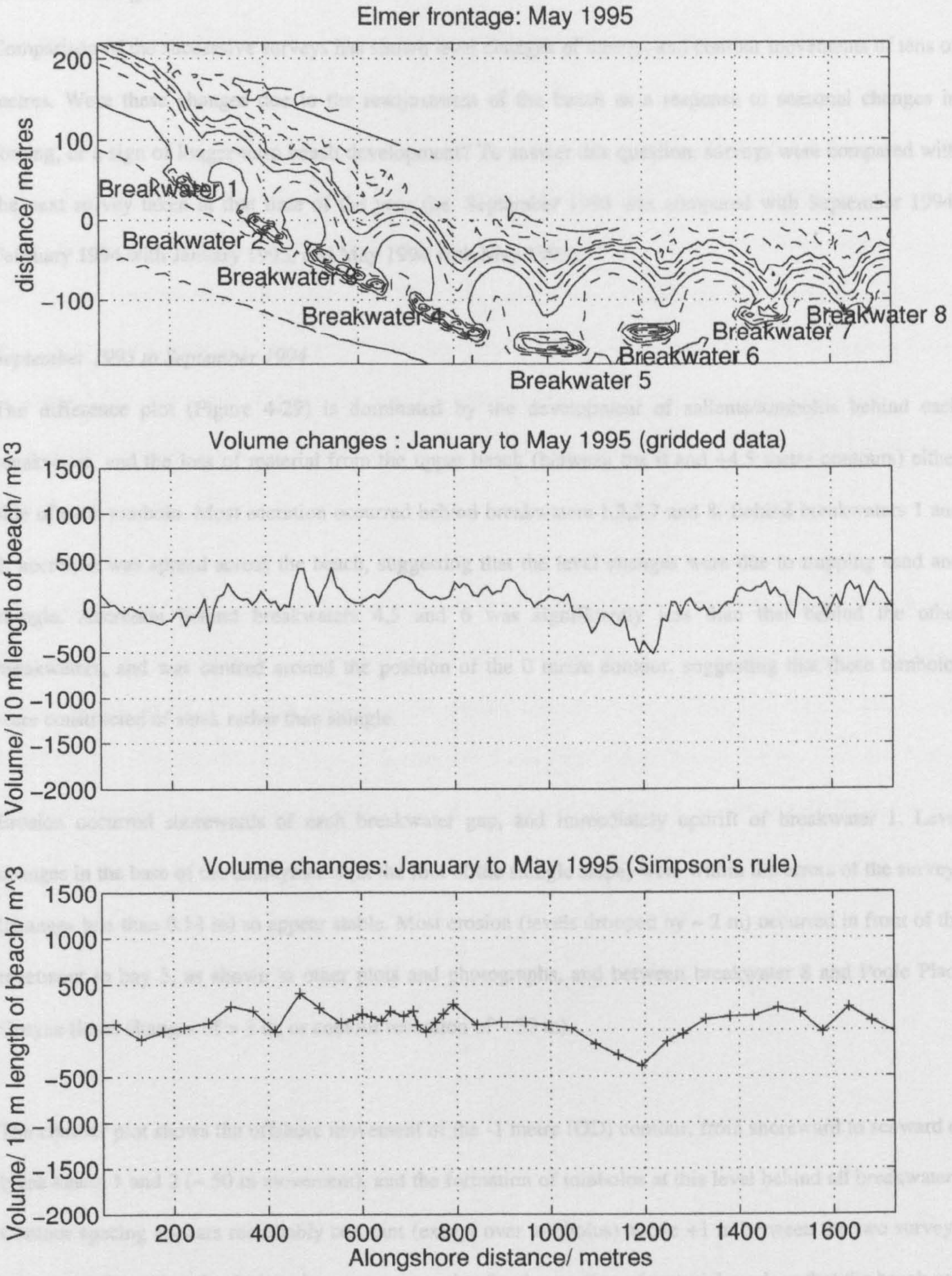

Figure 4-27 Volume changes between January and May 1995.

Annual Changes

Comparison of the successive surveys has shown level changes of metres, and contour movements of tens of metres. Were these changes due to the readjustment of the beach as a response to seasonal changes in forcing, or a sign of longer-term beach development? To answer this question, surveys were compared with the next survey taken at that time of the year (i.e. September 1993 was compared with September 1994, February 1994 with January 1995, and May 1994 with May 1995).

September 1993 to September 1994

The difference plot (Figure 4-29) is dominated by the development of salients/tombolos behind each breakwater, and the loss of material from the upper beach (between the 0 and +4.5 metre contours) either side of each tombolo. Most accretion occurred behind breakwaters 1,2,3,7 and 8. Behind breakwaters 1 and 2, accretion was spread across the beach, suggesting that the level changes were due to trapping sand and shingle. Accretion behind breakwaters 4,5 and 6 was significantly less than that behind the other breakwaters, and was centred around the position of the 0 metre contour, suggesting that these tombolos were constructed of sand, rather than shingle.

Erosion occurred shorewards of each breakwater gap, and immediately updrift of breakwater 1. Level changes in the base of the embayments (at the foot of the shingle slope) were within the errors of the surveys (changes less than 0.14 m) so appear stable. Most erosion (levels dropped by ~ 2 m) occurred in front of the revetment in bay 5, as shown in other plots and photographs, and between breakwater 8 and Poole Place Groyne (level changes of > 3 m, or contour recession of ~ 30 m).

The contour plot shows the offshore movement of the -1 metre (OD) contour, from shoreward to seaward of breakwaters 1 and 2 (~ 50 m movement), and the formation of tombolos at this level behind all breakwaters. Contour spacing appears reasonably constant (except over tombolos) above +1 m between the two surveys, suggesting that either the design slope was reasonable for the grading of material used, or that the beach was reworked to a 'natural', 'September' slope during construction (before the completion survey). Contour movements (Figure 4-29) confirm this. At low levels, movements are large over the salients/tombolos, but at higher levels the accretion is less - indicating a flattening of the beach profile. Towards the centre of the scheme however, and between +1 and +3 metre contour, movements appear to be similar at all levels.

Estimates of volume changes indicate an accretion of 28 900 m^3, based on the gridded data. Using Simpson's rule gave an accretion of 24 200 m^3. The contour movement method indicated an accretion of 3 000 m^3.

February 1994 to January 1995

Within the scheme, further salient growth occurs, although appears to be limited to behind breakwaters 1, 2 and 3. Behind breakwater 1, the salient is lengthened by ~ 15 m, and the bays between breakwaters 1 and 2, and between breakwaters 3 and 4 are further filled. The salient behind breakwater 3 is extended by ~ 20 m at the + 1 metre level, although higher levels show no further growth. This indicates that this accretion is due to sand deposition, rather than shingle. The level changes and contour plot are shown in Figure 4-31. Behind breakwater 4, the tombolo is widened at the -0.5 metre level, and the salient behind breakwater 5 reaches the breakwater.

Bay 5 differs from the updrift bays, in that it appears to be completely stable between the two surveys, with only slight erosion occurring around the edges of the bay at upper levels. The shoreward limit of the beach remains pinned by the revetment, and the profile appears unchanged. Bays 6 and 7 also appear stable, with slight erosion at the beach crest. Between breakwater 8 and Poole Place Groyne, the bay is eroded further (level changes of ~1.3 m - contour movement of ~ 25 m - shorewards of the + 4 metre contour level).

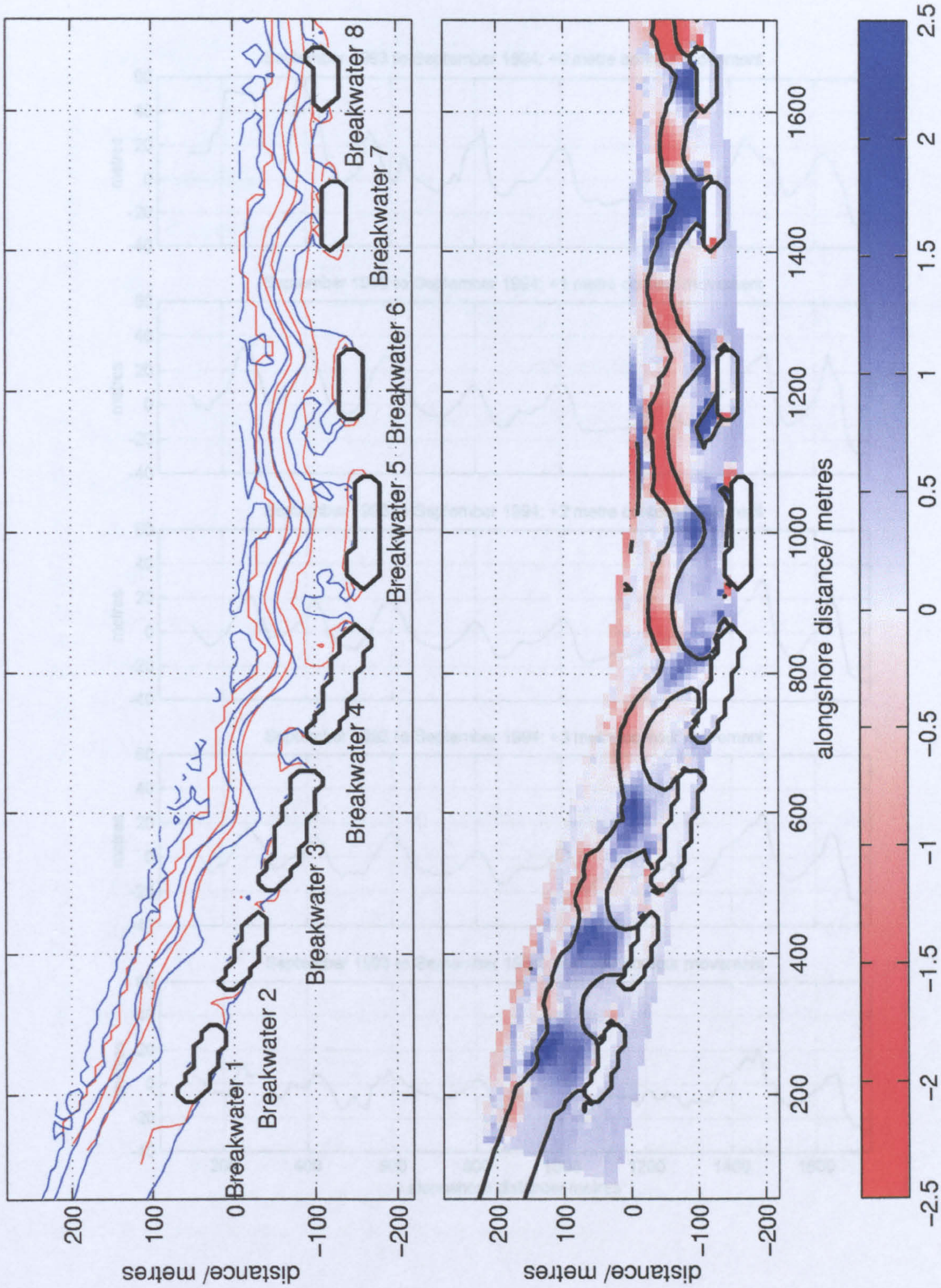

Figure 4-28 September 1993 (red) to September 1994 (blue) contour movements and level changes (m)

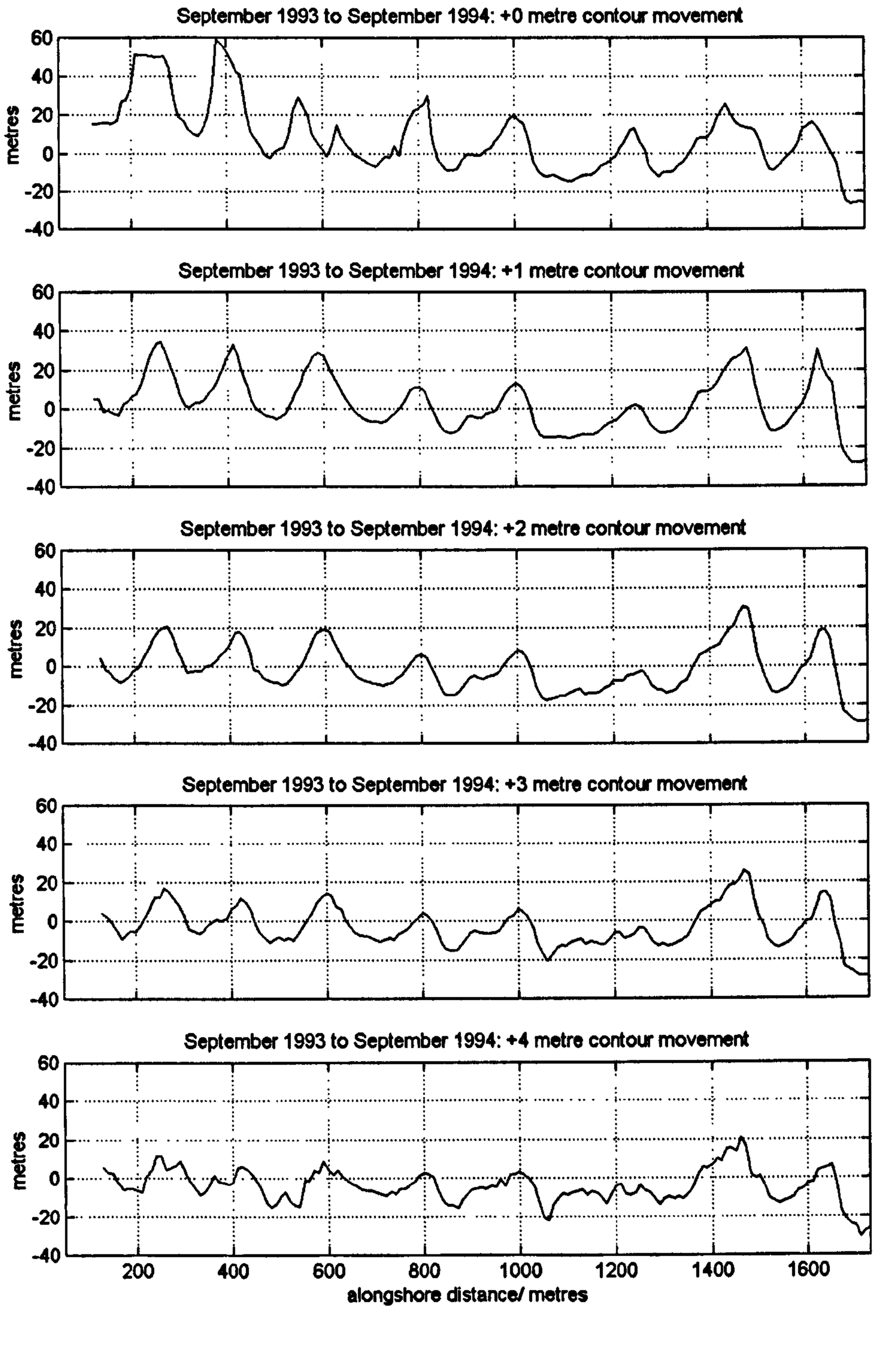

Figure 4-29 September 1993 to September 1994 contour movements at 0 to +4 m over Ordnance Datum

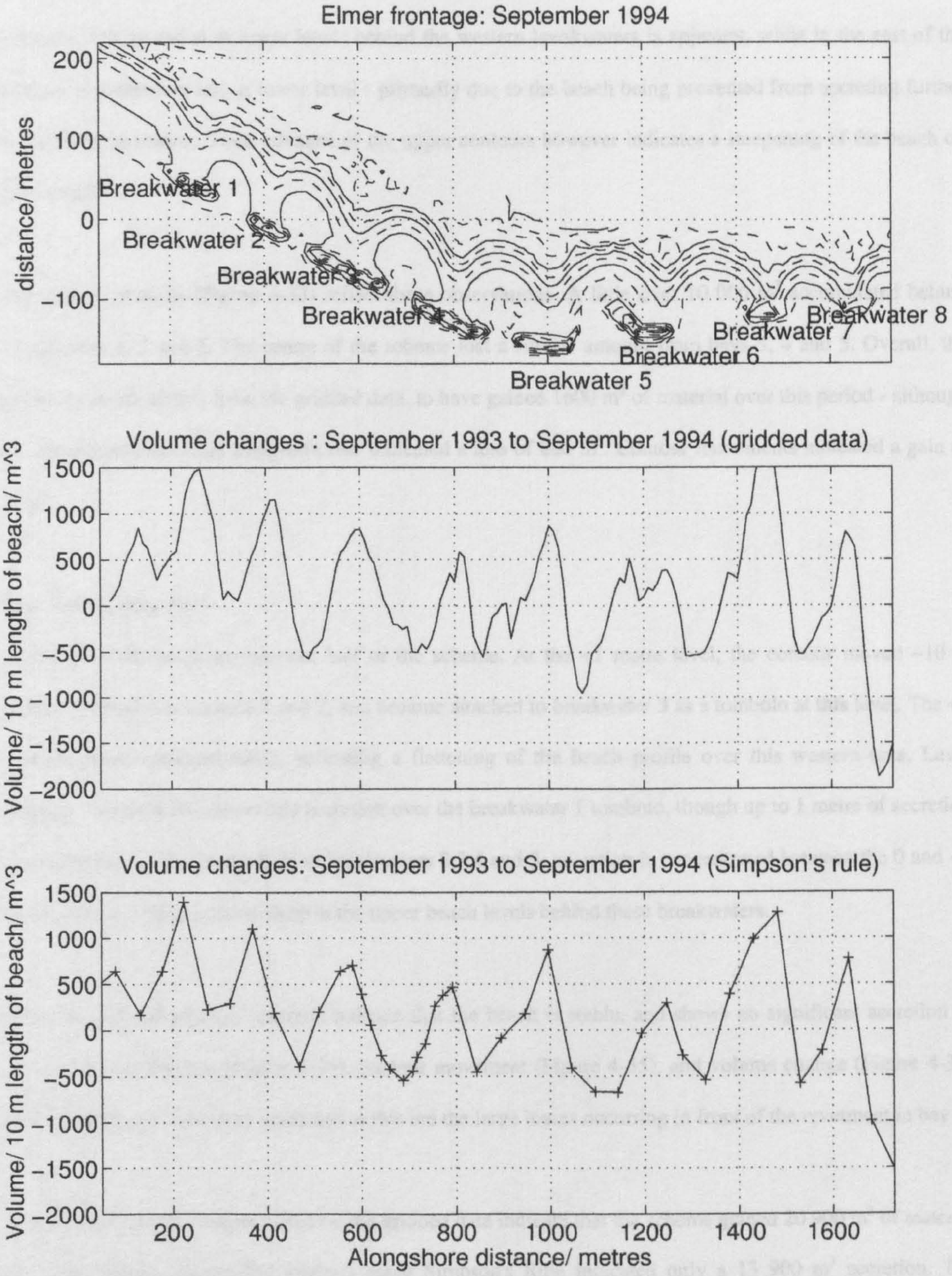

Figure 4-30 Volume changes, September 1993 to September 1994

Contour movements at different levels (Figure 4-32) again show the different behaviour of the lower contours. The accretion at lower levels behind the western breakwaters is apparent, while in the east of the scheme, movement is less at lower level - primarily due to the beach being prevented from accreting further by tombolo formation. Some advance of the upper contours however indicates a steepening of the beach on the tombolos.

The volume changes (Figure 4-33) reflect these observations. A little over 10 000 m^3 accumulated behind breakwaters 1, 2 and 3. The centre of the scheme lost a similar amount from bays 3, 4 and 5. Overall, the scheme was calculated, from the gridded data, to have gained 1600 m^3 of material over this period - although the calculations based on Simpson's rule indicated a loss of 800 m^3. Contour movements indicated a gain of 47 m^3.

May 1994 to May 1995

Accretion occurred in the western half of the scheme. At the +1 metre level, the contour moved ~10 m seaward behind breakwaters 1 and 2, and became attached to breakwater 3 as a tombolo at this level. The +3 metre contour remained static, indicating a flattening of the beach profile over this western area. Level changes (Figure 4-34) show little accretion over the breakwater 1 tombolo, though up to 1 metre of accretion occurs higher up the beach. Behind breakwaters 2,3,4 and 5, accretion is concentrated between the 0 and +1 metre contour. There is some drop in the upper beach levels behind these breakwaters.

In the east of the scheme, contours indicate that the beach is stable, and shows no significant accretion or erosion. The difference (Figure 4-34), contour movement (Figure 4-35), and volume change (Figure 4-36) plots confirm this, The only exception to this are the large losses occurring in front of the revetment in bay 5.

Calculating volume changes based on the gridded data indicate that the scheme gained 20 900 m^3 of material over this period. The profile analysis using Simpson's Rule indicated only a 13 900 m^3 accretion. The contour movements indicated a gain of 6 600 m^3.

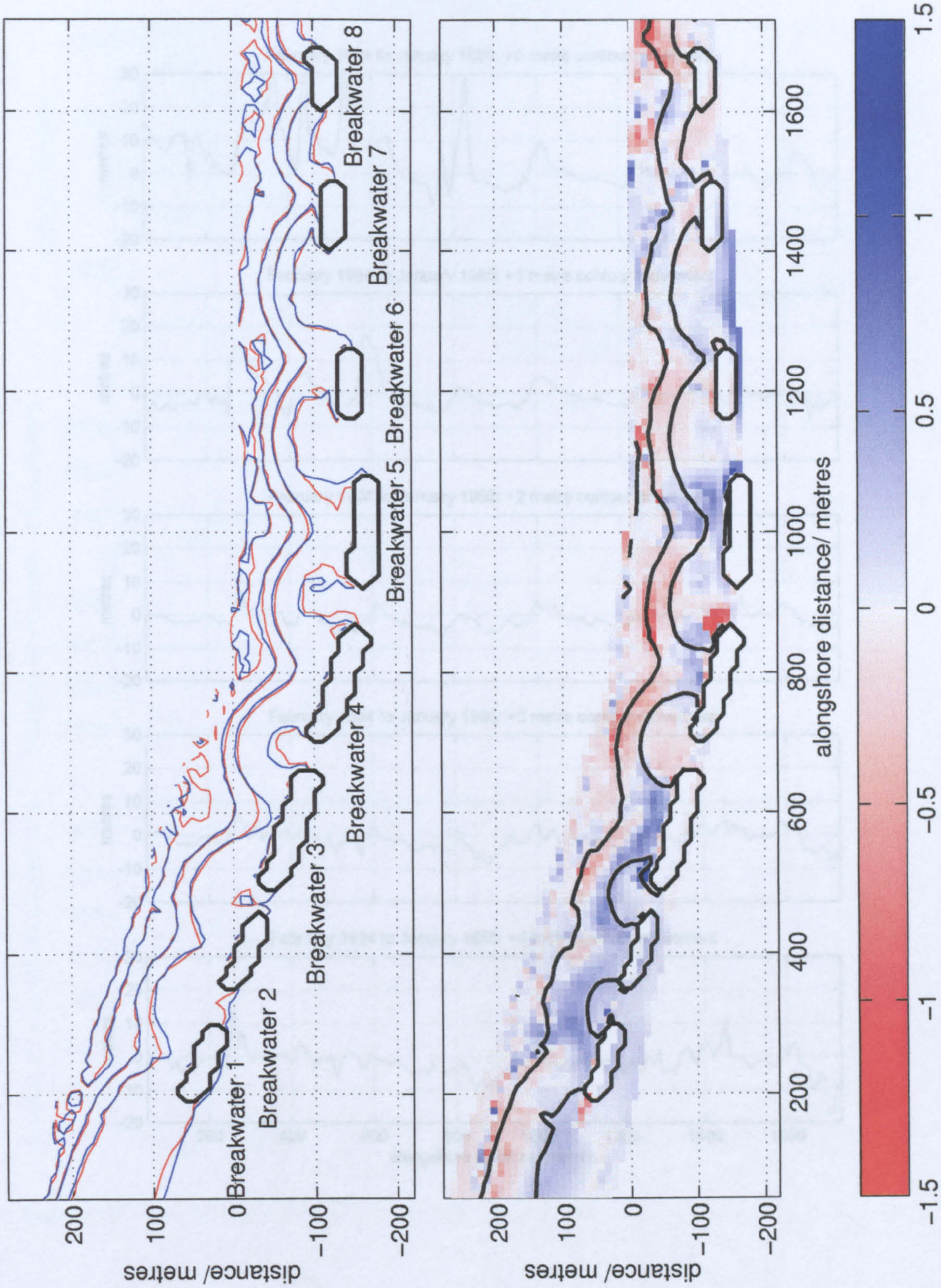

Figure 4-31 February 1994 (red) to January 1995 (blue) contour movements and level differences

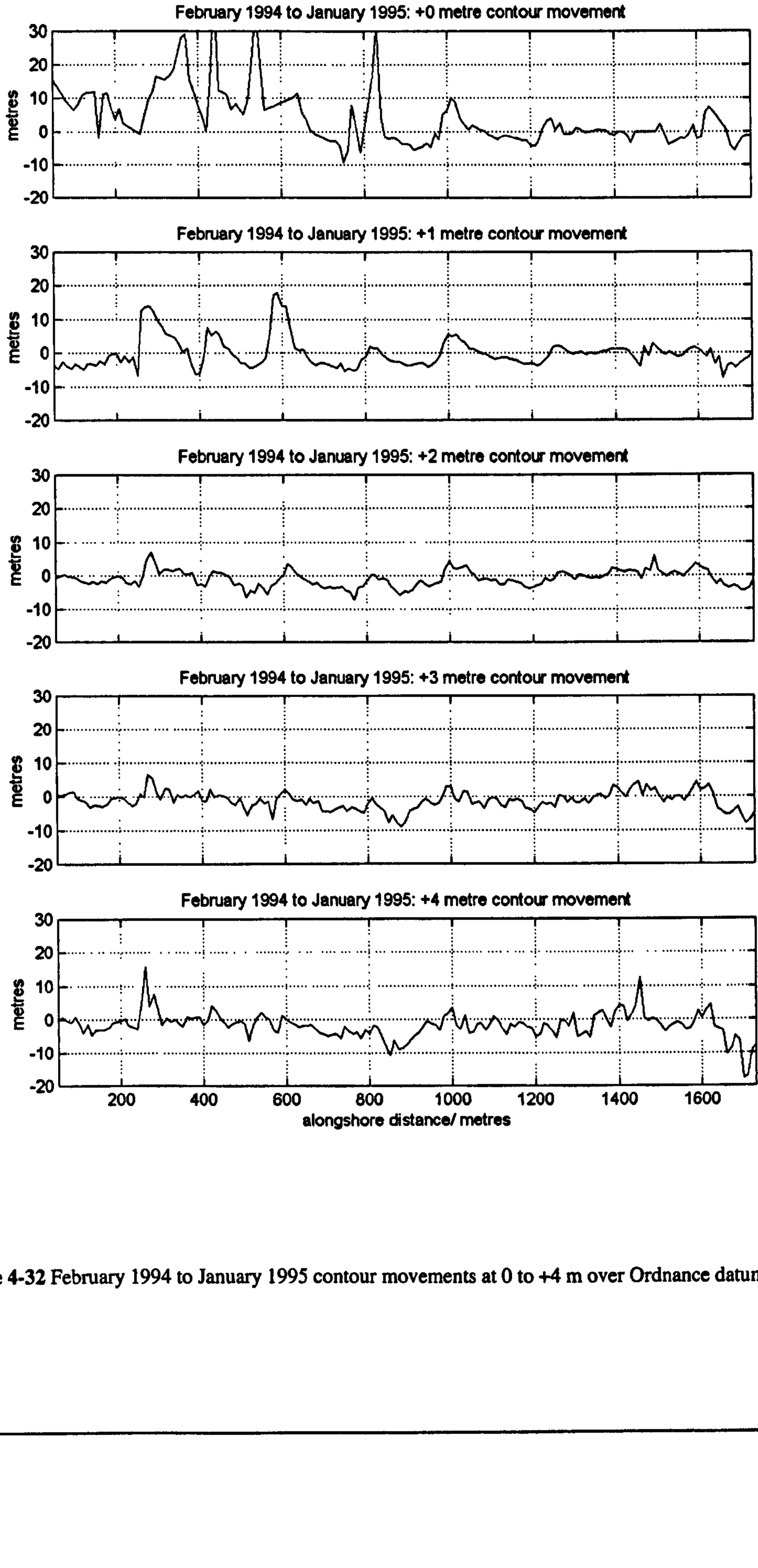

Figure 4-32 February 1994 to January 1995 contour movements at 0 to +4 m over Ordnance datum.

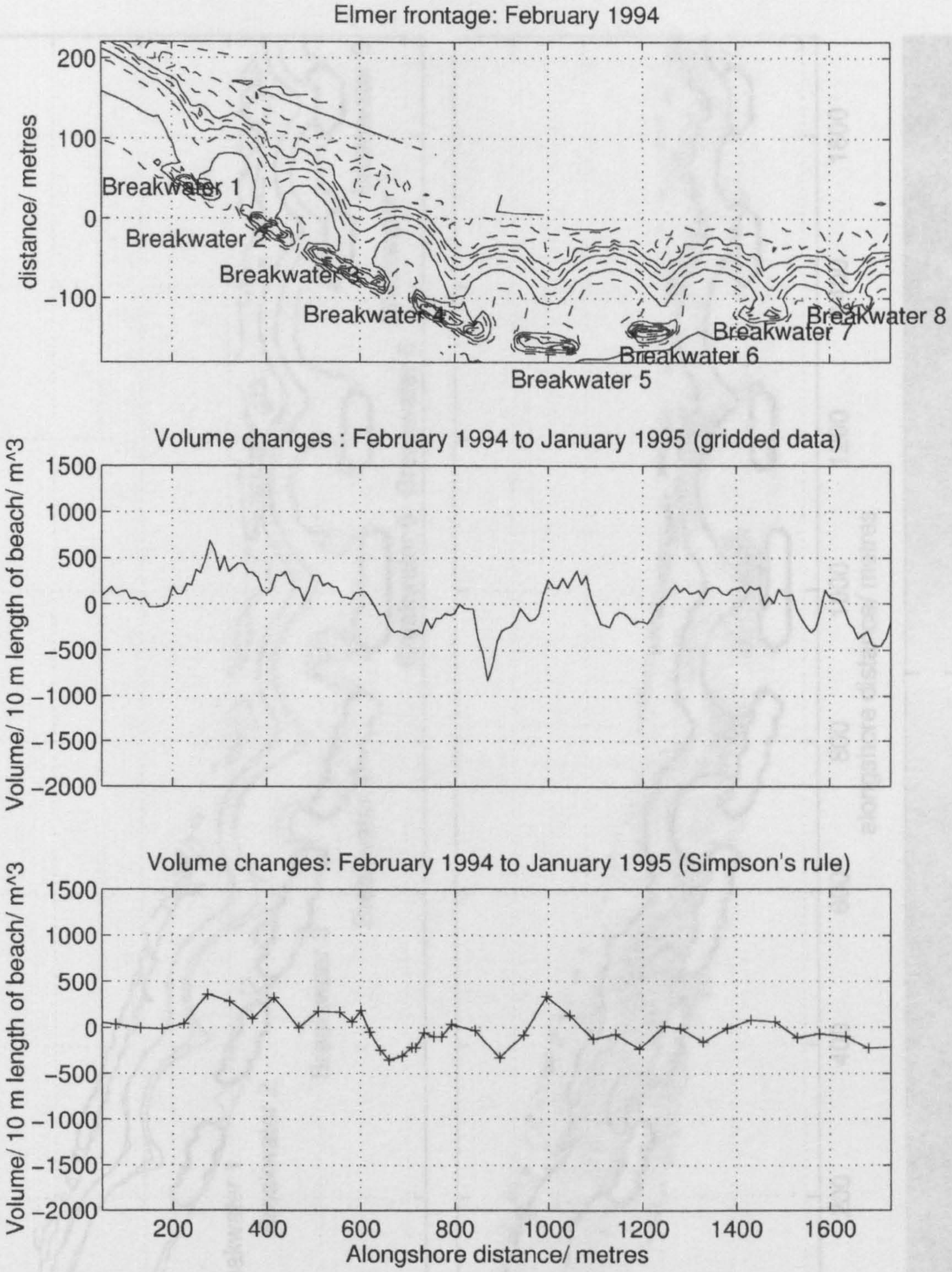

Figure 4-33 Volume changes between February 1994 to January 1995

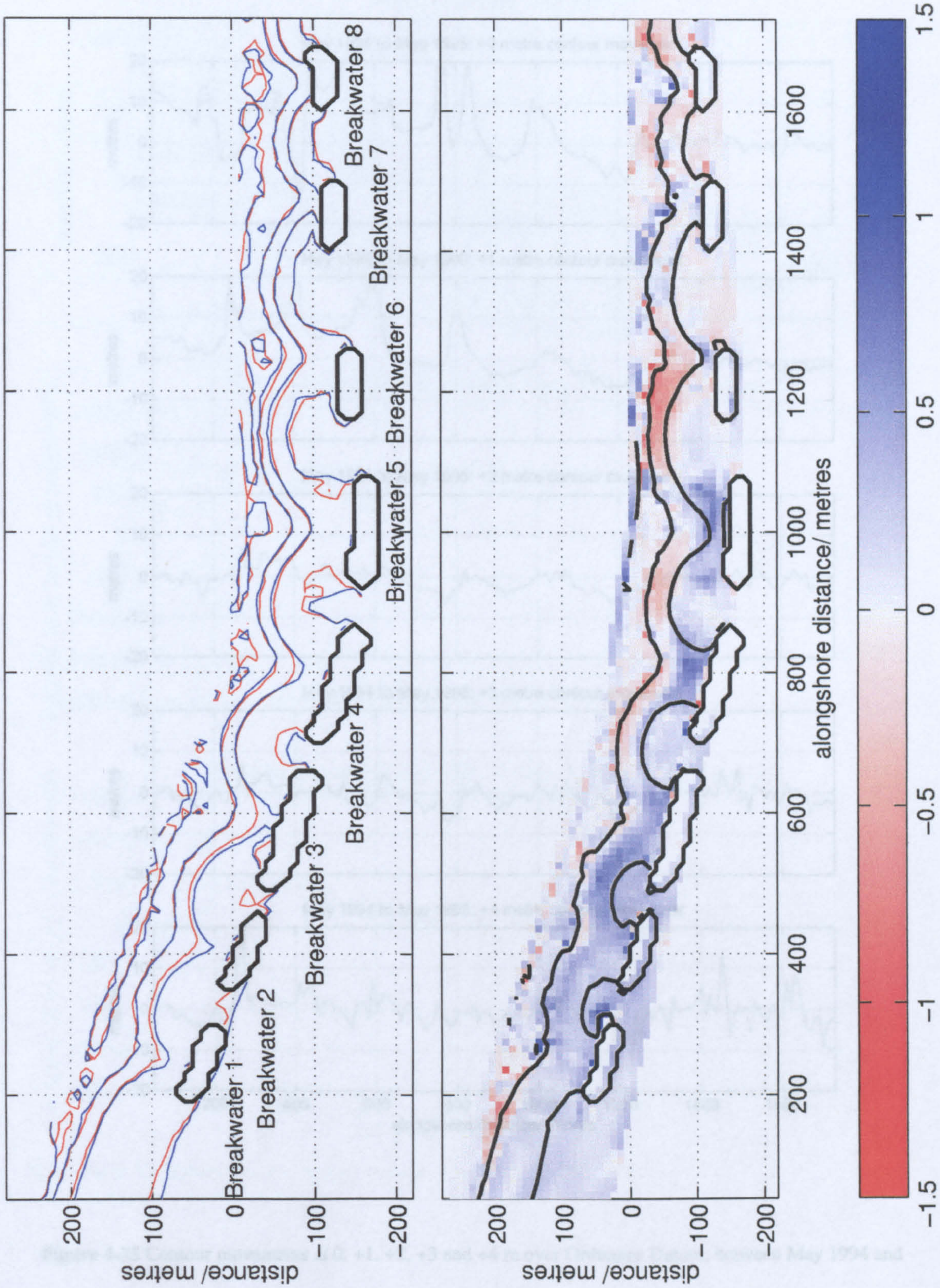

Figure 4-34 May 1994 (red) and May 1995 (blue) contour movements, and level differences

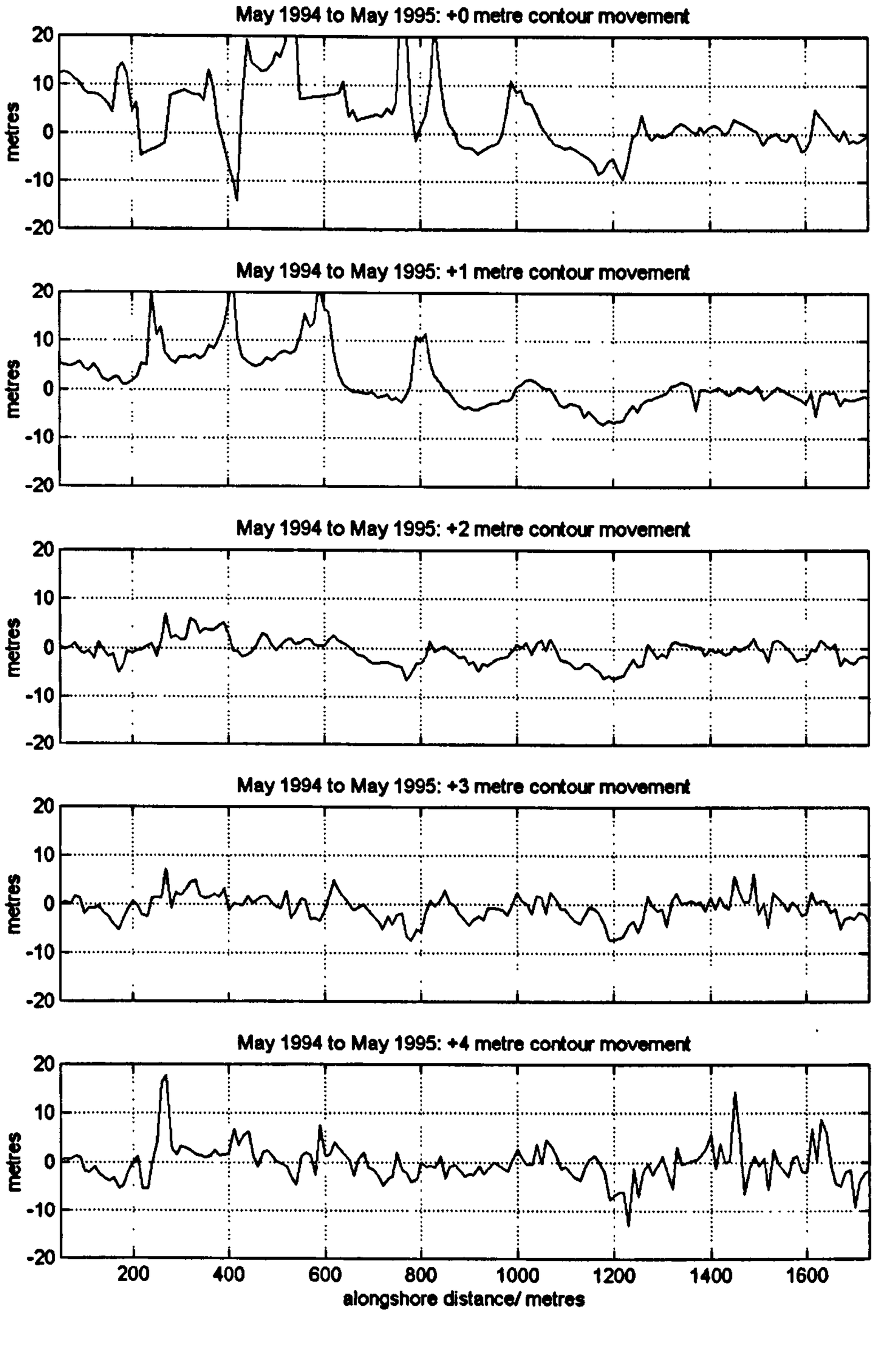

Figure 4-35 Contour movements at 0, +1, +2, +3 and +4 m over Ordnance Datum, between May 1994 and May 1995

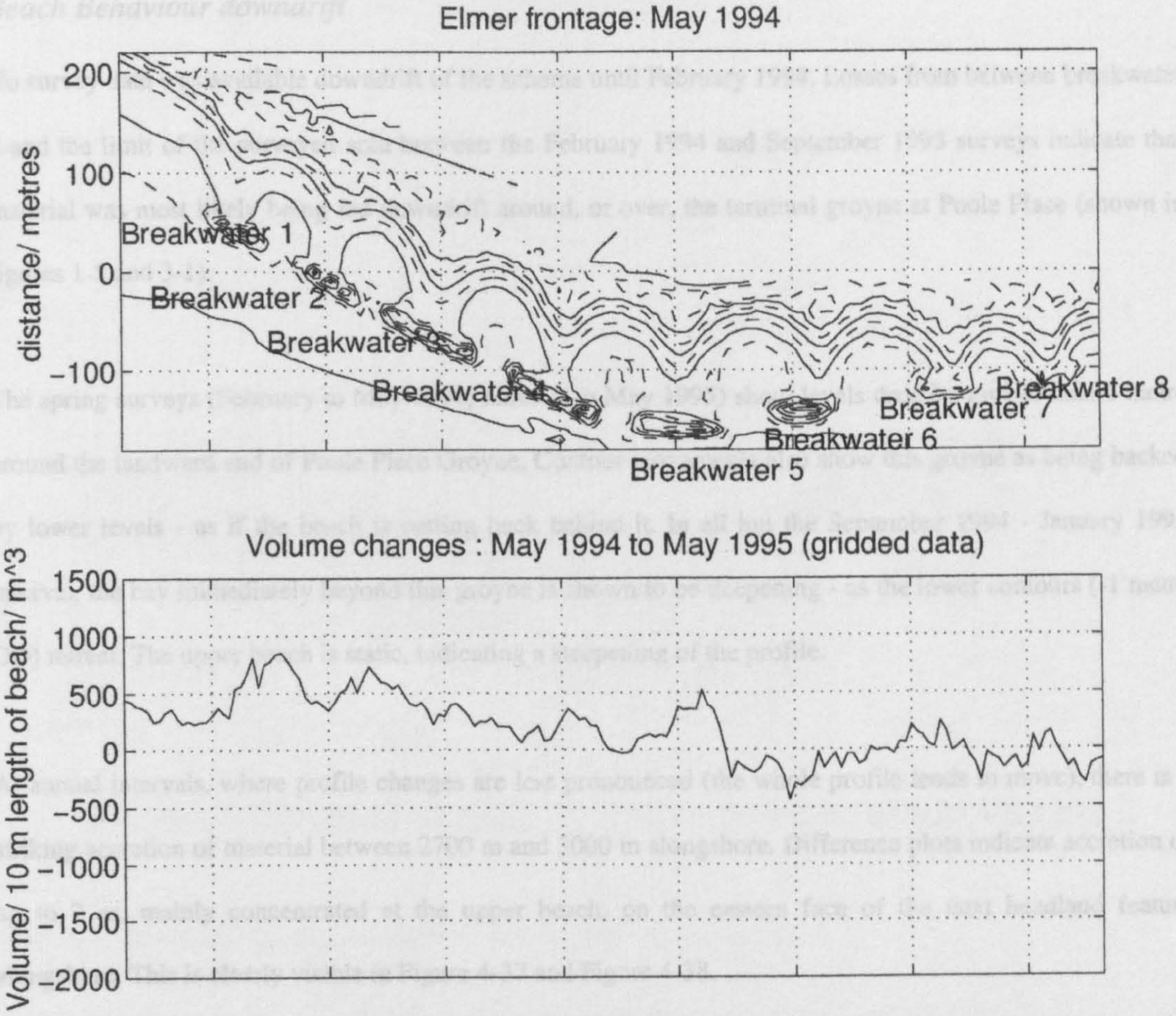

Figure 4-36 Alongshore volume changes between May 1994 and May 1995

Beach Behaviour downdrift

No survey data was available downdrift of the scheme until February 1994. Losses from between breakwater 8 and the limit of the surveyed area between the February 1994 and September 1993 surveys indicate that material was most likely being fed downdrift around, or over, the terminal groyne at Poole Place (shown in figures 1-5 and 3-1).

The spring surveys (February to May 1994; January to May 1995) show levels drop by greater than 1 metre around the landward end of Poole Place Groyne. Contour movements also show this groyne as being backed by lower levels - as if the beach is cutting back behind it. In all but the September 1994 - January 1995 interval, the bay immediately beyond this groyne is shown to be deepening - as the lower contours (-1 metre OD) retreat. The upper beach is static, indicating a steepening of the profile.

At annual intervals, where profile changes are less pronounced (the whole profile tends to move), there is a striking accretion of material between 2700 m and 3000 m alongshore. Difference plots indicate accretion of up to 2 m, mainly concentrated at the upper beach, on the eastern face of the next headland feature alongshore. This is clearly visible in Figure 4-37 and Figure 4-38.

Analysis of profile data to calculate volume changes indicate that between February 1994 and January 1995, the entire downdrift area lost 5200 m^3 of material. A similar figure was arrived at looking at the changes between May 1994 and May 1995.

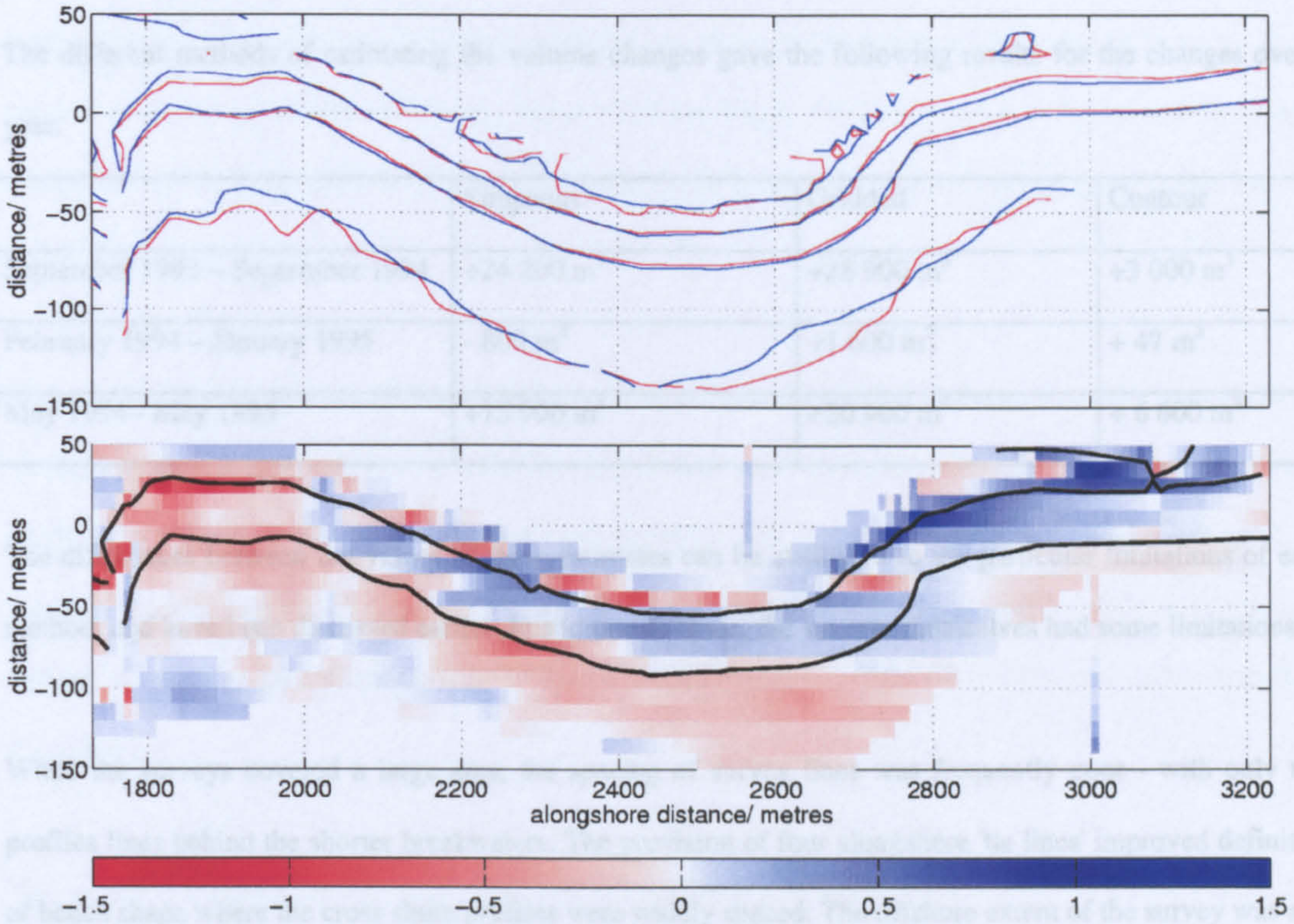

Figure 4-37 Downdrift beach development February 1994 to January 1995.

Contour plot shows February (red) and January (blue) contours at 1 metre intervals from -1 to +5 m OD.

Difference plot shows level changes

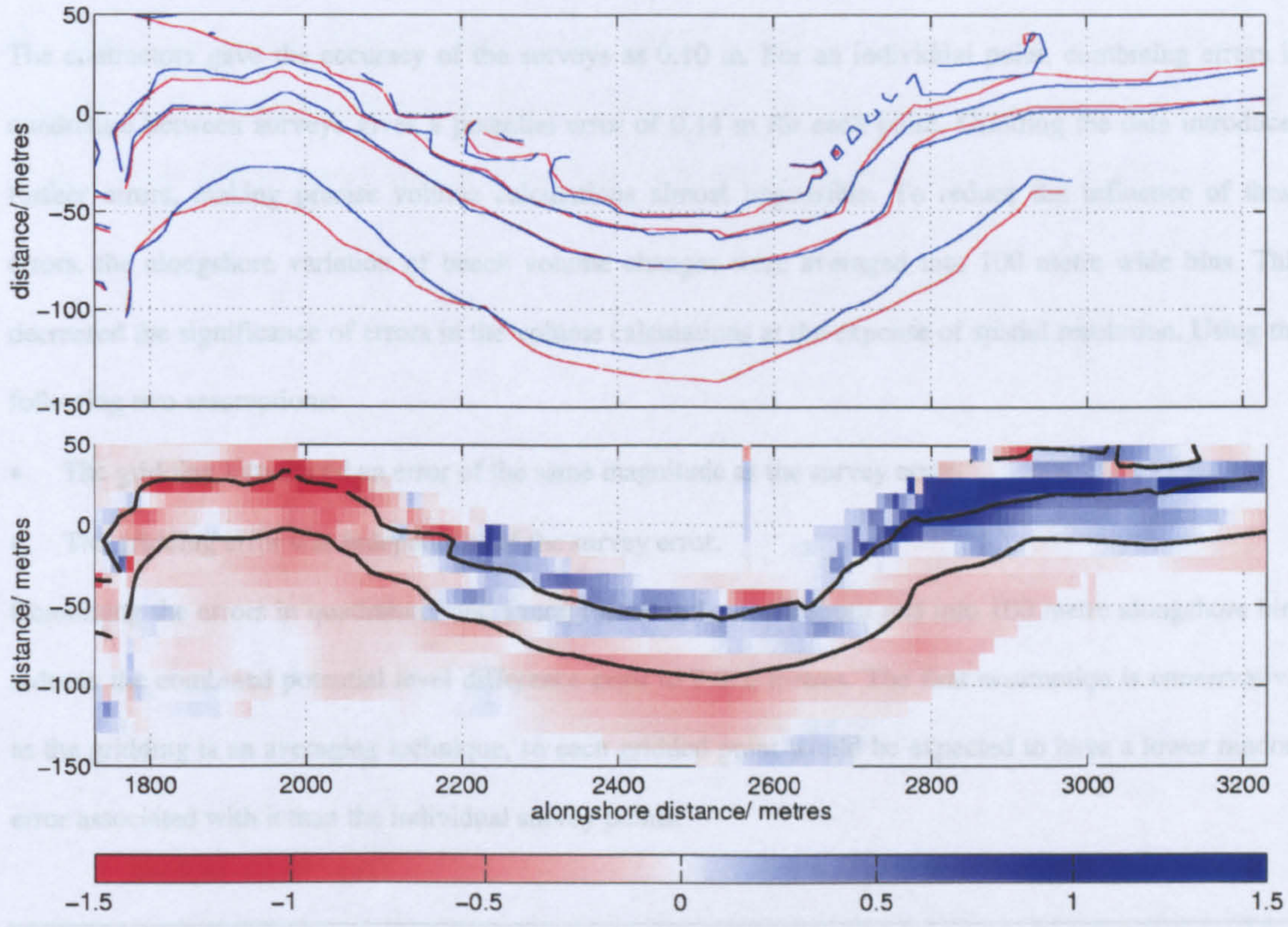

Figure 4-38 As above, for the period May 1994 to May 1995

Summary of Beach Development

The different methods of estimating the volume changes gave the following results for the changes over a year:

	Simpsons	Gridded	Contour
September 1993 – September 1994	+24 200 m^3	+28 900 m^3	+3 000 m^3
February 1994 – January 1995	- 800 m^3	+1 600 m^3	+ 47 m^3
May 1994 - May 1995	+13 900 m^3	+20 900 m^3	+ 6 600 m^3

The differences between the values of these estimates can be attributed to the particular limitations of each method, and have been discussed earlier. In addition to these, the surveys themselves had some limitations.

While the surveys covered a large area, the spacing of survey lines was frequently poor - with only two profiles lines behind the shorter breakwaters. The provision of four alongshore 'tie lines' improved definition of beach shape where the cross shore profiles were widely spaced. The offshore extent of the survey was also a problem. Occasionally (particularly in September 1994) the survey lines did not extend as far as the offshore rock platform - as the survey was not flown at the lowest possible tide. To make fair comparisons between surveys, only the area covered by the smallest survey was studied.

The contractors gave the accuracy of the surveys as 0.10 m. For an individual point, combining errors in quadrature between surveys gives a potential error of 0.14 m for each point. Gridding the data introduces further errors, making precise volume calculations almost impossible. To reduce the influence of these errors, the alongshore variation of beach volume changes were averaged into 100 metre wide bins. This decreased the significance of errors in the volume calculations at the expense of spatial resolution. Using the following two assumptions:

- The gridding introduced an error of the same magnitude as the survey error
- The gridding error was independent of the survey error.

Combining the errors in quadrature, and averaging over the cross shore and into 100 metre alongshore bins reduces the combined potential level difference error to 0.016 metres. The first assumption is conservative, as the gridding is an averaging technique, so each gridded point would be expected to have a lower random error associated with it than the individual survey points.

This averaging also has the effect of smoothing out local variations in accretion/erosion - for example where large amounts of accretion occur behind a breakwater and erosion occurs in the adjacent bay - to give a better overall view of scheme behaviour. Figure 4-39 and Figure 4-40 show the cumulative volume changes alongshore within the scheme, and downdrift, respectively, using values of volume change averaged into 100 metre bins.

The middle panel in Figure 4-39 demonstrates that volume changes after the first winter period did not change the overall pattern of accretion and erosion. Updrift (west of 500 m alongshore) there is net accretion, particularly behind breakwater 1.Between breakwaters 4 and 6, the scheme is basically stable, with the exception of the vicinity of bay 5, where there are significant losses which may contribute to the large amount of accretion behind breakwater 7. There are large losses of material from the downdrift extremity of the scheme.

The volume changes from February 1994 show the development of the scheme in more detail, though with the same overall story. The effect of the movement of material from behind breakwater 6 to bay 5 is visible in the September 1994 - January 1995 survey interval - although the very temporary effect of this work can be seen in the position of the January - May 1995 volume change,

Downdrift of the scheme (Figure 4-40) the erosion immediately beyond Poole Place Groyne is apparent. The next 600 m of shoreline appears stable however, and the area around 2800 m alongshore, to the east of a small headland feature, shows significant accretion - indicating the eastward migration of this feature.

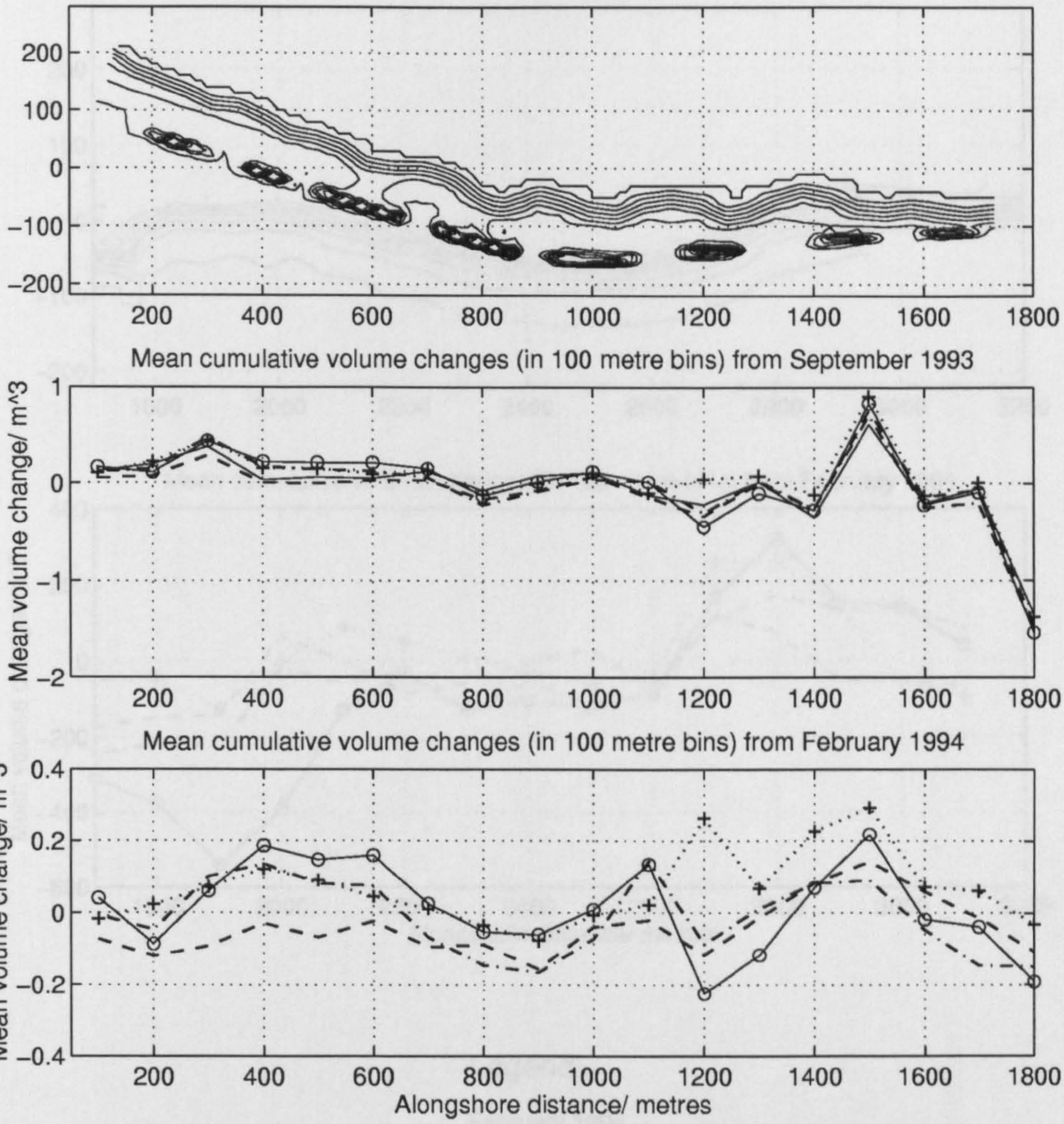

Figure 4-39 Cumulative volume changes within the renourished area - averaged over 100 metre (alongshore) bins.

Top panel shows shoreline as constructed. Middle panel shows volume changes from this position. Lower panel shows volume changes from the February 1994 position.

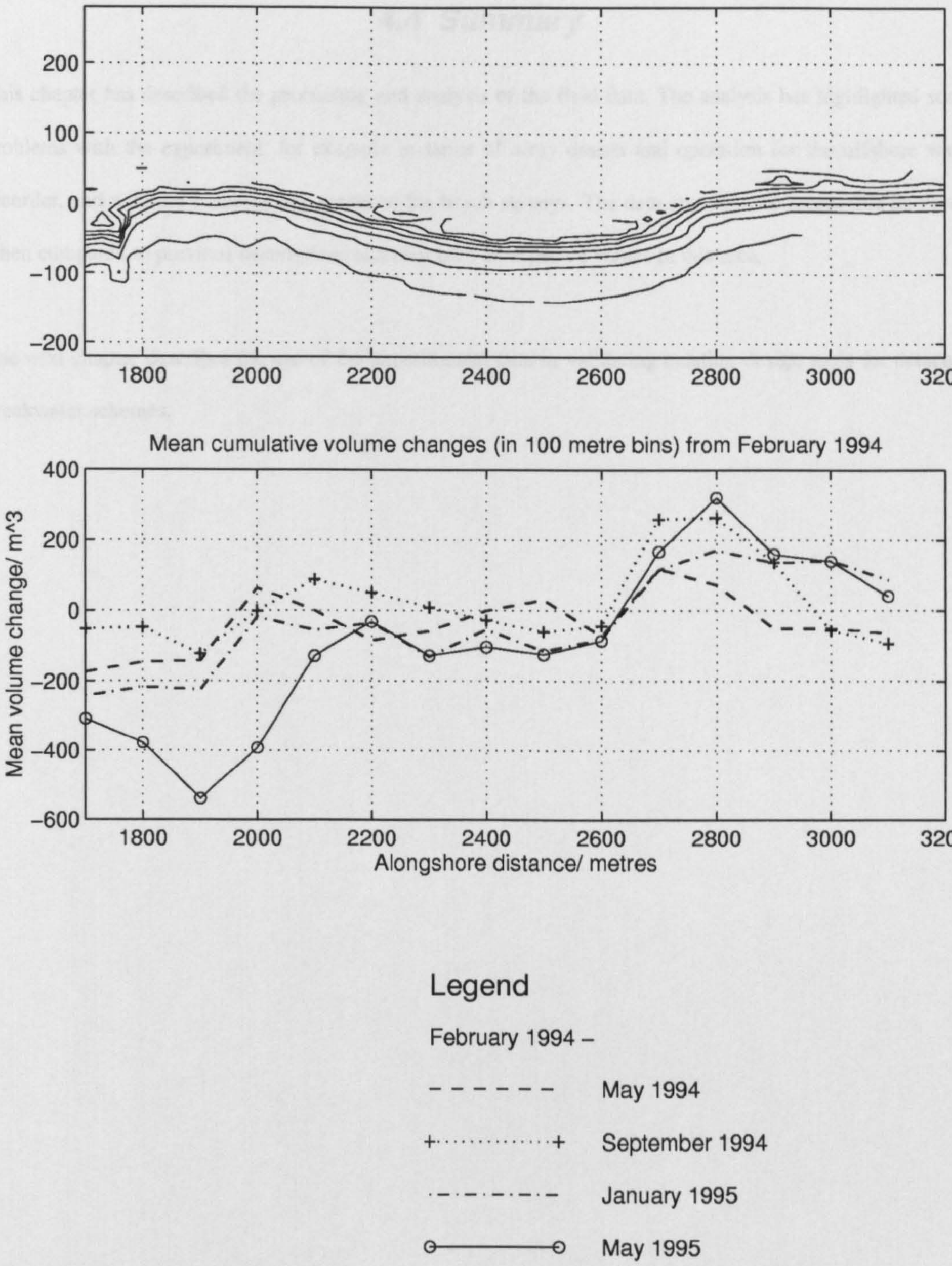

Figure 4-40 As **Figure 4-39**, but for the downdrift shoreline for the period between February 1994 and May 1995

4.4 Summary

This chapter has described the processing and analysis of the field data. The analysis has highlighted some problems with the experiment, for example in terms of array design and operation for the offshore wave recorder, and with the accuracy and extent of the beach surveys. The data appear to be reasonable however, when compared to previous descriptions and estimates of expected values in this area.

The next chapter describes the use of the experimental data in validating existing design tools for detached breakwater schemes.

5. Beach Plan Shape Modelling

5.1 Introduction

Plan shape models represent shoreline position in terms of the position of a single contour line on the beach face. Their application assumes that any changes in beach profile do not affect the shoreline position. This generally restricts their use to periods where profile changes due to storms or seasonality are insignificant - generally considered to be periods greater than one year.

For the study of shoreline response to detached breakwaters, two approaches to plan shape modelling exist. The first type is the geometrical, or empirical approach.. These models are based on observations of previously constructed schemes and natural pocket beaches. They assume that the beach plan adopts a certain shape in response to structures (such as log-spiral. parabolic or elliptic) and that the plan shape comes into equilibrium with the waves modified by the structure. Some models include wave conditions explicitly. Others assume that wave conditions only affect the rate at which a beach comes into equilibrium, but not the equilibrium shape.

The second class of model is the 'one-line' model. The same assumption about the significance of profile changes, and the resulting restriction to periods of greater than 1 year applies to these models. The basis of the one-line model is a longshore sediment transport equation. This frequently takes the form of a longshore power type relation of the type proposed by Inman and Bagnold (1963). The example of one-line models used in this study uses a modified form of the CERC equation that is presented in the Shore Protection Manual (Coastal Engineering Research Center, 1984).

The first half of this chapter describes the evaluation of geometrical modelling approaches when applied to the Elmer scheme. The second half describes the use and evaluation of the US Army Corps of Engineers GENESIS (Hanson, 1989) model using the Elmer field data.

5.2 Geometrical plan shape models

Four models were selected for evaluation. These were: Pope and Dean (1986); Suh and Dalrymple (1987); Ahrens and Cox (1990); and McCormick (1993). Of these, the Suh and Dalrymple model provides an estimate of salient length and the McCormick model predicts shoreline position. The Pope and Dean, and Ahrens and Cox models both describe the beach response in general terms.

5.2.1 Pope and Dean model

Pope and Dean (1986) proposed a system of classifying the effect of breakwater schemes in terms of their shoreline response. Beach response was divided into five bands, ranging from '*no sinuosity*' through '*subdued salients*', '*well-developed salients*', and '*periodic tombolos*' to '*permanent tombolos*'. The classification is based on the degree of protection afforded to a coastline (in terms of the ratio of breakwater length to gap length) plotted against the ratio of offshore distance to water depth at the structure. Preliminary results of a validation of this method were presented for low to moderate wave climates.

5.2.2 Ahrens and Cox model

Ahrens and Cox (1990) followed the classification scheme proposed by Pope and Dean, defining a beach response index I_s. The index is given by Equation 5-1.

$$I_s = \exp\left(1.72 - 0.41\frac{B}{G}\right)$$

Equation 5-1

Values of I_s less than 1 predict permanent tombolo formation, while values greater than 5 predict no sinuosity. This method differs from that presented by Pope and Dean, being based purely on the breakwater length and offshore distance. It ignores any effects of variable gap width.

5.2.3 Suh and Dalrymple model

This model was derived to fit the beach response observed in a set of physical model tests carried out with multiple breakwaters in a spiral wave basin, and also on prototype and model tests described in the literature. They observed that when non-dimensionalized with respect to the offshore distance, the breakwater length was the dominant parameter governing the sand trapping ability of a scheme. For multiple

breakwaters, the ratio of gap width to the square of the breakwater length was also considered important. The equation derived by the authors to predict salient length based on their data is given in Equation 5-2.

$$(S-X)^* = 14.8\left(\frac{G^*}{B^{*2}}\right)\exp\left[-2.83\left(\frac{G^*}{B^{*2}}\right)^{\frac{1}{2}}\right]$$

Equation 5-2

where *S-X* is the salient length. Characters marked with an asterisk represent values non-dimensionalized with respect to the offshore distance of the structure.

5.2.4 McCormick model

The McCormick (1993) model is based on the observation that bays formed behind detached breakwaters tend to be ellipsoid. This observation was based on aerial photographs, and on selected physical model data of Shinohara and Tsubaki (1966) and of Rosen and Vajda (1982). To predict the shoreline position, it is necessary to calculate the lengths of the major and minor axes of the shoreline ellipses, and the positions of the ellipse centres in relation to the breakwater positions. Equation 5-3 gives the length of the minor axis in relation to the offshore distance of the breakwater. The major axis length is given in Equation 5-6, and the offset of the ellipse centre from the breakwater centre is calculated with Equation 5-7.

$$\frac{b}{S} = 1 + 0.2\zeta_o \sin(\chi\zeta_o)$$

Equation 5-3

Where ζ_o and χ are given by:

$$\zeta_o = \frac{H_o}{\frac{L_o}{\tan\beta}}$$

Equation 5-4

$$\chi = -1.92\left(\frac{S}{B}\right)^2 + 9.92\left(\frac{S}{B}\right)$$

Equation 5-5

$$a = \sqrt{Ge^2 + b^2}$$

Equation 5-6

Where a is the length of the major axis, and b is the length of the minor axis. Ge is the distance between the ellipse centre and the breakwater tip. In the case of single breakwaters, this is given (relative to b) by:

$$\frac{Ge}{b} = \exp\left[19.4\tanh\left(0.91\frac{S}{B}\right)+\left(17.0\tanh\left(0.59\frac{S}{B}\right)\times\ln(\zeta_o)\right)-20.0\zeta_o\tanh\left(0.99\frac{S}{B}\right)\right]$$

Equation 5-7

Where multiple breakwaters are used, Ge is the distance from the breakwater tip to the midpoint of the gap. Where waves do not approach the shoreline normally, the frame of reference for drawing the shoreline is rotated such that the major axis of the ellipse is parallel to the wavefronts at the breakwater.

Validation for the model was carried out on four breakwaters within the 'Bay Ridge' prototype scheme in Chesapeake Bay. For the purposes of this evaluation, the predictions of salient length were extracted from this predicted shoreline position.

5.2.5 Model Application

None of the models above were derived from studies of macro-tidal beach response. To apply them to the Elmer site, the profile data and construction plans were analysed to provide information on the scheme geometry. To study the ability of these models to predict beach response at varying tidal levels, measurements of salient length, offshore distance and beach slope were extracted (for each breakwater) between the mid tide and mean high water spring tide level (2.4 metres higher) at 0.3 metre intervals. This information was then used to drive the models, and the predictions were compared with the observed findings. Offshore distances of the breakwaters are presented in Table 5-1, while measured salient lengths are presented in Table 5-2. Numbering of the breakwaters is the same as used in the previous chapter.

5.3 Results of geometrical model tests

5.3.1 Pope and Dean model

Figure 5-1 shows the predictions of beach response according to Pope and Dean's classification. Tombolo formation is only predicted to occur behind breakwaters 3 and 4, although the prediction of the limit between salient and tombolo for breakwater 3 is perfect. The model predicts the limited shoreline response behind breakwaters 1 and 2 at high tide. Tombolo formation at low water is not predicted at all.

The easternmost breakwaters (5,6,7 and 8) are all predicted to produce salients only, at all tidal levels. Tombolos were observed behind breakwaters 6,7 and 8 (between mean water level and +0.3, +1.2 and +1.2 metres respectively above mean water level).

Water level (over mean water level)	Break-water 1	Break-water 2	Break-water 3	Break-water 4	Break-water 5	Break-water 6	Break-water 7	Break-water 8
0	50.6	48.7	0	40.9	54.5	44.3	25.5	10.4
0.3	68.2	65.3	3.9	42.9	57.1	47.3	29.1	13.5
0.6	72.1	68.2	51.3	45.8	59.7	50.4	32.2	16.7
0.9	73.1	72.1	54.5	48.7	62.3	53.4	34.3	19.8
1.2	76	74	57.1	52.6	64.9	56.5	36.4	21.9
1.5	77.9	77.9	59.7	55.5	67.5	59.5	38.4	24
1.8	80.8	80.8	62.3	58.4	70.1	62.6	41	27.1
2.1	83.8	82.8	66.2	60.4	72.7	65.6	43.6	29.2
2.4	85.7	85.7	68.2	66.2	75.3	68.7	46.2	32.3

Table 5-1 Breakwater-shoreline distances at various tidal levels.

Water level (over mean water level)	Break-water 1	Break-water 2	Break-water 3	Break-water 4	Break-water 5	Break-water 6	Break-water 7	Break-water 8
0	51	49	0	41	30	44	26	10
0.3	68	65	4	43	21	15	29	14
0.6	72	64	51	46	18	9	32	17
0.9	54	35	55	16	16	5	34	20
1.2	35	27	38	14	14	1	34	19
1.5	27	23	28	5	12	-1	34	19
1.8	22	19	23	2	8	-2	35	20
2.1	22	11	21	0	8	-5	32	18
2.4	20	10	18	0	6	-7	31	17

Table 5-2 Observed salient lengths at various tidal levels

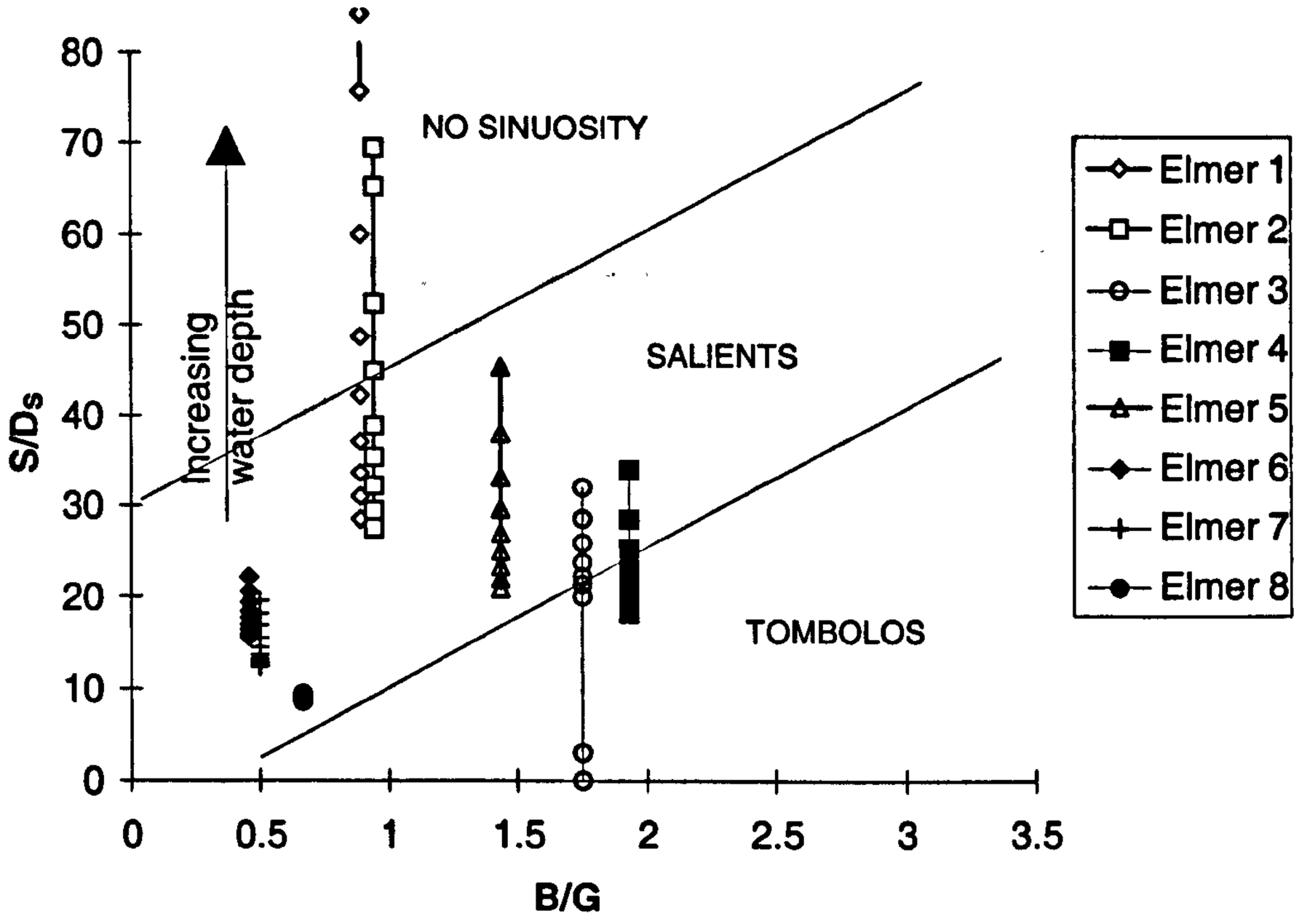

Figure 5-1 Elmer breakwaters plotted according to the classification scheme of Pope and Dean (1986)

5.3.2 Ahrens and Cox model

Figure 5-2 shows the effect of varying water depth on Ahrens and Cox's Beach Response Index, and the corresponding predictions of beach response. Breakwaters 1,2 and 6 are predicted to generate 'subdued salients' at all tidal levels. Breakwaters 5 and 7 are predicted to have 'well developed' salients. The remaining breakwaters (3,4 and 8) are predicted to have tombolos at low water, and well developed salients at high water. The model predicts the limit between tombolo and salient formation well for breakwater 3, but predictions of the level where tombolos become detached are less successful for the other breakwaters.

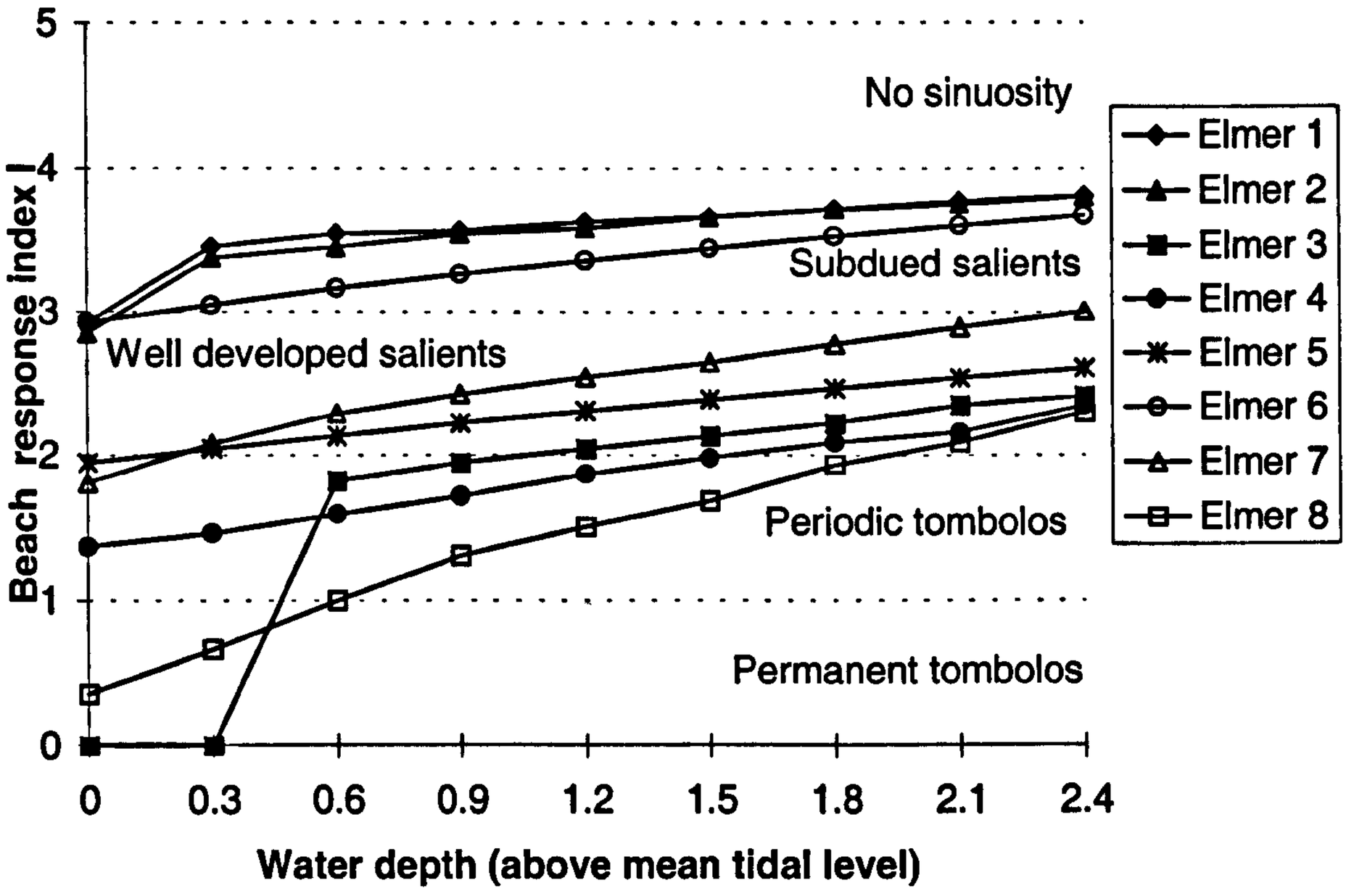

Figure 5-2 Breakwater index against tidal level, using the classification scheme of Ahrens and Cox (1990)

5.3.3 Suh and Dalrymple model

The model predictions from Suh and Dalrymple (1987) are shown in Figure 5-3. There is excellent agreement between observed and predicted salient lengths at the lower levels – i.e. when tombolos occur. As the tide rises, this model predicts steadily *increasing* salient lengths (the shoreline recedes faster away from the breakwater than over the salient – i.e. the beach slope away from the breakwater is less than that on the salient). This is contrary to the observed salient behaviour, but in line with the observations reported in Chasten *et al* (1993).

5.3.4 McCormick model

The response predicted by McCormick's model is shown in Figure 5-4. differs from this. Results are similar to those obtained using the Suh and Dalrymple model, in that at low water levels, the model predicted tombolo formation. For breakwaters 5 and 7, the salient length was predicted to reach a maximum length between high water and the mean water level. For all the other breakwaters, the model predicted steadily increasing salient lengths with increasing water depth, in a similar way to the Suh and Dalrymple model.

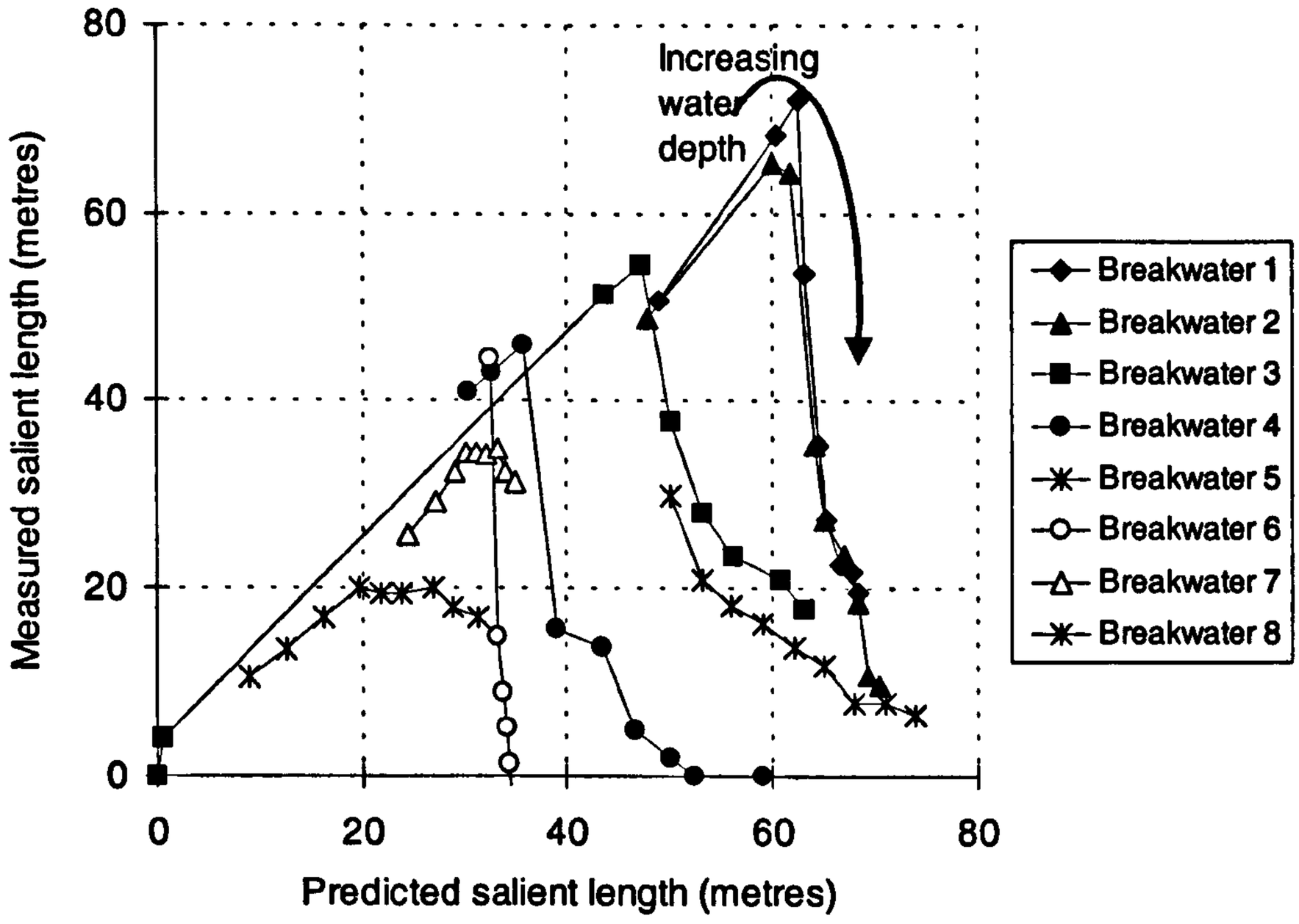

Figure 5-3 Comparison of observed and predicted salient lengths at Elmer, for each breakwater, at the range of tidal levels described in **Table 5-1**, using the method proposed by Suh and Dalrymple (1987).

5.4 Discussion

From these results, it appears that the methods of Suh & Dalrymple, and of McCormick, work very well for describing tombolo formation, but do not appear to be as reliable when modelling salient formation. This may be due to a tendency to over predict salient lengths, which is a characteristic that would be masked when comparing these models with field tombolos. This tendency has been observed previously and reported in Chasten *et al* (1993). As a counter to this however, both models described the lower salient and tombolo formation behind breakwater 4.

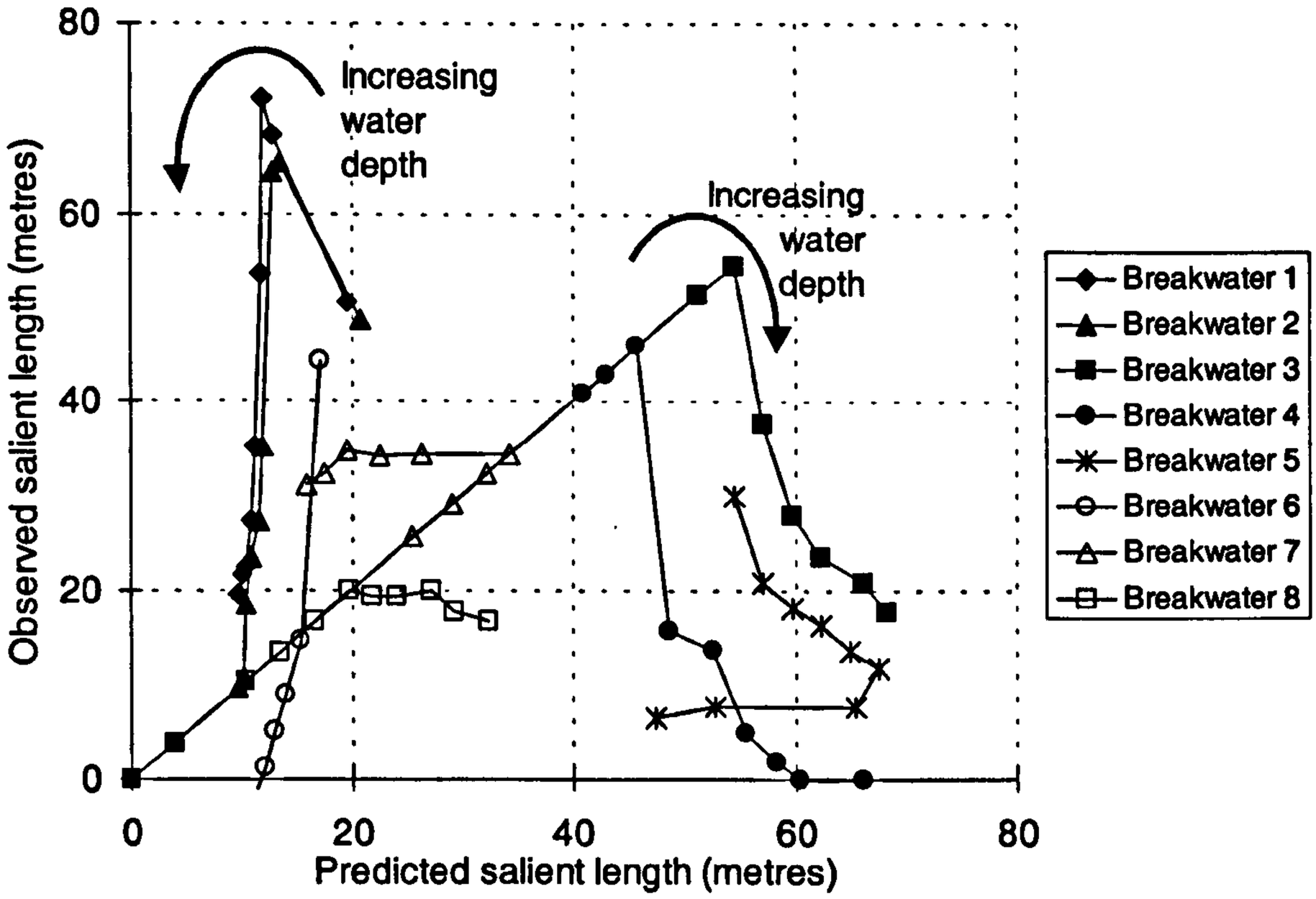

Figure 5-4 Comparison of observed and predicted salient lengths at Elmer, for each breakwater, at the range of tidal levels described in **Table 5-1**, using the method proposed by McCormick (1993).

The Suh and Dalrymple model was developed from physical model tests and prototype data where the gap widths between breakwaters was constant, and the beach response averaged across a scheme was evaluated. Where the gap widths are variable, as at Elmer, and individual salient lengths are required, the limits of applicability of this model may have been exceeded. Additionally, the study site is characterised by the bimodal nature of the beach. In the updrift west of the scheme, the tombolos are formed of sand, while the upper beach is gravel. In the (downdrift) east of the scheme, where the gap widths are wider, the tombolos are predominantly gravel. The formation of tombolos from finer material to the remainder of the beach leads to a difference in beach slope in the bays and on the tombolos. This in turn affects the rate at which parameters (non-dimensionalized against offshore distance) vary with depth. In the east of the scheme, this problem is less pronounced, due to the more uniform nature of the beach.

The more general predictors, of Pope and Dean, and Ahrens and Cox, were more successful in predicting beach response - due in part to the fact that as they only give general descriptions of a likely response. To

illustrate this, it is clear that in Figure 5-1, tombolos were not predicted to occur behind breakwater 7 or 8. The observed response, shown in Table 5-2, is that tombolos formed. The response predicted by this method does however lie close to the limit of salient tombolo formation presented by Pope and Dean. Thus the predictions are reasonable. The prediction of the response to 3 and 4 was excellent. The method failed in the predictions of 1 and 2. As mentioned previously, the net drift direction at Elmer was from west to east, and this has led to an increased accumulation of material behind the first two breakwaters, that has not (yet?) been passed through the system. It may be supposed therefore that the Pope and Dean predictions are best used where longshore transport into a system is not significant, such as in a pocket bay, or indeed in the middle of a scheme of breakwaters. This failure to predict the beach response to breakwaters 1 and 2 also occurs with Ahrens and Cox's technique, although this method does succeed in predicting the tombolos behind breakwater 8 (and less well) breakwater 7.

5.5 Conclusions

From the comparison of the predicted and observed salient lengths during this exercise, three of the predictive schemes (Ahrens and Cox, McCormick, and Pope and Dean) were unable to predict the behaviour of the updrift breakwaters. This suggests that these techniques are not suitable for use where there is significant longshore transport into a scheme, which restrict their use to the design of pocket beaches, or to the central portions of multiple breakwater schemes, where net longshore transport is expected to be low. The robustness of the simplest technique (Ahrens and Cox) is surprising, suggesting that even in multiple breakwater schemes, the ratio of breakwater length to offshore distance is still paramount in determining shoreline response.

The inability of these methods to predict shoreline positions behind detached breakwaters does make them of less use to design engineers. To improve our design capability, physically based numerical process models, validated against field measurements, are needed before we can confidently develop 'rules of thumb' to simplify design.

5.6 One line model tests

The principles behind one line modelling have been described in Chapter 2. For this study, the model chosen was the US Army Corps of Engineers model GENESIS (Hanson, 1989). This model is widely used by engineers, particularly in the United States. The model is supplied at no cost by the Corps, although users are required to register. Only the executable code is made available. The Corps supplied version 3 of the model, which runs under MS-DOS. A 32-bit version has since been released.

Version 3 differs from previous versions. New algorithms for wave diffraction were implemented, and a different procedure for computing the cumulative effect of energy diffracting from many sources on the shoreline position was introduced. Mechanical bypassing of sand is permitted within the model domain, a moving shoreline boundary condition is introduced, and a new method of representing groynes and jetties was applied. Tombolo formation still causes this one-line model to halt. This removes the need to parameterise the transport of material offshore of the breakwater. In addition to this, the numerical scheme used in GENESIS might be expected to have difficulty modelling sediment transport in areas where the shoreline is at a large angle to the longshore (x) axis of the model. This axis should be aligned with the overall trend of the shoreline. A tombolo shoreline deviates strongly from this trend. The way the model calculates transport on shorelines that are not parallel to the x-axis is described later in this chapter.

The model has no particular adaptations for representing a macro-tidal environment, or variable beach composition. Chu at al (1987) applied a specially adapted version of GENESIS to a macro-tidal site in Alaska. They adapted it such that the three pairs of sediment transport coefficients (K_1 and K_2) were chosen. Each pair controlled the sediment transport rates at either the high, mid or low tide levels – and so included the influence of grain size changes between high and low water. Gravens (pers. comm.) stated that this modification was felt to have had a negligible influence on either the calculated transport volumes, or the resulting shoreline configuration.

In these tests, the model was used to try to replicate the observed contour movements at Elmer. This would allow experience to be gained in using such a model in a macro-tidal environment, with a bimodal beach. The remainder of the chapter describes the equations within the model, and discusses the implications these

on the model behaviour. The model calibration procedure is then described, and the results are discussed in the light of other users' experiences with the model.

5.6.1 Model description

The sand transport formula at the heart of GENESIS is given Equation 5-8:

$$Q = (H^2 C_g)_b \left[a_1 \sin 2\theta_{bs} - a_2 \cos\theta_{bs} \frac{\partial H}{\partial x} \right]_b$$

Equation 5-8

Where: H is wave height; C_g wave group speed given by linear wave theory; b is a subscript to denote condition at breaking; θ is wave angle to the shoreline at breaking and x is the longshore co-ordinate.

Non dimensional parameters a_1 and a_2 are given as follows:

$$a_1 = \frac{K_1}{16(\rho_s/\rho - 1)(1-p)(1.416)^{5/2}}$$

Equation 5-9

$$a_2 = \frac{K_2}{8(\rho_s/\rho - 1)(1-p)\tan\beta(1.416)^{7/2}}$$

Equation 5-10

K_1 and K_2 are empirical coefficients, ρ_s is sediment density (set to 2650 kgm^{-3}), ρ is the seawater density (set to 1030 kgm^{-3}), p is sediment porosity (set to 0.4), and $\tan\beta$ is the mean beach slope (calculated from the shoreline to the maximum depth of longshore transport defined below).

5.6.2 Numerical Scheme

GENESIS solves the equation for the rate of change of shoreline position (Equation 2-18) using the volume sediment transport rate given in Equation 5-3. To simplify the numerical solution, GENESIS assumes that θ_{bs} is small, where

$$\theta_{bs} = \theta_b - \tan^{-1}\left(\frac{\partial y}{\partial x}\right)$$

Equation 5-11

i.e. it is the angle between the breaking waves (θ_b) and the shoreline. On a gently sloping beach, θ_b is small due to wave refraction, so for θ_{bs} to be small, then the shoreline slope must also be sufficiently small that the final term in Equation 5-11 can be approximated by $\frac{\partial y}{\partial x}$.

This allows the $\frac{\partial Q}{\partial x}$ term in Equation 2-18 to be replaced by $\frac{\partial(2\theta_{bs})}{\partial x} \approx 2\frac{\partial^2 y}{\partial x^2}$ if θ_b is assumed not to change with x. This allows Equation 2-18 to be re-written as Equation 5-12, a diffusion-type equation. This is solved implicitly using a Crank-Nicholson scheme (Crank, 1975).

$$\frac{\partial y}{\partial x} = \left(\frac{H^2 c_g}{D_B + D_C} \right) \left(2K_1 + K_2 \cos\theta_{bs} \frac{\partial H}{\partial x} \right) \frac{\partial^2 y}{\partial x^2}$$

Equation 5-12

To find the effect of this small angle assumption on the predicted transport rate, GENESIS was run for one time step, with a straight coastline parallel to the x-axis subject to wave attack from a single direction. This would allow the wave breaking conditions, and the sediment transport rate calculated by GENESIS to be seen before it was modified by any shoreline changes.

This test was repeated using offshore wave directions between 0° (shore normal) and +80°. The results of these tests were compared with a similar situation, where a straight shoreline (oriented at an angle of between 0° and 80° to the x-axis) was subject to waves that came in normally to the x-axis. The results of the GENESIS calculations are presented in Table 5-3 and Table 5-4. These tables show that for shoreline angles up to 60° to the x-axis, the small angle assumption does not significantly affect the calculated volume transport rate.

For these tests θ_b was constant throughout the model domain – as is required in the small angle assumption. In the case of beach development around detached breakwaters or groynes, this part of the assumption could also be invalidated. Larson *et al* (1987) show that the linearization of the shoreline equation starts to degrade the solution for accretion at a single, shore-normal groyne, when the initial breaking wave angle reaches

about 30°. Greater accretion rates were obtained using the small angle assumption in a numerical solution, than were obtained using an analytical solution containing the full $2\left[\alpha_o - \arctan\left(\frac{\partial y}{\partial x}\right)\right]$ term.

Similar shoreline curvatures exist behind detached breakwaters, with the similar implications for the accuracy of the estimates of sediment transport rates, and the resulting estimates of shoreline position.

Offshore (deep water)wave angle	Wave breaking angle to the x-axis	Wave breaking angle to the shoreline	Breaking wave height H_b (m)	Volume transport rate Q ($100 \times m^3/s$)
0	0	0	0.80	0
10	-1.97	-1.97	0.79	-0.36
20	-3.88	-3.88	0.78	-0.66
30	-5.68	-5.68	0.75	-0.87
40	-7.08	-7.08	0.71	-0.97
50	-8.17	-8.17	0.67	-0.94
60	-8.57	-8.57	0.61	-0.79
70	-8.50	-8.50	0.53	-0.54
80	-7.99	-7.99	0.40	-0.25

Table 5-3 Breaking wave conditions and sediment transport rate calculated by GENESIS, for a range of offshore wave angles, and a straight shoreline parallel to the x-axis. Offshore wave height was 0.50 metres, with a period of 10 seconds.

Shoreline angle to the x-axis	Wave breaking angle to the x-axis	Wave breaking angle to the shoreline	Breaking wave height H_b (m)	Volume transport rate Q ($100 \times m^3/s$)
0	0	0	0.80	0
10	8.03	-1.95	0.79	-0.37
20	16.10	-3.85	0.78	-0.67
30	24.41	-5.63	0.75	-0.88
40	32.94	-7.09	0.71	-0.97
50	41.85	-8.16	0.67	-0.94
60	38.57	-8.57	0.61	-1.82
70	28.50	-8.50	0.55	-1.85
80	17.99	-7.99	0.40	-0.76

Table 5-4 Breaking wave conditions and sediment transport rate calculated by GENESIS, for a range of shoreline angles to the x-axis, and a wave input normal to the x-axis. Offshore wave height was 0.50 metres, with a period of 10 seconds.

5.6.3 Preparation of Elmer input data

Beach data

Grain size

The GENESIS transport equation (Equation 5-8) shows no direct dependence on grain size. Grain size is used as an input parameter instead to describe the beach profile. The mean beach slope $\tan \beta$ is calculated from the median grain size (d_{50}) using Equation 2-27. The average beach slope is used in the second term in the transport equation, influencing transport due to longshore variations in wave height. Beach slope also influences the volume transport calculation through the wave breaking parameter γ, calculated using Equation 2-23.

To calculate the median grain size, it is recommended to fit observed beach profiles to templates published in GENESIS Technical Report 1 (Hanson and Kraus, 1989). If profile data is unavailable, then the median value of grain size in the surf zone should be used. In these tests, time averages of the observed Elmer beach profiles were calculated, and a least squares fitting procedure was used to find values of median grain size that generated best fitting 'Dean' profile. This procedure was used for all profile lines that were aligned with breakwater gaps and the average result was adopted. The resulting value of mean effective grain size was 4.67 mm (the range of values was from 1.6 to 10 mm). This compares with the median grain size of the original beach, which d_{50} equal to 11.0 mm on the upper slope, and 115 μm on the lower slope. The d_{50} of the imported material had a typical value of 14 mm.

Values of γ in the literature vary between 0.55 and 1.4 (Nelson, 1997). It can be seen from this figure that the method of Smith and Kraus (referred to in GENESIS technical report 1) tends to a value of γ of 0.56 as beach slope tends to 0. Observed values of the limiting ratio of breaking wave height to water depth at Elmer show γ to have a value of 0.52 (Chadwick *et al*, 1995). The predicted value of γ, based on Smith and Kraus, for a median grain size of 4.7 mm show that for an offshore wave steepness of more than 1/14, the value of γ is greater than 0.77. The result of this over-prediction of γ is that larger waves break in shallower water than would otherwise be the case. The increase in breaker height is just offset by the reduction in wave group velocity in the shallower water. Breaking wave angle is also reduced, resulting in lower estimates of transport rate than would be obtained with smaller values of γ.

The Active Beach Height and Depth of Closure

To convert the calculated beach volume changes into a distance moved by the modelled contour, it is necessary to know the 'active' beach height. In GENESIS, this is taken as the distance between the *'average berm height'*, and the *'depth of closure'*. These values are fixed along the modelled coast, although may vary in reality. Figure 5-5 shows the factors that control calculated beach volume, the effect of volume changes, and the importance of the active beach height.

Hallermeier (1983) introduced the concept of the depth of closure. The sub-aerial beach was divided into three zones: the *offshore zone* (where no changes in bathymetry occurred over long timescales); the *shoaling zone* (minimal changes in depth occurred); and the *littoral zone* (depth changes occur on relatively short timescales). The boundary between the littoral and shoaling zones was called the *depth of closure*.

By definition, the depth of closure can be found by observing beach profiles taken over the timescale of interest. The depth where the profiles start to show no change over this period is the profile closure depth.

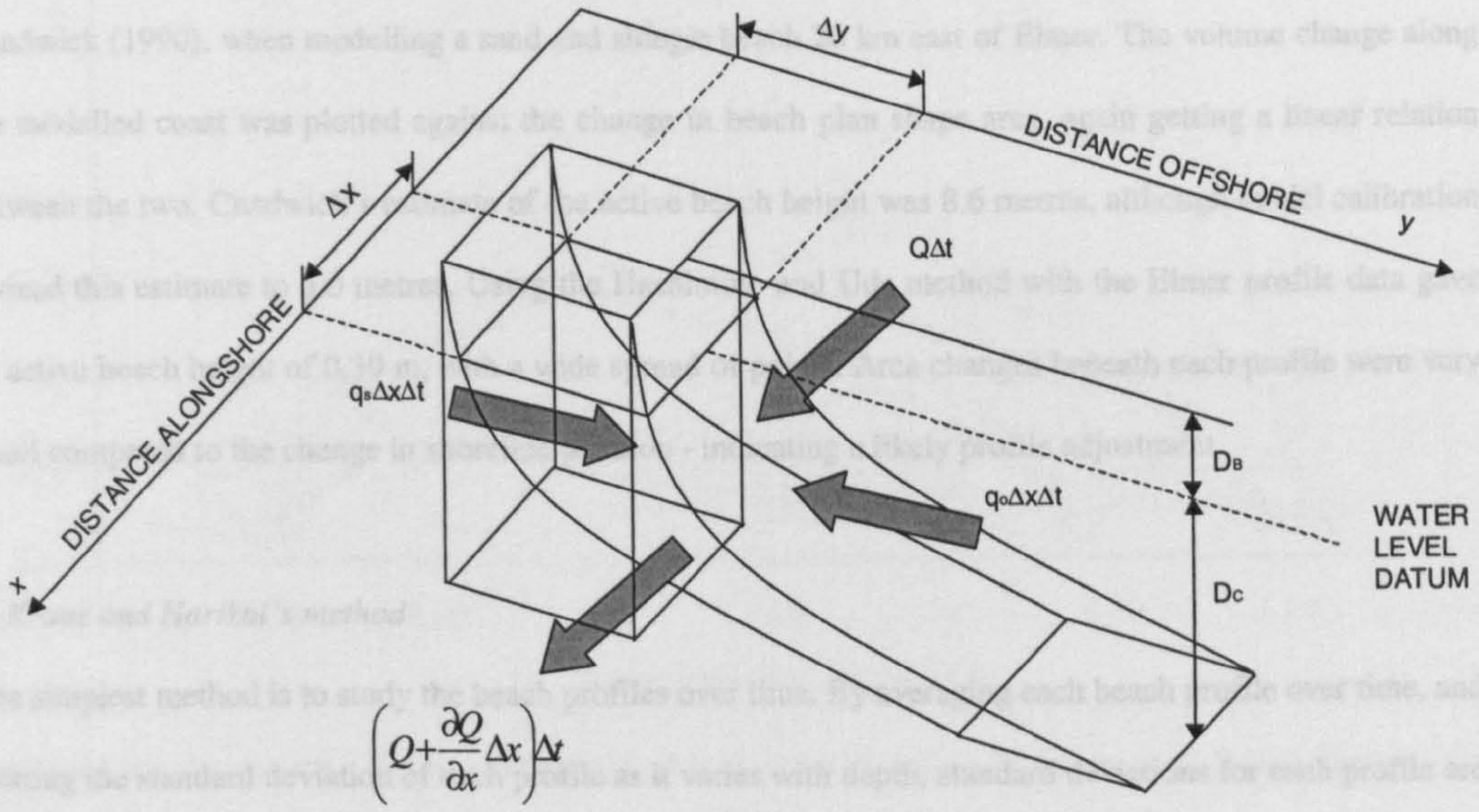

Figure 5-5 Definition sketch for shoreline change modelling, showing the definition of berm height D_B and closure depth D_C. After Hanson and Kraus 1989

Work by Nicholls (pers. comm.) looking at profile changes at Duck, North Carolina, show a time dependence on the depth of closure. It was found that 65% of profiles closed over a one or two-year period, while 30 % closed over four years, and only one profile closed over eight years. Thus, for model investigations of a couple of years, a depth of closure can be confidently defined. The effect of storms over longer periods is to drive the closure depth further offshore. This makes it difficult to define from profile studies, and also changes the value of the active beach height This in turn feeds back into the expected contour movements. Despite these difficulties, an estimate of the depth of closure is required for modelling. Three methods are available to help the estimate.

1) Method of Uda and Hashimoto (1980)

The method of Uda and Hashimoto (1980) involves calculating the area change under each profile, and the shoreline position change. Plotting the change in area (with units of square metres) against shoreline position change (units of metres), they found a reasonable linear trend between area change and shoreline position change. The gradient of the line describing this fit has the dimension of length (therefore units of metres) and they took this to be their active beach height. This was used in a slightly different form by Chadwick (1990), when modelling a sand and shingle beach 20 km east of Elmer. The volume change along the modelled coast was plotted against the change in beach plan shape area, again getting a linear relation between the two. Chadwick's estimate of the active beach height was 8.6 metres, although model calibration revised this estimate to 3.0 metres. Using the Hashimoto and Uda method with the Elmer profile data gave an active beach height of 0.39 m, with a wide spread of points. Area changes beneath each profile were very small compared to the change in shoreline position - indicating a likely profile adjustment.

2) Kraus and Harikai's method

The simplest method is to study the beach profiles over time. By averaging each beach profile over time, and plotting the standard deviation of each profile as it varies with depth, standard deviations for each profile are seen to tend towards the accuracy of the survey at both a shoreward limit (the berm height) and at a seaward limit (the depth of closure). This method was used by Kraus *et al* (1984) at Orai Beach in Japan. The result of employing this method at Elmer can be seen in Figure 5-6. There appears to be a minimum in the standard deviation in beach height at +5 m. Offshore, the lines appear to approach a minimum at around -1.8 m. It is unfortunate that the profile lines do not extend further offshore to better define this closure point. The

profile closure limit is clearly defined at Elmer however by the presence of the chalk platform. The limits of the active beach were taken as +5 metres and -1.8 metres above Ordnance Datum (AOD).

3) Hallermeier's method

The final method for calculating the closure depth is based on the extreme wave conditions averaged over a 12 hour period. This model is based on a sediment entrainment function. At the depth of closure, Hallermeier assumes that the near bed kinetic energy due to the highest 12 hour averaged wave height is sufficient to raise a grain by 0.015 of its diameter. Using the formula for depth of closure (Equation 2-28) with data collected at Elmer gives an annual deep water extreme wave (averaged over 12 hours) height of 1.72 m, and a corresponding period of 9.16 s. This gives a depth of closure of -0.22m. Hallermeier refers his values to the low tide mark, giving a value of around 3.15+0.22 m relative to Ordnance Datum, or around 1.5m deeper than that obtained by studying the profile variation with depth.

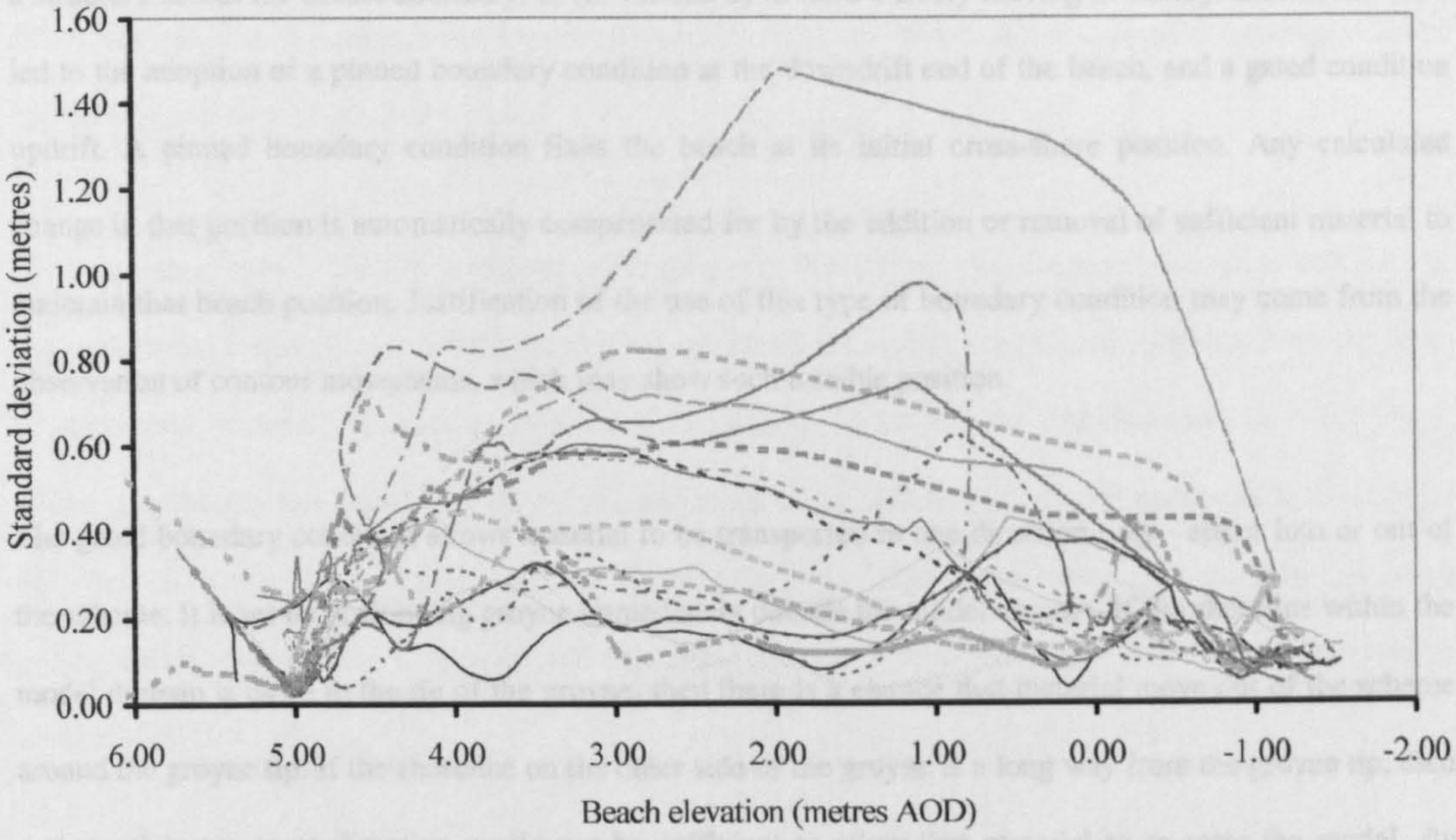

Figure 5-6 Plot of standard deviation of beach profiles against elevation for Elmer data. Based on the method of Kraus *et al* (1984)

Having calculated the active beach height, it was necessary to convert this into values for the depth of closure, and for the average berm height. This would then define the representative contour level. This is the height of the contour that is selected such that it's movement is considered representative of the entire beach

movement. A restriction on this choice was the inability of GENESIS to allow tombolos to form. This meant that the representative contour had to be higher up the beach than say, the mean tidal level, which would perhaps have been a more likely level to take. The choice to model a high contour should not influence the model output, since the beach is assumed to maintain a constant slope throughout the study - i.e. all contours are assumed to move equally either shorewards or seawards.

Beach position files were created from each of the aerial surveys. Because of the requirement for the beach contour to be monotonic in the x direction, it was necessary to rotate the beach data so that the orientation of Poole Place groyne was orthogonal to the *x* axis.

Boundary conditions

GENESIS allows the user to 'pin' the beach at the model boundaries, to apply a gated condition, by placing a structure across the model boundary, or (in version 3) to have a freely moving boundary. Calibration tests led to the adoption of a pinned boundary condition at the downdrift end of the beach, and a gated condition updrift. A pinned boundary condition fixes the beach at its initial cross-shore position. Any calculated change in that position is automatically compensated for by the addition or removal of sufficient material to maintain that beach position. Justification of the use of this type of boundary condition may come from the observation of contour movements, which may show such a stable position.

The gated boundary condition allows material to be transported in one direction only - either into or out of the scheme. It is set by positioning groyne immediately outside the model domain. If the shoreline within the model domain is close to the tip of the groyne, then there is a chance that material move out of the scheme around the groyne tip. If the shoreline on the other side of the groyne is a long way from the groyne tip, then a reversal in transport direction would not be sufficient to allow that material to re-enter the model. By reversing the shoreline to groyne tip distances, so that the outside shoreline is close to the tip, and the inner shoreline is further away, the condition can be made to favour the movement of sediment into the scheme. Allowing the boundaries free movement meant that there is no constraint on the shoreline position at the boundaries. In the early calibration runs of the model, this led to peculiar shoreline responses at the boundaries.

Structure data

Groynes

GENESIS requires values for the length of groynes used in simulations. Where groynes extend beyond the surf zone, they are classified as diffracting structures, otherwise they are considered only to interrupt longshore transport. For non-diffracting structures, GENESIS calculates the amount of sediment bypassing the seaward limit of the groyne. For all groynes, a permeability coefficient is required to simulate transport of material through or over a structure. Version 2 of GENESIS also required a value for the reduced beach slope in the vicinity of groynes. This was removed for version 3, which was the version tested in this study. Groynes affect the transport of material into, out of and beyond the scheme. They can be treated as calibration parameters helping to reproduce the observed transport rates into and out of the scheme. The GENESIS manuals recommend that the groyne permeabilities are 'tuned' in the calibration process to better represent beach changes in their vicinity.

The principle groyne in the Elmer scheme is the groyne at Poole Place that maintains the down drift limit of the constructed beach. This is a rock groyne that maintains the updrift beach level 5 metres above the level of the downdrift beach. Wooden groynes exist both updrift of the scheme, and downdrift of Poole Place. These groynes are low relative to the beach, and from aerial photographs do not appear to have a major influence on the beach plan shape, except at the very top of the beach. As a result, only one non-diffracting groyne was included in the tests, placed at the updrift boundary of the model domain to limit transport of material into the scheme.

Breakwaters

1) Transmission coefficients

GENESIS allows the inclusion of transmission coefficients for each breakwater. Energy can be transmitted through a breakwater by overtopping, and by wave penetration through the structure of the breakwater. The reef-type breakwaters employed at Elmer are expected to allow transmission by both mechanisms. Transmission through the structure was possible as the breakwaters had no rubble core, and had large

interstices between the armour stone blocks. Transmission through overtopping would most likely be restricted to high water and extreme wave events.

In GENESIS, the transmission coefficient for each breakwater is defined as the ratio of the height of the incident waves immediately seaward of the structure (and assuming no reflection from the structure) to the wave height immediately behind the breakwater. Thus a transmission coefficient of 1 is equivalent to no breakwater, while a value of 0 assumes no transmission. Given that wave transmission increases the wave energy behind the structure, it must reduce the longshore gradient in wave height in the vicinity of the breakwater, and thus have a similar effect to decreasing the value of K_2 in Equation 5-8. No variation of the transmission coefficient with wave steepness or structure property is assumed. In the GENESIS workbook, transmission coefficients are recommended to be used as a calibration parameter to 'knock back' salients that have grown too far, and/or too narrow in the calibration stages of the modelling exercise. Hanson, Kraus and Nakashima (1989) present this model of wave transmission, and its influence on shoreline development behind transmissive detached breakwaters in the Gulf of Mexico.

Formulae to calculate wave transmission through structures have been presented by van der Meer & Daeman (1994) and by Ahrens (1987) and their application is described in the CIRIA Manual on the Use of Rock in Coastal Engineering (CIRIA, 1996). An additional fieldwork exercise has taken place at Elmer to study the variation of transmission with tidal level (Simmonds *et al*, 1997).

Using a range of median rock sizes from 1.27 to 1.47 metres, an approximate cross-sectional-area of the breakwaters of 80 m^2, and freeboard and wave conditions derived from the observations, a histogram of wave transmission values was plotted. The mean value of the transmission coefficient was 0.32. Using the same input data, the method of Ahrens gives a value of 0.44. A preliminary value of 0.4 was found from the field tests at Elmer (D. Simmonds, pers. Comm.). Tests will investigate the influence of wave transmission on the model calibration.

2) Depths at breakwater tips

In addition to requiring the longshore and cross shore positions of breakwater tips, GENESIS also requires values for the depth at the breakwater tips. The depths at the tips are used in the diffraction calculations

described earlier in this chapter. There does not appear to be a method for updating the values of water depth at the tips as the beach moves.

Seawalls

Seawall positions were taken from the aerial survey data, and rotated to the modelling co-ordinate frame.

Bypassing and renourishment

GENESIS allows material to be added to the modelled beach during the simulation period. This has the effect of moving the modelled contour seaward by a user specified amount, to represent the new berm width after the material has come into equilibrium. The user specifies the start and end cells where the nourishment is to occur, and the dates when the beach fill operation starts and stops. Bypassing allows material to be taken from one part of the model domain and added elsewhere. Multiple nourishment and bypassing events are permitted in the model.

No additional renourishment took place at Elmer after the completion of the scheme, and no bypassing or renouishment was simulated in this modelling exercise. In September 1994, The NRA did remove an estimated 12 000 m^3 of material from the salients behind breakwaters 6 and 7, and place it in front of the revetment in bay 5. This handling took place after the aerial survey had been flown, so did not show in the autumn 1994 survey. The actual amount of material moved was not measured by the NRA, and the estimate of the volume of material moved was made by Arun District Council (R. Traynor, per. comm.). The material appeared to be quickly removed from the bay 5 beach, and was assumed to have moved back to its original position before the winter (January 1995) survey. Because of this, it was not modelled as part of this study.

Calibration Coefficients

The role of calibration coefficients in Equation 5-8 was described earlier in the chapter. To estimate suitable values for K_1, examples and relationships from the literature were sought. This section reviews the methods to obtain approximate values for the calibration coefficient K_1 for use in these tests.

Typical values of K_1 for a sandy beach are generally between 0.58 and 0.77 (Hanson and Kraus, 1991). A typical value adopted by HR Wallingford Ltd, for shingle transport on the U.K. south coast, are 0.02 to 0.04 (Brampton and Millard, 1996). To determine a suitable starting value for the Elmer calibration, typical transport rates were assessed from the literature, and then values of K_1 to reproduce those transport rates with the observed wave conditions were obtained. These were then compared with empirical relationships for K_1 from the literature.

Typical shingle transport volumes along the U.K. south coast vary between 5000 and 20000 cubic metres each year (Robert West and Partners, 1991). At Shoreham (20 km east of the study site), 15 000 cubic metres of material are transferred across the harbour mouth to maintain the feed to downdrift beaches (Holmes and Beverstock, 1996). For the design of the beach renourishment at Seaford, around 40 miles east of the Elmer scheme, volumes of sediment transport into the scheme were of the order of 5000 cubic metres per year, although movement within the scheme was estimated at 70 000 m^3yr^{-1}(reported in Brampton and Millard, 1996).

Assuming a straight coastline at Elmer, running 256°-076° (approximately west-south-west to east-north-east), and using the measured wave data, the mean volume transport rate (in m^3/s) was estimated. Bottom contours were assumed to be parallel, such that there was no longshore gradient in wave height. This reduced the transport volume to:

$$Q = \frac{\left(H^2 Cg\right)_b \left(K_1 \sin 2\theta\right)}{16\left(\rho_s/\rho - 1\right)\left(1-p\right)\left(1.416^{5/2}\right)}$$

Equation 5-13

K1 was adjusted to fit the calculated transport rate to the literature values. The observed wave data were transformed from the recorder position to breaking, using linear wave theory and an iterative method to find the breaking criteria. This provided an estimate of the mean transport rate (in m^3s^{-1}) which was then used to estimate an annual transport rate. Comparing this value with the expected (literature) values of between 5000 and 20000 m^3yr^{-1} gave an estimate of K_1 between 0.014 and 0.057. Taking the recycling volume used at Seaford as a maximum transport rate gave a value of K_1 of 0.20. This method could also have been used to provide a check on the estimated volume changes reported by the model. It does not however take into

account the influence of boundaries (and structures near boundaries) on preventing material entering the model domain. It does however provide a guide as to likely volume changes.

Kamphuis and Readshaw (1978), Vitale (1981), Kamphuis and Sayao (1982) and Ozhan (1982) all postulated relationships (based on laboratory data) between K and the Irribarren (surf similarity) number, ξ_b, where:

$$\xi_b = (\tan\beta)\left(\frac{H_b}{L_o}\right)^{-1/2}$$

Equation 5-14

Bodge and Kraus (1991) combined laboratory and field estimates of K and ξ_b to provide two expressions for K. The first was based on laboratory data alone, while the second combined laboratory and field data:

$$K = 0.37\ln\xi_b + 0.59$$

Equation 5-15 (Laboratory data only)

$$K = 0.22\ln\xi_b + 0.62$$

Equation 5-16 (Laboratory and field data)

Kamphuis (1990) proposed a relation based on 3D mobile-bed laboratory tests, using sands with a d_{50} of 0.105 and 0.18 mm. Following Bodge and Kraus' (1991) rearrangement of Kamphuis' equation, K can be written as follows:

$$K = K^* \frac{16 g^{0.25} \xi_b \sqrt{\gamma T_P}}{(2\pi)^{0.75}(d_{50}\tan\beta)^{0.25}\sin^{0.4}(2\theta_b)}$$

Equation 5-17

γ is the ratio of breaking wave height to water depth, T_P is the spectral peak period, ε_b is the Irribarren number and K^* is set to a value of 0.0013. Using the beach data and breaking wave conditions derived from the Elmer field study into these equations yielded estimates for K of 0.68 +/- 0.20 (Equation 5-15), 0.67 +/- 0.12 Equation 5-16) and 0.11 +/- 0.11 (Equation 5-17) (errors given as +/- 1 standard deviation).

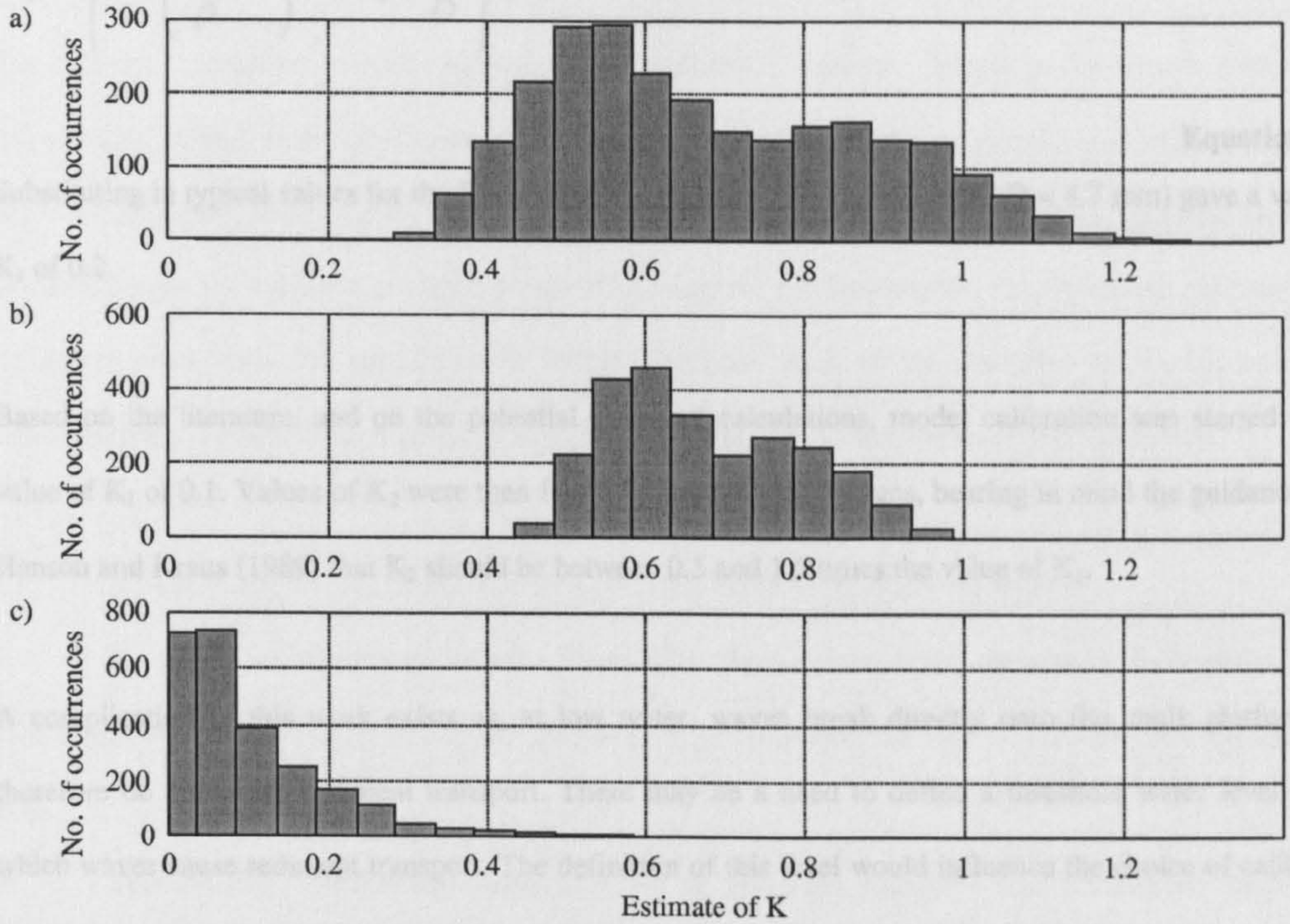

Figure 5-7 Histograms showing the distributions of estimates of the empirical longshore transport coefficient K_1.

where a) was calculated using Equation 5-15 and b) Equation 5-16, with an Irribarren number based on observed Elmer wave conditions and the time-mean effective beach slope. In c), Equation 5-17 is used, with the effective grain size for d_{50}.

Estimates of K_1 based on the equations presented in Bodge and Kraus are clustered around a median point of about 0.7 – close to the Shore Protection Manual recommended value of 0.77. The method based on Kamphuis gives substantially lower estimates of K_1. These estimates are more in line with other estimates of K_1 for shingle beaches.

Kamphuis et al (1986) studied a range of field data, and proposed the following modification give K_1 (called K_P in Equation 5-18) relative to the value of K_1 (called K) conventionally set to 0.77 in the CERC equation.

$$K_p = \left\{0.01\left(\frac{\rho_s}{\rho}-1\right)^{1/2}\tan\beta\frac{H_{bs}}{D}\right\}K$$

Equation 5-18

Substituting in typical values for the Elmer field site ($\tan\beta = 1/7$, $H_{bs} = 0.5$ and $D = 4.7$ mm) gave a value of K_1 of 0.2.

Based on the literature, and on the potential transport calculations, model calibration was started with a value of K_1 of 0.1. Values of K_2 were then found by iterative model runs, bearing in mind the guidance from Hanson and Kraus (1989) that K_2 should be between 0.5 and 1.5 times the value of K_1.

A complication to this work exists as, at low water, waves break directly onto the chalk platform and therefore do not cause sediment transport. There may be a need to define a threshold water level, above which waves cause sediment transport. The definition of this level would influence the choice of calibration coefficient, as the calibration coefficient may be used to compensate for either too high or too low a threshold level being adopted.

5.6.4 Model Calibration

The GENESIS Technical reference 1 defines model calibration as the 'procedure of reproducing with a model the changes in shoreline position that were measured over a certain time interval'. Verification is described as the 'process of applying the calibrated model to reproduce changes over a time interval different from the calibration interval.' The aim of the calibration exercise is to determine the values of the main parameters controlling known quantities - i.e. the net transport rate and volume changes in the study area. Local and more minor parameters are then used to optimise the calibration.

Model verification implies that the boundary conditions and calibration parameters remain constant and independent of the period over which the model is used. This assumes that no physical changes occur to the beach that may invalidate the model set-up, such as the construction of updrift structures that alter the model boundary conditions, or renourishment with a different material that alters the beach slope

Recommended calibration procedures

To perform a rigorous model calibration and validation exercise, beach position and composition information, as well as the directional wave data is required for both the calibration and validation periods. To meet the assumptions of one line modelling, these periods should ideally be annual, such that (seasonal) profile changes are averaged out over the period of interest. To illustrate the recommended calibration and validation procedures, the application of GENESIS to the study of the detached breakwater scheme at Lakeview Park, Lorain, Ohio is given by Hanson and Kraus. The procedure used was as follows:

1. K_1 was varied to give overall net transport rates close to the observed values
2. K_2 was varied alternately with the value YG1 (the distance of the shoreline outside the modelled area from the seaward end of the updrift groyne). YG1 controlled the flux of sediment into the modelled area.
3. Transmission coefficients were adjusted to give the 'correct' size of salients behind the breakwaters.
4. Breakwater positions were 'adjusted' to obtain better agreement between the modelled and observed shorelines. This adjustment was justified by the authors by arguing that it was difficult to precisely place the structures on a finite grid, and also because the model assumes that the structures were infinitely thin.
5. Qualitatively study the input and output files to check that the data is reasonable.

In addition to qualitatively comparing the modelled and observed shorelines in the calibration exercise, GENESIS offers a goodness of fit parameter called the 'calibration/validation error'. This is the average absolute difference in shoreline position between the final modelled and observed shoreline. This parameter is shown in Equation 5-19.

$$\text{Calibration/Validation Error} = \frac{1}{NN}\sum_{i=1}^{NN} abs\left(y_{observed}(i) - y_{predicted}(i)\right)$$

Equation 5-19

In the Lakeview Park case, verification data were not available (shoreline data was, but concurrent wave data was not). For the verification, predicted shoreline positions were compared with aerial photographs of the actual shoreline. This resulted in the value YG1 being increased. Running the model again with the new

value of YG1 and new shoreline data, but the original wave data, it was found that a 10% increase in wave height better replicated the observed shoreline changes. This variation was believed to be due to the natural year by year variability in wave conditions at the site.

Sensitivity Tests

The aim of the sensitivity testing is to show the effect of the original parameters on the model output. The hope is that the model is relatively insensitive to small changes in the input conditions. . Uncertainty in the input conditions (due to natural variability, measurement problems and data availability) means that there is uncertainty in the values of input parameters. If the model were sensitive to small changes in the input parameters, then the range of model output would be too large to be of use. The GENESIS Workbook (Technical Report 2 by Gravens, Kraus and Hanson, 1991) gives a more detailed description of the influence of uncertainty in the input parameters. The method applied in the Lakeview Park case was divided into two parts: beach data and wave conditions.

1. Beach data

K_1 was varied from 0.42 to 0.52. This caused an increase in the sand transport volume trapped by the scheme, but did not affect the shape of the final shoreline. Increasing K_2 from 0.12 to 0.22 led to an increase in salient length, and an increase in the amount of material lost from the western terminal groyne.

The modelled grain size was changed from 0.4 to 0.2 mm. The reduced beach slope pushed the breaker line further offshore. The structural parameters (breakwater position; depth at breakwater tips; depth at groyne tips) were not changed. The result was much greater material accreting behind the structures, although the authors recognised that this result was unrealistic, as GENESIS could not represent the expected increased loss of material offshore.

2. Wave data

While the transmission properties of the breakwaters in the Lakeview Park case were expected to be equal, it was found that by varying the transmission coefficients of each breakwater, it was possible to improve the fit of the predicted shoreline to the observed final shoreline position. The effect of reducing the transmission coefficients was to increase the salient length, without causing increased erosion in the embayments (thus

more material was retained by the scheme). Changing the input wave height had an effect similar to changing K_1. Changing the input wave direction by 10° had the expected result of increasing the observed transport.

The overall conclusion drawn from the sensitivity exercise was that the model was relatively insensitive to changes in the model parameters, and so could be used with confidence to describe and predict beach changes at this site.

5.6.5 Elmer model calibration

In addition to minimising the calibration/validation error (Equation 5-19) by fitting the modelled and observed shorelines, the observed volume changes need to be reproduced. The previous chapter showed that the volume change between September 1993 and September 1994 was an accretion of about 24 000 m^3 (calculated using Simpson's rule). Contour movements over this period showed this accretion to be mainly at lower beach levels, while the upper beach eroded. Thus at Elmer, one of the principle assumptions of one-line modelling - that the contours of the beach move in parallel - was invalid over this period.

The contours of the upper beach did move together, so it was decided to model the beach behaviour reproducing the movement of these contours. The volume change associated with the contour movements of the upper beach (assuming that they were replicated over the entire active profile) indicated a loss of 20000m^3. The model calibration would focus on minimising the calibration/ validation function, and replicating this loss of material.

This gave the problem that the model was apparently being calibrated to give an opposite trend to the observations. While this is true, the beach did not conform to the assumption of contours moving in parallel, although the upper, shingle beach did if considered separately from the lower beach. The shingle and sand portions of the beach appeared to behave separately also. The shingle beach lost material, while the sand beach gained twice the volume that was lost from the upper beach. While it is possible that the re-grading of the beach contributed to this, the large volume of accreted sand suggests that there was a supply of sand material to the beach, but little or no corresponding supply of shingle. In this case, the shingle portion of the

beach could be considered to be moving independently of the sand base, and so should be modelled separately.

The presence of tombolos on the sand beach made it impossible to model this using GENESIS. It could also be argued that the design engineer, interested in maintaining a certain, minimum berm width, is interested in the behaviour of the crest of the beach. Given the restrictions associated with one-line modelling, with GENESIS and the study site, it was felt that the approach outlined was reasonable.

Before calibrating the model by minimising the calibration error, the calibration errors were calculated between consecutive surveys. This gave a set of baseline calibration values that indicated whether the model was accounting for at least some of the variance seen in the contour position. The calibration errors were calculated by running GENESIS for one time step, with the initial shoreline position (SHORL file) described by one survey, and the calibration (SHORM) file containing data from subsequent surveys. The calculated calibration/verification error was output in the SETUP file, and checked by hand. Table 5-5 shows the calibration errors between successive surveys. Successful calibration would be indicated by values smaller than these.

	September 1993	February 1994	May 1994	September 1994	January 1995
September 1993	0				
February 1994	7.49515	0			
May 1994	8.11860	1.55525	0		
September 1994	8.48630	1.96385	1.15230	0	
January 1995	8.54625	1.95820	1.55445	1.83735	0
May 1995	9.20430	2.84125	1.97080	2.01160	1.95935

Table 5-5 Root-mean-square differences in the position of the observed +2m AOD contour line (from Equation 5-19).

The first calibration runs were carried out using the shoreline position data from February 1994 to January 1995, as this covered the period with the most complete wave data coverage. Initial tests concentrated on setting reasonable boundary conditions, and checking the position of the structures on the modelled grid. The first run allowed both the up- and down-drift boundaries to move freely. The result of this test was

unphysical shoreline positions close to the boundaries, although this did not appear to feed into the rest of the model domain.

The next test used a pinned updrift boundary condition. It was found that this was allowing too much material to enter the modelled scheme. The volume of material entering the scheme was reduced by applying a gated boundary condition by inserting a short groyne at the updrift limit of the model domain. The downdrift boundary was pinned, as it was not expected that material would enter the renourished area by travelling seaward of Poole Place groyne. Having set reasonable boundary conditions, the effects of varying the empirical transport coefficients on the model output were investigated.

Test name	K_1	K_2	Boundary conditions		Results	
			Updrift	Downdrift	Calibration error	Modelled volume change (m^3)
T1	0.1	0.05	Open, free to move	Open, free to move	63.68	$+5.86 \times 10^5$
T2	0.1	0.05	Pinned	Open, free to move	14.54	$+1.33 \times 10^5$
T3	0.1	0.05	Gated	Pinned	7.417	$+1.26 \times 10^5$
T4	0.1	0.075	Gated	Pinned	6.857	$+1.28 \times 10^4$
T5	0.1	0.2	Gated	Pinned	8.527	$+1.99 \times 10^4$

Table 5-6 Results of initial GENESIS tests on the Elmer field data

The low values of the mean square shoreline position differences shown in Table 5-5 indicate that the beach developed quickly between September 1993 and February 1994 (a mean difference in of 7 metres). After February 1994, changes were much smaller (mean differences of ~ 2 metres). To be able to calibrate a model down to these levels, and to see the effect of individual model parameters on the solution, would require an extremely sensitive model. Thus it would be difficult to see the relative importance of these parameters on the beach development. Thus, for the calibration exercise, the period September 1993 to September 1994 was used.

Selection of K_1

After setting boundary conditions that were reasonable, and gave reasonable beach responses, the model was run for a fixed value of K_2 (set to 0.1) and a range of K_1 values from 0.1 to 1.0. Breakwater transmission was set to 0.4, which fitted observations on site (Simmonds, per. comm.). The intention was to follow the

'textbook' example from Lakeview Park discussed earlier, in representing the volume changes observed within the scheme.

The results of these tests are presented in Table 5-7 in terms of the effect of K_1 on calibration errors, and on the observed volume changes. Figure 5-8 and Figure 5-9 show the range of shoreline positions created.

Test name	K_1	K_2	Calibration/ validation error	Modelled volume change (m^3)
T10	0.1	0.1	9.167	+7980
T20	0.2	0.1	10.419	+7840
T30	0.3	0.1	11.210	+4610
T40	0.4	0.1	12.016	-582
T50	0.5	0.1	12.928	-7080
T60	0.6	0.1	13.777	-14500
T70	0.7	0.1	14.566	-22600
T80*	0.8	0.1	13.872	-986
T90*	0.9	0.1	14.255	-8900
T99*	1.0	0.1	14.447	-19800

Table 5-7 Results of calibration tests looking at the effect of K_1 on model error, and on modelled volume change. Tests denoted with a * terminated prematurely due to tombolo formation

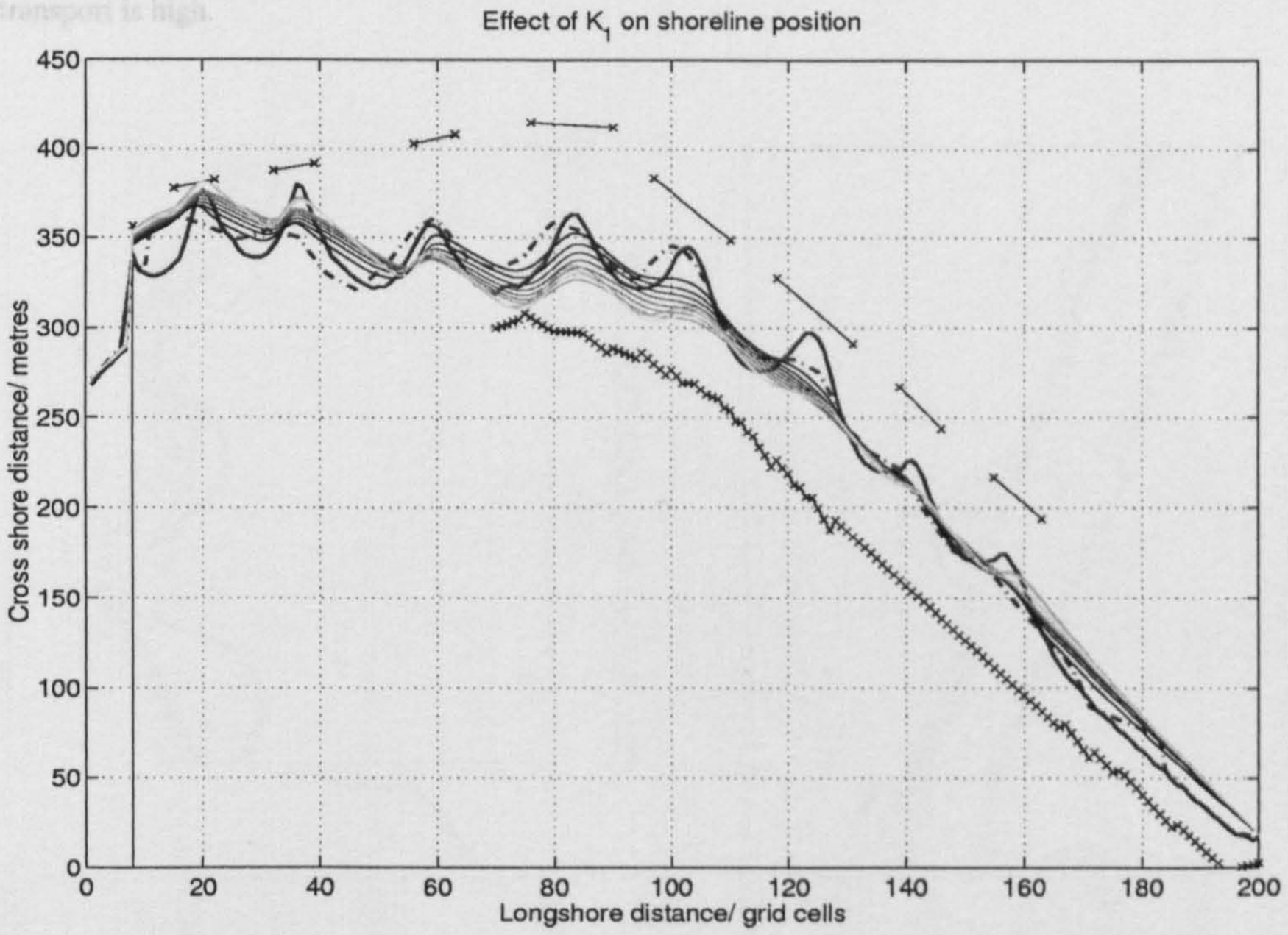

Figure 5-8 Effect of K_1 on modelled shorelines.

Lighter shorelines represent higher values of K_1, darker ones for low values. The thick solid shoreline is the final observed shoreline position. The initial shoreline is given by the thick dash-dot line. Breakwaters, groynes and seawalls are shown as crosses joined with straight lines. 1 grid cell is 10 metres wide.

The minimum in the calibration/validation error occurred for low values of K_1, as would be expected from the literature values discussed previously. The best representation of the observed (based on the +2 metre contour movements) volume changes were from the higher values of K_1 (particularly around $K_1 = 0.7$). Higher values of K_1 caused the model simulations to be terminated due to tombolo formation behind breakwater 8.

Figure 5-8 and Figure 5-9 show the effect of increasing K_1. Transport into the scheme increases with increasing K_1, as shown by the advancing shoreline behind breakwater 1. The presence of breakwater 1 reduces the transport locally, leading to the accumulation behind it. Transport towards the headland is reduced, leading to the erosion of the small salients built into the original beach plan. Around the headland position (80 - 120 cells alongshore) the beach is cut back almost to the sea wall for $K_1 = 1.0$. Material is also trapped by Poole Place Groyne and accumulates behind breakwater 8, leading to tombolo formation when transport is high.

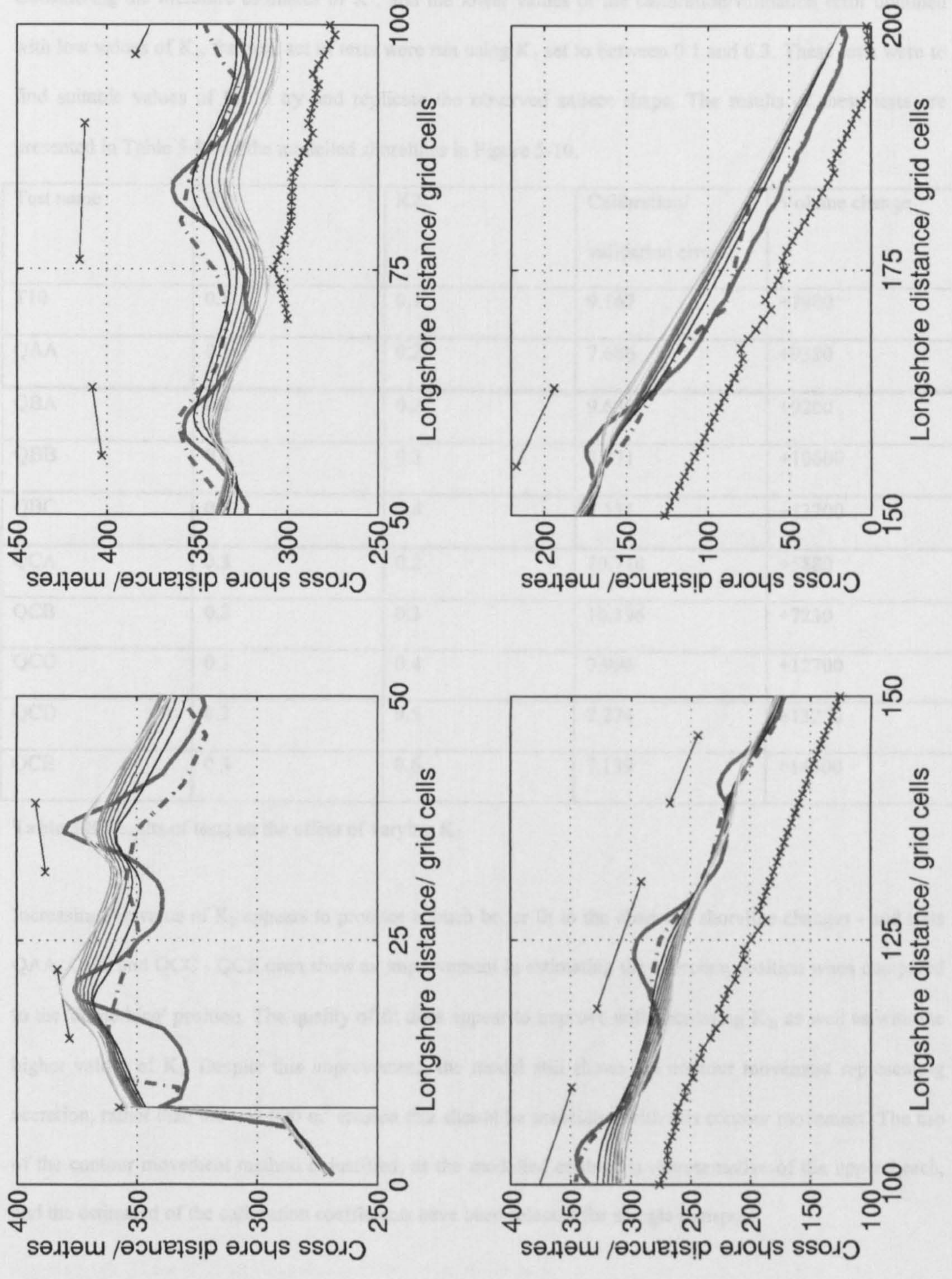

Figure 5-9 Tests on the influence of K_1 on modelled shoreline position.

Lighter shorelines represent higher values of K_1, darker ones for low values. The thick solid shoreline is the final observed shoreline position. The initial shoreline is given by the thick dash-dot line. Breakwaters, groynes and seawalls are shown as crosses joined with straight lines.

Considering the literature estimates of K_1, and the lower values of the calibration/validation error obtained with low values of K_1, the next set of tests were run using K_1 set to between 0.1 and 0.3. These tests were to find suitable values of K_2 to try and replicate the observed salient shape. The results of these tests are presented in Table 5-8 and the modelled shorelines in Figure 5-10.

Test name	K1	K2	Calibration/ validation error	Volume change
T10	0.1	0.1	9.167	+7980
QAA	0.1	0.2	7.686	+9380
QBA	0.2	0.2	9.639	+9200
QBB	0.2	0.3	8.871	+10600
QBC	0.2	0.4	7.151	+13700
QCA	0.3	0.2	10.710	+5880
QCB	0.3	0.3	10.196	+7230
QCC	0.3	0.4	7.996	+12700
QCD	0.3	0.5	7.274	+13200
QCE	0.3	0.6	7.139	+14300

Table 5-8 Results of tests on the effect of varying K_2

Increasing the value of K_2 appears to produce a much better fit to the observed shoreline changes - and tests QAA, QBC and QCC - QCE even show an improvement in estimating the shoreline position when compared to the 'do nothing' position. The quality of fit does appear to improve with increasing K_2, as well as with the higher values of K_1. Despite this improvement, the model still shows the contour movement representing accretion, rather than the ~20 000 m^3 erosion that should be associated with this contour movement. The use of the contour movement method is justified, as the modelled contour is representative of the upper beach, and the estimated of the calibration coefficients have been selected for shingle transport.

Differences between the modelled and observed shorelines are shown in Figure 5-11. Generally, the model is under predicting salient lengths, and not allowing sufficient erosion in the bays. The pinned updrift boundary is also allowing too much material to enter the model domain.

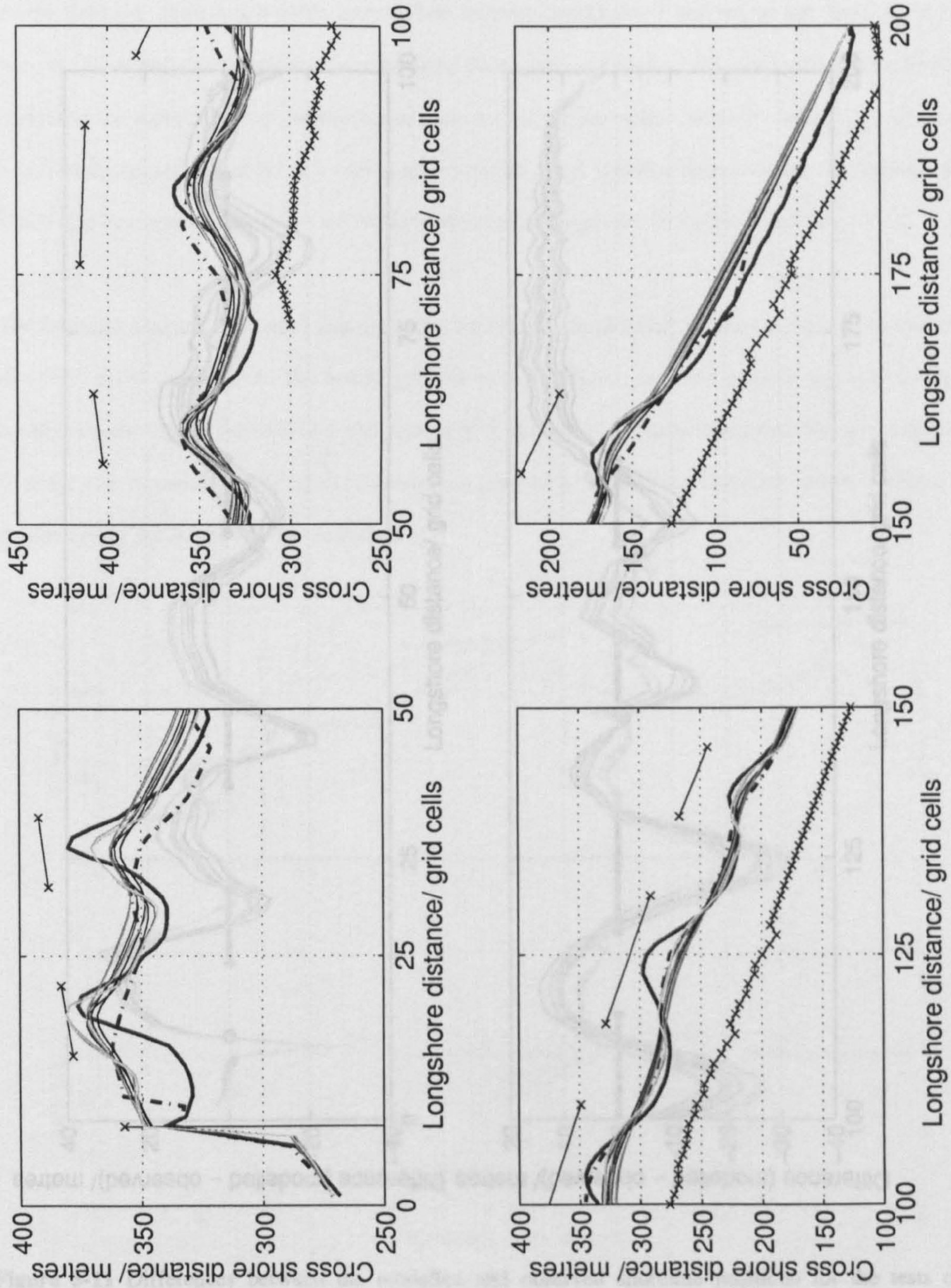

Figure 5-10 Effect of increasing K_2 up to twice the value of K_1.

Tests T10, QAA, QBA to QCE. Earlier tests (T10, QAA) are darker lines, later tests are lighter. Initial and final observed shorelines and structures are as for **Figure 5-9**.

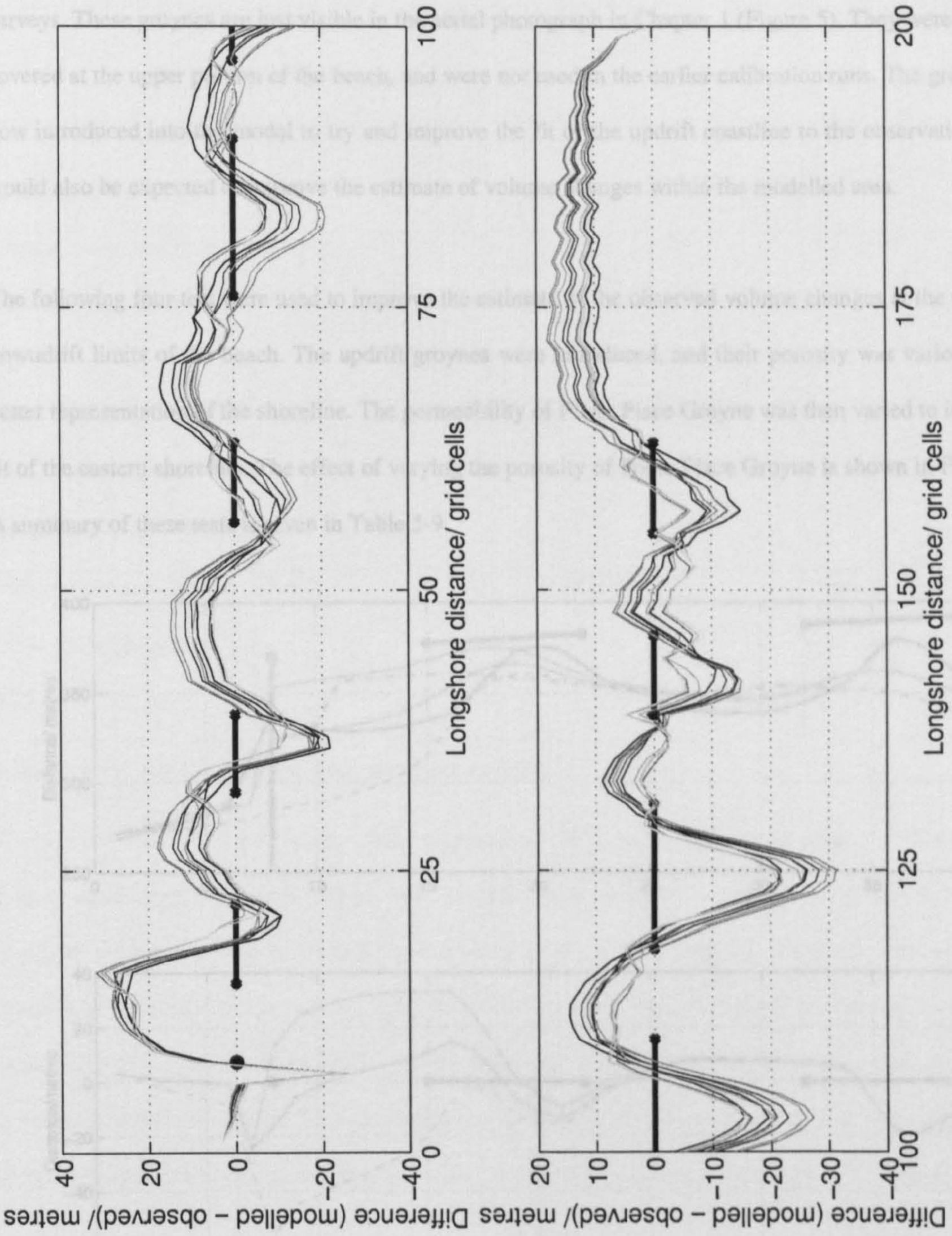

Figure 5-11 Differences between the modelled and observed shoreline positions for the tests on the influence of K_2.

Breakwater and groyne positions are denoted by the heavy lines and dot. The differences are shown such that darkest line represents tests T10, with the lines getting lighter towards test QCE.

At the field site, there is a wooden groyne field between breakwater 1 and the updrift limit of the beach surveys. These groynes are just visible in the aerial photograph in Chapter 1 (Figure 5). They were frequently covered at the upper portion of the beach, and were not used in the earlier calibration runs. The groynes were now introduced into the model to try and improve the fit of the updrift coastline to the observations, which would also be expected to improve the estimate of volume changes within the modelled area.

The following four test were used to improve the estimate of the observed volume changes at the updrift and downdrift limits of the beach. The updrift groynes were introduced, and their porosity was varied to give a better representation of the shoreline. The permeability of Poole Place Groyne was then varied to improve the fit of the eastern shoreline. The effect of varying the porosity of Poole Place Groyne is shown in Figure 5-12. A summary of these tests is given in Table 5-9.

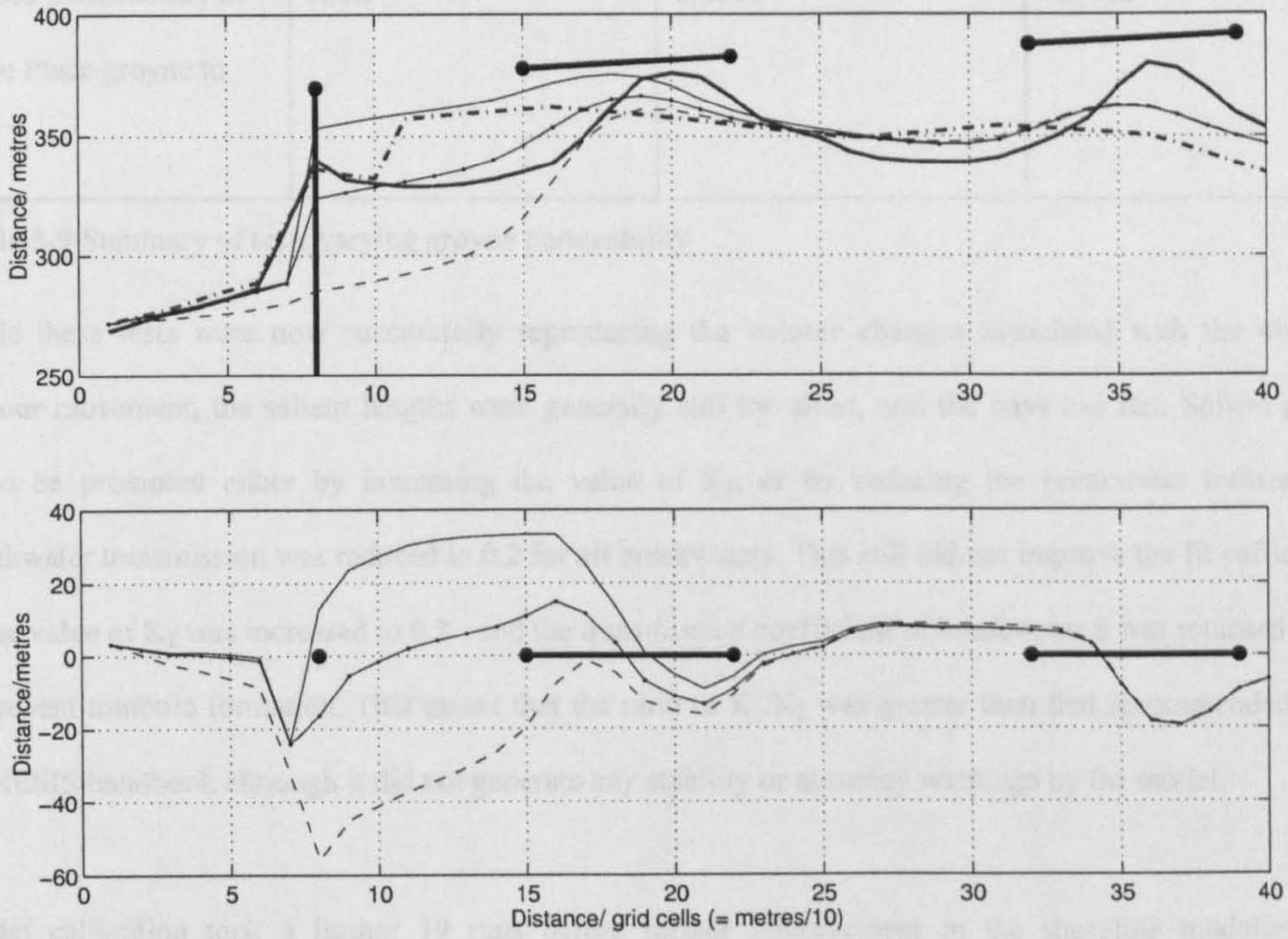

Figure 5-12 Effect of Poole Place Groyne (at grid cell 8) porosity on shoreline position.

Upper panel shows shoreline position (dash - dot and solid thick lines show initial and final observed shoreline position). Lower panel shows differences between observed and predicted shoreline positions for groyne porosity of 0 (solid line), 0.25 (dotted solid line) and 0.5 (dashed line).

Action	Test name	Calibration/validation error	Volume change (cubic metres)
Introduce impermeable updrift groynes	RAA	7.5700	+751
Change permeability of most updrift groyne to 0.5	RAB	7.5731	+792
Make Poole Place groyne semi-permeable (set permeability to 0.5)	RAC	7.9193	-44400
Reduce permeability of Poole Place groyne to 0.25	RAD	6.5871	-19000

Table 5-9 Summary of tests varying groyne permeability

While these tests were now successfully reproducing the volume changes associated with the observed contour movement, the salient lengths were generally still too short, and the bays too flat. Salient growth could be promoted either by increasing the value of K_2, or by reducing the breakwater transmission. Breakwater transmission was reduced to 0.2 for all breakwaters. This still did not improve the fit sufficiently, so the value of K_2 was increased to 0.3 - and the transmission coefficient of breakwater 8 was returned to 0.4, to prevent tombolo formation. This meant that the ratio of K_1:K_2 was greater than that recommended in the GENESIS handbook although it did not generate any stability or accuracy warnings by the model.

Model calibration took a further 19 runs before further improvement in the shoreline modelling was considered unattainable. The parameters of these tests are shown in Table 5-10, and Figure 5-14 shows the final shoreline and comparison with observations. The calibration/validation error was reduced to a minimum of 3.58, and a corresponding volume change of -20 200 m^3 was obtained.

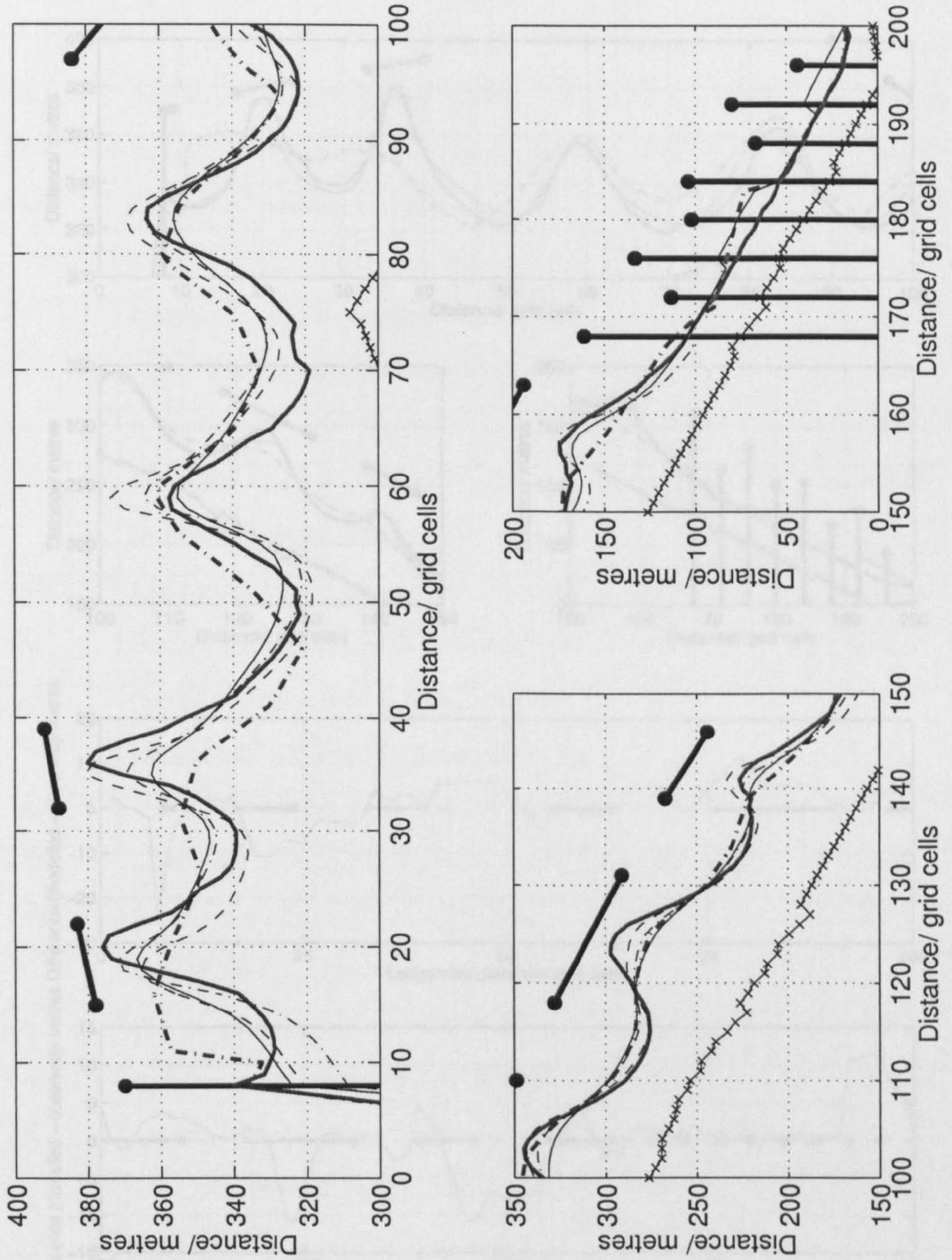

Figure 5-13 Shoreline predictions for tests on breakwater transmission and K_2.

Test: RAD (solid line: $K_2 = 0.2$; Transmission = 0.4);

RAE (dash-dot line: $K_2 = 0.2$, Transmission = 0.2)

RAF (dashed line: $K_2 = 0.3$; Transmission = 0.2 (0.4 behind breakwater 8).

The thick dash-dot and solid lines represent the initial and final shoreline positions.

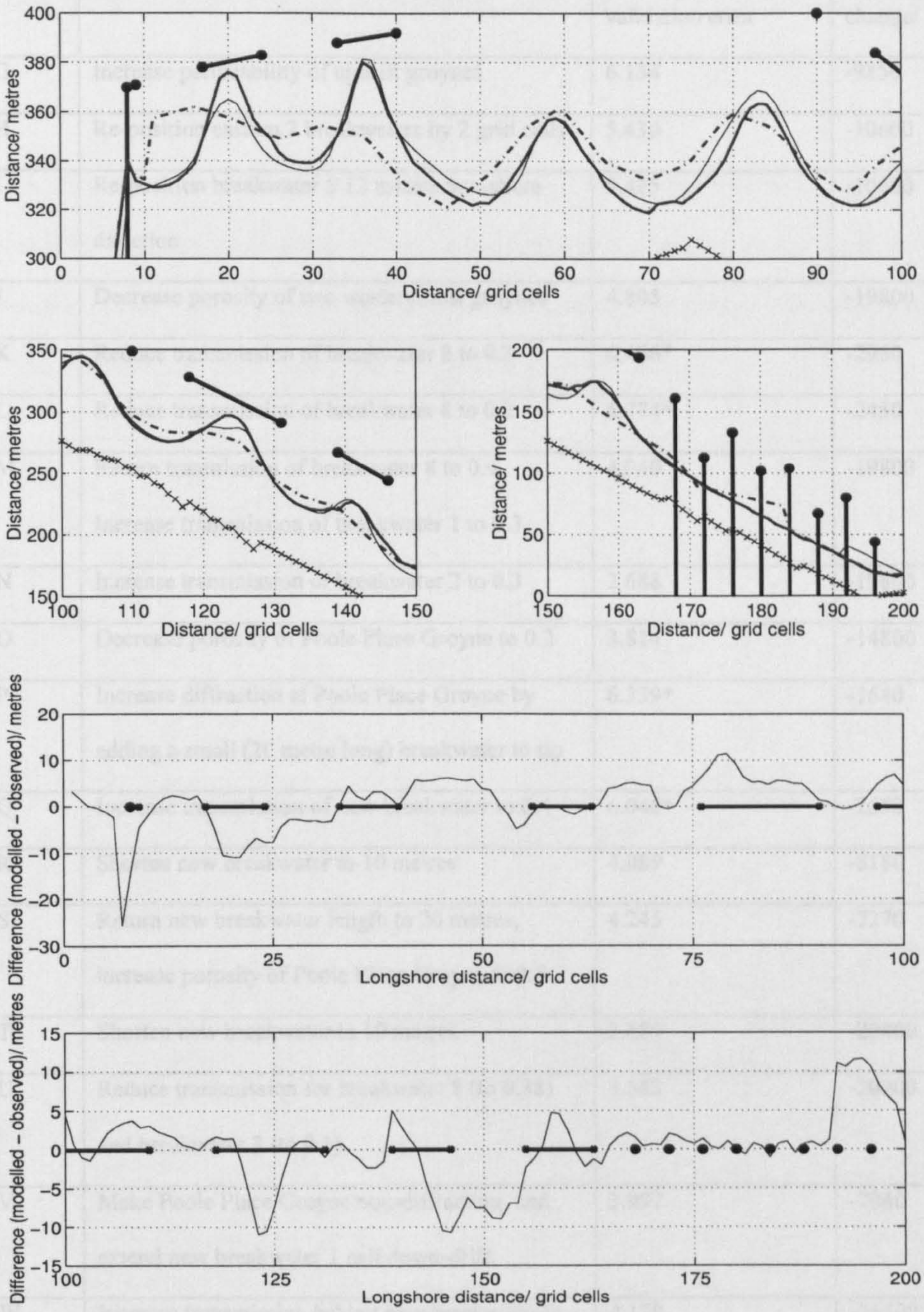

Figure 5-14 'Best attempt' calibrated shoreline (top panels) and difference between modelled and observed shorelines (lower panels)

Test name	Test description	Calibration/ validation error	Modelled volume change/ m^3
RAG	Increase permeability of updrift groynes	6.134	-9850
RAH	Re-position eastern 2 breakwaters by 2 grid cells	5.430	-10600
RAI	Re-position breakwater 5 12 metres in x-shore direction	5.425	-10600
RAJ	Decrease porosity of two westernmost groynes	4.805	-19800
RAK	Reduce transmission of breakwater 8 to 0.3	6.466*	-2960
RAL	Reduce transmission of breakwater 8 to 0.2	5.774*	-2450
RAM	Return tranmission of breakwater 8 to 0.4. Increase transmission of breakwater 1 to 0.3	4.040	-19800
RAN	Increase transmission of breakwater 2 to 0.3	3.688	-19800
RAO	Decrease porosity of Poole Place Groyne to 0.2	3.814	-14800
RAP	Increase diffraction at Poole Place Groyne by adding a small (20 metre long) breakwater to tip	6.339*	-1640
RAQ	Increase transmission of new breakwater to 0.4	6.048*	-2650
RAR	Shorten new breakwater to 10 metres	4.089	-8180
RAS	Return new breakwater length to 20 metres, increase porosity of Poole Place Groyne to 0.5	4.245	-7270
RAT	Shorten new breakwater to 10 metres	3.689	-20400
RAU	Reduce transmission for breakwater 8 (to 0.38) and breakwater 3 (to 0.1)	3.583	-20200
RAV	Make Poole Place Groyne non-diffracting, and extend new breakwater 1 cell down-drift.	3.997	-7040
RAW	Increase transmission behind new breakwater to 0.6	4.129	-26100
RAX	Increase porosity of Poole Place Groyne to 0.6	4.000	-6900
RAY	Reduce transmission of breakwater 3 to 0	3.655	-15100
RAZ	As RAU, but with breakwater 3 transmission = 0	3.608	-20200

Table 5-10 Summary of calibration model runs

The difference plots in Figure 5-14 show that the model still has difficulty representing the shape of the bay between breakwaters 1 and 2, the salient behind breakwater 3, and also the area down drift of Poole Place groyne.

Figure 5-15, shows that this section of the coast is curved, and with an angle to the *x*-axis of up to +/- 45°. Larson et al (1987) warn that where a shoreline is curved, and waves break at a large angle, then the small angle assumption (used when approximating the shoreline equation to a simple diffusion-type equation) is violated. This violation can cause inaccurate estimates of shoreline change.

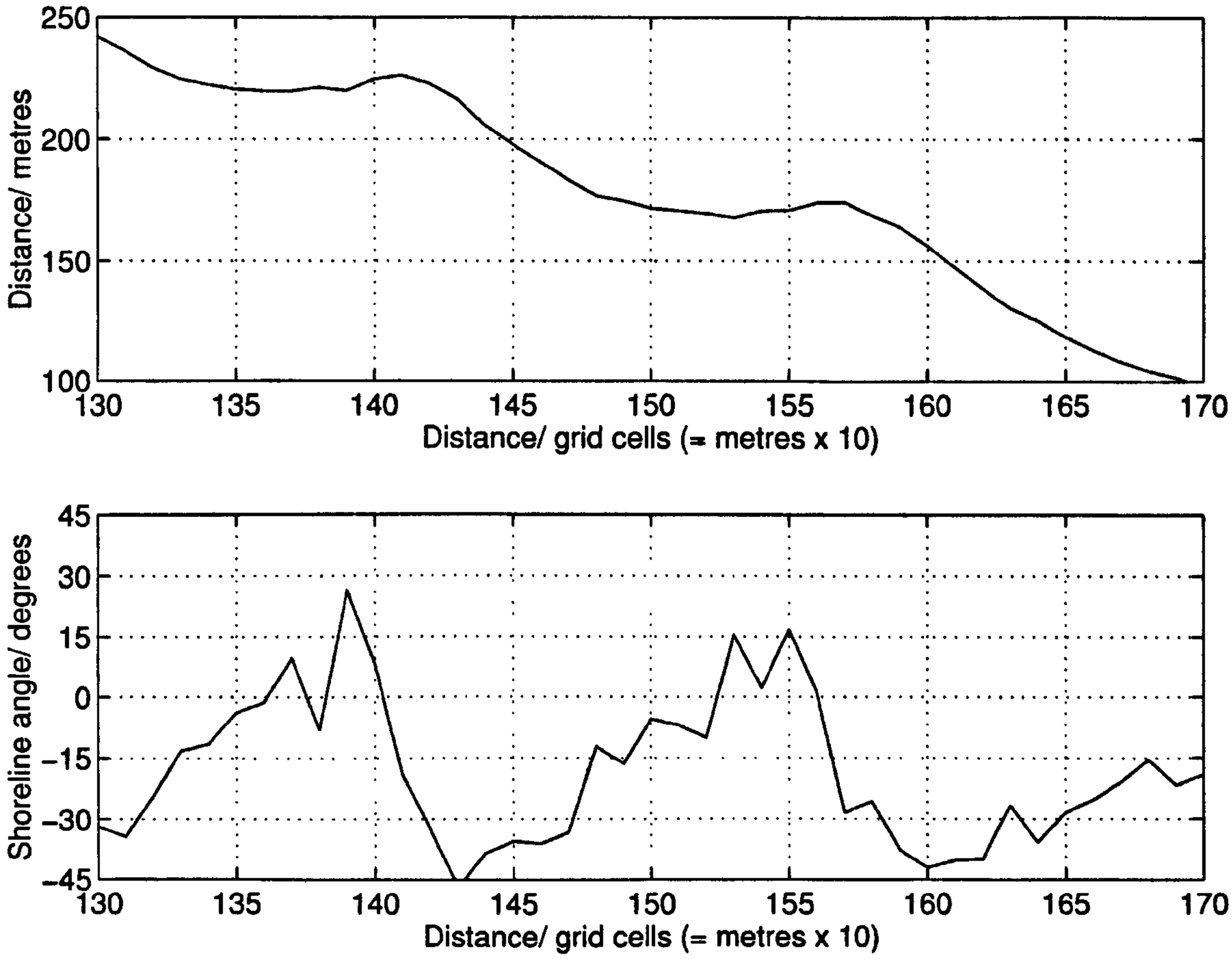

Figure 5-15 Observed shoreline and shoreline angle behind breakwaters 1 and 2

5.6.6 Model validation

Model validation should ideally use a completely independent set of data. This was not available from this experiment, although data from different annual periods, (and therefore different stages of scheme development) were available. The validation exercise was carried out with data from February 1994 to

January 1995, with the concurrent wave data. For the model to be representing these shoreline changes well, a calibration/validation error of less than 1.96 would have been required, and volume changes showing a loss of 11 000 m^3 of material (based on the movement of the 2 metre contour) would be necessary.

The initial test gave a calibration/ validation error of 5.13, and a volume change of -18 700 m^3. The shoreline position and differences from observations are shown in Figure 5-16 and Figure 5-17.

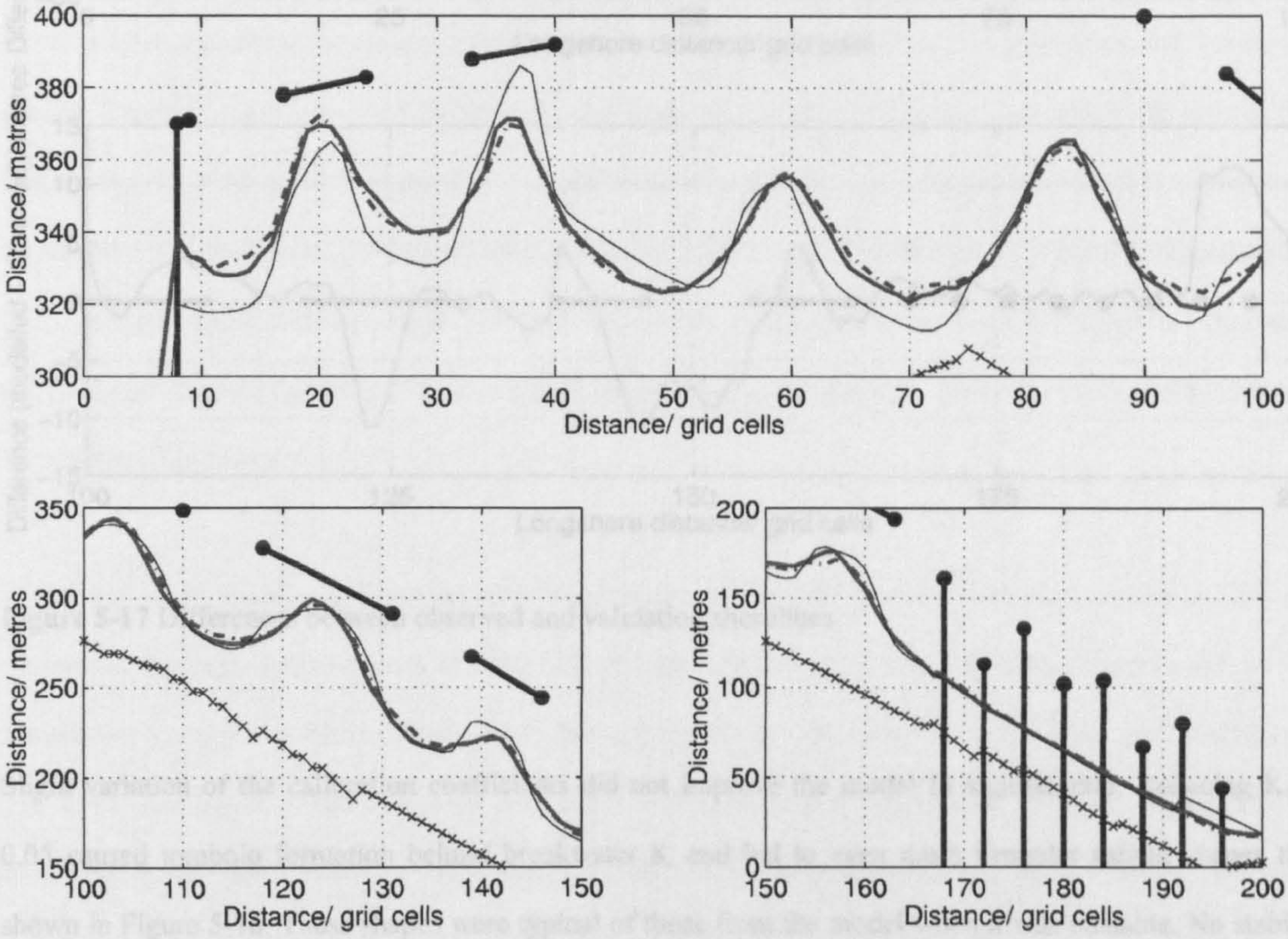

Figure 5-16 Shoreline positions from February 1994 - January 1995 validation run

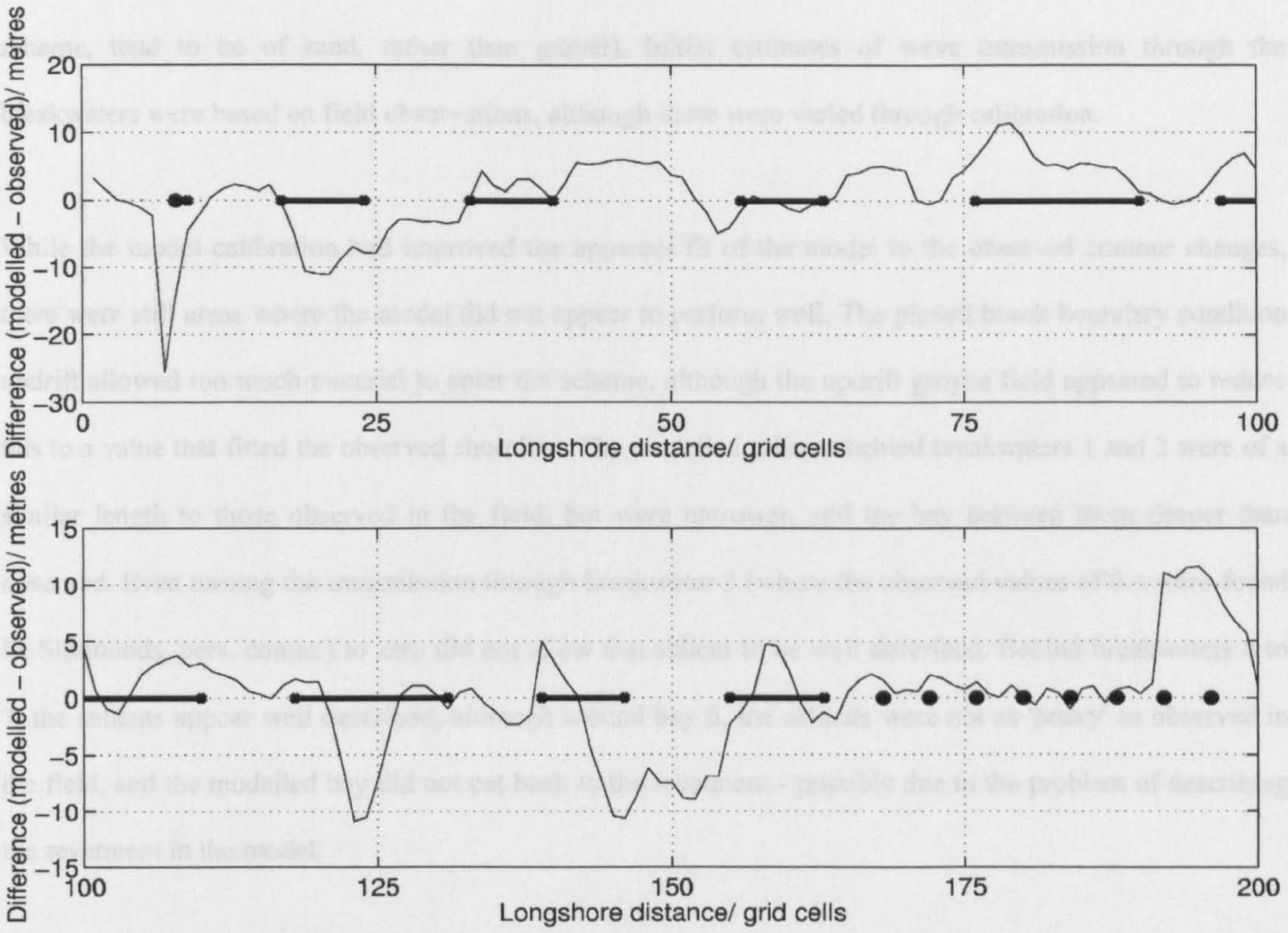

Figure 5-17 Differences between observed and validation shorelines

Slight variation of the calibration coefficients did not improve the model fit significantly. Reducing K_1 to 0.05 caused tombolo formation behind breakwater 8, and led to even more irregular salient shapes than shown in Figure 5-16. These shapes were typical of those from the model when it was unstable. No stability warnings were produced by the model however. Reducing K_2 to 0.2, and returning K_1 to 0.1 produced a smoother shoreline, although this caused salient lengths to be under predicted, particularly in the east of the scheme.

5.7 Discussion

The model calibration stage reduced the rms error in shoreline position from 8.5 metres to 3.5 metres, and also correctly modelled the expected volume change within the scheme due to the observed movement of the +2 metre contour. The value of K_1 used for this was reasonable, and in line with literature estimates. K_2 was higher than recommended by the GENESIS user guides, but was thought to be reasonable because of the

difference in composition of salients compared to the bays at that level (salients, particularly in the east of the scheme, tend to be of sand, rather than gravel). Initial estimates of wave transmission through the breakwaters were based on field observations, although these were varied through calibration.

While the model calibration had improved the apparent fit of the model to the observed contour changes, there were still areas where the model did not appear to perform well. The pinned beach boundary condition updrift allowed too much material to enter the scheme, although the updrift groyne field appeared to reduce this to a value that fitted the observed shoreline. The modelled salients behind breakwaters 1 and 2 were of a similar length to those observed in the field, but were narrower, and the bay between them deeper than observed. Even turning the transmission through breakwater 3 (where the observed values of 0.4 were found D. Simmonds, pers. comm.) to zero did not allow that salient to be well described. Behind breakwaters 4 to 7, the salients appear well described, although around bay 5, the salients were not as 'peaky' as observed in the field, and the modelled bay did not cut back to the revetment - possibly due to the problem of describing the revetment in the model.

Down drift of the headland, transport rates were greater, due to the more oblique wave approach, and also because of the larger gaps between breakwaters. The greatest difficulty was had representing the area around breakwater 8 and Poole Place Groyne. The observed salient was less than 10 metres from the breakwater at this level, making it difficult to tune the model to represent the salient well without causing tombolo formation. It was also difficult to model the accumulation of material against Poole Place Groyne, achieving a compromise between the material losses (groyne permeability) and accretion along it's length due to diffraction from the tip.

Model validation, against the February 1994 to January 1995 highlighted these problems further. Without changing any of the model parameters, the model gave a calibration error of 5.13. The updrift shoreline in the groyne field was again well described, and the salients behind breakwaters 1 to 4 were of reasonable length, but were more irregular in shape. Beyond breakwater 5, the comparison of modelled and observed shorelines deteriorated, with the predicted salients looking typical of those produced by too high a value of K_2.

Slight adjustment of the input parameters did not lead to a significant improvement in the fit of the model to the observed data, and sensitivity testing was problematic due to the formation of tombolos at the eastern two breakwaters.

The first lesson to be drawn from this evaluation of GENESIS is the importance of validating the model over a different period to that with which the model was calibrated. The calibration produced reasonable looking results, but they were not sustainable beyond the calibration period.

The contour changes described in the previous chapter demonstrated that during the first months of the scheme development, the beach contours did not move in parallel, invalidating one of the assumptions of one line modelling. This was due to the accretion of sand within the scheme at low levels, and the loss of gravel from the upper beach. A contour whose movement was representative of volume changes on the beach as a whole did probably exist on the lower beach, but the restriction of this particular one line model to not describing tombolos prevented its use.

To complicate matters further, salients in the west of the scheme were predominantly of sand, while in the east, they were of shingle. The ability to use a parameterisation of wave transmission to knock back, or promote, the growth of individual salients was useful. It was insufficient however to describe the development of the salient behind breakwater 3.The difference in composition of the beach behind the westernmost breakwaters also invalidates the assumption that the beach profile shape is constant.

No mention has been made yet of cross shore transport. With the accretion sand on the lower beach, and the loss of material at the top, it suggests that the profile flattened as it developed. The initial fill material was very poorly sorted (Axe, 1994) and so the improvement in sorting will lead to the removal of sand from the interstices of the gravel and its transport offshore (if only to the low tide level). This flattening of a renourished beach profile is not uncommon, and has been observed before, for example, by Work (1995).

All these points suggest that the assumptions of one line modelling in general, and GENESIS in particular, are too restrictive for the description of a newly renourished beach in the vicinity of detached breakwaters. That GENESIS cannot describe tombolo formation limits its applicability in this case. This limitation is not

common to all one line models, although observations from laboratory tests (for example Suh and Dalrymple, 1987) suggest that as tombolos form, material is transported offshore more frequently.

An n-line model (such as that described by Perlin and Dean, 1983) would not suffer from the same need to have parallel contour movements at all levels, and would also be numerically simple enough to average out short-term processes to make it of value for longer term modelling. A suitable next step would be the application of an n-line model to this beach.

To understand the more complex changes that have caused problems in this modelling exercise, the next chapter describes the use of a purely empirical technique to try and describe the different modes of behaviour that exist in the survey data.

PAGES

MISSING

IN

ORIGINAL

6. Empirical orthogonal function analysis

6.1 Introduction

The previous chapter described attempts to model the plan shape of the renourished beach at Elmer using purely empirical methods (based on the expected response of a beach to detached breakwaters) and also using a one line model (which represented some of the processes expected to describe the beach development). The lack of success in modelling the beach plan shape with these models, and the complexity apparent in the beach morphology (chapter 4) suggests that there is a need for another approach to try and understand the beach dynamics. This chapter presents the analysis of the beach morphology data using empirical orthogonal functions.

6.1.1 Empirical orthogonal function analysis

The EOF procedure is one of a family of inverse techniques. The term 'EOF' was first adopted by Lorenz (1956) in the field of statistical weather prediction. It allows a spatially and temporally varying quantity, in this case beach elevation, to be described in terms of a linear combination of orthogonal spatial predictors, or modes. The net response of these modes, as a function of time accounts for the combined variance of all the observations (Emery and Thompson, 1998).

Principal component (or 'empirical orthogonal function') analysis for the study of beach profile data was first presented by Winant *et al* (1975), in a study of three profiles at Torrey Pines beach, California. Most profile variance was accounted for by the three largest eigenvalues. The spatial eigenfunction associated with the largest eigenvalue was called the '*mean beach function*', and was related to the time - averaged beach profile. The spatial function associated with the next largest eigenvalue had strong maxima at the position of the summer berm, and a minimum at the winter bar position, and so was named the '*bar-berm function*'. The third function had a maximum at the position of the low tide terrace, and was called the '*terrace function*'. In Winant *et al*'s study, the temporal eigenfunction associated with the largest eigenvalue showed no seasonal variation, but second largest eigenvalue exhibited strong annual periodicity, reaching a maximum in the late summer (August-September), and a minimum in the spring (March).

This work was extended by Aubrey (1979) for the same data set. He observed that the regular periodic behaviour of the bar-berm function meant that it could be used as a predictor for the seasonal volume changes on the beach.

This method of analysis has since been applied to a wide variety locations, including the U.K. east coast (Aranuvachapun and Johnson, 1979), the Baltic and Black Sea (Pruszak, 1993) and to renourished beaches on the Atlantic coasts of Spain and the United States (e.g. Medina *et al*, 1991; Larson *et al*, 1997). The technique has also been extended to two spatial dimensions, and has also been used as the basis for a predictive model of beach changes (Uda and Hashimoto, 1980; Hsu *et al*, 1994). This work follows the one dimensional method described by Winant *et al* and Aranuvachapun and Johnson (1979).

6.1.2 Methodology

To calculate the eigenfunctions and corresponding eigenvalues for this data, each profile line was interpolated to give beach elevations at 1 metre (horizontal) intervals along its length (so that each profile was made up of exactly coincident points). For each profile, a matrix H was then constructed. Each row of H consisted of values of beach elevation along the profile at a particular time, while each column of H showed the time series of beach elevation for a particular point on that profile. From this matrix, two square symmetric correlation matrices A and B were formed, where

$$A = \frac{H'H}{tx}, \quad B = \frac{HH'}{tx}$$

Equation 6-1

The variables t and x represent the number of data points in time, and in space respectively.

These matrices each have a set of eigenvalues λ_n and corresponding eigenfunctions e_{nx} and e_{nt} respectively, defined by the following equations:

$$Ae_{nx} = \lambda_n e_{nx}, \quad Be_{nt} = \lambda_n e_{nt}$$

Equation 6-2

where the subscript x labels the spatial eigenfunction derived from matrix A, and subscript t labels the temporal eigenfunction calculated from B. The eigenvalues are then ranked by percentage of variance (where

the variance is defined as the *mean square value* of the data), such that the first eigenfunction explains most of the variance. The magnitudes of the eigenvalues associated with beach profile data decrease rapidly. The proportion of the total variance described by each eigenfunction is found from its corresponding eigenvalue, and therefore the relative importance of the eigenfunctions in determining the beach profile configuration can be observed.

Given that most of the variance in the signal is associated with the first three modes, the remaining eigenfunctions and values can generally be discarded as containing noise. In this way, eigenfunctions are frequently used to filter noisy data - for example from satellite images. Where the entire data set contains random data, the analysis apportions the variance associated with each eigenfunction equally, so that eigenvalues cannot be ranked (Stauffer et al, 1985).

6.2 Analysis of Elmer profiles

6.2.1 Eigenvalues

Figure 6-1 shows the percentage of variance associated with the first eigenfunction (the *mean beach* function), as it varies alongshore from updrift of the breakwater scheme, to 1500 metres downdrift of it. The top panel shows the Elmer topography (contour interval 1 m) calculated from the mean beach function.

The proportion of variance associated with the first eigenfunction is between 98 and 100% throughout the study site. Updrift of the renourished area (between -470 and 0 metres alongshore), in an area of narrow beach fronting a vertical seawall, the associated variance is lower than that observed further east. In the western half of the scheme, the proportion of variance is generally greater than 99.5%.

Continuing eastwards through the scheme, the proportion of variance continues to increase, to a maximum, around the position of the seventh breakwater (around +1400 metres alongshore). For the next 600 metres, the proportion of variance decreases steadily, reaching a minimum of 98.5% in the embayment down-drift of the terminal groyne. Between this point and then end of the surveyed area (+2000 to +3200 metres alongshore), the proportion of variance remains fairly constant, at around 99.5%.

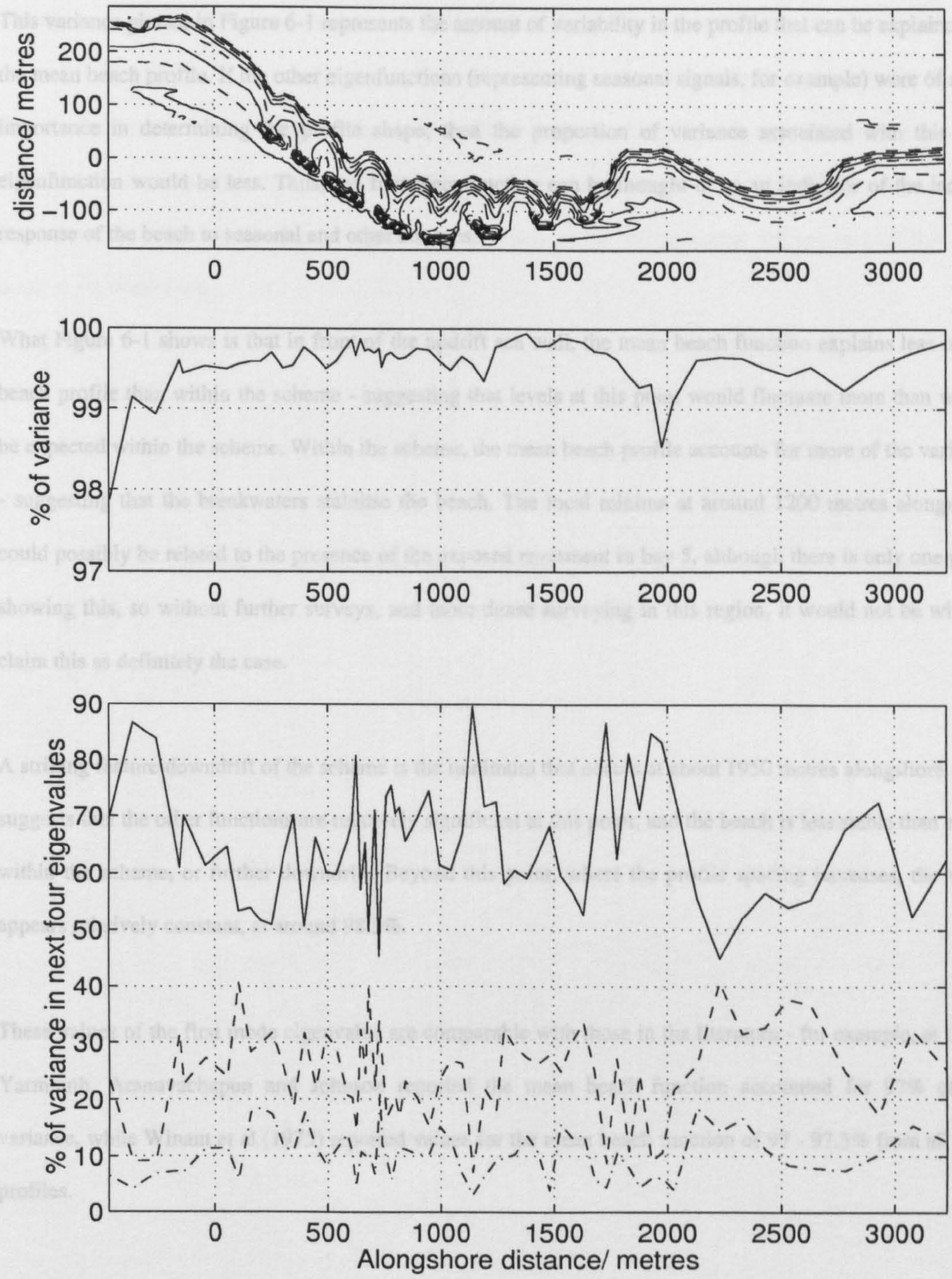

Figure 6-1 Variation of variance associated with the first four eigenfunctions with longshore distance.

Top panel is a contour plot of the mean beach topography (calculated from the gridded mean beach function). Contours at 1 metre intervals between -2 to +5 metres over Ordnance Datum. Middle panel shows the longshore variation of the first eigenvalue as a percentage of the total variance. The bottom panel shows the proportion of the remaining variance associated with the next three eigenvalues.

This variance plotted in Figure 6-1 represents the amount of variability in the profile that can be explained by the mean beach profile. If the other eigenfunctions (representing seasonal signals, for example) were of more importance in determining the profile shape, then the proportion of variance associated with this first eigenfunction would be less. Thus, the first eigenfunction can be thought of as an indicator of the lack of response of the beach to seasonal and other changes.

What Figure 6-1 shows is that in front of the updrift sea wall, the mean beach function explains less of the beach profile than within the scheme - suggesting that levels at this point would fluctuate more than would be expected within the scheme. Within the scheme, the mean beach profile accounts for more of the variance - suggesting that the breakwaters stabilise the beach. The local minima at around 1200 metres alongshore could possibly be related to the presence of the exposed revetment in bay 5, although there is only one point showing this, so without further surveys, and more dense surveying in this region, it would not be wise to claim this as definitely the case.

A striking feature downdrift of the scheme is the minimum that occurs at about 1950 metres alongshore. This suggests that the other functions are relatively significant at this point, and the beach is less stable than either within the scheme, or further downdrift. Beyond this point, where the profile spacing increases, the value appears relatively constant, at around 98.5%.

These values of the first mode eigenvalue are comparable with those in the literature - for example, at Great Yarmouth, Aranuvachapun and Johnson reported the mean beach function accounted for 97% of the variance, while Winant et al (1975) reported values for the mean beach function of 97 - 97.5% from all their profiles.

6.2.2 Eigenfunctions

Spatial eigenfunctions were calculated from the data using the method described above. The functions obtained from updrift and downdrift of the scheme were similar to those described by Winant et al (1975). Figure 6-2 shows typical results from the analysis. The mean beach profile is clearly visible, and maxima

exist in the bar-berm function at the onshore end of the profile, as well as at 190 metres in the cross shore. The third eigenfunction shows a maximum at 255 metres alongshore at the middle of the upper beach slope.

The results from behind the breakwater show a different response. While the mean beach function still describes the beach profile, there is no well-defined maximum in the bar-berm function. There is however a large peak in the terrace function over the central portion of the salient. Large minima in both functions occur at the breakwater.

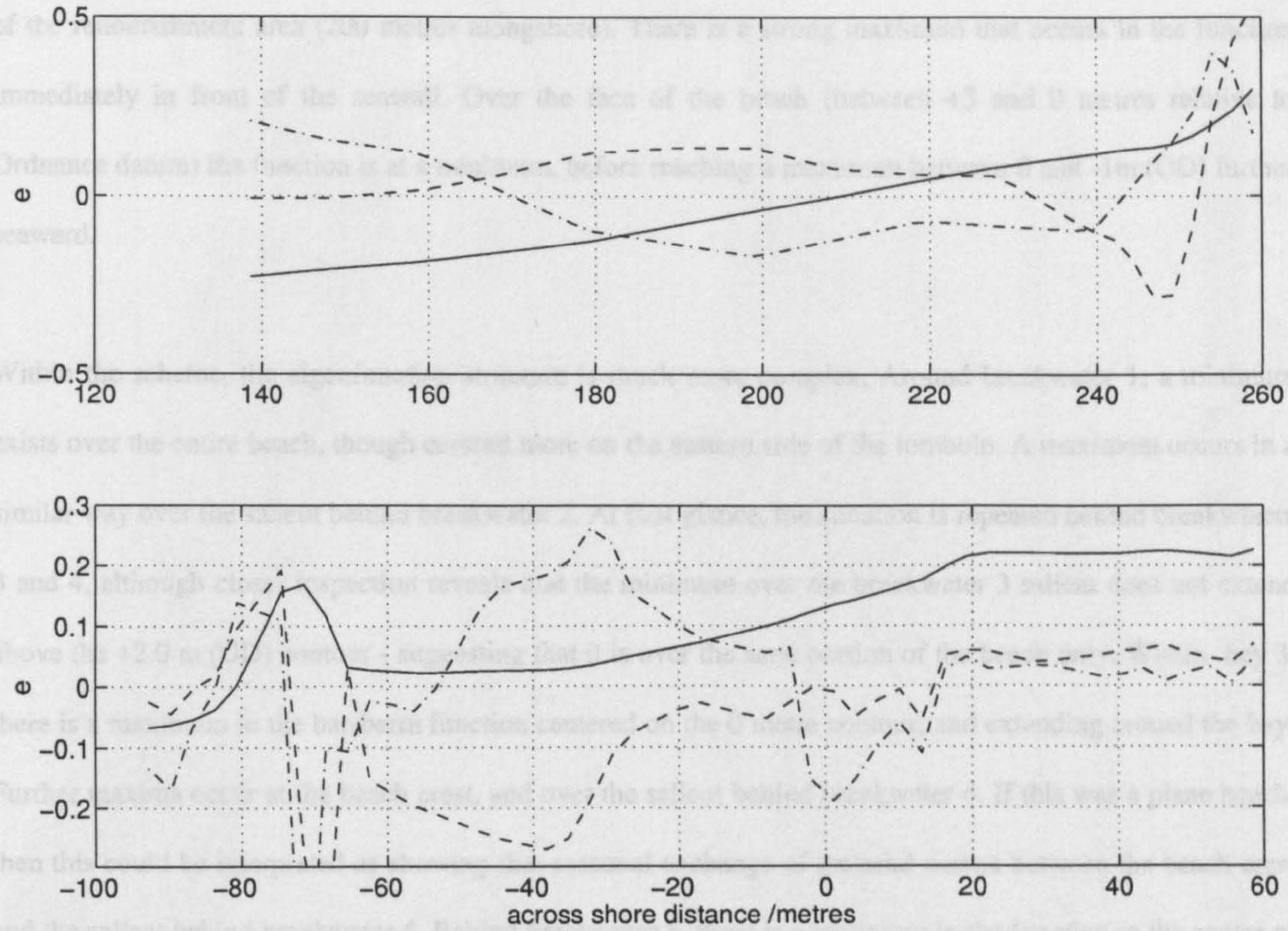

Figure 6-2 Example of eigenfunctions calculated using Elmer data.

Top panel shows eigenfunctions from profile 1 (updrift of scheme). Solid line is the first eigenfunction called by Winant et al (1975) the 'mean beach function'. The dashed line is the second eigenfunction (the bar berm function). The dash-dot line is the third eigenfunction (the terrace function). The lower panel shows the same calculation for profile 20, across a breakwater)

After calculating the spatial eigenfunctions, they were gridded and contoured. Figure 6-3 shows the variation of the second eigenfunction (the *bar berm* function) across the study site. The top panel shows the western end of the scheme. Blue colours show positive values of the bar berm function, while red shows negative values. From these, berm and bar positions may be inferred. The lower panel shows the same information for the eastern end of the study site. The dashed lines in each panel represent the actual beach morphology from the first (*mean beach*) eigenfunction.

Starting to the west of the scheme, the results of the bar-berm function are remarkably uniform up to the start of the renourishment area (200 metres alongshore). There is a strong maximum that occurs in the function immediately in front of the seawall. Over the face of the beach (between +3 and 0 metres relative to Ordnance datum) the function is at a minimum, before reaching a maximum between 0 and -1m (OD) further seaward.

Within the scheme, the eigenfunction structure is much more complex. Around breakwater 1, a minimum exists over the entire beach, though centred more on the eastern side of the tombolo. A maximum occurs in a similar way over the salient behind breakwater 2. At first glance, the situation is repeated behind breakwtaers 3 and 4, although closer inspection reveals that the minimum over the breakwater 3 salient does not extend above the +2.0 m (OD) contour - suggesting that it is over the sand portion of the beach only. Within bay 3, there is a maximum in the bar-berm function centered on the 0 metre contour, and extending around the bay. Further maxima occur at the beach crest, and over the salient behind breakwater 4. If this was a plane beach, then this could be interpreted as showing that seasonal exchange of material occurs between the beach crest and the salient behind breakwater 4. Behind breakwater 5, there is a minimum in the function in the centre of the salient, but a maximum on the flanks. Further maxima occur on the salients behind breakwater 6 and 8, and locally at the edges of bays 5 and 6.

Downdrift of the scheme there is an extensive minimum between Poole Place Groyne and 2100 metres alongshore - extending from the beach crest to the -2m (OD) level. Beyond this, a maximum becomes defined at the +5 metre level, and also (weakly) at the -1 metre level, indicating a return to the classical cross-shore behaviour observed updrift of the scheme.

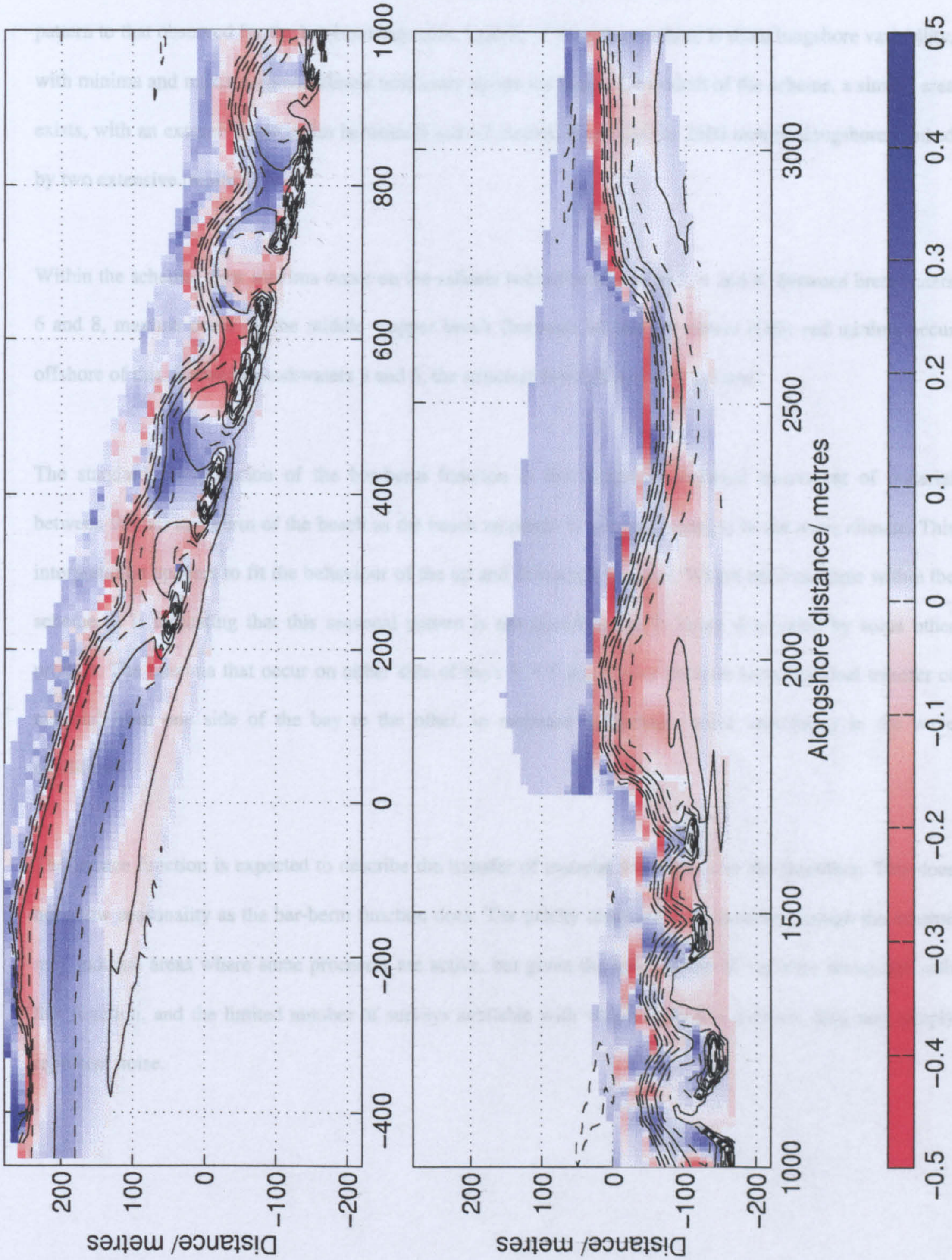

Figure 6-3 Gridded bar - berm eigenfunction (i.e. the second mode eigenfunction) based on the Elmer data.

Colours represent values of the function, related to the colorbar below the graph. Mean beach positions (caluclated from the mean beach function (first mode) are overlaid.

Figure 6-4 shows the variability of the terrace function through the study site. This exhibits a different pattern to that observed for the bar-berm function. Updrift of the scheme, there is more longshore variability, with minima and maxima spread almost uniformly across the beach. Downdrift of the scheme, a similar area exists, with an extensive maximum between 0 and +2 metres, from 2100 to 2600 metres alongshore flanked by two extensive minima.

Within the scheme, clear maxima occur on the salients behind breakwaters 2, 4 and 8. Between breakwaters 6 and 8, maxima occur on the middle - upper beach (between +2 and +5 metres (OD) and minima occur offshore of this. Between breakwaters 3 and 5, the structure is much less well defined.

The standard interpretation of the bar-berm function is that describes seasonal movement of material between the bar and berm of the beach as the beach responds to seasonal changes in the wave climate. This interpretation appears to fit the behaviour of the up and downdrift beaches. Where minima occur within the scheme, it is indicating that this seasonal pattern is not occurring, or is being dominated by some other process. The maxima that occur on either side of bays 3, 4 5 and 6 may indicate some seasonal transfer of material from one side of the bay to the other, in response to perhaps, some seasonality in the wave conditions.

The terrace function is expected to describe the transfer of material from dunes to the shoreface. This does not show seasonality as the bar-berm function does. The patchy distribution of maxima through the scheme may indicate areas where some processes are active, but given the low amount of variance associated with this function, and the limited number of surveys available with which to do this analysis, they may simply represent noise.

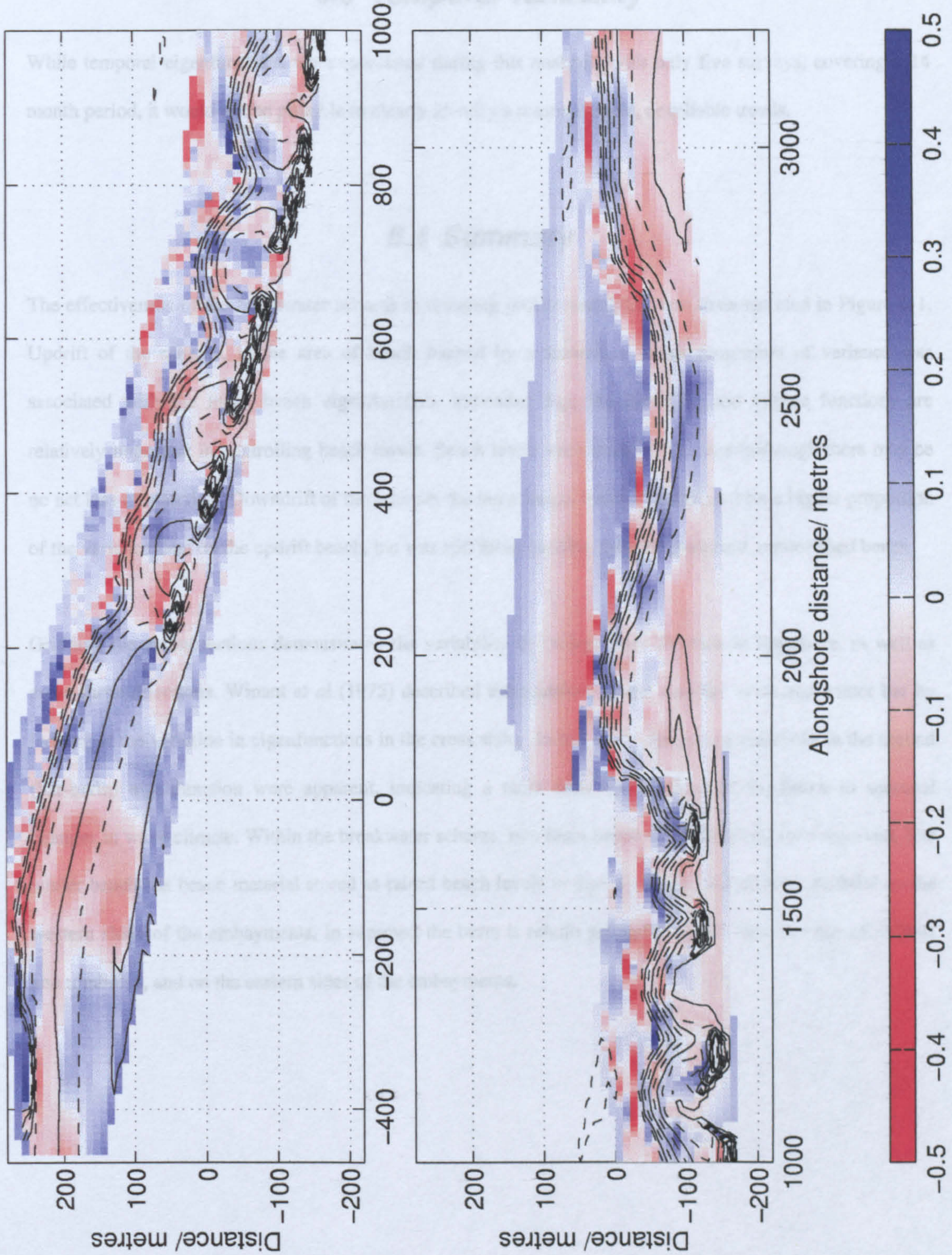

Figure 6-4 Gridded values of the third eigenfunction (the 'terrace' function) showing alongshore variability

6.3 Temporal variability

While temporal eigenfunctions were calculated during this analysis, with only five surveys, covering a 14 month period, it would not be possible to clearly identify a seasonal cycle, or reliable trends.

6.4 Summary

The effectiveness of the breakwater scheme in reducing profile variability was demonstrated in Figure 6-1. Updrift of the scheme, in the area of beach backed by a seawall, a lower proportion of variance was associated with the mean beach eigenfunction, indicating that the bar-berm and terrace functions are relatively important in controlling beach levels. Beach levels vary more in this area (although there may be no net loss of material). Downdrift of the scheme, the mean beach function accounted for a higher proportion of the variance than on the updrift beach, but was still more variable than the protected, renourished beach.

Gridding the eigenfunctions demonstrated the variability in the bar berm function in longshore, as well as cross shore directions. Winant *et al* (1975) described the locations of the summer berm and winter bar by looking at the variation in eigenfunctions in the cross shore. In this study, longshore variations in the second (bar-berm) eigenfunction were apparent, indicating a more complex response of the beach to seasonal changes in wave climate. Within the breakwater scheme, two main beach configurations were observed. The winter beach has beach material stored as raised beach levels in the bay floors, and as more material on the western slope of the embayments. In summer, the berm is rebuilt primarily on the western sides of salients and tombolos, and on the eastern sides of the embayments.

7. Discussion and Conclusions

7.1 Summary of work

The literature presented in Chapter 2 demonstrated the broad range of spatial and temporal scales over which beach morphology changes, and the limitations to predictability that prevent high resolution, wave by wave models from describing beach changes over seasonal to inter-annual periods. This, the absence of design guidance and experience of detached breakwaters in macro-tidal environments, and the lack of critical evaluations of numerical models of shoreline change motivated the present study.

The subsequent chapters described the collection of a large, high quality set of directional wave data, giving a description of the forces driving the beach development. Concurrent topographic surveys were commissioned to map the beach development, and sediment sampling and current metering were also undertaken. A photographic log was kept, showing the beach development in a more qualitative way.

Current design techniques for predicting beach plan shapes were evaluated, and problems found in their application to a macro-tidal beach were presented. Finally, a statistical technique was used to investigate areas of standing oscillations in the beach topography.

7.1.1 Discussion of the data set

The data set collected at Elmer provides a valuable resource for this and future research. Wave recorders were levelled into the same reference frame, making possible the direct comparison of data, including mean levels, from offshore to the shoreline. This allows further study, for example, of wave setup behind the breakwaters for various wave conditions and water levels. Wave data has been banked to CD-ROM, although to realise its full value, the data and associated meta-data should be made available on the web for use by other researchers. Data may also be used to contribute to an investigation of combined surge and wave activity on the Arun coast.

The beach survey data is also a vital resource. The six surveys presented describe the initial development of a large coastal engineering scheme, and are more valuable because they were taken over a period when the wave forcing on the scheme is well known. When combined with long term (annual - decadal) monitoring of

the coastline, the value of these first surveys increases, as they become suitable for model development and evaluation for the study of longer term trends. It is desirable that this data also be made available to other researchers.

The current meter data were collected simultaneously with the wave data, and can give some understanding of the circulation behind the breakwaters. The deployment of these instruments in the intertidal zone means that data were recorded within and seaward of the surf zone. This may give some information on the cross shore structure of the nearshore circulation. Linking in the current meter data with laboratory observations may also help with the understanding of differences between hydraulic models and prototype observations, to improve the design and interpretation of hydraulic model results.

Complete data sets documenting the initial development of large coastal engineering projects are extremely rare, and the critical use of such data sets for the evaluation of numerical modelling methods is not common. As a result, the data produced by this study is of importance to the coastal engineering community.

7.1.2 Calibration

Calibration of the wave recorders was presented in Chapter 3. There was an inter-comparison between the recording systems prior to deployment, and also instruments were calibrated using sensor-specific methods. The IWCM calibration allowed the frequency response, as well as the mean values from the instrument to be determined, as discussed in Borges (1993). Although the calibration was not in-situ, it was carried out on each staff individually before and after deployment. As each staff was replaced every couple of months, calibration of the IWCM was ongoing throughout the study period. The calibration of the offshore pressure array was less satisfactory. While the relative transducer gains and offsets were calculated and found to be stable to within a percentage point over a servicing interval (4-5 months), the only absolute calibration of the instrument was done prior to deployment and afterwards. The only in-situ calibration involved the comparison of mean values with predicted tidal levels, which showed the instrument to be good to 5% after taking into account a static inverse barometer effect. While this value is good, it did not involve the comparison of the instrument with a more accurate method, so cannot be considered a genuine calibration.

Given that both recorders were levelled to the same datum, it would have been possible to directly compare the mean levels from each system over periods with low sea level variance (and thus minimal set up effects behind the breakwaters). This would have provided an external calibration on the offshore wave recorder.

7.1.3 Typicality of wave data

Extreme values

Measured wave conditions were compared with values of extreme events, and with modelled (hindcasted) wave conditions used in the scheme design. Wind conditions during the experiment were also compared with climatological values from the Department of Energy's Metocean Parameters report (1989). Overall, the measured maximum sustained gusts during the sampling year were 90% of the expected maximum, although this figure hides the month by month variability.

Comparing the measured wave conditions to extreme events in the literature led to a discussion of techniques for calculating return values of wave heights, based on the methods presented in the British Standard (BS 6349 part 1; 1984). The importance of using the extreme value distribution that best fits the observed data was apparent, as was the sensitivity of methods that use a limiting wave height parameter to the value of that parameter. An example was presented using the Weibull distribution (which did provide the best fit to the data). Variation of the lower limiting wave height between 0.17 m (the final lower limit in this analysis) and 0.3 m. led to a change in the estimate of the 100 year return wave height from 3.9 to 5.5 m.

Comparison with estimated conditions

The measured wave conditions were compared with the predicted wave conditions used in the scheme construction. These predicted values were based on conditions calculated by refracting and shoaling offshore waves predicted by the U.K. Meteorological Office's Fine Mesh Wave Model. This comparison demonstrated that the predictions over-predicted the maximum wave height and failed to predict the presence and height of long period (period > 15 s) swell. The predictions also over-predicted the number of short period, low wave events. In the middle of the range (heights between 0.5 and 2 m, periods between 4 and 8 s) the agreement between the predictions and the observations was excellent.

In terms of assessing the typicality of the measured data, this comparison was less successful, as the assessment could equally be seen as a validation of the wave model. Assuming the model to be correct, the maximum values of Hm_0 measured at Elmer were 60 % less than those predicted by the model, and longer (peak) period waves were more frequent.

The difference in measured and predicted maximum wave heights agrees qualitatively with the comparison of extreme wind conditions. The absence of very long period swell in the model could be blamed on poor de-trending of the observed data - leading to low frequency harmonics being introduced into the analysis. It is felt that these long period swell are real however, as the de-trending method is widely used, and anecdotal evidence of surfers suggest that long period wave conditions do occur several times each year on the Arun coastline (M. Davidson, pers. comm.).

The methods described above give no more than a qualitative estimate of how the measured wave conditions compare with the mean wave climate. Long-term (decadal) wave records do not generally exist around the UK coastline to allow a direct comparison. Long term records of storm surges do exist in the eastern English Channel, and could be used to compare with observed surge levels during the study period to get an estimate of 'storminess'. This would have the advantage over the wind speed (gust) comparison method that it would actually be a comparison of observations of the sea's response to atmospheric forcing.

Comparison of the modelled and observed wave conditions was surprisingly good, although the development of wave generation and transformation models is still an active area of research (Booij et al, 1999). A hindcasted wave climatology for the North Atlantic has been generated from historical atmospheric pressure records, as part of the WASA project (WASA Group, 1998). A better estimate of the regional wave climate could be obtained by combining the offshore estimates with a model more suited to nearshore wave generation and transformation. The EUROWAVES project (Barstow et al, 1998) seeks to provide atlases of coastal wave conditions for Europe. These would provide a useful resource for the assessment of observed wave conditions.

7.1.4 Beach surveys

Survey method

The survey method adopted was justified in Chapter 3, on the grounds of the length of beach to be surveyed over a low tide window. The greatest problem with this method is the poor vertical accuracy. This becomes a problem when calculating volume changes, although as the scheme was monitored during its initial development, the level changes observed were large enough to be significant.

An external contractor carried out the beach surveys. This means that they were presented as a product, and the user must trust that they are within the standard set in the contract, with no mistakes. The survey cost meant that re-analysis of survey photographs, to obtain some understanding of the processing errors, was not possible. It also meant that the actual surveys could not be flown frequently or repeated. Thus there is a problem of the representativeness of each survey. Do the surveys actually show the seasonal variation in the beach topography, or do they suffer from aliasing, and in fact reflect a badly sampled, higher frequency signal?

It is difficult to answer this criticism fully. Shingle beaches are known to respond very quickly to changing wave conditions (Powell, 1990), and so aliasing would be expected. Comparison of surveys taken a year apart suggests that the observed beach gradients are very similar, while larger differences exist between successive surveys. This suggests that the surveys are representative of their season.

Two approaches may answer this point. Either many, frequent surveys are made to try to resolve high frequency beach changes, and thus provide a 'mean' beach condition for each season, or the surveys are extended in time, but with a similar frequency to before. As well as providing additional information on the scheme development, an eigenfunction approach may be used, for example, to confidently separate the seasonal, trend and 'noise' components of the survey.

Volume calculations

Analysis of the beach data raised several problems. A variety of packages exist for the gridding of data from irregular to regular grids. The complexity and accuracy of these methods are extremely variable. The range of techniques available in packages such as Surfer or PV-Wave should serve as a warning that the validation of gridding routines, and the calculation of residuals, should be a regular procedure - at least until a 'standard' method is adopted for the processing of nearshore morphological data. Without this calculation, the effect of gridding on the error budget cannot be quantified

Volume changes were calculated using a variety of techniques. The simplest approach involved the subtraction of the gridded matrices of beach elevation. This provided an excellent visual description of the level changes. Area changes under the cross-shore profiles were calculated using Simpson's rule. Finally, to provide a comparison with the volume change estimates of the one line modelling, volume changes based on contour movements were calculated - although only for the 0, +1, +2, +3 and +4 m (OD) levels where the

contours were approximately monotonic. Calculations of the volume changes from survey to survey within the scheme are shown in Table 7-1.

Method	September 1993 - February 1994	February - May 1994	May - September 1994	September 1994 - January 1995	January 1995 - May 1995
Simpsons rule	+17600	-2600	+9200	-7400	+12200
Gridded data	+6200	-10400	+33300	-21400	+900
Contour movements	+300	-2900	+6000	-3000	+3800

Table 7-1 Volume changes (in m^3) between successive surveys, estimated by different techniques

The discrepancy between the volume changes estimated by different methods is disturbing. The largest difference is of the order of 24 000 m^3. The gridded data set consists of 3300 cells, each of 100 m^2 surface area. The average level difference per cell required to generate this discrepancy is 0.07 m, within the error of the surveys, and comparable to the errors introduced by gridding the data.

The 'absolute' volume changes hide a great deal of information. A large proportion of the beach level changes were significant - at least locally, if not when averaged over the whole beach. This is clear from the level changes plotted in Chapter 5. Data were gridded to 10 × 10 m cells. The profile spacing was only 10 metres in the instrumented part of the beach, and varied between 30 and 50 metres away from this area. Gridding to a coarser resolution would have meant that grid cell levels were based on the mean of many data points, and would have been more statistically significant (although spatial resolution would have been lost). In addition, although data points along profile lines were not coincident, the profile lines generally were. By calculating the level differences based on the profile lines, and gridding the differences would have meant that only one gridding operation (and introduction of errors) was required.

Analysis of beach surveys demonstrated that sand accretion was important at this site. This accretion came in part from a sorting of the renourishment material, but the trapping of sand moving alongshore was also significant - demonstrated by the growth of the salients behind breakwaters 1 and 2 Some shingle was also trapped (particularly behind breakwater 1). Losses from the eastern end of the scheme may be sufficient minimise the down drift effects of the scheme. The main areas of erosion came from in front of the revetment in bay 5, and also immediately downdrift of Poole Place Groyne.

7.2 Beach Modelling

7.2.1 Empirical approaches

The evaluation of the empirical modelling techniques indicated that of the techniques assessed, usable results came from those that gave a general description of the beach response, rather than a specific value of salient length. Of these, the Ahrens and Cox (1990) method included only breakwater length and offshore distance as input parameters, though still performed reasonably beyond breakwaters 1 and 2. Pope and Dean (1986) included gap width and water depth as input parameters. This performed better than other schemes, though still failed to predict the large amount of salient growth behind breakwaters 1 and 2.

This failure to describe the salient formation behind breakwaters 1 and 2 suggests that the methods do not work well where there is longshore transport into the lee of the breakwaters (in addition to that caused by the breakwaters themselves).

The other methods of course gave perfect predictions where there were tombolos at lower tidal levels.. The Suh and Dalrymple model continued to predict increasing salient lengths as the breakwaters became further offshore (as the tide rose), although the observations showed salient length to be decreasing. McCormick (1993) showed a similar, though less uniform, response, and also had problems describing the behaviour of breakwaters 1 and 2.

While these models (particularly Pope and Dean) may be of some use as a very rough guide to beach response, they do not appear to be good enough to use for confident scheme design. The Hsu and Silvester data analysis for single breakwaters, and described briefly in Chapter 5, predicts tombolo formation when the ratio of breakwater length to offshore distance has a value of around 5. This would suggest that a 100 m breakwater would need to be 20 m from the shore before a tombolo formed. This is obviously ridiculous when compared with field and laboratory observations

Observing a breakwater scheme in a macro-tidal environment leads to a questioning of the assumptions behind these methods. They assume that the salient length is defined as the horizontal distance from the initial beach line to the furthest extent of dry beach, and yet as the tide drops, it can be seen that the salient is the visible part of the body of sand deposited behind the breakwater, which is hidden at high water. The

models seek to describe the point where a salient connects to the breakwater and becomes a tombolo. The formation of the tombolo is of interest, because of its effect of blocking longshore sediment transport, and possibly diverting it offshore. Where the beach slope is small however, this blocking will probably occur even though the shore line is some distance from the breakwater.

There are several ways that this evaluation could be developed. The McCormick (1993) and the Hsu and Silvester (1990) models both give predictions of shoreline position. How well do they represent the entire scheme response to the breakwaters, at the range of tidal levels observed?

How sensitive are the results from all the methods to the estimate of breakwater position, or gap width? This is of interest, as the models ask for a distance from the shoreline to the breakwater. The Elmer breakwaters varied from 4 m wide at the crest, to about 25 m wide at the toe. This latter distance is about a third of the maximum distance between the breakwaters and the shore, so the value used would be expected to be significant

All the models assume that the beach reaches some form of equilibrium with the breakwaters. Only the McCormick model includes the effect of waves (in the form of wave steepness) or grain size. This suggests that most models consider that the beach response does not change with changing wave conditions. This seems to be unreasonable, as it would rule out, for example, seasonal changes in beach position. This also accounts for the difficulty the models had with representing the response of breakwaters 1 and 2, which have trapped material entering the scheme, and have generated larger salients than would have been expected given their dimensions.

7.2.2 GENESIS tests

Evaluation of beach morphology models is usually hampered by a lack of high quality data. There is frequently a need to rely on, for example, hindcasted wave data when wave chronology could be important. The fieldwork provided the high quality data needed for a comprehensive model evaluation. Additional fieldwork, motivated by the results of the initial study also provided information on wave transmission through the breakwaters (Simmonds et al, 1997). It was hoped that the US Army Corps model GENESIS could be calibrated and validated against this data.

The model evaluation did not result in specific guidelines for applying the model to this type of scheme. There were two major problems. The first concerned the beach behaviour. Analysis of the data in Chapter 4 showed that most of the volume changes experienced over the site were due to the accretion of sand. The contour movements below the 0 m OD level were not the same as the movements higher up the beach. This invalidates one of the fundamental assumptions of one-line modelling - that the beach contours all move in parallel (or the profile shape is constant). The second problem lay in the inability of the model to allow beach development after tombolo formation. This limitation led to the selection of a contour from the upper beach (which did not form a tombolo), but prevented the selection of a contour that represented the beach volume changes as a whole.

The model was calibrated to reproduce both the volume changes and the contour movements associated with the selected contour between September 1993 and September 1994. After many model runs, the calibration error (rms difference between the observed and predicted contour position) was reduced to a value of 3.58 m. This is similar to the value obtained by Chu et al (1987), when they applied GENESIS to a straight macro-tidal beach in Alaska. For the 'textbook' case study at Lakeview Park (Hanson and Kraus, 1989) the error was reduced to 4.04 ft.

The 'best' fit shoreline had been produced using a value of K_1 that was reasonable for a shingle beach. The value of K_2 selected however was higher than was recommended by the GENESIS handbooks, which warn that shoreline change may become exaggerated in the vicinity of coastal structures, and that numerical instability might occur. Despite this high value of K_2, to describe the salient formation well it was necessary to reduce the breakwater transmission coefficients from the initial value of 0.4 to promote the salient growth. It was still not possible to describe the salient formation behind breakwater 3. Reducing the transmission coefficient further here did not enhance the salient formation, while increasing K_2 further did lead to unreasonable salient formation elsewhere.

The high value of K_2 was required because salients at Elmer are formed mostly of sand, whereas the beach material is shingle at this level in the bays. Sand transport is generally characterised by a larger transport coefficient than shingle, so the larger coefficient may be necessary to represent the sand transport. It was thought that K_1 was not important within the scheme, as diffraction effects (described through K_2) would dominate. Transport due to oblique wave approach was important to control the volume of material entering and leaving the site, and also the orientation of the bays. Higher values of K_1 led to flatter bays that were

strongly aligned to the wave approach, giving a saw-tooth shaped shoreline. The plan shapes produced this way were qualitatively similar to those produced by Vine and Coates (1992) from hydraulic model tests using anthracite

Model validation was not successful. The record length (14 months of wave data, 21 months of surveys) was insufficient to provide data for a separate validation period. It was decided to allow the calibration and validation periods to overlap. To benefit from the available wave record, the validation was done using data from the period of February 1994 to January 1995. Strictly speaking, if model validation is successful, there should not be any further adjustment of model parameters beyond what were set in the calibration exercise. This rule is not always adhered to, and in the Lakeview Park exercise (Hanson and Kraus, 1989) there was further adjustment of the model after validation to better fit the observations. The Elmer validation runs were unable to represent the observed contour movements, which were extremely small at this level.

There has been discussion of GENESIS in the literature. Young *et al* (1995) cite McAnally (1989), who criticised the two step modelling approach as being simplistic, a misuse of data, and leading users into having undue confidence in the results. The final point seems reasonable, as a semi-empirical model can only be valid over the range of conditions against which it was calibrated. A change in boundary conditions, for example due to a change in the updrift sediment supply, would be expected to invalidate a model calibration.

Young *et al* (1995) then criticise the use of averaged values in GENESIS, when natural processes are complex and may not be best described by their mean values. They also criticise the inability of the model to represent extreme events, and the neglect of the underlying geology in the modelling exercise. The technique of averaging input conditions was defended by de Vriend (1992) for medium to long term models, of which GENESIS is typical. This discussion is presented in chapter 2.

Young *et al* (1995) do raise that the need for a quantification of the magnitude of uncertainty in model parameters. This follows a general trend towards more probablistic methods of describing coastal change. They also call for the source code of models such as GENESIS to be made available, to widen the scrutiny of such models. This would be a welcome step, as it would make GENESIS available as a modelling framework to test the validity of, for example, different transport formulae, and allow the development of the model to allow its application to a wider range of sites than is currently possible.

7.2.3 Recommendations

The inability of GENESIS to represent beach changes at Elmer was due to its unsuitability for use at this particular site. In part, this unsuitability is down to the inability of the model to describe tombolo formation, but also it was due to the differing behaviour of the sand and shingle parts of the beach. If the tombolo problem were solved, then it might be possible to model a 'representative' contour adequately for engineering purposes.

It is possible to include tombolo formation in one-line models. The UNIBEST model does allow tombolo formation for cases of oblique wave approach but, not having a wave height gradient term, cannot produce tombolos for direct wave approach (Ahmed, A., 1997). To allow tombolo formation, the back of the breakwater can be treated in a similar way to a seawall. As material is fed to the tombolo, it gets higher, until its height equals the level of the top of the active beach height. After this, additional material causes the tombolo to broaden.

With a breakwater parallel to the x-axis, the shoreline at the tombolo is likely to be normal to the x-axis. This would violate the small-angle assumption used in deriving the numerical scheme, leading to poor estimates of shoreline change in this area. Use of a numerical scheme that does not rely on the small angle assumption, such as that proposed by Kamphuis (1992) would eliminate this problem.

Allowing tombolo formation requires some parameterisation of sediment bypassing seaward of the breakwater. Without this, a single breakwater could impound all material travelling alongshore, leading to a 'pinned' coastline position at the breakwater tip that would be unreasonable, and affect the shoreline position updrift. This could be avoided by adopting a similar system to bypassing at groynes, where a proportion of the beach below the modelled contour, and offshore of the groyne tip (or breakwater) is passed to the alongshore. Whether such material in reality is lost to the system, reintroduced downdrift of the breakwater, or simply deposited on the breakwater's seaward face and made available for further transport is currently unknown. The way in which a model should deal with this is open.

A problem of allowing material to settle on the front face of the breakwater, and for the beach to develop seaward of the structure (as is possible for groynes) is that the tombolo may develop towards the updrift end of a long breakwater. Further beach growth along the breakwater could lead to the existence of the beach line

at two cross-shore positions in the same grid cell. This would mean that the beach profile in these cells would not be monotonic, in breach of a basic assumption of one-line modelling. A pragmatic approach to solve this problem could be to allow the shoreline to develop in front of a breakwater, and to terminate the simulation if a shoreline overlap occurs.

In its present form, the model was of some use in understanding the difference in weighting attached to the two transport processes (due to oblique wave approach, and due to longshore gradients in wave height). Comparison of these results with the hydraulic model tests (Vine and Coates, 1992) suggested that the over-prediction of longshore transport in the laboratory tests, due to the use of a low density model sediment, contributed to flatter salients developing behind the modelled breakwaters. A similar effect was achieved in the numerical model by increasing the transport rate coefficients.

The final beach configuration in the hydraulic model was constructed at Elmer, to provide a beach planform that was closer to the expected equilibrium, and to reduce the re-working of the imported beach material. Due to the under-prediction of salient lengths in the hydraulic model study, this was not wholly successful. The development of longer salients could be attributed to the sorting of the fill material – releasing fines that were not used in the hydraulic tests - and is also attributable to the entrapment of sand moving alongshore.

In the hydraulic model tests, only the upper (shingle) portion of the beach was mobile. Transport was assumed to only occur at high water, and the lengths of tests were calculated on the basis that the beach was only subject to waves for 50% of the time. Below the level of the interface between sand and shingle, the existing (pre-construction) bathymetry was moulded in concrete. The inability of the lower modelled beach to respond to the breakwaters meant that the salient development could not be properly modelled in the hydraulic tests. No lower beach material – whether from the re-working of the beach fill, or from updrift – was available in the model to settle behind the breakwaters. Thus, the hydraulic model beach could not reach the same equilibrium plan shape as was observed in the field.

The presence of sand at Elmer does increase the amenity value of the beach, without detracting from the beach performance as a coastal protection structure. Sand trapping structures are not common in the Selsey - Brighton littoral cell, as shingle is recognised as the primary beach material, and most groynes are constructed to trap shingle. To understand and design a beach, with control structures, to reduce wave

overtopping of a sea wall, the hydraulic tests were certainly adequate. To understand the development of the Elmer frontage however, the behaviour of both sand and shingle must be considered.

The GENESIS restriction to salient, rather than full tombolo, formation meant that it was not possible to try the method of Chu *et al* (1987) for including the effect of variable sediment composition and a macro-tidal environment. In their Alaskan study, they used different values for K_1 and K_2 to represent material at the beach crest, mid tide and low water beach levels. Discussion with one of the authors of the Alaskan study (M. Gravens, pers. comm.) suggested that the effect of this enhancement of GENESIS was small. It is attractive to increase the complexity of GENESIS by including additional, simple enhancements in this way. With this enhancement though, perhaps the depth at the wave input should be varied, the berm height and closure depth altered to be relative to this level, and the grain size used in the calculations should be changed to represent the grain size at the tidal level. Increasing the level of detail in the model input will probably not be of benefit when the modelling approach is so simple.

In the potential transport calculations, used to estimate a suitable value for K_1, use of a depth threshold (below which waves were excluded from the calculation, as they were not expected to reach the active beach) did not have a significant impact on the calculated sediment transport until the threshold was set to exclude all but the waves recorded at the very highest tidal levels. This demonstrated the dominance of storm events in longshore transport calculations. It also showed that the inclusion of the low tide wave conditions did not greatly influence the calculated transport. If the user is constrained by a slow computer, or is modelling a particularly large area or a long time period, then removal of the lower wave conditions could be used to speed up the calculations. One-line models are not suitable for modelling the storm response of beaches however, so the effect of including large wave events should be monitored closely, to ensure that they don't lead to excessive shoreline changes.

The 'best' model calibration run used a value for K_1 of 0.10. This was higher than that recommended by Brampton and Millard (1996) for a nearby stretch of coast. Where wave data is available, and an approximate transport rate is known, then the fitting of the potential to the observed transport rate gave a reasonable range of values of K_1. The methods of Kamphuis (1990) and Kamphuis et al (1986) both gave estimates for K_1 close to those finally selected. The 'best fit' modelled shoreline was found with a value of K_2 of 0.3. Hanson and Kraus (1989) recommend that K_2 should not exceed twice the value of K_1. The K_2 value gave a 'standard' level of salient development across the model domain, which could then be fine tuned using

structure parameters. The breakwater transmission coefficients and groyne porosities were used as fitting tools. The result was that the breakwaters were given transmission coefficients between 0 (breakwater 3) and 0.4. A field study of transmission demonstrated that breakwater 3 had a mean transmission coefficient of about 0.4 (Simmonds, pers. comm.). It would be expected that the two eastern breakwaters would be more transmissive however, as the crest level was 1 metre lower.

The small-angle assumption, resulting from the derivation of the numerical solution to the shoreline equation, imposes limitations on the shoreline angle to the x-axis. This presents a problem when attempting to model a headland area such as Elmer. The actual assumption was shown to be robust when a straight shoreline was used, and the angle between the shoreline and the x-axis was up to 70°. Problems would be expected to occur when the shoreline angle is both large, and varying with x. This situation was studied by Larson et al (1987), comparing analytical and numerical solutions to the shoreline change equation for a semicircular shoreline, and also for a shoreline adjacent to a groyne. It was claimed that the approximation was reasonable for breaking wave angles of up to 30°. While most of the model domain was within these limits, around the terminal groyne, and over some salients, these limits were exceeded. The model solutions are thus least accurate around structures and headlands, where there is strong shoreline curvature and large shoreline angles to the x-axis.

Around structures, it is not possible to remove this problem altogether if using this approximation. To reduce the problem, the headland could be divided into two model domains, each broadly parallel to the x-axis, and modelled separately. Dealing with the boundaries between the two domains would be likely to introduce further problems, however. A better solution would be the use of a scheme which did not rely on the small angle assumption, such as that presented by Kamphuis (1992).

7.3 Empirical Orthogonal Function analysis

The EOF analysis was undertaken to try and find areas of periodic behaviour in the beach morphology, particularly 3D effects that could not be described by 1-line modelling approaches. The eigenvalues showed the variance associated with each of the three main functions introduced by Winant et al (1975). The most variance was associated with the mean beach function. Plotting this indicated that seasonal movements and noise were least within the scheme, while greatest changes were immediately downdrift of the scheme, and updrift of the scheme, in front of a sea wall. The second eigenvalue (variance associated with the bar-berm

seasonal movement of material) peaked at these points, and also in front of the revetment between breakwaters 5 and 6. This suggests that seasonal movements account for a larger proportion of the beach variance at these points. It can be inferred that the scheme has the effect of stabilising the protected area of beach.

The gridded eigenfunctions showed a simple seasonal cross shore movement of material updrift of the scheme. The picture within the scheme was much more complex, suggesting that seasonal movements do not follow a simple onshore offshore pattern. Downdrift of the scheme, the system does not return to the simple cross shore pattern observed updrift, except possibly towards the limit of the surveys.

The influence of structures on beach seasonality has been observed before (Wijnberg and Terwindt, 1995), although several decades of survey data were available for this work. Hsu et al (1994) state that 1 year of data is sufficient to generate these functions, although it is clear that a longer record must be required to resolve functions with periods of longer than six months, and to improve the confidence in the estimates made. A longer record would also allow the identification of 'noise' in the data (i.e. contributions to the variance that cannot be explained by the 3 principle functions described above). A longer record would also allow the generation of an empirical model, based on the eigenfunction behaviour, such as that produced by Hsu et al (1994). While temporal eigenfunctions were calculated, the short record length did not allow seasonal behaviour to be inferred.

This work did demonstrate the complex 3-dimensional nature of the seasonal beach changes. This cannot be explained with a one line model. To understand the actual beach response over the time scale of the study, a coastal area model is required, including effects of cross shore transport.

7.4 Conclusions and Recommendations for future work

The project length was insufficient to allow sufficient data to be collected to allow the full evaluation long term models of beach development, while the frequency of surveys was insufficient for short-term (storm response) model evaluation. The data set is of use however for evaluating medium-term methods of modelling the beach development. As a result, equilibrium approaches to beach plan shapes were tested, and the applicability and assumptions of the US Army Corps model GENESIS were investigated. GENESIS was chosen for evaluation as it is probably the most widely used, and cited, example of a one-line numerical

model. Despite this, it has not been subject to evaluation outside the US Army Corps of Engineers, or with such a complete set of evaluation data.

Analysis of the field data highlighted differences in the scheme development from that expected from the hydraulic model tests used in the scheme design. Salient development in the field was greater than estimated by the hydraulic model tests. This was due to the hydraulic model tests being intended to provide design guidance to prevent the overtopping of the seawall that backs the Elmer beach. For hydraulic tests to attempt to model the actual salient formation and beach development, it is probably necessary to represent both sand and shingle in the model tests. The fixed bathymetry must be modelled to the beach closure depth, rather than to the limit of shingle coverage, as done in this case. This would allow the salients to develop properly – and to influence the modelled wave field in a way that was not possible in these tests because of the slope associated with the sediment size used. Further laboratory work is necessary to determine the effects of modelling both sediment types – and to properly understand the limits of what can be inferred from tests where only one sediment type is used.

The forcing on the beach was measured during this study, and the modification of the waves through diffraction was measured at the shoreline. The GENESIS modelling used wave transmission as a calibration parameter, and it may be of importance at Elmer, where the breakwaters were constructed without a rubble core. This has since been investigated by Simmonds *et al* (1997). Hydraulic model testing of detached breakwaters since showed that the classical twin gyre circulation pattern is not always observed (S. Ilic, pers. comm.). There is a need for improved understanding of the fluid behaviour to understand the mechanism behind the nearshore circulation.

The field site studied was novel in that it was a macro-tidal site, with detached breakwaters, with a mixed sand-shingle beach, subject to beach renourishment. Each of these conditions is worthy of research on their own. Offshore sourced aggregate is a common material for beach recharge schemes in the U.K. It frequently forms cliffs on the beach, and is extremely poorly sorted. To understand the sorting of the material, the resulting changes in beach profile and porosity, the timescales over which the profile develops, and the expected losses of material, there is a need for a dedicated monitoring study of a similar renourished beach. Ideally this should be away from the influence of control structures, so that the inherent behaviour of the renourished material can be studied. This will allow the influence of structures, and the behaviour of the

beach material to be understood independently, and the influence of one on the other to be assessed. In turn, this will lead to better scheme design, and more effective use of a limited resource in the future.

To improve the understanding of the breakwater scheme behaviour, there is a need for a coastal area model to be developed. Ideally this should be developed as a co-operative research tool, for use and further development by as wide a range of users as possible, in a similar way that some ocean models (e.g. the Princeton Ocean Model, Mellor and Blumberg, 1980) are sometimes developed. The aim of such a model would be to develop the understanding of processes that govern topographic change around breakwaters. This in turn will lead to better parameterisation of processes for improved engineering applications.

8. References

'Island Stopping', 1993, *New Civil Engineer*, 1st April, p 18

Ackers P. and White W.R. 1973, 'Sediment transport: New approach and analysis', *Journal of the Hydraulics Division of the ASCE*, HY 11

Adept Scientific Micro Systems Ltd., 1990, *Graftool*, Adept Scientific Micro Systems, Letchworth, Herts, U.K.

Ahrens J.P., 1987, 'Characteristics of reef breakwaters', *Technical Report CERC 87-17*, Coastal Engineering Research Centre, Vicksburg, M.S.

Ahrens J.P. and Cox J. 1990, 'Design and performance of reef breakwaters', *Journal of Coastal Research*, vol 6(1), pp. 61-75

Aranuvachapun S. & Johnson J.A., 1979, 'Beach profiles at Gorleston and Great Yarmouth', *Coastal Engineering*, vol 2, pp. 201-213.

Aubrey D.G., 1979, 'Seasonal patterns of onshore/offshore movement', *Journal of Geophysical Research*, vol 84 C10, pp. 6347-6354.

Aubrey D.G. and Emery K.O., 1993, 'Recent global sea levels and land levels', in *'Climate and Sea Level Change, observations, projections and implications'*, ed R.A. Warrick, E.M. Barrow and T.M.L.Wigley, pp 45-56

Axe P.G., 1994, 'Elmer frontage beach development - a preliminary report', *University of Plymouth School of Civil and Structural Engineering Report 94003*, Plymouth, U.K.

Axe P.G. & Bird P.A.D., 1994, 'Wave studies at Felpham Beach (West Sussex) - 11th February - 24th June, 1993', *University of Plymouth School of Civil and Structural Engineering Report 94001/C*, Plymouth, U.K.

Bakker W.T. 1968,'The dynamics of a coast with a groyne system', *Proceedings 11th International Conference on Coastal Engineering*,ed. B. Edge, ASCE, New York, pp. 492-517.

Barber N.F. 1963, 'The directional resolving power of an array of wave detectors', in *Ocean Wave Spectra*, Prentice Hall, pp 137-150

Barber P.C. and Davies C.D. 1985, 'Offshore breakwaters - Leasowe Bay', *Proceedings of the Institution of Civil Engineers*, vol. 78 part 1, pp. 85-109.

Barstow S.F, G.A.Athanassoulis, L. Cavaleri, and H.E. Krogstad, 1998, 'EUROWAVES – a user friendly tool for the evaluation of wave conditions at any European coastal location'. *Poster paper at the 3rd European Marine Science and Technology Conference, 23-27 May 1998*, Lisbon,Portugal.

Beltram L.M. and Southgate H.N. 1996, 'Time series analysis of long term beach level data from Lincolnshore, UK', *Proceedings of Coastal Dynamics '95*, ASCE, New York.

Berkhoff J.C.W., 1972, 'Computation of combined refraction diffraction', *Proceedings of the 13th International Conference on Coastal Engineering*, ed. B. Edge, ASCE, New York, pp. 471-490.

Bijker E.W., 1971, 'Longshore transport computations', *Proceedings ASCE Waterways, Harbours and Coastal Engineering Division*. WW4

Bird P.A.D. & Bullock G.N., 1991, 'Field measurements of the wave climate', in *Developments in coastal engineering*, eds D.H. Peregrine and J.H. Loveless, Bristol University, U.K., pp 25-34

Bird P.A.D., 1993, 'Measurements and analysis of sea waves near a reflective structure'. *Unpublished Ph.D thesis*, University of Plymouth, Plymouth, UK

Bodge K.R. and N.C. Kraus, 1991, 'Critical examination of longshore transport rate magnitude', *Proceedings of Coastal Sediments '91*, ed. N.C. Kraus, ASCE, pp. 139-155

Bokhove O and Peregrine D.H. 1999, 'The generation of longshore currents and eddies by breaking waves in the surf zone', *Annales Geophysicae*

Booij N., Ris R.C., & Holthuijsen L.H. 1999, 'A third-generation wave model for coastal regions - 1. Model description and validation', *Journal of geophysical research-oceans*, vol.104, no.C4, pp.7649-7666.

Borges, J.C.V. 1993, 'Wave climate & shingle beach response', *Unpublished Ph.D thesis*, University of Brighton, Brighton, UK

Brampton A.H. & Motyka J.M. 1985, 'Modelling the plan-shape of shingle beaches', *Offshore and Coastal Modelling: Lecture notes on coastal and estuarine studies*, vol. 12, Eds, P.P.G. Dyke, A.O. Moscardini and E.H. Robson, Springer-Verlag, Berlin.

Brampton A.H. & K. Millard, 1996, 'The effectiveness of the Seaford beach renourishment programme', in *Partnership in Coastal Zone Management*, ed: J Taussik and J Mitchell, pp 623-629

Bray M.J. Carter D.J. & Hooke J.M. 1995, 'Littoral cell definition and budgets for central southern England', *Journal of Coastal Research*, vol 11 no.2, pp 381-400.

Briand M.H.G. and Kamphuis J.W. 1990, 'A micro-computer based quasi-3D sediment transport model', *Proceedings of the 22nd International Conference on Coastal Engineering* , ed. B. Edge, ASCE, New York, pp 2159-2172

Briggs J.B., Thompson E.F., and Vincent C.L., 1995, 'Wave diffraction around a breakwater', *Journal of Waterways, Port Coastal and Ocean Engineering*, vol. 121, pp. 23-35

British Standards Institute 1984, *BS 6349: British standard code of practice for maritime structures, Part 1 General Criteria (and amendments)*, British Standards Institution, London U.K.

British Standards Institute,1984-1990, *BS 812, parts 100-103: Testing aggregates*, British Standards Institution, London U.K.

Capon J., Greenfield R.J., & Kolker R.J., 1967, 'Multidimensional maximum-likelihood processing of a large aperture seismic array', *Proceedings of the IEEE* vol 55 pp 192-211

Carr J.H. and Stelzriede, M.E. 1952, 'Diffraction of water waves by breakwaters', *Gravity Waves*, Circular No. 521, US National Bureau of Standards, New York, pp. 109-125.

Chadwick A.J. 1989, 'Field measurements and numerical model verification of coastal shingle transport', *Advances in water modelling and measurement*, ed. M.H.Palmer, BHRA., pp. 381-402.

Chadwick A.J., 1990, 'Nearshore waves and longshore shingle transport', *Unpublished Ph.D. thesis*, Brighton Polytechnic, Brighton, U.K.

Chadwick A.J., 1991, 'An unsteady flow bore model for sediment transport in broken waves. Part 1: the development of the numerical model', *Proceedings of the Institution of Civil Engineers Part 2*, vol 91, pp 719-737

Chadwick, A. J., Pope, D. J., Borges, J. and Ilic, S. 1995, 'Shoreline Directional Wave Spectra, Pt1: An Investigation of Spectra and Directional Analysis Techniques', *Proceedings of the Institution of Civil Engineers (Water Maritime and Energy)*, vol 112, issue 3, pp. 198-209.

Chasten M.A., Rosati J.D., McCormick J.W. and Randall R.E. 1993, 'Engineering design guidance for detached breakwaters as shoreline stabilization structures'. *Coastal Engineering Research Centre Technical Report CERC-93-19*, US Army Waterways Experiment Station, Vicksburg. MS.

Chu Y., Gravens M.B., Smith J.M., Gorman L.T. and Chen H.S., 1987,' Beach erosion control study, Homer Spit, Alaska', *Technical Report CERC-87-15*, US Army Waterway Experiment Station, Vicksburg, MS.

CIRIA, 1996, *Beach management manual*, eds J.D Simm., A.H.Brampton, N.W Beech. and J.W Brooke., CIRIA report 153, Westminster, London, UK

Coastal Engineering Research Centre, 1984, *Shore protection manual*, US Army Waterways Research Station, Vicksburg, MS

Coates T.T. 1994, 'Physical modelling of the response of shingle beaches in the presence of control structures', *Proceedings of Coastal Dynamics '94*, eds: Arcilla AS, Stive MJF, Kraus NC, ASCE, New York, pp.924-937.

Copeland G.J.M. 1985, 'A numerical model of the propagation of short gravity waves and the resulting circulation around nearshore structures', *Unpublished Ph.D. thesis*, University of Liverpool, Liverpool, U.K.

Cowell P.J. and Roy P.S., 1988, *Shoreface transgression model: programming guide*. Report of the Coastal Studies Unit, University of Sydney, Sydney.

Crank J., 1975, *The mathematics of diffusion*, 2nd edn, Clarendon Press, Oxford, England.

Dales, D.C. and M. Al-Mahouk, 1991, 'Application of a 3D beach response model to the Norfolk coast'. *Proceedings MAFF Conference of River and Coastal Engineers*, Ministry of Agriculture, Fisheries and Food, London, UK

Dally W.R. and Pope J., 1986, 'Detached breakwaters for shoreline protection'. *Tech Report CERC-86-1*, US Army Waterways Experiment Station, Vicksburg, MS

Damgaard J.S. and Soulsby R.L. 1996, 'Longshore bed-load transport', in *Proceedings of the 25th International Conference on Coastal Engineering*, ed B. Edge, ASCE, New York, pp. 3614-3627

Davidson, M.A. 1992, 'Implementation of linear wave theory in the frequency domain for the conversion of sea bed pressure to surface elevation', *University of Plymouth Department of Civil and Structural Engineering Internal report SCSE 92008*, Plymouth, U.K.

Davidson, M.A. 1993. 'Optimal Spectral Analysis Procedures for Wave Records', *University of Plymouth School of Civil and Structural Engineering Research Report No. SCSE 93-002*, Plymouth, UK

Davidson M.A., Russell P.E., Huntley D.A., and Hardisty J., 1993, 'Tidal asymmetry in suspended sand transport on a macrotidal intermediate beach'. *Marine Geology*, vol. 110, no 3-4, pp. 333 – 353.

Davidson M.A., Bird P.A.D., Bullock G.N., and Huntley D.A., 1994, "Wave reflection: Field measurements analysis and theoretical developments", *Proceedings of Coastal Dynamics '94*, ASCE, New York, pp 642-655.

Davidson M.A., Bird P.A.D. Huntley D.A. & Bullock G.N. 1996, 'Prediction of wave reflection from rock structures: an integration of field and laboratory data', *Proceedings of the 25th International Conference on Coastal Engineering*, ed. B. Edge, ASCE, New York, pp 2077-2086

Davies M.H. and Kamphuis J.W. 1985, 'Littoral transport rate', *Proceedings of the Canadian Coastal Engineering Conference*, pp 223 - 240

De Vriend H. and Ribberink J.S. 1988, 'A quasi 3D mathematical model of coastal morphology', *Proceedings of the 21st International Conference of Coastal Engineering*, ed B. Edge, ASCE, New York, pp. 1689-1703.

De Vriend H. 1992, 'Mathematical modelling of 3D coastal morphology', *Proceedings of the short course on the design and reliability of coastal structures*, Scuola di S. Giovanni Evangelista, Venice, 1-3 October 1992

De Vriend H.J. 1986, '2DH computation of transient sea bed evolutions', *Proceedings of the 20th International Conference on Coastal Engineering*, ed. B. Edge, ASCE, New York, pp. 1689-1712.

Dean R.G., 1977, 'Equilibrium beach profiles: US Atlantic and Gulf coasts', *Ocean engineering report no. 12*, Department of Civil Engineering, University of Delaware, Newark DE

Del Valle, R., R. Medina, and M.A. Losada, 1993, 'Dependence of coefficient K on grain size', *Journal of Waterway, Port, Coastal and Ocean Engineering*, vol 119 no 5, pp 568 - 574

Department of Energy, 1989, 'Metocean parameters – parameters other than waves', *Report OTH 89 299*, HMSO, London.

Dingemans M.W., Radder A.C., de Vriend H.J. 1987, 'Computation of the driving forces of wave-induced currents', *Coastal Engineering*, vol. 11(5/6), pp. 539-563.

Emery W.J. and Thompson R.E., 1998, *Data analysis methods in physical oceanography*, 1st edn, Pergamon Press, Oxford, U.K.

Engelund F. and Hansen E. 1967, 'A monograph on sediment transport in alluvial streams', *Teknisk Forlag*, Copenhagen. Denmark.

Fisher P.R. and O'Hare T.J. 1996, 'Modelling sand transport on macro-tidal beaches', *Proceedings of the 25th International Conference on Coastal Engineering*, ed. B. Edge, ASCE, New York, pp. 2994 – 3005.

Fleming C.A. 1993a, 'Groynes, offshore breakwaters and artificial headlands', in *Coastal, estuarial and harbour engineers reference book*, eds M.B. Abbott and W.A. Price, E. & F.N. Spon Ltd., Andover, U.K.

Fleming C.A. 1993b, 'Beach response modelling', in *Coastal, estuarial and harbour engineers reference book*, eds M.B. Abbott and W.A. Price, E & F.N. Spon Ltd, Andover, U.K.

Fleming C.A, Pinchin B.M. and Nairn R.B. 1986, 'Evaluation of models of nearshore processes', *Proceedings of the 20th International Conference on Coastal Engineering*, ed. B. Edge, ASCE, New York, pp. 1116-1131.

Goda Y. 1985, *Random seas and the design of maritime structures*, University of Tokyo Press, Tokyo, Japan.

Goda Y., Takayama T. and Suzuki Y., 1978, 'Diffraction diagrams for directional random waves', *Proceedings of the 16th International Conference on Coastal Engineering*, ed. B. Edge, ASCE, New York, pp. 628-650

Golden Software Inc., 1984, *Surfer*, Golden Software, Golden, Colorado, U.S.A.

Gourlay M.R., 1976, 'Non uniform longshore currents', *Proceedings 15th International Conference Coastal Engineering*, ed. B. Edge, ASCE, New York, pp. 701-720.

Gravens M., Kraus N.C. & Hanson H., 1991, *GENESIS Technical reference 2, Workbook and system users manual*, CERC Technical Report CERC 89-19, US Army Waterways Experiment Station, Vicksburg, M.S.

Hallermeier, R.J. 1983, 'Sand transport limits in coastal structure design', *Proceedings of Coastal Structures '83*, ASCE, New York, pp 703-716

Halliday D. & Resnick R., 1978, *Physics, parts 1 and 2*, 3rd edn, Wiley, Bognor Regis, U.K.

Hamm L., Madsen P.A. and Peregrine D.H. 1993, 'Wave transformation in the nearshore zone: A review', *Coastal Engineering*, vol. 21, pp. 5-39

Hanson H., 1989, 'GENESIS- A generalized shoreline change numerical model', *Journal of Coastal Research*, vol. 5(1), pp. 1-27.

Hanson H. and Kraus N.C. 1989, 'GENESIS: Generalized model of simulating shoreline change. Report 1', *Technical Reference CERC 89-19*, US Army Waterways Experiment Station, Vicksburg, MS.

Hanson H. Kraus N. and Nakashima L., 1989, 'Shoreline change behind transmissive detached breakwaters'. *Proceedings of Coastal Zone '89*, ASCE, New York, pp. 568-582

Hanson H., and Kraus N.C., 1990, 'Shoreline response to a single transmissive breakwater', *Proceedings 22nd International Conference on Coastal Engineering*, ed. B. Edge, ASCE, New York,

Hanson H., and Kraus N.C., 1991, 'Numerical simulation of shoreline change at Lorain, Ohio', *Journal of Waterways, Port, Coastal and Ocean Engineering*, vol 117 no 1, pp 1-18

Holland B. & Coughlan P. 1994, 'The Elmer coastal defence scheme', *Proceedings of MAFF conference of river and coastal engineers*, Ministry of Agriculture, Fisheries and Food, London, UK

Holmes C.W. & Beverstock P., 1996, 'The beach management plan for Lancing and Shoreham', in: *Partnership in Coastal Zone Management*, ed: J Taussik & J Mitchell, p 361-368

Horikawa K., (ed), 1988, *Nearshore dynamics and coastal processes - Theory, measurement and predictive models*, University of Tokyo Press, Tokyo, Japan.

Horikawa K. 1996, 'History of coastal engineering in Japan', in *History and Heritage of Coastal Engineering*, ed. N.C. Kraus, ASCE, New York, pp. 336-374.

HR Wallingford Ltd. 1988, 'Wave recording at Littlehampton, 1985-1986', *Report EX 1462*, HR Wallingford Ltd., Wallingford, Oxon.

HR Wallingford Ltd. 1991, 'Wave climate change and its impact on UK coastal management', *Report SR 260*, HR Wallingford Ltd , Wallingford, Oxon.

HR Wallingford Ltd. 1992a, 'Offshore breakwaters physical model study', *Report IT 383*, HR Wallingford Ltd., Wallingford, Oxon

HR Wallingford Ltd. 1992b, 'Elmer 3D Physical Model Study', *Report EX 2529*, HR Wallingford Ltd., Wallingford, Oxon

HR Wallingford Ltd. 1994, 'Wave conditions along the Arun coastline: A guide for contractors', *Report EX3026*, HR Wallingford Ltd., Wallingford, Oxon.

Hsu J.R.C., Silvester R., and Xia Y.M., 1987, 'New characteristics of equilibrium shaped bays'. *Proceedings of the 8th Australian Conference on Coastal and Ocean Engineering.*, Institution of Engineers, pp. 140-144

Hsu J.R.C. and Silvester R., 1990, 'Accretion behind a single offshore breakwater'. *Journal Waterways, Port, Coastal, and Ocean Engineering.*, ASCE, vol. 116(3), pp. 367-380

Hsu T-W., Ou S-H. and Wang S.K., 1994, 'On the prediction of beach changes by a new 2D empirical eigenfunction model'. *Coastal Engineering*, vol 23, pp. 255-270

Hunt J.F., 1979, 'Direct solution of the wave dispersion equation', *Journal of Waterways, Port, Coastal and Ocean Engineering*, vol. 105 no WW4, pp 457-459.

Ilic S, 1994, 'The role of offshore breakwaters in coastal defence - comparison of the two measurement systems', *University of Plymouth School of Civil and Structural Engineering Report SCSE-94002*, University of Plymouth, Plymouth, U.K.

Ilic S., 1999, 'Transformation of multi-directional sea - field and computational study'. *Unpublished Ph.D. thesis*, University of Plymouth, Plymouth, U.K.

Ingles M. 1996, 'The Sidmouth Coastal Protection Scheme', *Unpublished MSc. Dissertation*, University of Plymouth. Plymouth, U.K.

Inman D.L. and Bagnold R.A, 1963, 'Beach and nearshore processes Part II, littoral processes', in: *The Sea, vol 3*, ed: Hill M.N. Wiley-Interscience, Bognor Regis, U.K., pp 529-533.

Isobe, M. and Kondo, K. 1984, ' Method for estimating directional wave spectrum in incident and reflected wave field', *Proceedings of the 19th International Conference on Coastal Engineering*, ed B. Edge, ASCE, New York, pp 467-483.

Jago C.F., and Hardisty J. 1984, 'Sedimentology and morpho-dynamics of a macrotidal beach, Pendine Sands, SW Wales', *Marine Geology*, vol. 60, pp. 123-154.

Janssen M.C. 1993, 'Beach profile development under random waves', *unpublished M.Sc. thesis*, Imperial College of Science and Technology, London

Johnson J.W., O'Brien M.P. and Isaacs J.D. 1948, 'Graphical construction of wave refraction diagrams', *U.S. Navy Hydrographic Office Publication*, No. 605

Kamphuis J.W. 1990, 'Alongshore sediment transport rate', *Proceedings of 22nd International Conference on Coastal Engineering*, ed. B. Edge, ASCE, New York, pp. 2402-2415.

Kamphuis J.W. 1991, 'Alongshore sediment transport rate', *Journal of Waterways, Port, Coastal and Ocean Engineering.*, vol. 117, pp. 624-640

Kamphuis J.W. 1992, 'Computation of coastal morphology', *Proceedings of the short course on the design and reliability of coastal structures*, Scuola di S. Giovanni Evangelista, Venice, 1-3 October 1992,

Kamphuis J.W. 1994, 'One dimensional modelling of coastal morphology', *EU MAST Advanced Study Course in Coastal Engineering*. Bologna, Italy

Kamphuis J.W. and J.S. Readshaw, 1978, 'A model study of alongshore sediment rate', *Proceedings of the 16th International Conference on Coastal Engineering*, ed. B. Edge, ASCE, New York, pp 1656-1674

Kamphuis J.W. and O.J. Sayao, 1982, 'Model tests on littoral sand transport rate', *Proceedings 18th International Coastal Engineering Conference*, ed. B. Edge, ASCE, New York, pp 1305-1325

Kamphuis, J.W., M.H. Davies, R.B. Nairn, and O.J. Sayao, 1986, 'Calculation of littoral sand transport rate', *Coastal Engineering*, vol. 10(1), pp. 1-21

Kobayashi N, G.S. De Silva, K.D. Watson, 1989, 'Wave transformation and swash oscillation on gentle and steep slopes', *Journal of Geophysical Research*, 94 C1, pp. 951-966

Komar P.D. and Inman D.L., 1970, 'Longshore transport on beaches'. *Journal of Geophysical Research.* Vol. 75, pp. 5914-5927.

Kraus N.C., 1982, 'Pragmatic calculation of the breaking wave height and angle between structures', *Proceedings of the 29th Japanese Coastal Engineering Conference*, Japan Society of Civil Engineers, pp 295-299.

Kraus N.C. 1984, 'Estimate of breaking wave height behind structures', *Journal of Waterways, Port, Coastal and Ocean Engineering*, vol. 110 no 2, pp. 276-282.

Kraus, N and Harikai S., 1983, 'Numerical model of shoreline change at Oarai beach'. *Coastal Engineering.*, vol. 7, pp. 1-28

Lacombe H, 1952, 'The diffraction of a swell: A practical approximate solution and its justification', *Gravity Waves*, circular no 521, US National Bureau Standards, New York, pp. 129-140

Lamb H.H., 1932, *Hydrodynamics*, 6th edn, Dover Press, Englewood Cliffs, N.J.

Larson M., H. Hanson, N.C. Kraus, and M.B. Gravens, 1997, 'Beach topography response to nourishment at Ocean City, Maryland', *Proceedings of Coastal Dynamics '97*, ASCE, New York, pp 844-853

LeBlond, P.H., 1972, 'On the formation of spiral beaches', *Proceedings 13th International Conference on Coastal Engineering*,ed. B. Edge, ASCE, New York, pp. 1331-1346.

Liberatore G. 1992, 'Detached breakwaters and their use in Italy', *Proceedings of the short course on the design and reliability of coastal structures*, Scuola di S. Giovanni Evangelista, Venice, 1-3 October 1992 pp. 373-395.

Longuet-Higgins M.S., 1970a, 'Longshore currents generated by obliquely incident sea waves, Part 1', *Journal of Geophysical Research*, vol. 75(33), pp.

Longuet-Higgins M.S., 1970b, 'Longshore currents generated by obliquely incident sea waves, Part 2', *Journal of Geophysical Research*, vol. 75(33), pp.

Longuet-Higgins M.S. and Stewart R.W. 1962, 'Radiation stress and mass transport in gravity waves, with application to "surf beats"', *Journal of Fluid Mechanics*, vol. 13, pp 481-504.

Longuet-Higgins M.S. and Stewart R.W. 1964, 'Radiation stresses in water waves; a physical discussion, with applications', *Deep Sea Research*, vol. 11, pp. 529-562.

Lorenz E., 1956, 'Empirical orthogonal functions and statistical weather prediction'. *Scientific report no 1.*, Air Force Cambridge Research Center, Air Research and Development Command, Cambridge, M.A.

Loveless J.H., Grant G.T., and Karlsson R.I. 1996, 'The effect of groundwater flows on scour at coastal structures', in *Proceedings of the 25th International Conference on Coastal Engineering*, ed B. Edge, ASCE, New York, pp. 2152-2165

Madsen P.A., Sørensen O.R & Schäffer H.A., 1997, 'Surf zone dynamics simulated by a Boussinesq type model. Part 1. Model description and cross-shore motion of regular waves', *Coastal Engineering*, vol. 32, pp. 255-287.

Mathworks Inc., 1993, *Matlab*, The Mathworks Inc., Natick, Boston, M.A.

Matsuoka M. & Ozawa Y., 1983, 'Application of a numerical model to the prediction of shoreline changes', in: *Proceedings of Coastal Structures '83*, ASCE, New York, pp 649 – 659

McAnally W.H., 1989, 'Lessons from ten years sediment modelling', In: *Sediment Transport Modeling* ed: Wang S.S.Y., ASCE, New York, pp 350-355

McCormick M.E., 1993, 'Equilibrium shoreline response to breakwaters', *Journal Waterways, Port, Coastal, and Ocean Engineering.*, vol. 119(6), pp. 657-670.

Medina R., M.A. Losada, R.A. Dalrymple & A.J. Roldan, 1991, 'Cross shore sediment transport determined by EOF method', *Proceedings of Coastal Sediments '91*,ed. N.C. Kraus, ASCE, New York, pp 187-210

Mellor G.L. & A.F. Blumberg 1978, 'A coastal ocean numerical model', in: *"Mathematical Modeling of Estuarine Physics," Proceedings of an International Symposium, Hamburg, Germany, August 24-26*, eds. J. Sundermann & K-P. Holz, Springer-Verlag, Berlin, pp. 203-219

Memos C.D. 1980, 'Water waves diffracted by two breakwaters', *Journal of Hydraulic Research.*, vol. 18(4) pp. 343-357

Ministry of Agriculture, Fisheries and Food 1994, *Coastal Protection Survey of England*, MAFF, London.

Mitsuyasu H., 1975, 'Observations of the directional spectrum of ocean waves using a cloverleaf buoy', *Journal of Physical Oceanography*, vol 5(4), pp 750-760

Moore, B. 1982, 'Beach profile evolution in response to changes in water level and wave height', *Unpublished M.S. thesis*, Department of Civil Engineering, University of Delaware, Newark, DE

Morse, P.M. and Rubinstein P.J. 1938, 'The diffraction of waves by ribbons and by slits'. *Physical Review*, vol. 54, pp. 895-898.

Nairn R.B., 1988, 'Prediction of wave height and mean return flow in cross shore sediment transport modelling' *IAHR Symposium on Mathematical Modelling of Sediment Transport in the Coastal Zone*, Copenhagen.

National Rivers Authority, 1992, *Sea defence survey*, National Rivers Authority, Bristol

Nelson R.C. 1997, 'Height limits in top down and bottom up wave environments', *Coastal Engineering*, vol. 32, pp. 247-254.

Nicholls R.J. and Wright P., 1991, 'Longshore transport of pebbles, experimental estimates of K', *Proceedings of Coastal Sediments '91*, ed. N.C. Kraus, ASCE, New York, pp. 920-933.

Nir Y. 1982,' Offshore artificial structures and their influence on the Israel and Sinai Mediterranean beaches', *Proceedings of the 18th International Conference on Coastal Engineering*. ed B. Edge, ASCE, New York, 1837-1857

Osaza H., and Brampton A.H., 1980, 'Mathematical modelling of beaches backed by a seawall', *Coastal Engineering*, vol. 4, pp. 47-64.

Ozhan, E., 1982, 'Laboratory study of breaker type effect on longshore sand transport', in: *Mechanics of Sediment Transport Proceedings of Euromech 156*, eds: B.M. Sumer & A. Muller, A.A. Balkema, Rotterdam, 265-274

Pawka S.S., 1983, 'Island shadows in wave directional spectra', *Journal of Geophysical Research*, vol 88 no C4, pp 2579-2591

Pelnard-Considere, R., 1956, 'Essai de theorie de l'evolution des formes de rivage en plages de sable et de galets'. *4th Journees de l'Hydraulique, Les energies de la Mer*, Question III, Rapport No.1, pp. 289-298.

Penney W.G. and Price A.T. 1952, 'The diffraction theory of sea waves, and the shelter afforded by breakwaters', *Philosophical transactions of the Royal Society of London*. Part A vol. 244(882) pp. 236-253

Perlin M and Dean R.G. 1978, 'Prediction of beach planforms with littoral controls'. *Proceedings of the 16th International Conference Coastal Engineering*. ed B. Edge, ASCE, New York, pp. 1818-1838.

Perlin M and Dean R.G.,1985, '3D model of bathymetric response to structures', *Journal of Waterways, Port Coastal and Ocean Engineering*, v111 part 2, 153-170

Perlin M. 1979, 'Predicting beach planforms in the lee of a breakwater', *Proceedings of Coastal Structures '79*, ASCE, New York, pp. 792-808.

Pethick J. and Burd F. 1993, *Coastal defence and the environment: a guide to good practise*, Ministry of Agriculture, Fisheries and Food, U.K.

Pope J. and Dean J.L., 1986, 'Development of design criteria for segmented breakwaters', in: *Proceedings 20th International Conference Coastal Engineering*, ed: B. Edge, ASCE, New York, pp 2144-2158

Pos J.D. & Kilner F.A. 1987, 'Breakwater gap wave diffraction: an experimental and numerical study'. *Journal of Waterways, Port, Coastal and Ocean Engineering*. vol. 113, pp. 1-21.

Powell K., 1990, 'Predicting the short term profile response for shingle beaches'. *Report SR 219*, HR Wallingford Ltd., Wallingford, Oxon.

Pruszak, Z., 1993, 'The analysis of beach profile changes using Dean's method and empirical orthogonal functions', *Coastal Engineering* vol 19, pp 245-261

Putnam J.A., W.H. Munk & M.A.Traylor, 1949, 'The prediction of longshore currents', *Transactions of the AGU*, vol 30, pp 337-345

Radder A.C., 1979, 'On the parabolic equation method for water wave propagation', *Journal of Fluid Mechanics*, vol. 95(1), pp. 159-176.

Rendel Palmer and Tritton Ltd. 1996, 'History of coastal engineering in Great Britain', in *History and heritage of coastal engineering*, ed. N.C. Kraus, ASCE, New York, pp. 214-274.

Robert West and Partners Ltd., 1991, *Joint Coastal Defence Study*, Robert West and Partners, Orpington, London.

Rosatti J.D. & Truitt C.L. 1990, 'An alternative design approach for detached breakwater projects'. *Miscellaneous Paper CERC-90-7*, US Army Waterways Experiment Station, Vicksburg, MS.

Rosen D.S. & Vajda M., 1982, 'Sedimentological influences of detached breakwaters', *Proceedings 18th International Conference on Coastal Engineering*, ed. B. Edge, ASCE, New York, pp.1930-1949.

Sauvage de St Marc M.G., & Vincent M.G. 1954, 'Transport littoral, formation de fleches et de tombolo', *Proceedings 5th International Conference on Coastal Engineering*. Council on Wave Research, pp. 296-327

Schäffer H.F., Madsen P.A. & Diegaard R., 1993, 'A Boussinesq model for waves breaking in shallow water', *Coastal Engineering*, vol. 20, pp. 185-202.

Schoonees J.S. & Theron A.K. 1994, 'Accuracy and applicability of the SPM longshore transport formula', *Proceedings 24th International Conference on Coastal Engineering*, ed. B. Edge, ASCE, New York, pp. 2595-2609.

Shinohara K. & Tsubaki T., 1966, 'Model study on the study of change of shoreline of sandy beach by offshore breakwater'. *Proceedings 10th International Conference on Coastal Engineering*, ed. B. Edge, ASCE, New York, pp. 550-564.

Silvester R., 1970, 'Growth of crenulate shape bays to equilibrium', *Journal of Waterways and Harbours Division of the ASCE*, Vol. 96(WW2), pp. 275-287.

Silvester R & Ho S-K, 1972,'Use of crenulate shaped bays to stabilize coasts', *Proceedings 13th International Conference on Coastal Engineering*, ed. B. Edge, ASCE, New York, pp. 1347-1365.

Simmonds D.J. A.J. Chadwick, P.A.D. Bird and D.J. Pope, 1997, 'Field measurements of wave transmission through a rubble mound breakwater', *Proceedings of Coastal Dynamics '97*, ASCE, New York, pp 734-743

Smallman J. and Porter D. 1985, 'Wave diffraction by two inclined semi-infinite breakwaters', *Proceedings of the International Conference of Numerical Hydraulic Modelling of Ports and Harbours*, pp 269-278.

Sommerfeld A. 1896, 'Mathematische Theorie der Diffraktion', *Mathematische Annalen*, vol 47, pp. 317-374

Sørensen O.R., Schäffer H.A., & Madsen P.A. 1998, 'Surf zone dynamics simulated by a Boussinesq type model, III. Wave-induced horizontal nearshore circulations', *Coastal Engineering*, vol. 33, pp. 155-176.

Stauffer D.F., Garton E.O. & R.K. Steinhorst, 1985, 'A comparison of principal components from real and random data', *Ecology*, vol 66(6), pp 1693-1698

Suh K. and Dalrymple R.A., 1987, 'Offshore breakwaters in laboratory and field', *Journal Waterways, Port, Coastal and Ocean Engineering.*, vol 113 no 2, pp. 105-121

Svendsen I.A. and Brink-Kjær O. 1973, 'Shoaling of cnoidal waves', *Proceedings of the 13th International Conference on Coastal Engineering*, ed. B. Edge, ASCE, New York, pp. 365-383 .

Thompson G. 1992, 'Coastal Modelling Strategy', *Proceedings of the Institution Civil Engineers: Water Maritime & Energy*, vol. 96, pp. 179-180.

Toyoshima O. 1976, 'Seabed changes due to detached breakwaters', in *Proceedings of the 15th International Conference on Coastal Engineering*, ed B. Edge, ASCE, New York, pp. 365-383

Toyoshima O. 1982, 'Variation in foreshore due to detached breakwaters', in *Proceedings of the 18th International Conference on Coastal Engineering*, ed. B. Edge, ASCE, New York, pp. 365-383

Uda T. & Hashimoto H., 1980, 'Application of an empirical prediction model of beach profile change to the Ogawara coast', *Coastal Engineering in Japan*, v 23, pp 191-204

Van der Graaff J. & van Overeem J. 1979, 'Evaluation of sediment transport formulae in coastal engineering practice', *Coastal Engineering* vol. 3, pp. 1-32.

Van der Meer, J.W. & I.F.R. Daemen, 1994, 'Stability and wave transmission at low crested rubble mound structures', *Journal of Waterways, Port, Coastal and Ocean Engineering*, vol 120, no 1, pp 1-19

Van Hijum E. & Pilarczyk K.W. 1982, 'Equilibrium profile and longshore transport of coarse material under regular and irregular wave attack', *Delft Hydraulics Laboratory publication 274*, Delft Hydraulics Ltd., Delft.

Vitale, P., 1981, 'Movable bed laboratory experiments comparing radiation stress and energy flux factor as predictors of longshore transport rate', *CERC Research Manuscript 81-4*, US Army Waterways Experiment Station, Vicksburg, MS

WASA Group, 1998, 'Changing waves and storms in the northeast Atlantic?', *Bull. American Meteorological Society*, vol 79, 741-760

Watanabe A., Maruyama K., Shimizu T. & Sakakiyama T., 1986, 'Numerical prediction model of three dimensional beach deformation around a structure', *Coastal Engineering in Japan*, vol. 29, pp. 179-194.

Wijnberg K.M., & Terwindt J.H.J., 1995, 'Extracting decadal morphological behaviour long-term bathymetric surveys along the Holland coast using eigenfunction analysis', *Marine Geology* vol. 126,pp. 301-330

Winant C.D., Inman D.L. & Nordstrom C.E., 1975, 'Description of seasonal beach changes using empirical eigenfunctions', *Journal of Geophysical Research*, vol 80 no 15, pp 1979-1986

Work P.A. & Dean R.G., 1995, 'Assessment and prediction of beach-nourishment evolution', *Journal of Waterways, Port, Coastal and Ocean Engineering*, vol 121 no 3, pp 182-190

Wright L.D., Nielsen P., Short A.D., & Green M.O., 1982, 'Morphodynamics of a macrotidal beach', *Marine Geology*, vol. 50, pp. 97 –128.

Yasso, W.E. 1965, 'Plan geometry of headland-bay beaches'. *Journal of Geology*. vol 73, pp. 702-713.

Young R.S., Pilkey O.H., Bush D.M. & Thieler R.E., 1995, 'A discussion of the Generalized Model for Simulating Shoreline Change (GENESIS)', *Journal of Coastal Research*, vol 11 no 3, pp. 875-886